MODELLING BIOLOGICAL MACROMOLECULES IN SOLUTION:
THE GENERAL TRI-AXIAL ELLIPSOID

Stephen Ernest Harding, M.A. (Oxon), M.Sc.

PhD Dissertation

University of Leicester

1980

MODELLING BIOLOGICAL MACROMOLECULES IN SOLUTION:

THE GENERAL TRI-AXIAL ELLIPSOID

by

STEPHEN ERNEST HARDING, M.A. (Oxon), M.Sc.

A thesis submitted in partial fulfilment

of the regulations governing the Ph.D.

degree at the University of Leicester.

Department of Biochemistry,   June, 1980

School of Biological Sciences,

Adrian Building,

University of Leicester,

University Road,

Leicester, LE1 7RH

To Anne

'. . . God, in the beginning form'd Matter in solid,

massy, hard, impenetrable, moveable particles . . .'

Newton, <u>Opticks</u>, 1717, Query 31.

Abstract

Hydrodynamic shape functions for modelling biological macromolecules in solution in terms of an ellipsoid of revolution model are reviewed. Several new, hitherto unpublished shape functions whose experimental determination does not require knowledge of the swollen molecular volume in solution, are given. The limitations and inadequacies of this model are explained. The viscosity increment ν for a dilute dispersion of tri-axial ellipsoids of semi-axes $a > b > c$, under dominant Brownian motion is derived and an explicit expression in terms of a, b and c is given. Knowledge of the viscosity increment alone is not sufficient to uniquely determine the axial ratios (a/b, b/c) because (i) in order to determine ν, knowledge of the swollen volume in solution is required and (ii) a particular value for ν has a line solution of possible values for (a/b, b/c). (i) is dealt with by combining ν with the tri-axial frictional ratio function P to give the tri-axial R function and (ii) by combining graphically the R line solution with δ_+ and δ_- swelling independent line solutions. The experimental determination of δ_+ and δ_- requires the resolution of a 2-term electric birefringence decay into its component relaxation times; current data analysis techniques are however not satisfactory for resolving close relaxation times (as for globular proteins) with the current experimental precision. It is however shown by exhaustive computer simulation that using a new R-constrained non-linear least squares iterative analysis this is now possible. It is thus concluded that the general tri-axial ellipsoid as a model for the gross conformation of biological macromolecules in solution can now be employed.

CONTENTS

.

LIST OF TABLES

LIST OF FIGURES

PREFACE

Preface

There are two basic approaches for determining the gross
conformation of a biological macromolecule in solution. One is to assume
a structure (generally an array of spheres of varying sizes) and then
calculate its hydrodynamic properties, for example the intrinsic
viscosity, sedimentation coefficient, translational diffusion coefficient,
and then see how much these predicted properties differ from the
experimentally determined properties for the unknown structure. The
model is then successively changed or 'refined' until the predicted
properties converge to agree with the actual properties. This method has
been developed by Bloomfield, Garcia de la Torre and co-workers
(Bloomfield et al, 1967, Garcia de la Torre & Bloomfield, 1977a,b,c, 1978,
Wilson & Bloomfield, 1979a,b, Garcia Bernal & Garcia de la Torre, 1980).
There is however a serious drawback in that the final calculated structure
may not be the only one which gives these properties.

The alternative approach is to calculate the structure directly from
the known hydrodynamic properties. Some general model must of course be
assumed, but although the models available from this approach are less
precise (the most general before the commencement of this study being an
ellipsoid with two equal axes) it does not suffer from the uniqueness
problem. This approach was first developed by Stokes (1851, 1880) in
terms of a simple spherical model calculated from the translational
frictional property and the rotational frictional property and again for
a spherical model by Einstein (1906 – with a correction in 1911) from the
viscosity property. Although the current state of theoretical, experimental
and data analysis techniques allows use of the '2 equal axes' ellipsoid
("ellipsoid of revolution"), it is clear from a simple perusal of

crystallographic models that for many biological structures this model is a very poor approximation to the true structure.

The aim of this thesis is thus twofold: the first is to review all the current ellipsoid of revolution shape functions (in which some new, hitherto unpublished functions are given) and the second is to develop the current theoretical and data analysis techniques to show that with current experimental precision the restriction of two equal axes on the ellipsoid model can now, in principle at least, be dispensed with to allow use of the more general "tri-axial ellipsoid" model.

I would like to thank my friends and colleagues in this Department for making my stay here an enjoyable one, and finally my Mother for her great patience whilst typing this manuscript.

C H A P T E R   1

The Mass, Size and Shape of Macromolecules in

Solution: The Ellipsoid of Revolution Model

1.1. Macromolecular Structure in Solution

The concept of a unique structure for a biological macromolecule in solution and in crystallized form has only relatively recently been established beyond dispute. Prior to the work of Svedberg the view was commonly taken (Sorensen, 1930) that proteins and other macromolecules exist in solution not as unique structures but as dissociable complexes containing possibly several components, that the equilibrium state was dependent on circumstances (for example the composition of the solution) and any components precipitated are not necessarily to be identified with those occurring in solution. Researchers were consequently surprised at the ultracentrifuge results of Svedberg and his co-workers (Svedberg & Pedersen, 1940) which strongly suggested the molecular homogeneity of many protein systems. Thus, in striking contrast to the polydispersity of many polymer systems (such as carbohydrates, rubber or polystyrene) it was deduced that carefully prepared protein solutions contain one, or at the most a few, different molecular species. This deduction was derived mainly from the observation that boundary spreading observed in the sedimentation of protein solutions could be identified with separately measured translational diffusion coefficients. Bresler and Talmud (1944) suggested however that a monodisperse protein really contains a distribution of molecular weights with a sharply defined maximum. This surmise is, on the other hand, strongly opposed by the immunological properties of proteins (Alexander & Johnson, 1949) together with the overwhelming evidence now available from protein crystallography (Kendrew et al, 1958, Perutz et al, 1960, Blake et al, 1965, Feldman, 1976) which support the idea of discrete individual structures.

X-ray crystallography is by far the most accurate method for determining these structures. Unfortunately this technique is also the most laborious, requiring several researchers working for a period of months to determine the structure of a single globular protein. The calculated structures are also of the 'fossilized' form of the macromolecule which may not necessarily be the same in solution. There are many techniques available, such as nuclear magnetic resonance, electron spin resonance, fluorescence and other spectroscopic techniques which can give much detailed information about the dynamic properties of localized regions of macromolecules in solution (for example, the active sites of enzymes are being extensively studied). These techniques cannot however give information as to the overall macromolecular mass, size and shape. For this one needs to consider the hydrodynamic properties of solutions of the macromolecule (although scattering phenomena can also give useful information), which allows determination of the molecular weight, simple 'hydrodynamically equivalent' mathematical models for the structure and also the size (including the swelling due to solvent association) of the macromolecule.

1.1.1. <u>Mass</u>

The 'inertial mass' of a body can be defined as the quantity of matter in it, or as the ratio of the force applied to its acceleration (Newton's 2nd Law of Motion). For a macromolecule we conveniently express the mass by the 'Molecular Weight' (M_r) which is defined as the ratio of the mass of the macromolecule to that of one sixteenth of an oxygen O_{16} atom, and is expressed in grams.

The mass of fluid displaced by a macromolecule in a solution will

equal the product of the volume displaced and the density of the solution $(M_r \bar{v}/N_A)\rho_o$, where M_r is the molecular weight, N_A Avogadro's number, ρ_o the solution density and $\bar{v}$ the partial specific volume of the macromolecule, i.e. the volume increase when unit mass (generally one gram) of solute is added to an infinite volume of the solvent at constant temperature and pressure

$$\bar{v} = \left(\frac{\partial \bar{v}}{\partial m}\right)_{T,p}$$

(1)

The 'Archimedean mass' (i.e. the buoyant mass) of a macromolecule (Van Holde, 1971) in solution will equal the true mass minus the mass of the fluid displaced:

$$= \frac{M_r}{N_A} - \left[\frac{M_r}{N_A} \bar{v}\right]\rho_o = \frac{M_r}{N_A}(1 - \bar{v}\rho_o)$$

(2)

The molecular weight of a macromolecular solute can be measured from many methods, for example sedimentation velocity and translational diffusion, osmosis, light or x-ray scattering, or most precisely from a sequence analysis. A recent review of these methods is given by Rowe (1978). The partial specific volume can be found either from a concentration determination followed by a densimetric analysis (Kratky et al, 1969, 1973), or for a protein, from Traube's rule (Rowe, 1978). This rule may possibly also be applicable to nucleic acids (Pearce et al, 1975).

1.1.2. Size

The size of a rigid macromolecule in solution will differ from that in the anhydrous state because of associated solvent. The hydrodynamic or swollen specific volume $\bar{v}_s$, will now comprise of the partial specific

volume, $\bar{v}$, the bound solvent that adheres to the hydrophilic particle

surface, and 'entrained' solvent which may be trapped in the various

cavities and indentations in the macromolecule (Figure 1). The ratio

$\bar{v}_s / \bar{v}$ is known as the 'swelling' of the macromolecule and is equal

to unity if the macromolecule is anhydrous and compact in solution.

The swollen specific volume can be simply related to the "effective"

hydrodynamic volume V_e i.e. the swollen volume of a single macromolecule

in a homogeneous solution:

$$V_e = \frac{\bar{v}_s M_r}{N_A}$$

(3)

1.1.3. Shape

Owing to the difficulties in developing theoretical relationships

between the shape of a macromolecule and experimentally measurable

parameters, only rather simple 'hydrodynamically equivalent' models are

currently available, the boundaries of which can be described by a simple

mathematical equation; these are (Figure 2) rods, discs and ellipsoids

of revolution (Tanford, 1961).

An ellipsoid of revolution is formed by rotating an ellipse either

about the major axis (prolate ellipsoid) or about the minor axis (oblate

ellipsoid) and thus has the necessary restriction that two of the three axes

must be equal. In the limit of large axial ratio, a prolate ellipsoid

(2 minor axes, 1 major) becomes a good approximation to a rod whilst an

oblate ellipsoid (2 major axes, 1 minor) becomes a good approximation to

a disc. Consequently, physical biochemists have tended to use the

ellipsoid of revolution model to determine the hydrodynamically equivalent

shape of a rigid macromolecule in solution.

It should be made clear at this stage that many macromolecules cannot

be modelled by any of these rigid structures as they have no preferred

structure in solution: these 'randomly coiled' macromolecules can only be represented by probability configurations. Many other macromolecules have a well defined rigid structure but cannot be reasonably modelled, judging from the x-ray models at least, by any ellipsoid. The L-shaped Transfer RNA molecule is an outstanding example (Kim, 1974).

1.2. The Hydrodynamic Properties of a Macromolecular Solution

The hydrodynamic properties of a macromolecular solution, which are used to determine these structures, can be conveniently divided into three broad classes:

(i)   The viscosity property, which concerns the effect of the dissolved macromolecule on the bulk motion of the fluid when a shear gradient is . applied.

(ii) The translational frictional property, which concerns the movement of the macromolecule through its solution when some form of external force is applied. This can be a centrifugal field in a sedimentation experiment or a concentration gradient (i.e. a gradient of chemical potential) in a translational diffusion experiment.

(iii) The rotational frictional property, which concerns the disorienting effect on the macromolecule by the local Brownian motion of the surrounding solvent molecules.

1.3.   The Viscosity Property of a Macromolecular Solution

The viscosity of a fluid is a measure of its resistance to flow and may be simply defined for a simple shearing flow[*] (Figure 3) in terms of the shearing stress σ and the shear rate G:

$$\sigma = \eta G \qquad\qquad (4)$$

_____

[*] For the equations describing a more general flow see Batchelor (1967).

where η is known as the viscosity coefficient. If η is a proportionality
constant independent of the shear rate the fluid is said to be Newtonian.
However, if the constituent molecules show preferred orientations, this
will alter the retarding forces between adjacent fluid elements and hence
the internal friction or viscosity coefficient. This non-Newtonian
effect will occur in solutions containing highly asymmetric or easily
deformable molecules and at high shear rates (Batchelor, 1967); this forms
the basis of flow birefringence experiments (see 1.5.3). For characterizing
the macromolecule in solution we can set the conditions (i.e. very low shear
rates) so that the Newtonian condition prevails, whereas the chemical engineer
would be more interested in the general flow properties.

Using equation (4) we can simply relate the viscosity coefficient to
the energy dissipation during flow. Writing σ as a tangential force per unit
area (F/A) and the shear rate as the velocity gradient ((dx/dt)/Δy):

$$\frac{F}{A} = \eta \ \frac{1}{\Delta y} \frac{dx}{dt}$$

Multiplying both sides by G:

$$\frac{F \ dx}{A \Delta y dt} = \eta \ G^2$$

Since AΔy is the volume of the element under consideration, then

$$\left\langle \frac{dW}{dt} \right\rangle = G^2 \eta$$

(5)

where <dW/dt> is the mean energy dissipated per unit volume.

The effect of dissolved or suspended macromolecules which are assumed
to occupy a volume φ of fluid, is to disturb the streamlines of the
fluid motion and to reduce the volume of the fluid in which the same
overall deformation takes place. Thus the internal friction, the viscosity

coefficient and hence the energy dissipated is increased. This increase can be represented by:

$$\left\langle \frac{dW}{dt} \right\rangle_{inc} = G^2 (\eta - \eta_o) = G^2 \eta_o \nu\phi \tag{6}$$

where η is the viscosity coefficient of the solution and η_o that of the solvent. Rewriting:

$$\eta = \eta_o (1 + \nu\phi) \tag{7}$$

Here ν is defined as the viscosity increment and is a function of the shape of the particle. Again, rewriting equation (7):

$$\frac{\eta}{\eta_o} - 1 = \eta_{sp} = \nu\phi$$

where η_{sp} is the specific viscosity. This equation only applies to an infinitely dilute solution in which no solute-solute interactions occur. For finite concentrations:

$$\eta_{sp} = \nu\phi + \nu_1\phi^2 + \nu_2\phi^3 + \ldots \ldots$$

or, replacing ϕ by $c\bar{v}_s$, where c is the concentration and $\bar{v}_s$ the swollen specific volume:

$$\eta_{red} = \frac{\eta_{sp}}{c} = \nu\bar{v}_s + \nu_1\bar{v}_s^2 c + \nu_2\bar{v}_s^3 c^2 + \ldots \ldots$$

where η_{red} is the reduced specific viscosity. As the concentration approaches zero, η_{red} tends to a limiting value, known as the intrinsic viscosity, $[\eta]$. This can therefore be found by extrapolating a plot of η_{red} versus concentration to infinite dilution, and, if the swollen specific volume, $\bar{v}_s$ is known (section 1.1.2.), ν can also be found:

$$\nu = \frac{[\eta]}{\bar{v}_s} = \frac{[\eta]M_r}{V_e N_A} \tag{8}$$

An approximate value for ν can be estimated for 'globular' proteins by using the partial specific volume $\bar{v}$ and assuming that $\bar{v}_s / \bar{v}$ is ~ 1.4 for globular proteins. A full review of the experimental techniques for determining the intrinsic viscosity, $[\eta]$ is given by Yang (1961).

Einstein (1906, 1911) was the first to determine an explicit value for ν for a specific particle shape, i.e. a sphere, by solving the equations of motion for the flow using spherical harmonics. His assumptions were:

(i) the particles are large enough compared to the solvent molecules so that the surrounding fluid can be regarded as a continuum and Euler's (Batchelor, 1967) equations concerning the change of flow through specific volume elements rather than the complicated Lagrange equations for particle motion can be used,

(ii) the dimensions of the particles are however considered very much less than the spatial variations in the velocity flow field,

(iii) the flow rates are small enough so that squared terms concerning the velocity (and hence normal stress effects) can be neglected and that the inertia or mass forces can be neglected.

Using these assumptions and considering the increase in the average dissipation of energy per unit volume, he found that $\nu = 2.5$, and was independent of particle size. This result has been confirmed experimentally for polystyrene latex spheres by Cheng & Schachman (1955).

Jeffrey (1922) attempted to extend this theory to find ν as a function of axial ratio for ellipsoids of revolution, using ellipsoidal harmonics to solve the equations for the fluid flow. Owing to the non-isotropic nature of ellipsoids, the hydrodynamic torques on the ellipsoids were shown to have two effects:

(a) the first effect tends to make the particle rotate on average with the local undisturbed angular velocity of the fluid,

(b) the second effect tends to orient the minor axis parallel to the flow for prolate ellipsoids and perpindicular to the flow for oblate ellipsoids. As a result, the fluid is no longer isotropic and an energy dissipation analysis fails to give a unique value for the axial ratio for a given value of ν (Brenner, 1972a). However, if the particles are sufficiently small the randomizing effect of the Brownian motion of the surrounding solvent molecules counteracts the orientational tendancy of the hydrodynamic torque (b) so that the particles are randomly oriented (Simha, 1940) and rotate on average with the local angular velocity of the fluid. The solution is then statistically isotropic, allowing an energy dissipation analysis to be used to obtain an unambiguous solution for ν in terms of the axial ratio for prolate and oblate ellipsoids of revolution. Simha (1940) was thus able to obtain a formula which has been shown to give good agreement with experiment (Mehl, Oncley & Simha, 1940):

$$\nu = \frac{1}{ab^2} \left\{ \frac{2\alpha_0{}''}{15b^2\alpha_0{}'\beta_0{}'} + \frac{7}{15b^2\alpha_0{}'} + \frac{2}{5} \left[\frac{\beta_0{}'(a^2 + b^2) + 2\beta_0{}''}{\beta_0{}'[2a^2b^2\beta_0{}' + (a^2 + b^2)\beta_0{}'']} \right] \right\}$$

(9)

where a,b,b are the three semi-axes of the ellipsoid (b > a for oblate and b < a for prolate), and the α_0' etc. which depend on a and b are elliptic integrals given by Jeffrey (1922) (Appendix I). This relation could be solved numerically for both cases and a table of values for ν as a function of axial ratio was given by Mehl, Oncley & Simha (1940).

The function is plotted in Figure 4. In the limit of large axial ratio

p (=b/a)

$$\nu \sim \frac{1/p^2}{15(\ell n(2/p)-3/2)} + \frac{1/p^2}{5(\ell n(2/p)-1/2)} + \frac{14}{15} \quad \text{(prolate)}$$

(10a)

$$\nu \sim \frac{16}{15} \tan^{-1}(p) \quad \text{(oblate)}$$

(10b)

These formulae agree with the independent derivations of Kuhn & Kuhn

(1945) and Kirkwood (1967).

Simha apparently did not assume that the particles were on average

rotating with the local angular velocity of the fluid but with zero

angular velocity. This objection was raised by Saito (1951) who however

obtained exactly the same result (equation 9) despite assuming particles

on average rotating with the same local angular velocity of the fluid.

He suggested that Simha "probably made some error in his calculation"

without actually finding it. We will show in the next Chapter that Simha

had apparently arrived at the correct result by making the wrong assumption

and then missing out a whole series of terms in his calculation.

1.4. The Translational Frictional Property of Macromolecular Solutes

The ease with which a macromolecule moves through its solution under

the influence of an applied external force field will depend on its shape

and size. The coefficient generally used to describe this ease is the

frictional coefficient, f, defined as the ratio of the frictional force

to the terminal velocity of the particle. Stokes (1851) using spherical

harmonics again and assumptions similar to Einstein's (section 1.3)

derived the well-known relation between the frictional coefficient f and

the radius R of a spherical particle:

$$f = 6\pi\eta_0 R \tag{11}$$

where η_0 is the viscosity of the solvent. Perrin (1936) and independently Herzog, Illig and Kudar (1934) extended Stokes equation to cover the case of general ellipsoidal particles:

$$\frac{f}{f_0} = \frac{2}{(abc)^{1/3} \int_0^\infty \frac{d\lambda}{[(a^2+\lambda)(b^2+\lambda)(c^2+\lambda)]^{\frac{1}{2}}}} \tag{12}$$

where f_0 is the corresponding coefficient for a sphere of the same volume:

$$f_0 = 6\pi\eta_0(abc)^{1/3} = 6\pi\eta_0 \left(\frac{3V_e}{4\pi}\right)^{1/3} \tag{13}$$

V_e is the molecular swollen volume, defined in section 1.1.2. The integral in equation (12) is elliptic and could only be solved for the special case of ellipsoids of revolution. For prolate ellipsoids ($p = (b/a) < 1$):

$$\frac{f}{f_0} = \frac{(1 - p^2)}{p^{2/3}\tan^{-1}(p^2-1)^{\frac{1}{2}}} \tag{14a}$$

and for oblate ellipsoids ($p = (b/a) > 1$)

$$\frac{f}{f_0} = \frac{(p^2 - 1)}{p^{2/3}\tan^{-1}(p^2-1)^{\frac{1}{2}}} \tag{14b}$$

and can easily be plotted as a function of axial ratio (Figure 5). The translational frictional ratio f/f_0 can be measured experimentally either from a translational diffusion experiment, where the driving force is a concentration gradient, or from ultracentrifugation, where the driving force is a centrifugal field.

1.4.1. <u>Translational Diffusion</u>

The translational diffusion coefficient, D, is related to the frictional coefficient, f, at a particular particle concentration, c, by the relation:

$$D_c = \frac{kT}{f} \left\{ 1 + c\, \frac{\partial \ln \gamma}{\partial c} \right\}$$ (15)

(van Holde, 1971), where γ is the 'activity coefficient', a measure of the concentration gradient. Extrapolating D_c to infinite dilution gives the Einstein relation (Einstein 1905, Tanford, 1961):

$$D = \frac{kT}{f}$$ (16)

By assuming the concentration gradient to be in one direction only, and applying Fick's laws (Tanford, 1961) for a two-component system, a simple relation for finding D experimentally can be derived, in terms of the area under, A, and the maximum height of, H, a concentration gradient (dc/dx) versus distance (x) curve:

$$\left(\frac{A}{H}\right)^2 = 4\pi D_c t$$

Thus a plot of $(A/H)^2$ versus time, t, in a 'free diffusion of a sharp boundary experiment' will give D_c from the gradient (Tanford, 1961, van Holde, 1971). D_c can be extrapolated to infinite dilution after repeating the procedure for several solute concentrations. Unfortunately, few laboratories have the apparatus required for an accurate determination of D using this method. A fast and accurate method for determining diffusion coefficients has been developed using quasi-elastic laser light scattering (Chu, 1974, Cummins & Pike, 1973, Berne & Pecora, 1974); the fluctuations of solute particles from the equilibrium state are a function of the diffusion

coefficients and with adequate instrumentation for signal analysis can be time-resolved.

From equation (16), the frictional ratio can be found from the translational diffusion coefficient using the relation

$$\frac{f}{f_o} = \frac{D_o}{D}$$

(17)

where D_o is the translational diffusion coefficient for a sphere of the same volume and molecular weight:

$$D_o = \frac{kT}{f_o} = \frac{kT}{6\pi\eta_o} \left(\frac{4\pi}{3V_e}\right)^{1/3}$$

(18)

1.4.2. Sedimentation Velocity

In a sedimentation velocity experiment, using an analytical ultracentrifuge (van Holde, 1971), the macromolecules quickly attain the terminal velocity, whence

$$\frac{M_r}{N_A} (1 - \bar{v} \rho_o)\omega^2 r = f \frac{dr}{dt}$$

where ρ_o is the solution density, r the distance from the centre of rotation of the solution/solvent boundary, ω the speed of rotation and $M_r(1 - \bar{v}\rho_o)/N_A$ the 'buoyant mass' defined in section 1.1.1. Rearranging:

$$\frac{M_r(1 - \bar{v} \rho_o)}{N_A f} = \frac{dr/dt}{\omega^2 r} = s_c$$

(19)

where s_c is the sedimentation coefficient at a particular solute concentration. In a sedimentation velocity experiment the movement of the boundary between solution and solvent is monitored as a function of time using the property of change of refractive index with change in

concentration, hence optical techniques such as scanning Schlieren optics or ultra-violet absorption can be used (Lloyd, 1974). If we rearrange and integrate equation (19) we find that

$$s_c = \frac{1}{\omega^2} \frac{\Delta \ln r}{\Delta t}$$

thus by plotting $\log_e r$ versus t and knowing the angular velocity ω, s_c can be found from the gradient. The sedimentation coefficient s_c is a function of solute concentration, thus is normally extrapolated to infinite dilution to give the sedimentation coefficient, s, which is characteristic of any macromolecular solute. From equation (19) it can be seen that the frictional ratio f/f_o will be given by

$$\frac{f}{f_o} = \frac{s_o}{s}$$

where s_o is the sedimentation coefficient for a compact ·sphere of the same molecular weight and volume. From equations (19) and (13):

$$s_o = \frac{M_r(1 - \bar{v} \, \rho_o)}{N_A \, f_o} = \frac{M_r(1 - \bar{v}\rho_o)}{N_A \, 6\pi\eta_o} \cdot \left(\frac{4\pi}{3V_e}\right)^{1/3} \tag{20a}$$

and thus the frictional ratio can be found, provided s, M_r, $\bar{v}$, ρ_o, η_o and the swollen molecular volume, V_e are known:

$$\frac{f}{f_o} = \frac{M_r(1 - \bar{v} \, \rho_o)}{N_A \, 6\pi\eta_o \, s} \left(\frac{4\pi}{3V_e}\right)^{1/3} \tag{20b}$$

1.5. The Rotational Frictional Property of Macromolecular Solutes

The ability of a macromolecule to rotate under the influence of the local Brownian motion of the neighbouring solvent molecules will depend on its size and shape. By analogy with the translational frictional

coefficient, we can define, for rotation about a specific particle axis, a rotational frictional coefficient, ζ_i, as the torque which must be applied to cause the particle to rotate with unit angular velocity. For a general ellipsoidal particle there will be three rotational frictional coefficients corresponding to rotation about each of the three axes; for an ellipsoid of revolution there will be two, and for a spherical particle, one. Each rotational frictional coefficeint can be related to a rotational diffusion constant by analogy with the Einstein relation (1905) (equation 16):

$$\theta_i = \frac{kT}{\zeta_i} \qquad (21)$$

where θ_i is defined as the ratio of the mean squared angular displacement of the axis to the time elapsed (Tanford, 1961). In a typical rotational frictional experiment an initial orientation of the macromolecule is produced by some external field. If, for example, the macromolecules in a solution are oriented with their "a" axis parallel to an orienting field and the field is suddenly removed, the macromolecules will then relax due to the Brownian motion and tend to assume a random configuration by rotating about the b and c axes. We therefore conveniently define a rotational relaxation time in terms of the rotational diffusion constants (θ_b, θ_c about the b,c axes respectively) by

$$\varrho_a = \frac{1}{\theta_c + \theta_b} \qquad (22a)$$

There will be similar relations describing relaxation of the b and c axes:

$$\varrho_b = \frac{1}{\theta_c + \theta_a} \quad ; \quad \varrho_c = \frac{1}{\theta_a + \theta_b} \qquad (22b,c)$$

By analogy with the translational frictional case, Stokes (1880) using spherical harmonic solutions of the equations of motion with the boundary condition that the fluid in contact with the particle rotates with the same angular velocity (i.e. the 'no-slip' condition) derived an equation linking the rotational frictional coefficient with its radius, R:

$$\zeta = 8\pi\eta_o R^3$$

(23)

Edwardes (1893) extended this equation to the case of general ellipsoidal particles. After a correction for a numerical error (Perrin, 1934), these are:

$$\zeta_a = \frac{16\pi\eta_o}{3} \frac{b^2 + c^2}{b^2\beta_o + c^2\gamma_o}$$

$$\zeta_b = \frac{16\pi\eta_o}{3} \frac{c^2 + a^2}{c^2\gamma_o + a^2\alpha_o}$$

$$\zeta_c = \frac{16\pi\eta_o}{3} \frac{a^2 + b^2}{c^2\gamma_o + a^2\alpha_o}$$

(24)

where again the α_o etc. are elliptic integrals defined by Jeffrey (1922) - see Appendix I. The expressions on the right hand side of equations (24) are functions not only of shape but of volume as well; the corresponding rotational frictional ratios however, are not.

$$\frac{\zeta_a}{\zeta_o} = \frac{\theta_o}{\theta_a} = \frac{2}{3abc} \frac{b^2 + c^2}{b^2\beta_o + c^2\gamma_o}$$

$$\frac{\zeta_b}{\zeta_o} = \frac{\theta_o}{\theta_b} = \frac{2}{3abc} \frac{c^2 + a^2}{c^2\gamma_o + a^2\alpha_o}$$

$$\frac{\zeta_c}{\zeta_o} = \frac{\theta_o}{\theta_c} = \frac{2}{3abc} \frac{a^2 + b^2}{a^2\alpha_o + b^2\beta_o}$$

(25)

where ζ_o $(= 8\pi\eta_o abc)$ & θ_o $(= kT/\zeta_o)$ are the corresponding coefficients for spheres of the same volume, and can be found experimentally only if the swollen molecular volume, V_e is known:

$$\zeta_o = 6\eta_o V_e \ ) \ \theta_o = kT/6\eta_o V_e$$

(26a,b)

The corresponding rotational relaxation time ratios are:

$$\frac{\rho_a}{\rho_o} = \frac{2}{\left[\dfrac{\theta_b}{\theta_o} + \dfrac{\theta_c}{\theta_o}\right]}$$

$$\frac{\rho_b}{\rho_o} = \frac{2}{\left[\dfrac{\theta_c}{\theta_o} + \dfrac{\theta_a}{\theta_o}\right]}$$

$$\frac{\rho_c}{\rho_o} = \frac{2}{\left[\dfrac{\theta_a}{\theta_o} + \dfrac{\theta_b}{\theta_o}\right]}$$

(27a)

where $\rho_o = 1/2 \theta_o$.

(27b)

Unfortunately, as for the translational frictional coefficients, the elliptic integrals could only be solved analytically for the special case of ellipsoids of revolution of semi-axes a, b=c (Gans, 1928, Perrin, 1934). Although numerically equivalent, Gans uses the less manageable 'eccentricity' ($\epsilon = 1 - b/a$) rather than the axial ratio ($p = b/a$), hence the equations of Perrin are generally used:

$$\frac{\zeta_a}{\zeta_o} = \frac{\theta_o}{\theta_a} = \frac{2}{3} \frac{(1 - p^2)}{(1 - p^2 S)}$$

$$\frac{\zeta_b}{\zeta_o} = \frac{\theta_o}{\theta_b} = \frac{2}{3} \frac{(1 - p^4)}{p^2 [S(2-p^2) - 1]}$$

$$(28a)$$

where

$$S = (1 - p^2)^{-\frac{1}{2}} \ln\{[1 + (1-p^2)^{\frac{1}{2}}]/p\}$$

for a prolate ellipsoid ($p<1$), and

$$S = (p^2 - 1)^{-\frac{1}{2}} \tan^{-1} [(p^2 - 1)^{\frac{1}{2}}]$$

for an oblate ellipsoid ($p>1$).

The rotational diffusion ratio θ_i/θ_o ($i=a,b$) can be related to experimental parameters using equations (26b):

$$\frac{\theta_i}{\theta_o} = \frac{6\eta_o V_e}{kT} | \theta_i$$

$$(28b)$$

The corresponding rotational relaxation time ratios were also given by Perrin (1934) but contained an error of sign involving S. The correct result was given by Koenig (1975):

$$\frac{\rho_a}{\rho_o} = \frac{\theta_o}{\theta_b} = \frac{2(1 - p^4)}{3p^2[S(2-p^2) - 1]}$$

$$\frac{\rho_b}{\rho_o} = \frac{2}{\left(\frac{\theta_a}{\theta_o} + \frac{\theta_b}{\theta_o}\right)} = \frac{4(1 - p^4)}{3[p^2S(1-2p^2) + 1]} \tag{29a}$$

These may be related to experimental parameters by combining equations (26b, 27b):

$$\frac{\rho_i}{\rho_o} = \frac{kT}{3\eta_o V_e} \dot{\rho}_i \tag{29b}$$

All these functions ($\zeta_i/\zeta_o = \theta_o/\theta_o$, ρ_i/ρ_o) are plotted as functions of axial ratio in Figure 6. It should also be pointed out that, like the translational functions the rotational diffusion coefficients and relaxation times are functions of concentration (Riddiford & Jennings, 1967) and should be extrapolated to infinite dilution. The same is also true for the harmonic mean relaxation time, the birefringence decay constants and the fluorescence depolarisation relaxation times mentioned below. The various experimental methods for determining all these shape parameters will now be discussed.

1.5.1. Dielectric Dispersion

The capacity of a condenser filled with a solution of the macromolecule is measured as a function of the applied sinusoidal voltage across it

(Edsall, 1953). The 'dielectric increment' or increase in the dielectric
constant, ε, due to the presence of the solute is given by

$$\Delta\varepsilon = \varepsilon - \varepsilon_o = \frac{C}{C_v} - \frac{C_o}{C_v} \tag{30}$$

where ε_o is the dielectric constant of the solvent and C, C_o and C_v
are the capacities of respectively, the solution, solvent and vacuo.
At sufficiently small frequencies, the dipolar macromolecules can keep
pace with the alternating field, and the dielectric constant will remain
at its 'static' value. At sufficiently high fields, the rotation of the
macromolecule about a particular axis will no longer follow the field and
its contribution, $\Delta\varepsilon_\infty$ to the dielectric constant is that of a non-polar
substancd (Oncley, 1940); thus over a certain critical range
characteristic of the size and shape of the macromolecule, the dielectric
constant decreases as the frequency increases. The frequency corresponding
to the mid-point of the dispersion curve is known as the 'critical
frequency'. For a general particle with three rotational relaxation times
ρ_a, ρ_b, ρ_c, there will be three critical frequencies:

$$\nu_a = 2\pi\rho_a \quad ; \quad \nu_b = 2\pi\rho_b \quad ; \quad \nu_c = 2\pi\rho_c \tag{31}$$

For an ellipsoid of revolution there will be two (since $\rho_b = \rho_c$) or one,
either if the dipolar axis is parallel to the rotation axis of symmetry
or for a spherical particle. Typical dielectric dispersion curves for
ellipsoids of revolution of various axial ratios are shown in Figure 7
(from Oncley, 1940)

Even in the most favourable case, $\theta = 45^o$, resolution is poor for
axial ratios less than 9 (Squire, 1978). Application of this method is

also limited by the fact that, due to electrode polarization, only

solutions of low ionic strength can be used, thus restricting the use

to proteins of high solubility.

1.5.2. <u>Electric Birefringence</u>

Polarized light incident on a solution of macromolecules oriented by

an elctric field will be split into perpendicular components because the

refractive index will be different for directions parallel and

perpéndicular to the electric dipole moment (Benoit, 1951). The solution

is then said to be birefringent and the amount of birefringence will

depend on the nature and concentration of the macromolecules.

The decay due to Brownian motion of the birefringence when the field

is suddenly switched off is most interesting since this will be

independent of the electric properties of the macromolecules (apart from

the initial amplitude of the decay) but dependent on their size and

asymmetry, assuming the solution to be homogeneous. The solution must

be rendered homogeneous by, say, ultracentrifugation for removing larger

impurities, followed by gel filtration for fine purification. The number

of terms in the exponential decay will be dependent on the particle

asymmetry, assuming that the particles are small enough so that the

Rayleigh - Gans - Debye scattering theory applies (i.e. particle dimensions

less than $\lambda/20$). Ridgeway (1966, 1968) has shown that a general particle

will have two relaxation times, τ_+, τ_- or two decay constants, θ_+ $(=1/6\tau_+)$,

θ_- $(=1/6\tau_-)$:

$$\Delta n = \frac{N}{2n_\ell} (A_+ e^{-6\theta_+ t} + A_- e^{-6\theta_- t})$$

$$(32)$$

where Δn is the birefringence, N is the number density of particles in

suspension, n_ℓ the refractive index of the solvent and A_+ complicated

expressions depending on the initial particle orientations and their

dielectric and diffusion properties. Unfortunately, although Ridgeway

provided relationships linking θ_+ with the size and shape of general

tri-axial ellipsoids (see Chapters 3 and 4), only one relaxation time

has been resolved from the experimental exponential decays for homogeneous

solutions. Thus the method has been restricted to ellipsoids of revolution

($A_- = 0$) for which Benoit (1951) had shown previously that, for an initial

birefringence n_0,

$$\Delta n = \frac{N}{2n_\ell} A e^{-6\theta_b t} = n_0 e^{-6\theta_b t}$$

(33)

assuming the electric dipole axis coincides with the rotational axis of

symmetry. For spherical particles there would be no birefringence.

1.5.3. Flow Birefringence

The aligning field can also be produced, if the macromolecules are

highly asymmetric, by large flow velocity gradients in the annular space

between two concentric cylinders, one rotary and one stationary (van Holde,

1971, Squire, 1978). The orientation of the macromolecules will again be

opposed by rotational Brownian motion, and for a constant shear rate, there

will be an equilibrium distribution of orientation states. Results for

early studies are discussed by Cerf and Scheraga (1952) and by Tanford

(1961). This method has the advantage that the steady state birefringence

can now be used to derive shape parameters, since this will be independent

of the electric properties of the macromolecule. However, the method has the

serious disadvantage in that relaxation experiments are virtually impossible,

and also the use is restricted to highly asymmetric molecules (Squire, 1978).

1.5.4. Fluorescence Depolarization

This method applies to those macromolecules that possess a fluorescent group or a chromophore (Cantor & Tao, 1971). If an electron in a chromophore is excited to a higher energy state by the absorption of radiation, then instead of the energy being dissipated non-radiatively in the form of heat as it returns to the ground state, it loses only part of its energy as heat as it returns to the lowest vibrational level of the excited state, but then re-radiates the rest. This will necessarily be of lower energy (hence longer wavelength) than the incident radiation. This phenomenon is called fluorescence.

If the macromolecule is irradiated with polarized light, and if, in the 10^{-8} to 10^{-7} seconds it takes for the energy to be re-radiated the macromolecule has changed its orientation due to Brownian motion, there will be a net depolarization of the incident light. If the solution is continuously irradiated then a steady state depolarization will be reached depending on the ratio of the fluorescence decay time, τ^* to the harmonic mean of the three rotational relaxation times (equations 27), τ_h (Perrin, 1934):

$$\left(\frac{1}{P} - \frac{1}{3}\right) = \left(\frac{1}{P_o} - \frac{1}{3}\right) \left(1 + \frac{3\tau^*}{\tau_h}\right)$$

(34)

P is the polarization (i.e. the ratio of the difference in intensities of light polarized parallel and perpindicular to the incident beam to their sum), P_o is the intrinsic polarization of the fluorescence (the polarization that would be observed if no rotation had occurred) and τ_h is defined by

$$\frac{1}{\tau_h} = \frac{1}{3} \left(\frac{1}{\varrho_a} + \frac{1}{\varrho_b} + \frac{1}{\varrho_c} \right)$$

(35)

for general ellipsoids, or for ellipsoids of revolution ($\varrho_b = \varrho_c$):

$$\frac{1}{\tau_h} = \frac{1}{3} \left(\frac{1}{\varrho_a} + \frac{2}{\varrho_b} \right)$$

The harmonic mean relaxation time ratio τ_h / τ_o can thus be plotted as a function of axial ratio (Figure 8), where τ_o is the corresponding coefficient for a sphere of the same molecular weight and volume:

$$\tau_o = \frac{3\,\eta_o\,V_e}{kT}$$

(36a)

Thus τ_h / τ_o can be related to experimental parameters by:

$$\frac{\tau_h}{\tau_o} = \frac{kT\tau_h}{3\eta_o V_e}$$

(36b)

Equation (34) is not particularly useful as it stands, since neither P_o nor τ_h are known. If τ_h is approximated by $\tau_h \sim \tau_o$ (i.e. $= 3\eta_o V_e / kT$) then:

$$\left(\frac{1}{P} - \frac{1}{3} \right) = \left(\frac{1}{P_o} - \frac{1}{3} \right) \left(1 + \frac{kT\tau^*}{\eta_o V_e} \right)$$

(37)

If measurements are then made in solutions of varying viscosity (for example by adding glycerol) and/or temperature, $(1/P - 1/3)$ can be plotted against T/η_o, $1/P_o$ can be found from the intercept and hence τ_h

from the gradient, assuming τ^* can be found independently. A major disadvantage of this method is that by adding glycerol or changing the temperature the swelling due to solvation may be altered: also an independent estimate for τ^* is required.

A more accurate method in principle is nanosecond fluorescence depolarization decay (Cantor & Tao, 1971). Here the solution is irradiated with polarized light pulses of very short duration ($\sim$1ns). The anisotropy, A is measured by determining the intensity of emission polarized parallel to ($I_\parallel$) and perpindicular to ($I_\perp$) the incident pulse:

$$A = \frac{I_\parallel - I_\perp}{I_\parallel + 2I_\perp} \qquad .$$

$$(38)$$

For a rigid spherical macromolecule, the anisotropy decay is described by a single exponential term (Jablonski, 1961)

$$A(t) = A_o e^{-t/\tau_o}$$

$$(39)$$

with $\tau_o = \eta_o V_e / kT$. For a rigid ellipsoid of revolution, Memming (1961) and Wahl (1966) have shown that the anisotropy is a sum of three exponential terms:

$$A(t) = \alpha_1 e^{-t/\tau_1} + \alpha_2 e^{-t/\tau_2} + \alpha_3 e^{-t/\tau_3}$$

$$(40)$$

where

$$\tau_1 = \frac{1}{6\theta_b} \quad ; \quad \tau_2 = \frac{1}{5\theta_b + \theta_a} \quad ; \quad \tau_3 = \frac{1}{2\theta_b + 4\theta_a}$$

$$(41)$$

The fluorescence decay time ratios are plotted in Figure 9 where τ_o is the corresponding coefficient for a sphere of the same molecular weight and volume:

$$\tau_o = \frac{\eta_o V_e}{kT} = \frac{4\pi\eta_o ab^2}{3kT}$$

Thus the fluorescence anisotropy decay time ratios can be related to experimental parameters by

$$\frac{\tau_j}{\tau_o} = \frac{kT\tau_j}{\eta_o V_e} \qquad (j=1,2,3)$$

$$(42)$$

The values of the component amplitudes α_1, α_2, α_3 and hence the dominant relaxation time will depend on the angle between the transition moment of the chromophore to the rotation axis of symmetry of the ellipsoid of revolution. Unfortunately, resolution of a multi-term exponential decay into its components is notoriously difficult (Jost, 1978), even for relaxation times differing in orders of magnitude; this is coupled to the problem that the observed decay will be a convolution of the finite cut-off time of the incident pulse, the fluorescence decay and the anisotropy decay. There are also more serious problems:

(i)   since the fluorescence itself decays within about 10ns, only molecules with very short relaxation times can be investigated,

(ii)   most macromolecules do not contain a chromophoric group such as tryptophan; thus one must be introduced. This may significantly alter the true conformation of the molecule,

(iii) even if the macromolecule contains tryptophan, the decay is not

perfectly exponential, due to interference between the side chain and

the indole ring,

(iv) rotation of the chromophore, or of a fragment of the macromolecule

to which the chromophore is attached, with respect to the rest of the

macromolecule may occur: Munro et al (1979) have given evidence for

internal rotation of the tryptophan residue in <u>Staphylococcus aureus</u>

nuclease B (M_r = 14,100) and <u>Pseudomonas aeruginosa</u> azurin (M_r = 14,000).

1.6. <u>Scattering</u>

Absorption and hence fluorescence phenomena can only occur when the

frequency of the exciting radiation is the same as or near to that of an

allowed transition frequency of the molecule. However, at other wave-

lengths electro-optic interaction can still occur; the electric vector

of the incident radiation polarizes the molecule by attracting the

nuclear mass and repelling the electron clouds. The frequency of

oscillation of the incident radiation is the same as that of the induced

oscillating dipole; however, the waves emitted are by Huyghens principle

spherical and hence the radiation is scattered in all directions.

The scattering by a solution of macromolecules is most rigorously

analysed by considering the local concentration fluctuations of the

solution; however, if we consider the particle as small compared with the

wavelength of the incident light and the solution to be so dilute so that

each particle can be considered independently, relations can be derived

between particle shape in terms of the 'radius of gyration' (Tanford,

1961) and the scattering (van de Hulst, 1957). For small particles ($<\lambda/20$)

interference effects between radiation scattered by different parts of the

macromolecule can be neglected, and the following relation between

molecular weight, M_r and the scattering can be derived:

$$\frac{Hc}{\tau} = \frac{1}{M_r} + 2B.c$$

where c is the particle concentration, H is the scattering constant

($\alpha \lambda^{-4}$, and the square of the refractive index increment, dn/dc),

B the second virial coefficient and τ is a measure of the relative

scattering perpindicular to the incident beam (i.e. the fraction of light

scattered (van Holde, 1971)). Hence if Hc/τ is plotted versus

concentration, the molecular weight can in principle be determined from

the intercept. For large particles (d~λ/20) destructive interference

occurs between light scattered from different parts of the macromolecule.

Light scattered in the forward direction cannot however be subject to

destructive interference. Unfortunately this cannot be viewed directly,

but if the scattering is studied over a range of angles it can be

extrapolated to the forward direction. This involves extrapolating to

zero-angle and to zero-concentration using the so-called Zimm plot

(Zimm, 1948, Stacey, 1956, Tanford, 1961). The slope of the c=0 line

gives the radius of gyration of the particle, R_G, i.e. the mean extension

of mass from the centre of gravity. For a sphere of radius R, $R_G = \sqrt{3/5}\,R$,

and for a large rod of length L, $R_G = L/\sqrt{12}$, thus light scattering can be

used to obtain information about conformation in solution, where particular

models for which R can be specified are applicable. Holtzer and Lowey

(1956) showed by this method that L = 1500 $\overset{o}{A}$ if myosin could be reasonably

modelled by a long rod. Martin (1964) has shown that the radius of gyration

can be related to the axial ratio of the equivalent ellipsoid of

revolution provided that the swollen volume is known:

$$R_G^2 = \left(\frac{3V_e}{4\pi}\right)^{2/3} \left(\frac{5p^{4/3} + 4p^{-2/3}}{15}\right)$$

(43a)

for a prolate ellipsoid and

$$R_G^2 = \left(\frac{3V_e}{4\pi}\right)^{2/3} \left(\frac{p^{4/3} + 2p^{-2/3}}{5}\right)$$

(43b)

for an oblate ellipsoid.

An explicit relation relating R_G to axial ratio alone can be found by 'reducing' it

$$(R_G)_{red} = \left(\frac{4\pi}{3V_e}\right)^{1/3} R_G = \left(\frac{5p^{4/3} + 4p^{-2/3}}{15}\right)^{\frac{1}{2}}$$

(44a)

for a prolate ellipsoid and

$$(R_G)_{red} = \left(\frac{4\pi}{3V_e}\right)^{1/3} R_G = \left(\frac{p^{4/3} + 2p^{-2/3}}{5}\right)^{\frac{1}{2}}$$

(44b)

for an oblate ellipsoid.

This is plotted in Figure 10. Experimental determination of $(R_G)_{red}$ requires of course a knowledge of V_e.

The same analysis can be used for laser light scattering as this gives good time resolution for rapidly changing solutions (for example aggregation of macromolecules, randomly coiled macromolecules). However a major difficulty with all light scattering experiments is that all

solutions, glassware etc., must be dust free; removal, without damage to the biological solute, poses great difficulties. Due to diffraction effects it is also difficult to measure scattering angles less than about five degrees, thus a clear extrapolation to zero angle may not be possible. Another major difficulty is that, since the resolving power depends on $(R_G/\lambda)^2$, the method fails for macromolecules below about 100 $\overset{o}{A}$ (although M_r may still be found). Reducing the wavelength of the incident radiation does not help (until down to the x-ray region) since below 200nm most biological materials absorb very strongly. A method of low angle x-ray scattering (LAXR) has also been developed (Beeman et al, 1957). However, due to very strong diffraction and interference effects, the scattering is almost entirely confined to a very narrow wavelength range. On the other hand, it is possible to collimate the x-ray beam much better than a light beam, thus measurements can be made to a low enough angle to a more reasonable extrapolation to zero angle.

Deductions about the size and shape of macromolecules from scattering information is generally restricted however, since any simple interpretation of the radius of gyration must assume that the macromolecule is homogeneous (uniform electron density). If, therefore, the particle contains fluid filled cavities or indentations or a monolayer of bound solvent, the dimensions of any assumed model calculated from the R_G will be incorrect. This problem does not apply to the determination of the hydrodynamic shape parameters considered previously since these phenomena do not depend on interactions with or properties of the interior of the macromolecules.

1.7. The Problem of Swelling due to Solvation

In order to determine from experimental data the ellipsoid

of revolution shape functions mentioned so far, a knowledge of the

swelling due to solvation (i.e. V_e) is required:

$$\nu = \frac{[\eta]}{\bar{v}_s} \equiv \frac{[\eta]M_r}{N_A V_e} \tag{8}$$

$$\frac{f}{f_o} \equiv \frac{M_r(1 - \bar{v}\rho_o)}{N_A 6\pi\eta_o s} \left(\frac{4\pi}{3V_e}\right)^{1/3} \tag{20b}$$

$$\frac{\theta_i}{\theta_o} = \frac{\zeta_o}{\zeta_i} = \frac{6\eta_o V_e}{kT} \theta_i \tag{28b}$$

$$\frac{\varrho_i}{\varrho_o} = \frac{kT}{3\eta_o V_e} \varrho_i \qquad (i = a,b). \tag{29b}$$

$$\frac{\tau_h}{\tau_o} = \frac{kT}{3\eta_o V_e} \tau_h \tag{36b}$$

$$\frac{\tau_j}{\tau_o} = \frac{kT}{\eta_o V_e} \tau_j \qquad (j=1,2,3) \tag{42b}$$

$$(R_G)_{red} = \left(\frac{4\pi}{3V_e}\right)^{1/3} R_G \tag{44}$$

The first significant attempt at dealing with this problem was due

to Oncley (1941) using a graphical analysis: If V_e is fixed then a single

value of the shape parameter being considered will correspond to a single

value of the axial ratio. If, however, V_e is assumed to have a range of

possible values, then a single value of the shape parameter will have a

'line solution' of possible values of the axial ratio. This is shown in Figures 11a and 11b for the viscosity increment and translational frictional coefficient. However, if line solutions for two or more of the different shape parameters are compared, then in principle a unique value for the axial ratio and effective volume can be found from the intersection. On the other hand, in practice these curves could only be made to intersect by imposing large experimental errors on the data, and in one case - pepsin - the curves do not cross at all (Figure 12). Here Oncley uses as his abscissa the 'hydration factor' w, related to the effective volume, V_e by:

$$w = \rho_0(\bar{v}_s - \bar{v}) = \rho_0 \left[\frac{N_A V_e}{M_r} - \bar{v} \right]$$

A different approach would be to eliminate V_e simultaneously by combining any two of the shape parameters together. The effective volume can then also be found by back substitution into the equations. This naturally assumes, as does the Oncley approach, that the axial ratio and the swelling are the same for both types of experiment. Scheraga and Mandelkern (1953) combined equations (8) and (20b) to produce a swelling-independent function β (Figure 13):

$$\beta = \frac{N_A^{1/3}}{(16200\pi^2)^{1/3}} \frac{\nu^{1/3}}{f/f_0}$$

(45a)

or in terms of experimental parameters, from

$$\beta \equiv \frac{N_A \, s[\eta]^{1/3} \eta_0}{M_r^{2/3} (1 - \bar{v}\rho_0) 100^{1/3}}$$

(45b)

where [η] is in ml/gm. Scheraga and Mandelkern also combined equation (8) with equations (28b) to produce swelling independent δ_a and δ_b functions (Figure 14), although in their original paper, only δ_b is given:

$$\delta_i = \frac{\zeta_o}{\zeta_i}\, \nu = \frac{\theta_i}{\theta_o}\, \nu \equiv \frac{6\eta_o \theta_i [\eta] M_r}{N_A\, kT}$$

(46)

(i=a,b)

Scheraga (1961) later combined (20b) with (28b) to produce swelling independent μ_a, μ_b functions (Figure 15) although again only μ_b was given:

$$\mu_i = \left(\frac{f_o}{f}\right)\left(\frac{\zeta_i}{\zeta_o}\right)^{1/3} \equiv \frac{3\pi^{2/3} s}{\theta_i^{1/3}} \cdot \frac{N_A (kT)^{1/3} \eta_o^{2/3}}{M_r(1 - \bar{v}\rho_o)} = \frac{3\pi^{2/3} D}{\theta_i^{1/3}} \left(\frac{\eta_o}{kT}\right)^{2/3}$$

(47)

(i=a,b)

Squire et al (1968) combined equation (20b) with (29b) to produce swelling independent γ_a and γ_b functions:

$$\gamma_i = \left(\frac{f}{f_o}\right)^3 \frac{\rho_o}{\rho_i} \equiv \frac{1}{54\pi^2 N_A^3 kT} \cdot \frac{M_r^3(1 - \bar{v}\rho_o)}{s^3 \eta_o^2 \, \rho_i}$$

(48)

(i=a,b)

Squire later (1970) combined (20b) with (36b) to give a swelling independent Ψ function (Figure 16)

$$\Psi \left(\frac{\tau_o}{\tau_h}\right)^{1/3}\left(\frac{f}{f_o}\right) \equiv \left(\frac{4\pi\eta_o}{kT}\right)^{1/3} \cdot \frac{M_r(1 - \bar{v}\rho_o)}{6\pi\eta_o N_A s}\left(\frac{1}{\tau_h}\right)^{1/3}$$

(49)

Plots of the Squire γ_a and γ_b parameters as functions of axial ratio are

given in Figure 16. A similar swelling independent function can be

obtained by combining the viscosity increment, equation (8) instead of

equation (20b) with (36b) (see Appendix II and Harding, 1980a):

$$\Lambda = \left(\frac{\tau_o}{\tau_h}\right) \nu \equiv \frac{3\eta_o [\eta] M_r}{N_A \, kT \, \tau_h}$$

(50)

(Figure 17). Also, by combining equation (8) instead of (20b) with

equation (29b), swelling independent ε_a, ε_b functions are produced

(Figure 18):

$$\varepsilon_i = \nu \, \frac{\varrho_o}{\varrho_i} \equiv \frac{3\eta_o [\eta] M_r}{N_A \, kT \, \varrho_i}$$

(51)

(i=a, b)

By combining (8) with the fluorescence anisotropy relaxation times (42b)

three new functions, κ_1, κ_2, κ_3 are produced (Figure 19):

$$\kappa_j = \nu \, \frac{\tau_o}{\tau_j} = \frac{\eta_o [\eta] M_r}{N_A \, kT \, \tau_j} \qquad (j=1,2,3)$$

(52)

Alternatively, combining equation (20b) with equation (42b)(Figure 20):

$$\xi_j = \left(\frac{f}{f_o}\right)^3 \frac{\tau_o}{\tau_j} \equiv \frac{m_r^{\,3} \, (1 - \bar{v}\rho_o)^3}{162 N_A^{\,3} \, kT \eta^2 \eta_o^{\,2} s^3 \tau_j} \qquad (j = 1, 2, 3)$$

(53)

As far as the author is aware, the Λ, ε_i, κ_j and ξ_j functions are new

and have not been published before. These functions are tabulated for

axial ratios between 1 and 10 (Table 1).

Martin (1964) eliminated the requirement of knowledge of the swollen

volume for scattering experiments by combining (44) simultaneously with

either the translational frictional function (Figure 21):

$$\gamma \equiv \frac{R_G \, \eta_o \, D}{kT} \equiv \frac{R_G \, \eta_o \, N_A \, s}{M_r (1 - \bar{v}\rho_o)} = \frac{1}{6\pi} \, \frac{f_o}{f} \left[\frac{5p^{4/3} + 4p^{-2/3}}{15} \right]^{\frac{1}{2}}$$

(prolate ellipsoid)

$$= \frac{1}{6\pi} \, \frac{f_o}{f} \left[\frac{p^{4/3} + 2p^{-2/3}}{5} \right]^{\frac{1}{2}}$$

(oblate ellipsoid)

or the viscosity increment (Figure 22):

$$\alpha \equiv \frac{R_G}{[\eta]^{1/3} M_r^{1/3}} = \frac{75}{\pi N_A} \left[\frac{5p^{4/3} + 4p^{-2/3}}{15} \right]^{\frac{1}{2}} \cdot \frac{1}{\nu^{1/3}}$$

(prolate ellipsoid)

$$= \frac{75}{\pi N_A} \left[\frac{p^{4/3} + 2p^{-2/3}}{5} \right]^{\frac{1}{2}} \cdot \frac{1}{\nu^{1/3}}$$

(oblate ellipsoid)

where p is the axial ratio defined in section 1.4.

The molecular covolume has also been given as a function of shape and swollen volume by Nichol et al (1977) for prolate and oblate ellipsoids

$$U = N_A \, V_e \left\{ 2 + \frac{3}{2} \left[\frac{1 + \sin^{-1}\varepsilon}{\varepsilon(1 - \varepsilon^2)^{\frac{1}{2}}} \right] \right.$$

$$\left. \left[1 + \frac{1 - \varepsilon^2}{2\varepsilon} \ln \frac{1 + \varepsilon}{1 - \varepsilon} \right] \right\}$$

(54)

where the ellipticity ε is related to the axial ratio by

$$\varepsilon = \sqrt{1 - \frac{b^2}{a^2}}$$

for prolate ellipsoids (b<a), and

$$\varepsilon = \sqrt{1 - \frac{a^2}{b^2}}$$

for oblate ellipsoids (b>a). By 'reducing' U we obtain a function U_{red} in terms of shape alone:

$$U_{red} = \frac{U}{N_A V_e} = 2 + \frac{3}{2} \left[1 + \frac{1 + \sin^{-1}\varepsilon}{\varepsilon(1 - \varepsilon^2)^{\frac{1}{2}}} \right]$$

$$\left[1 + \frac{1 - \varepsilon^2}{2\varepsilon} \ln \frac{1 + \varepsilon}{1 - \varepsilon} \right] \tag{55}$$

The covolume U can be found from a sedimentation equilibrium experiment in terms of the activity coefficient, as outlined by Nichol et al (1977) although in order to determine U_{red}, a knowledge of V_e is still required. Nichol et al (1977) however eliminated V_e by solving equation (55) simultaneously with the translational frictional ratio (equation 20b) to produce the swelling independent ψ function (not to be confused with the Squire Ψ function)

$$\psi = \frac{U_{red}}{162\pi^2} \left(\frac{f_o}{f} \right)^3 \equiv \frac{U \eta^3 N_A^2 s^3}{M_r^3 (1 - \bar{v}\rho_o)^3} \tag{56}$$

As seen from Figure 23, ψ has the advantage that no prior decision has to be made as to whether the macromolecule is better modelled either by a prolate or oblate ellipsoid. Unfortunately, for typical globular macromolecules (small axial ratios), the parameter is still very

sensitive to experimental error: this is clear from Nichol et al's

results for ovalbumin, whose axial ratio they found to be 2.5:1 with

a standard error of 3. This is largely due to the large number of

terms on the right hand side of equation (56), several of them cubed.

U_{red} can of course be combined with any of the equations (8), (20b),

(28b), (29b), (36b), (42b) to eliminate V_e. For example, if (55) is

combined with the viscosity increment (8), a new swelling independent

function is produced (Figure 24) (Harding, 1980b):

$$\Pi = \frac{U_{red}}{v} \cong \frac{U}{[\eta]M_r}$$

(57)

Values of the Π function for various axial ratios are given in Table 1.

The results for hemoglobin are in excellent agreement with those found

from x-ray crystallography (see Appendix III).

1.7.1. Hydrodynamic non-ideality: the R function

The viscosity, translational frictional and rotational parameters

considered so far are normally those extrapolated to zero concentration

in order to negate the effect of the net volume excluded by the particles

and solute-solute interaction. However, the nature of the concentration

dependence of these parameters, particularly the sedimentation coefficient·

"s" and the reduced specific viscosity, η_{sp}/c, has now been shown by Rowe

(1977) to give valuable information as to the conformation and swelling

in solution and also an estimate of the "goodness of fit" of an ellipsoid

for the macromolecule in solution.

The variation of s and η_{sp}/c with concentration can be represented

by regression parameters k_s, and k_η:

$$s_c = s(1 - k_s c) \tag{58}$$

$$\frac{\eta_{sp}}{c} = [\eta] (1 + k_\eta c) . \tag{59}$$

where k_s and k_η are, respectively, the sedimentation and viscosity

concentration regression coefficients. These approximate linear

equations are valid only for dilute solutions. A universal equation has

been derived by Rowe (see Appendix IV) for all solute concentrations up

to ϕ_p, the critical packing fraction:

$$\frac{s_c}{s} \frac{f_o}{f} = \frac{[\eta]}{\eta_{sp}/c} = 1 - gc \tag{60a}$$

where

$$gc = \frac{kc - (2\phi_p - 1)(c\bar{v}_s/\phi_p)^2}{kc - 2\bar{v}_s c + 1} \tag{60b}$$

where $k = k_s$ (sedimentation) or $k = k_\eta$ (viscosity). This provides a more

accurate method for extrapolating to infinite dilution to obtain $[\eta]$

and "s", and also for finding k_s and k_η , from a given set of data, by

minimising:

$$\{w_i[s_i - f(k_s, \bar{v}_s, s, c_i, \phi_p)]\}^2$$

$(w_i = \text{weight})$ \hfill (61)

This procedure is unstable if k_s, $\bar{v}_s$ and s (or the corresponding viscosity

parameters) are all taken to be independent variables. However, if we

assume $\bar{v}_s = k_s/4$ for globular proteins, or assume $\bar{v}_s$ from the ratio $\bar{v}_s/\bar{v}$

$= k'_\eta/k'_s$, where k'_η and k'_s are the parameters found from the approximate fit (equations 58 & 59), a stable fit may be found.

Rowe (1977) has shown that the swelling, $\bar{v}_s/\bar{v}$, can be found from:

$$\frac{\bar{v}_s}{\bar{v}} = \frac{k_\eta}{k_s}$$

(62)

Therefore

$$V_e = \frac{M_r \bar{v}_s}{N_A} = \frac{M_r}{N_A} \cdot \frac{k_\eta}{k_s} \cdot \bar{v}$$

(63)

The value of $\bar{v}_s/\bar{v}$ and hence V_e thus found is independent of any assumed model for the protein. Since the determination of V_e by back substitution into the equations given at the beginning of 1.7. after the axial ratio has been determined is dependent on the model chosen (i.e. an ellipsoid of revolution), an estimate for the "goodness of fit" of an ellipsoid of revolution is now available by comparing the model dependent V_e with model independent V_e (or, equivalently, $\bar{v}_s$ or $\bar{v}_s/\bar{v}$).

This theory also provides a new shape function "R", which is independent of particle swelling:

$$R = \frac{2}{v} \left(1 + \left(\frac{f}{f_o}\right)^3 \right) \equiv \frac{k_s}{[\eta]}$$

(64)

Wales & Van Holde (1954) had previously reported that the ratio $k_s/[\eta]$ was some unknown function of shape and equal to 1.6 for spherical particles; this agrees with that predicted by equation (44) (Figure 13). R varies rather rapidly with axial ratio for ellipsoids, even for low axial ratio, and this function provides a precise method for characterizing the axial ratio of relatively symmetrical particles.

Besides its greater sensitivity than the β function (or the Ψ function),

R has several other advantages:

(1) unlike β computation of R does not require knowledge of the absolute

solute concentration (Rowe, 1977)

(2) less data is required to compute R and hence the error in the final

function is minimized. As rotational parameters are generally very

difficult to determine, as will be evident from the earlier parts of this

chapter, the R function is also to be preferred over swelling independent

functions involving these. The R function is also to be preferred over

the scattering γ and α functions mainly because of the particle

homogeneity problem mentioned in section 1.6. The β function can still

however be useful, precisely because of its lack of variation for oblate

ellipsoids, in deciding whether the macromolecule is better modelled by

either a prolate or an oblate ellipsoid. Experimental values for β and

$k_s/[\eta]$ ($\equiv$R) have been tabulated for a wide range of proteins by Creeth

& Knight (1965). Values of β below the theoretical minimum of 2.112×10^6

and above 1.6 for R may indicate that some proteins cannot be modelled by an

equivalent ellipsoid of revolution. This has been suggested for Bovine

serum albumin (BSA). A table of values of axial ratio calculated from

the R function for recent data, together with a comparison of their

'model dependent' estimates for $\bar{v}_s/\bar{v}$ with their 'model independent'

estimates to determine the 'goodness of fit' of an ellipsoid of

revolution, is given in Table 2.

1.8. Comment

Although a hydrodynamically equivalent ellipsoid of revolution

model can now be fitted with much greater precision to many rigid

macromolecules with the aid of the R function (and possibly the Π function)

the distinction still has to be made as to whether the macromolecule

is better modelled either by a prolate or an oblate model. It is clear

from a perusal of the crystallographic models of many globular proteins

such as carboxypeptidase, myoglobin and ribonuclease (Table 3) that in

many cases this is quite arbitrary and indeed in some cases is

impossible

It would be a significant step forward therefore if the restriction

of two equal axes on the ellipsoid were removed to allow use of the more

general tri-axial ellipsoid. However, either due to the lack of the

theoretical relationships linking the axial dimensions of the ellipsoid

with experimental parameters, or, even if they are available, due to the

lack of the necessary experimental precision, numerical inversion

procedures or data analysis techniques, this model has not, to date, been

available. The aim of the rest of this thesis is to show that the general

tri-axial ellipsoid can now be successfully employed to model biological

macromolecules in solution. We will start by deriving the tri-axial

viscosity increment equation.

Table 1. Values of Λ, ε_a, ε_b, κ_1, κ_2, κ_3, ξ_1, ξ_2, ξ_3 and Π for

prolate and oblate ellipsoids of revolution

axial ratio	1	2	3	4	5	6	7	8	9	10
Λ_p	2.500	2.490	2.692	3.071	3.575	4.177	4.862	5.624	6.457	7.359
Λ_o	2.500	2.356	2.187	2.070	1.989	1.931	1.887	1.854	1.827	1.805
$\varepsilon_{a,p}$	2.500	1.932	1.574	1.373	1.251	1.171	1.115	1.075	1.044	1.020
$\varepsilon_{a,o}$	2.500	2.522	2.343	2.202	2.102	2.029	1.974	1.931	1.896	1.868
$\varepsilon_{b,p}$	2.500	2.768	3.250	3.920	4.737	5.679	6.736	7.899	9.164	10.528
$\varepsilon_{b,o}$	2.500	2.273	2.110	2.003	1.932	1.882	1.844	1.815	1.792	1.774
$\kappa_{1,p}$	2.500	1.932	1.574	1.373	1.251	1.171	1.115	1.075	1.044	1.020
$\kappa_{1,o}$	2.500	2.522	2.343	2.202	2.102	2.029	1.974	1.931	1.896	1.868
$\kappa_{2,p}$	2.500	2.211	2.133	2.222	2.413	2.674	2.989	3.349	3.751	4.189
$\kappa_{2,o}$	2.500	2.439	2.265	2.136	2.045	1.980	1.930	1.892	1.862	1.837
$\kappa_{3,p}$	2.500	3.047	3.809	4.769	5.899	7.182	8.609	10.174	11.871	13.698
$\kappa_{3,o}$	2.500	2.190	2.032	1.937	1.875	1.832	1.801	1.777	1.758	1.742
$\xi_{1,p}$	1.000	0.756	0.588	0.487	0.421	0.374	0.340	0.313	0.292	0.275
$\xi_{1,o}$	1.000	1.000	0.920	0.860	0.818	0.787	0.763	0.745	0.731	0.719
$\xi_{2,p}$	1.000	0.865	0.797	0.788	0.811	0.854	0.911	0.976	1.051	1.129
$\xi_{2,o}$	1.000	0.967	0.890	0.834	0.796	0.768	0.747	0.731	0.718	0.707
$\xi_{3,p}$	1.000	1.192	1.423	1.691	1.983	2.295	2.623	2.966	3.322	3.690
$\xi_{3,o}$	1.000	0.868	0.798	0.757	0.729	0.711	0.697	0.686	0.678	0.671
Π_p	3.200	3.122	2.960	2.778	2.601	2.438	2.291	2.159	2.041	1.935
Π_o	3.200	3.180	3.179	3.192	3.208	3.225	3.241	3.255	3.268	3.280

subscript p: prolate ellipsoid

o: oblate ellipsoid

Table 2. Use of the R function to predict the conformation of various macromolecules in solution in terms of an ellipsoid of revolution model

Protein	k_s ml/gm	k_η ml/gm	$[\eta]$ ml/gm	R	axial ratio	model dependent (v_s/v)	model independent $(\bar{v}_s/\bar{v})$	Conclusion
Apoferritin[1]	8	12	5.16	1.55	1.45*†	2.6*†	1.5	spherical
BSA[2]	5.5	7.7	2.75	2.0	—	—	1.4	not a hydrodynamic ellipsoid (cf β< 2.1)
Fibrinogen[3]	7	14	7.8	0.9	6.3†	1.1†	2.0	prolate ellipsoid ~6:1. Agrees with electron microscopy (Hall & Slayter, 1959)
C-protein[4]	11	15.4	12.6	0.87	26.0,6.65*†	0.9,2.12*†	1.4	oblate ellipsoid ~25:1
Myosin[5]	85	92	234	0.38	30†	4.3†	1.1	not hydrodynamic ellipsoids of revolution
Synthetic A-filaments[6]	160.8	366	176	0.9	19.5†	16†	2.3	not hydrodynamic ellipsoids of revolution
Collagen sonicates[7]								
(i) M_r = 352,000	308	880	1252	0.246	80†	2.28†	2.85	prolate ~80:1
(ii) M_r = 330,000	291	756	1078	0.270	64†	2.85†	2.60	prolate ~65:1
(iii) M_r = 273,000	241	564	639	0.377	30†	6.12†	2.34	not hydrodynamic ellipsoids of revolution
(iv) M_r = 227,000	193	428	400	0.483	18†	9.13†	2.22	not hydrodynamic ellipsoids of revolution

† prolate ellipsoid, * oblate ellipsoid. Refs: 1&2 Rowe & Pancholi (unpub.), 3 Rowe & Mihalyi (unpub.), 4 Offer et al (1973), 5 Emes (1977), Emes & Rowe (1978a), 6 Emes (1977), Emes & Rowe (1978b), 7 from Nisihara & Doty (1958)

Table 3. Crystallographic dimensions of some globular proteins

Protein	Dimensions (Å)	Reference
Carboxypeptidase	50 x 42 x 38	Lipscomb (1971)
Myoglobin	43 x 35 x 23	Kendrew et al (1958)
Cytochrome c	25 x 25 x 35	Dickerson & Geiss (1969)
Lysosyme	45 x 30 x 30	Blake et al (1965)
Ribonuclease	38 x 28 x 22	Kartha et al (1967)
Pre - albumin	70 x 55 x 50	Blake et al (1978)
Hemoglobin	64 x 55 x 50	Perutz et al (1960)

$\boxed{/\!/\!/} \equiv \bar{V}$
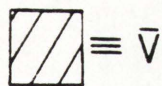
$\overline{}\overline{}$ associated solvent

● trapped or entrained solvent
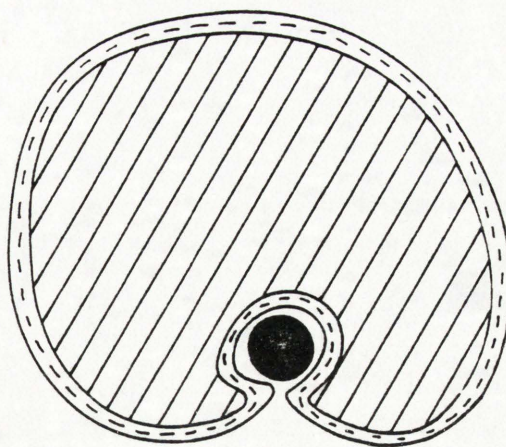
<u>Figure 1.</u> A macromolecule in solution is generally swollen due to solvent association

Rod
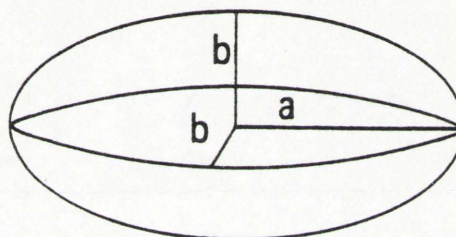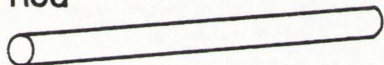
Prolate ellipsoid of revolution (b< a)

<u>Figure 2.</u> Mathematical models for macromolecules in solution

Disc
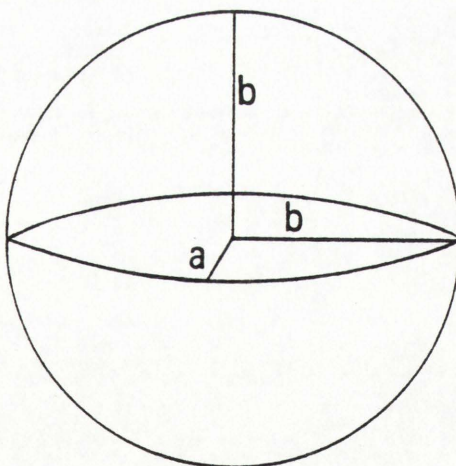
Oblate ellipsoid of revolution (b> a)

stress σ → velocity V →
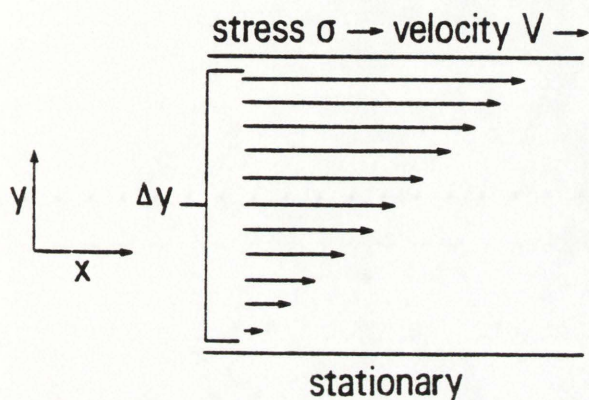
length of arrows are proportional to the fluid velocity at that value of y

<u>Figure 3.</u> Shearing of a Newtonian fluid between parallel plates (from Van Holde, 1971)

stationary
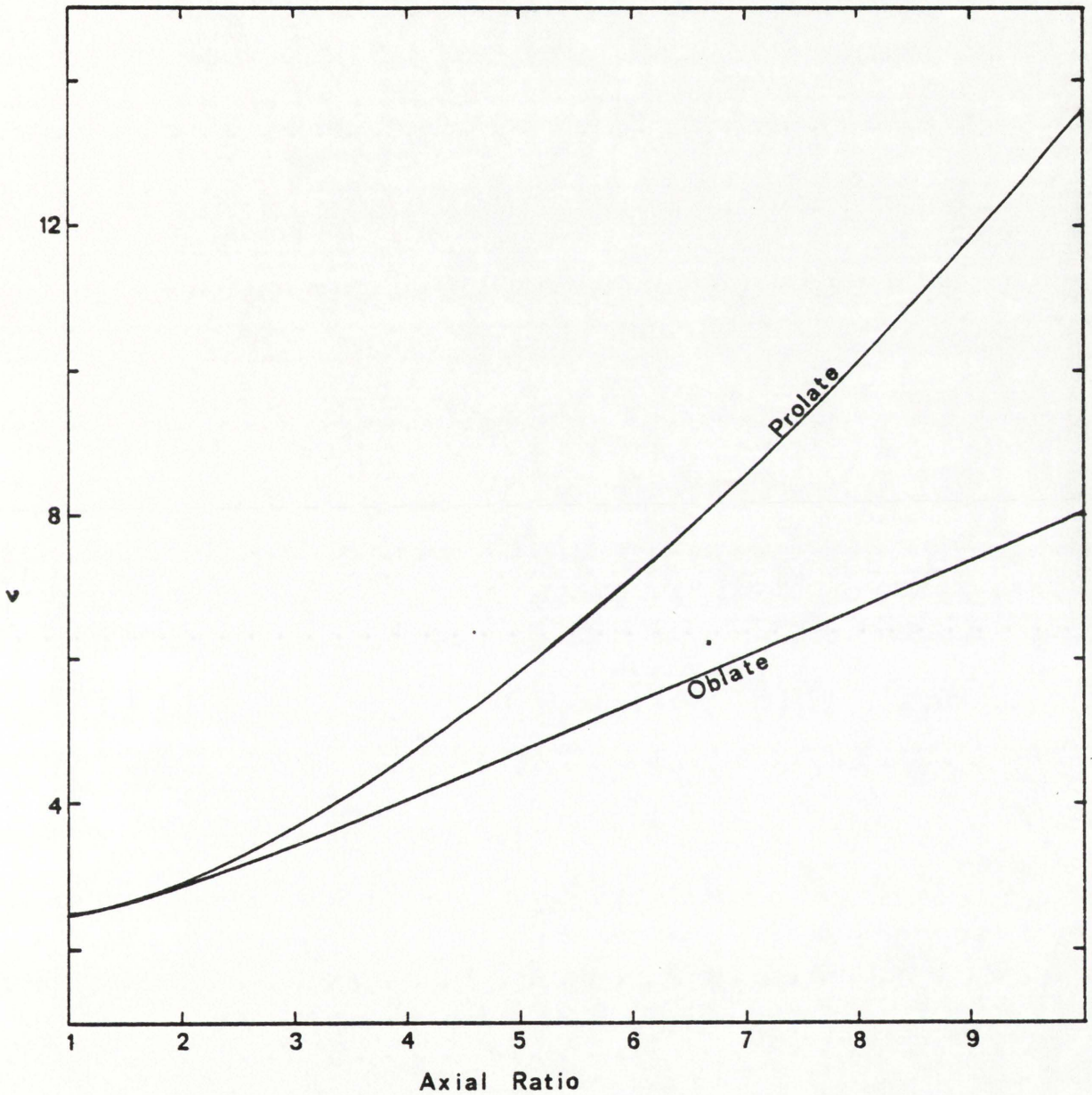
Figure 4. Plot of the viscosity increment as a function of axial ratio

for ellipsoids of revolution
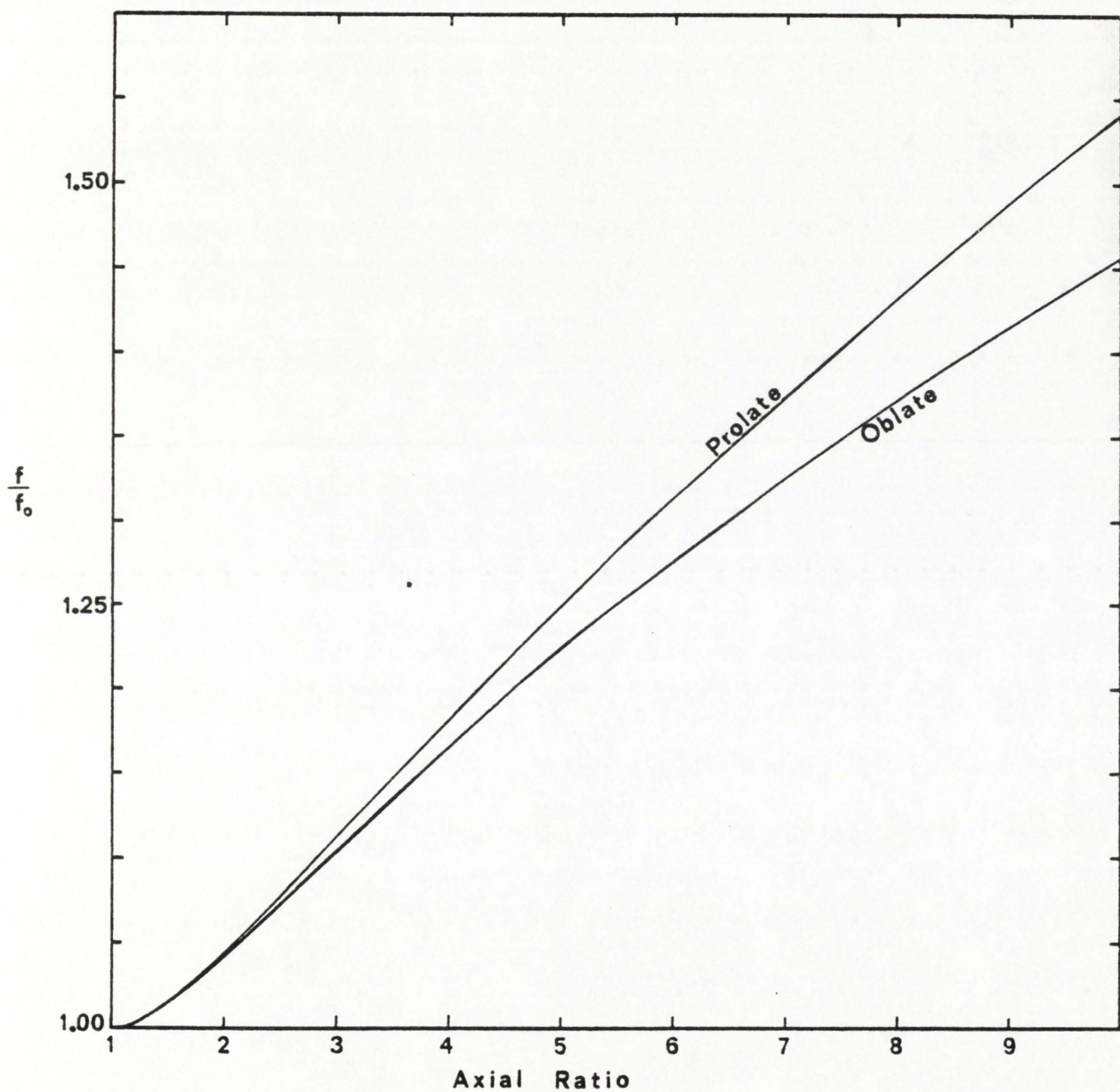
Figure 5. Plot of the translational frictional ratio (the "Perrin

function") as a function of axial ratio for ellipsoids
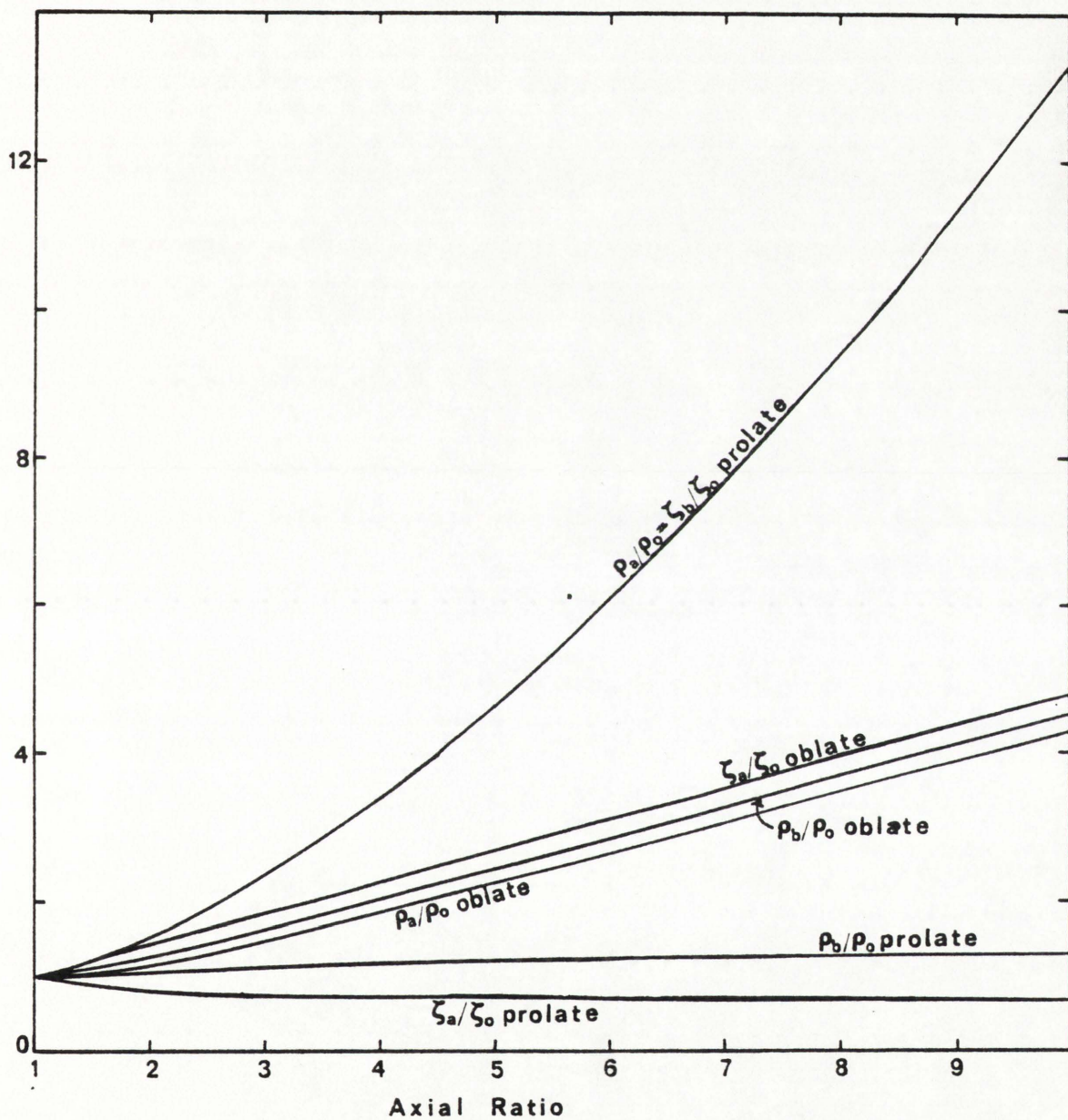
of revolution

Figure 6. Plot of the rotational diffusion coefficient ratios and
rotational relaxation time ratios as a function of axial
ratio for ellipsoids of revolution

Figure 7. Dielectric dispersion curves for prolate ellipsoids of

revolution. Constant dipole angle ($\theta = 45^{\circ}$) and varying

axial ratio (a/b from 1 to 50). From Oncley (1940)

Log$_{10}$ Relative Frequency ν/ν_o

$(\epsilon - \epsilon_\infty)/(\epsilon_o - \epsilon_\infty)$

Relative Contribution to Dielectric Constant:

a/b =

$\Delta t_a/\Delta t_b = 1$
(Dipolar Angle
=45°)

21
4
9
16
25
50

$\dfrac{\tau_h}{\tau_o}$
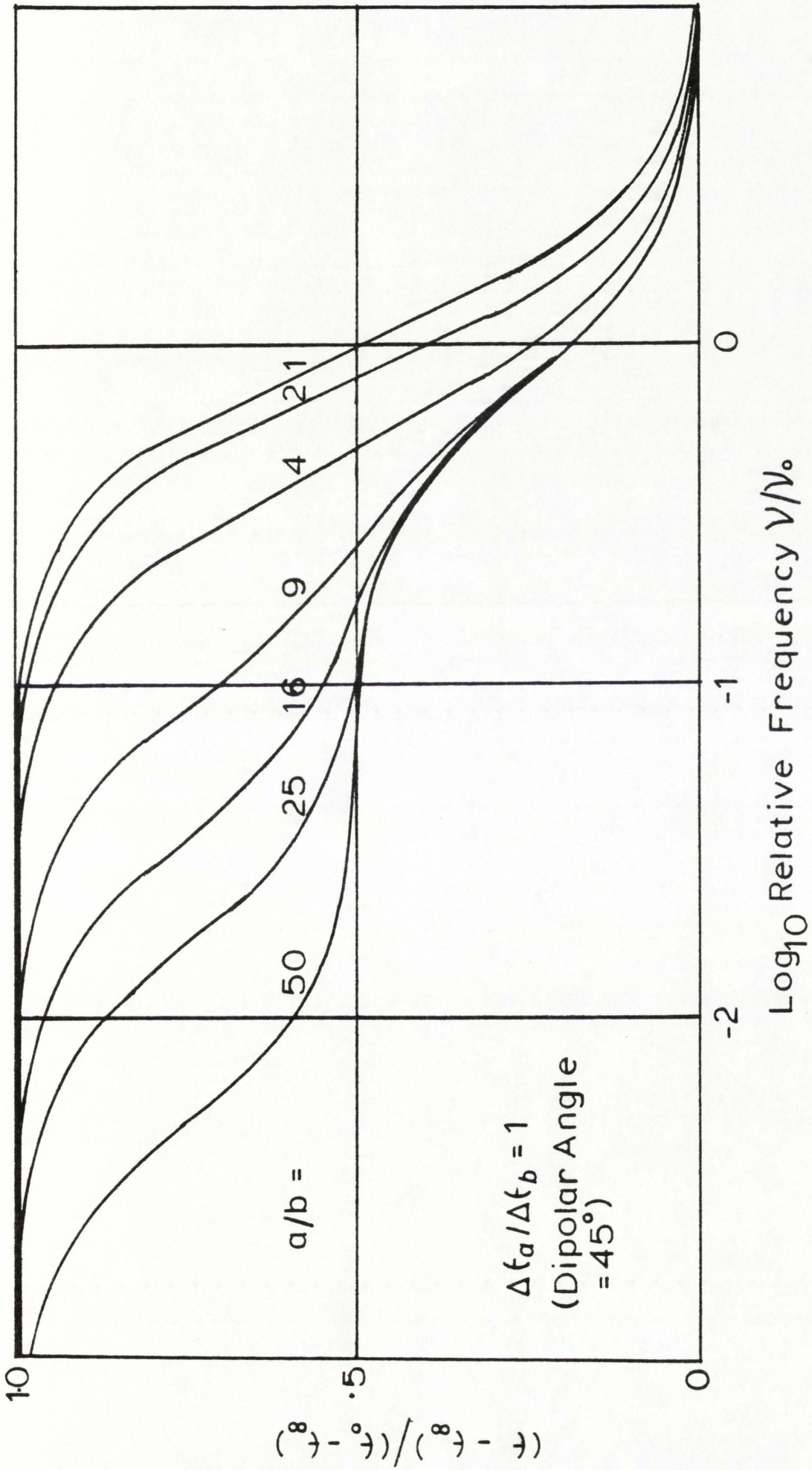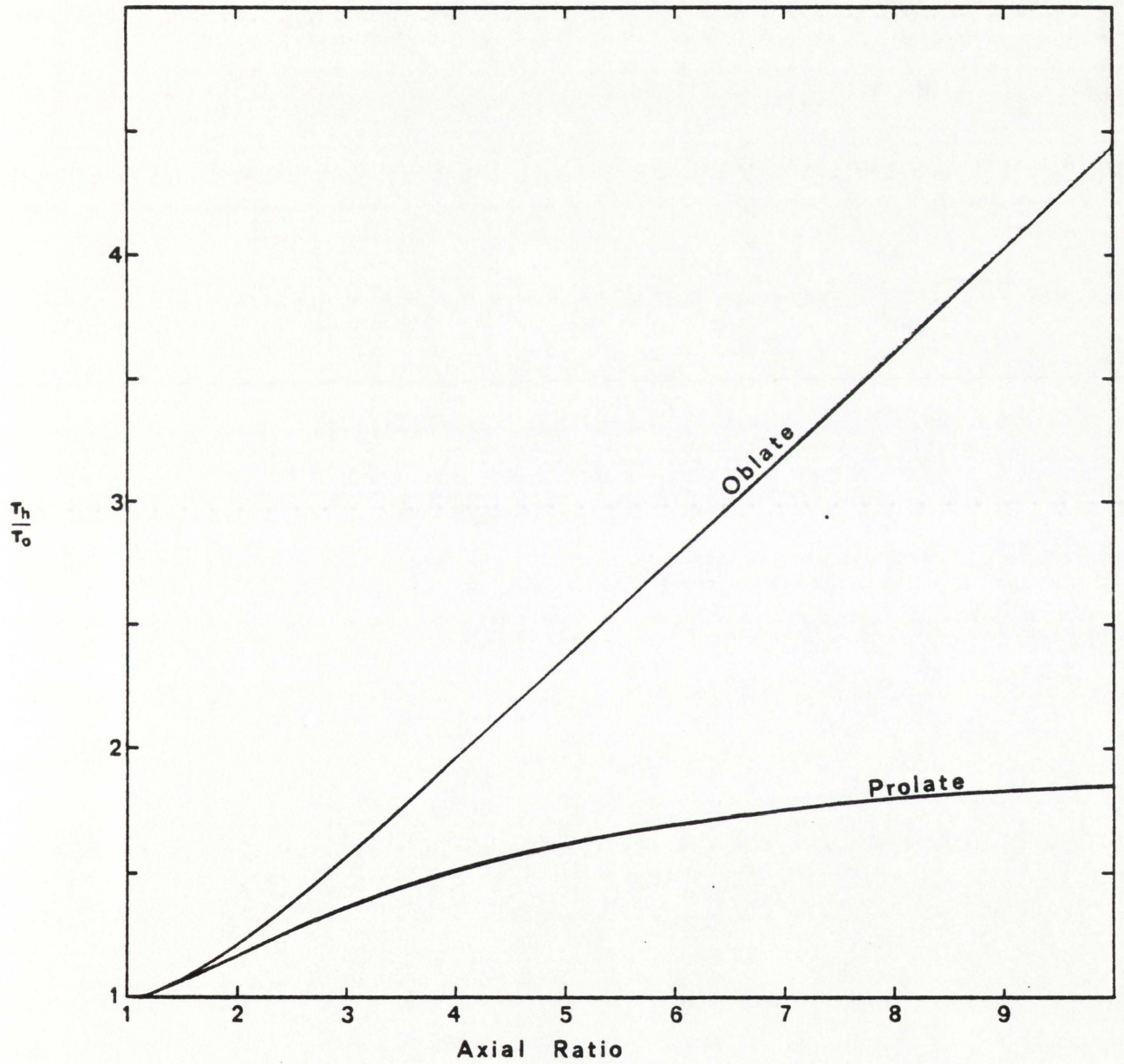
Axial Ratio

Figure 8. Plot of the harmonic mean rotational relaxation time ratio
as a function of axial ratio for ellipsoids of revolution
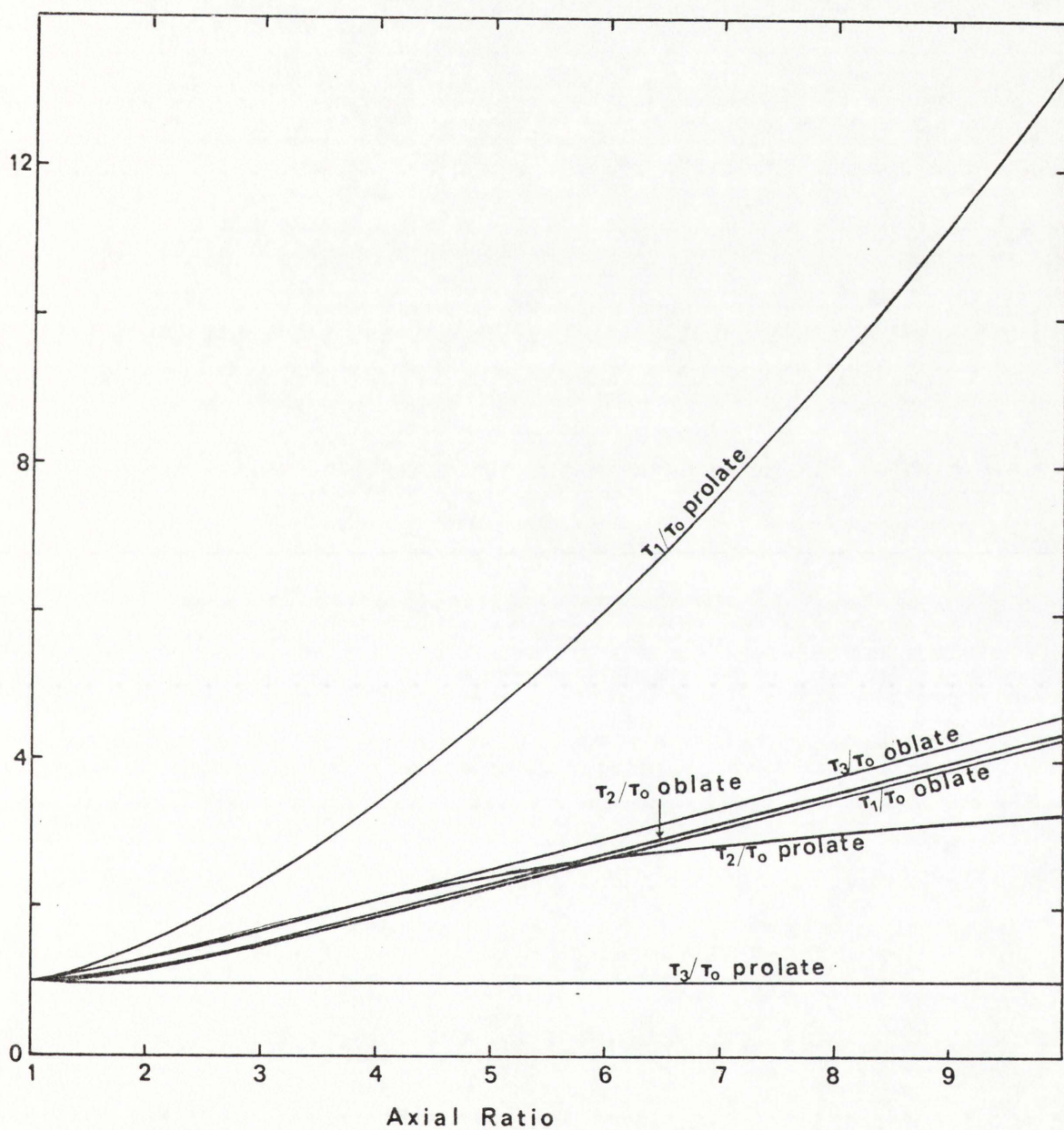
Figure 9. Plot of the fluorescence anisotropy relaxation time ratios as a function of axial ratio for ellipsoids of revolution
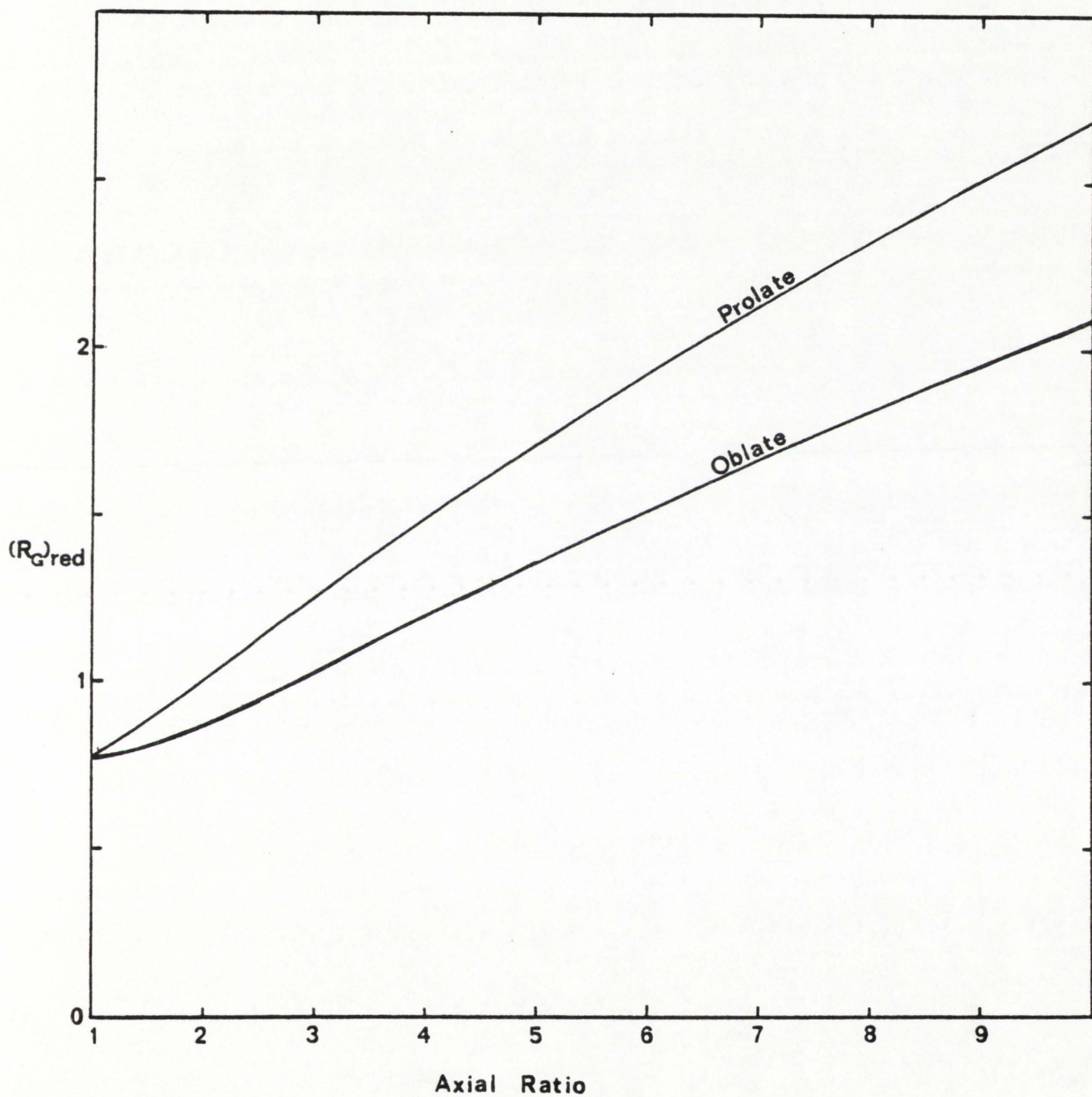
Figure 10. Plot of the 'reduced' radius of gyration as a function of

axial ratio for ellipsoids of revolution

Figure 11. (a) <u>Values of axial ratio and hydration as a function of</u>

$\nu(\bar{v}_s/\bar{v})$. Contour lines denote values of $\nu(\bar{v}_s/\bar{v})$

(b) As above, but as a function of $(f/f_0).(\bar{v}_s/\bar{v})^{1/3}$.

Contour lines denote values of $(f/f_0).(\bar{v}_s/\bar{v})^{1/3}$

(from Oncley, 1941)

(a)

AXIAL RATIO, a/b.

HYDRATION
Grams of Water per Gram of Protein

(b)

AXIAL RATIO, a/b.

HYDRATION
Grams of Water per Gram of Protein
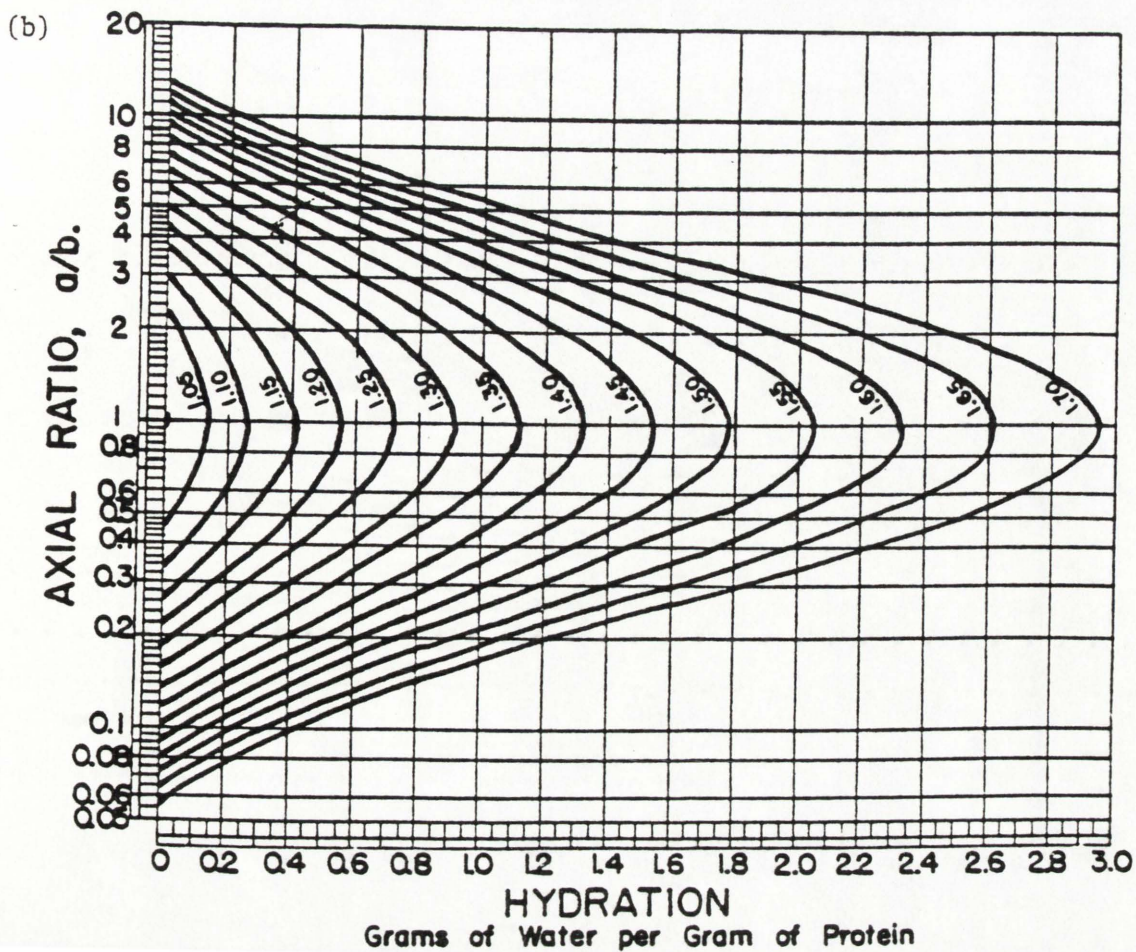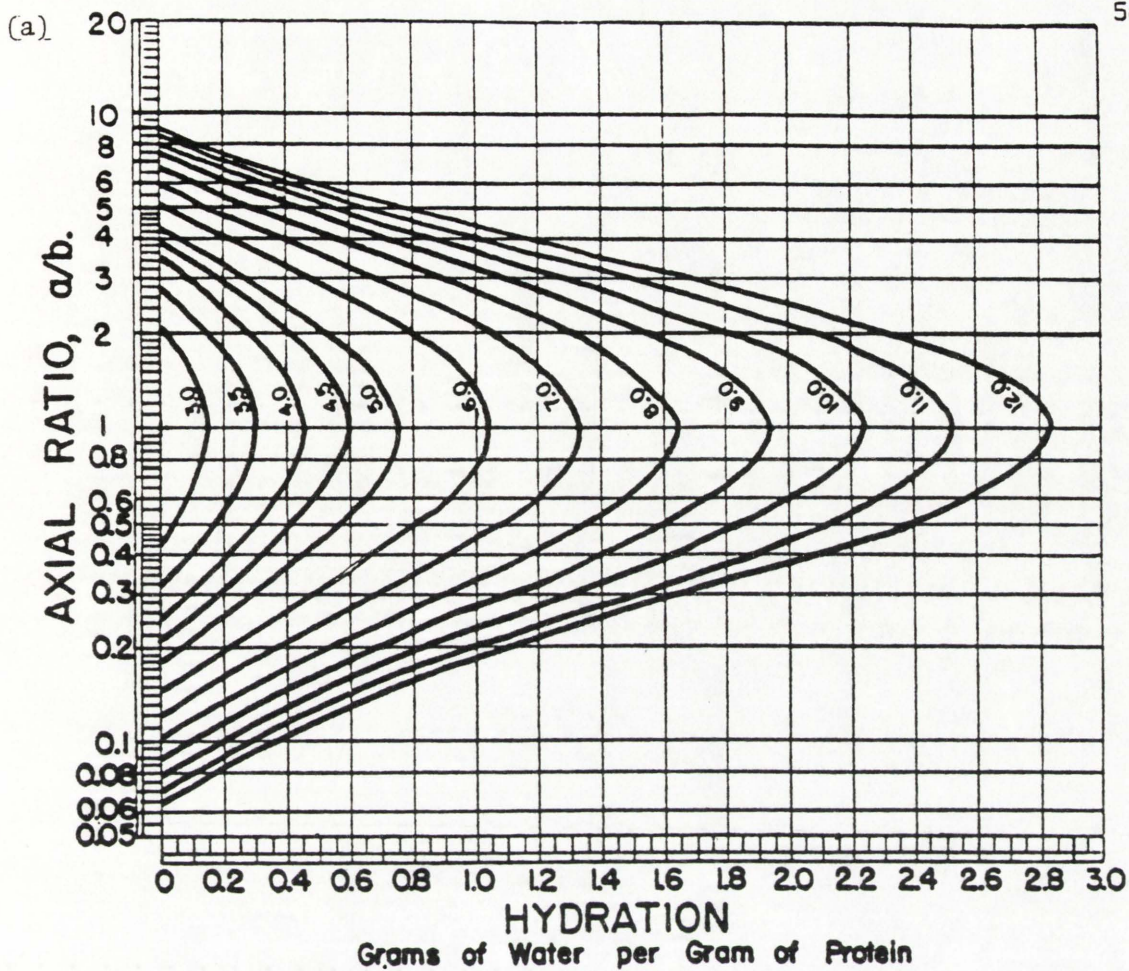
Figure 12. Asymmetry and hydration (i.e. solvent association) of certain protein molecules. (from Oncley, 1941)

Serum Albumin   Edestin   Lactoglobulin

Hemoglobin   Insulin   Pepsin   Egg Albumin

AXIAL RATIO, a/b.

HYDRATION
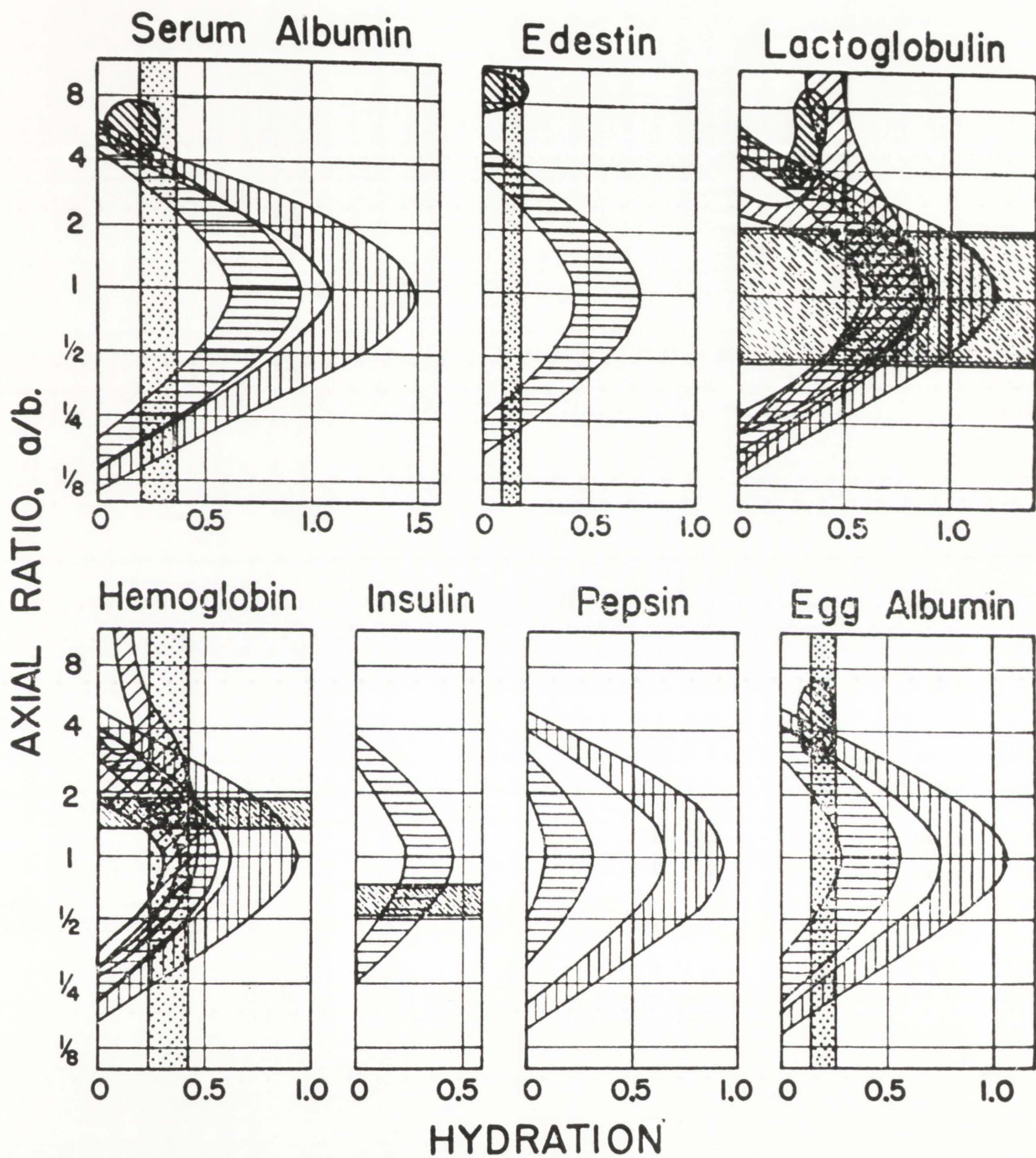
Grams of Water per Gram of Protein

From frictional ratio (assuming ±4% error)

From viscosity coefficient (assuming ±10% error)

From crystal density (assuming ±25% error)

From X-ray studies

From dielectric dispersion, with one relaxation time

From dielectric dispersion, with two relaxation times
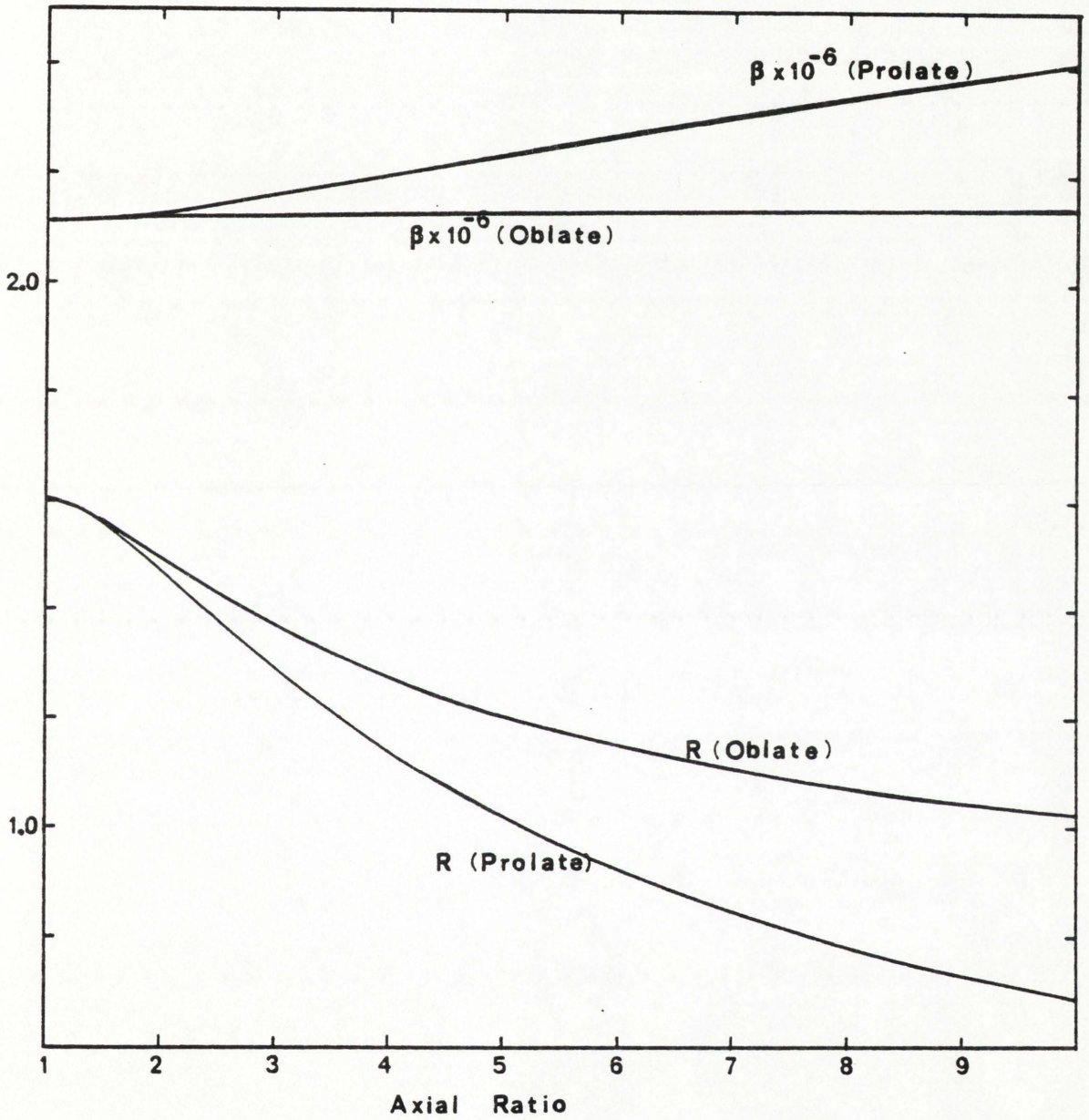
Figure 13. Plot of the Scheraga & Mandelkern β ($\times 10^{-6}$) and Rowe R functions versus axial ratio for ellipsoids of revolution
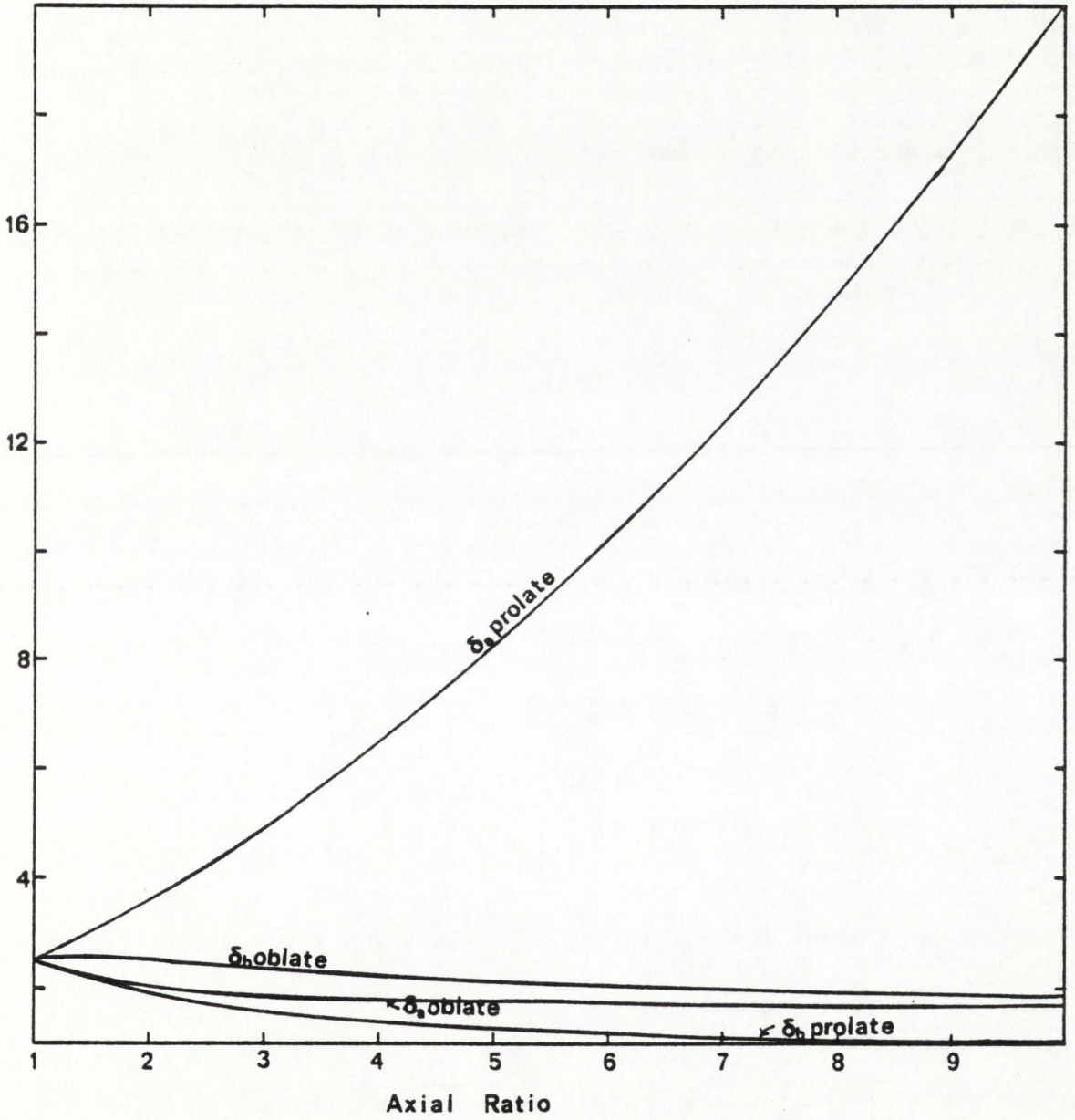
Figure 14. Plot of δ_a and δ_b as functions of axial ratio for ellipsoids of revolution
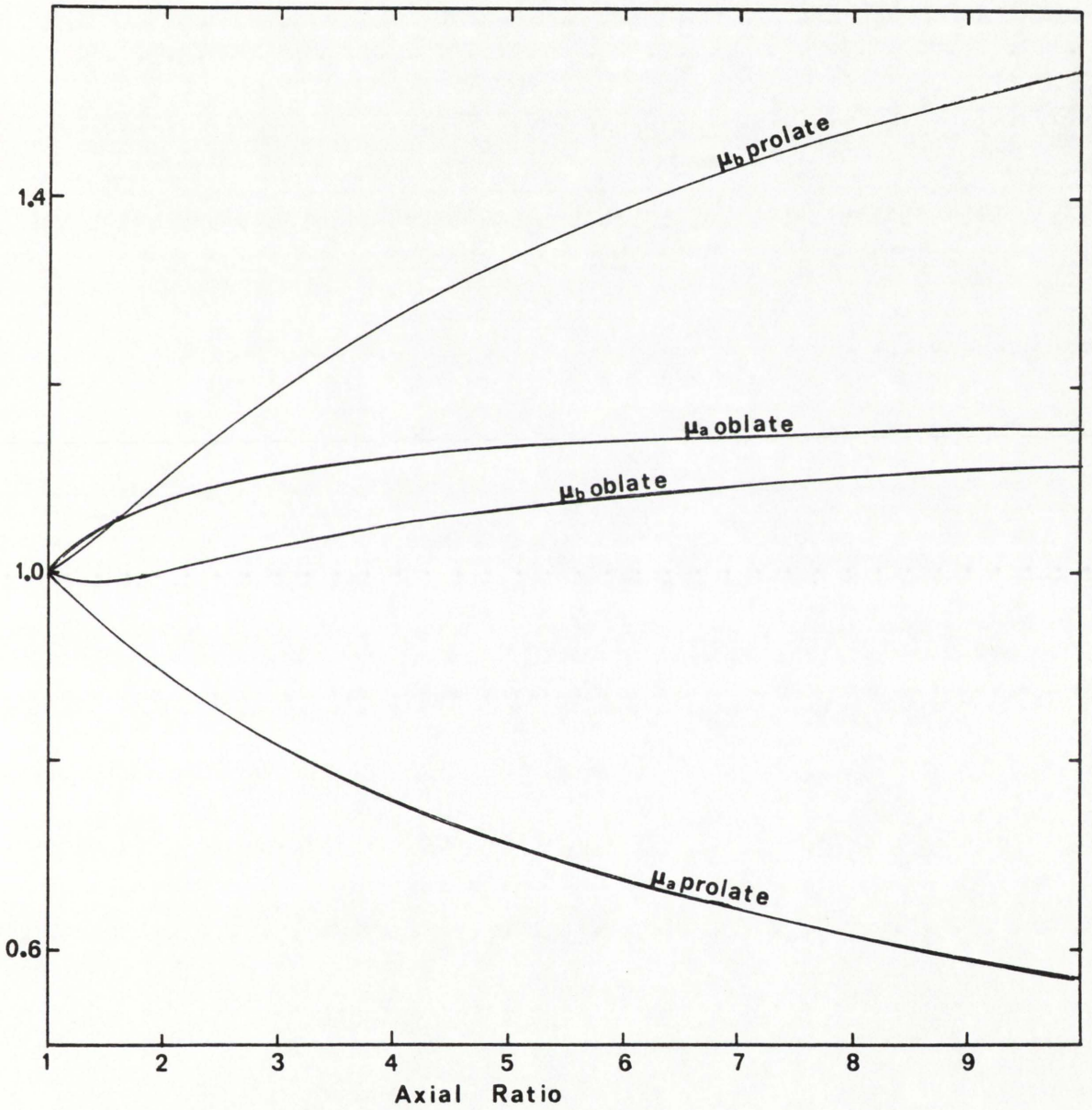
Figure 15. Plot of μ_a and μ_b as functions of axial ratio for ellipsoids of revolution
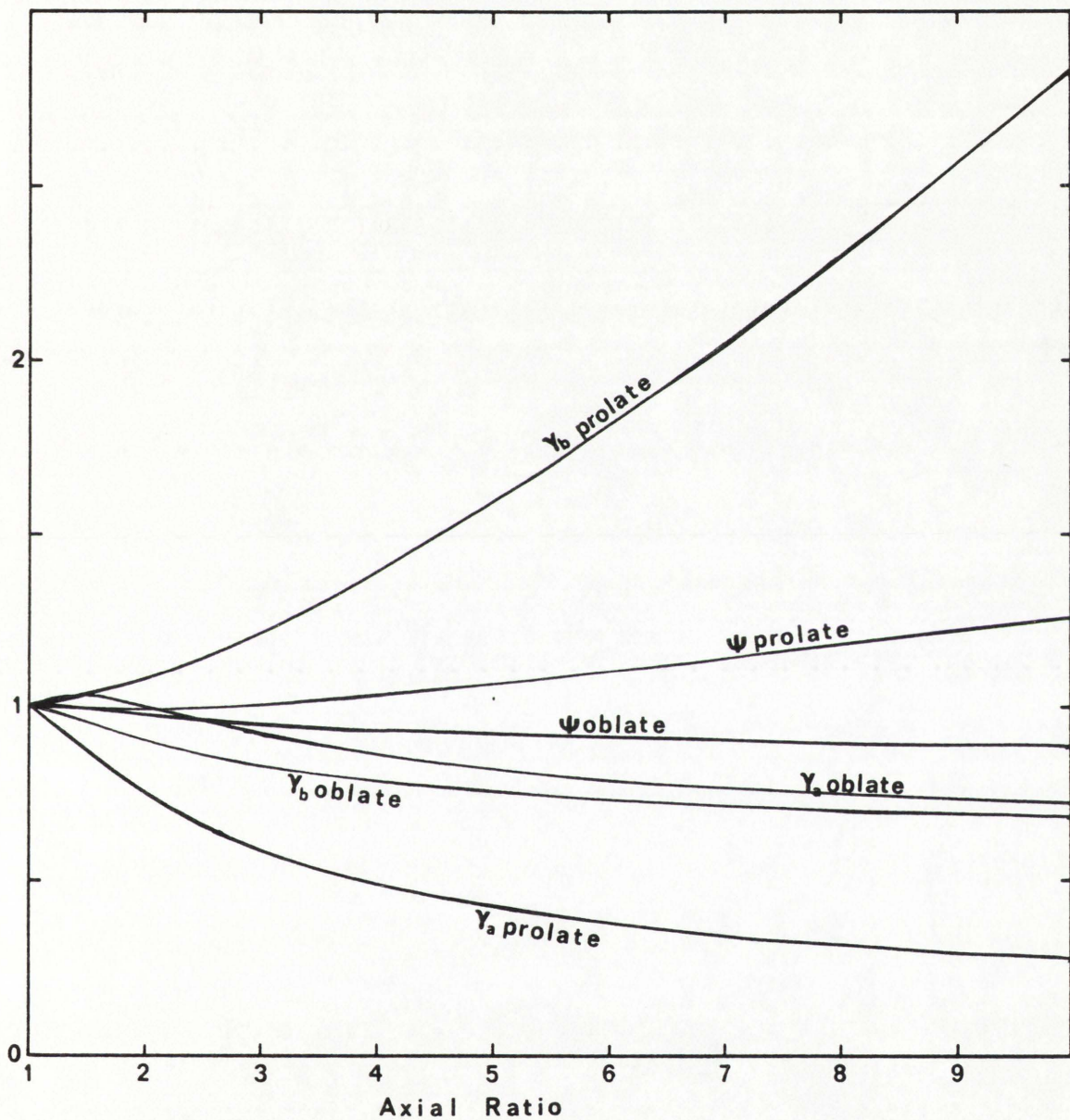
Figure 16. Plot of γ_a, γ_b and Ψ as functions of axial ratio for ellipsoids of revolution
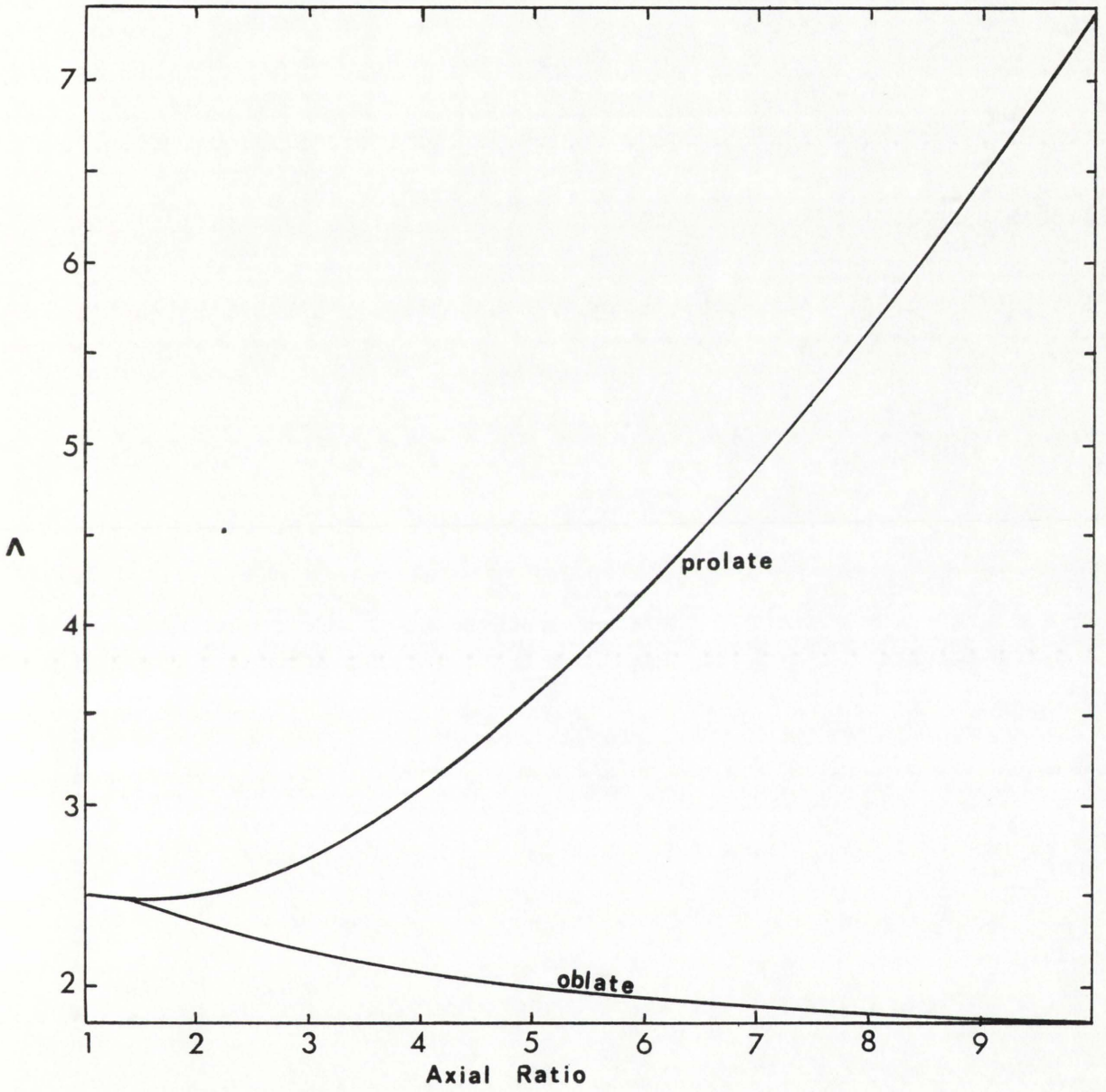
Figure 17.   Plot of Λ as a function of axial ratio for ellipsoids
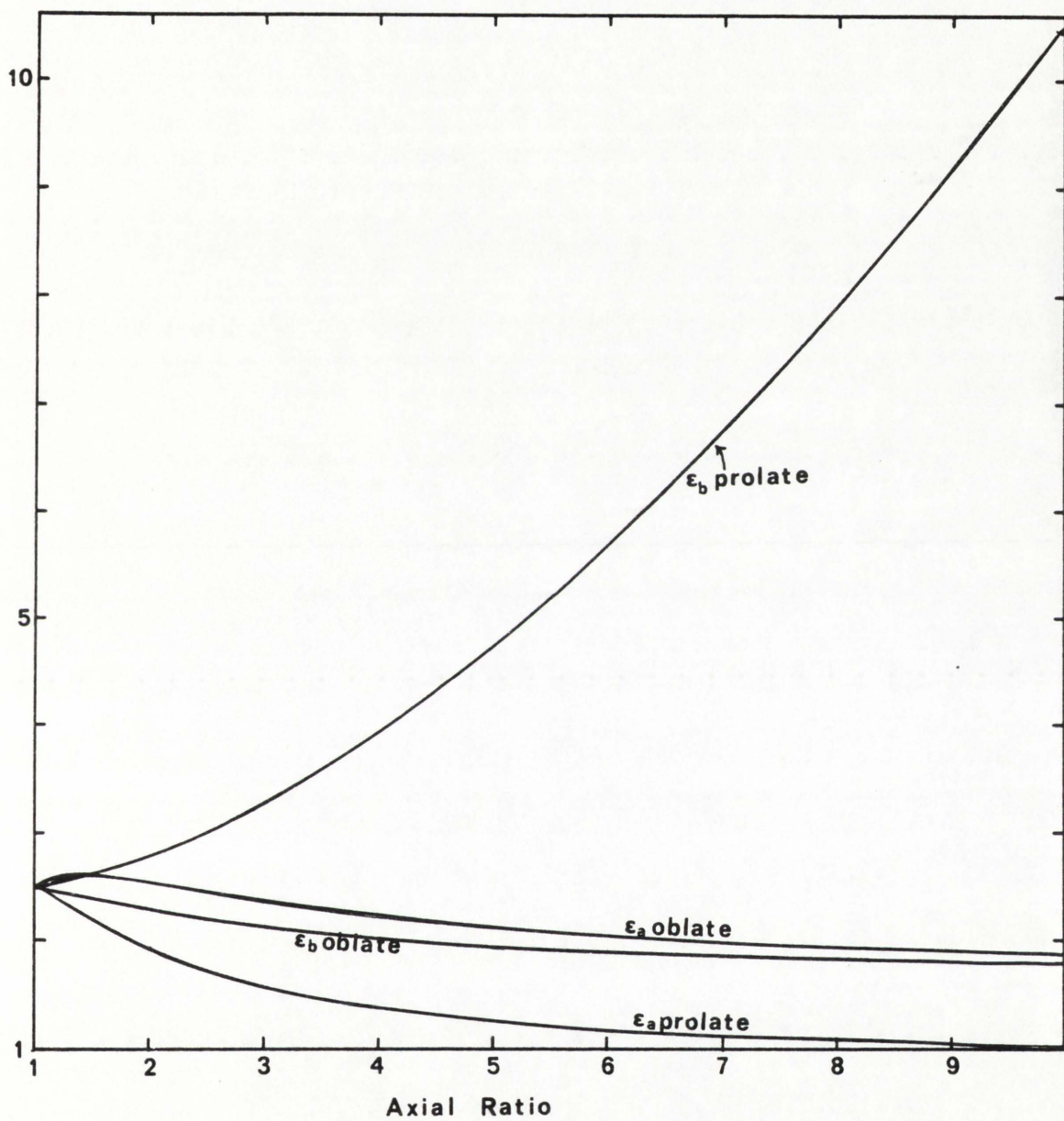
of revolution

Figure 18. Plot of ε_a and ε_b as functions of axial ratio for ellipsoids
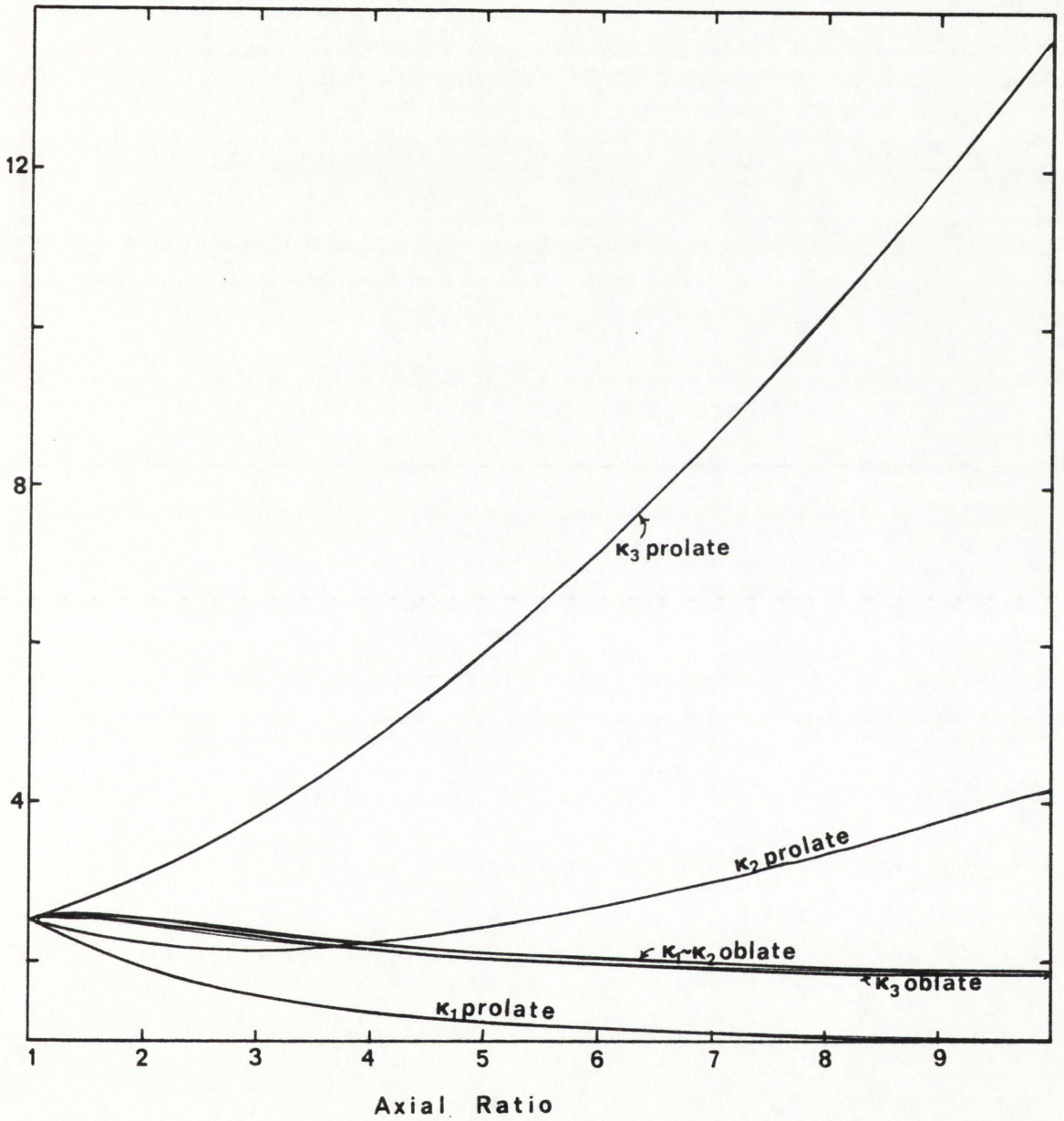
of revolution

<u>Figure 19.</u> Plot of κ_1, κ_2 and κ_3 as functions of axial ratio for ellipsoids
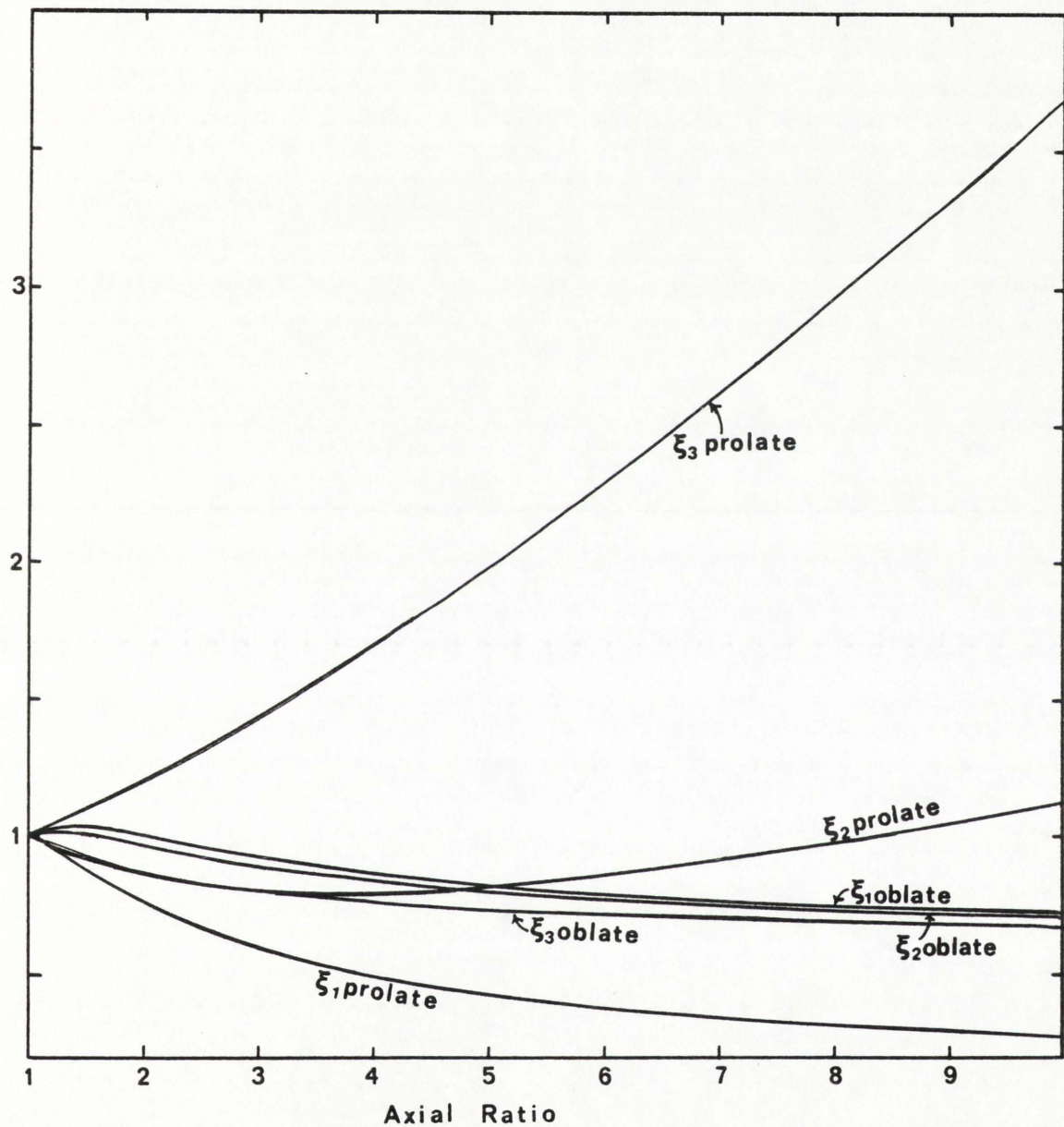
of revolution

Figure 20. Plot of ξ_1, ξ_2 and ξ_3 as functions of axial ratio for ellipsoids of revolution
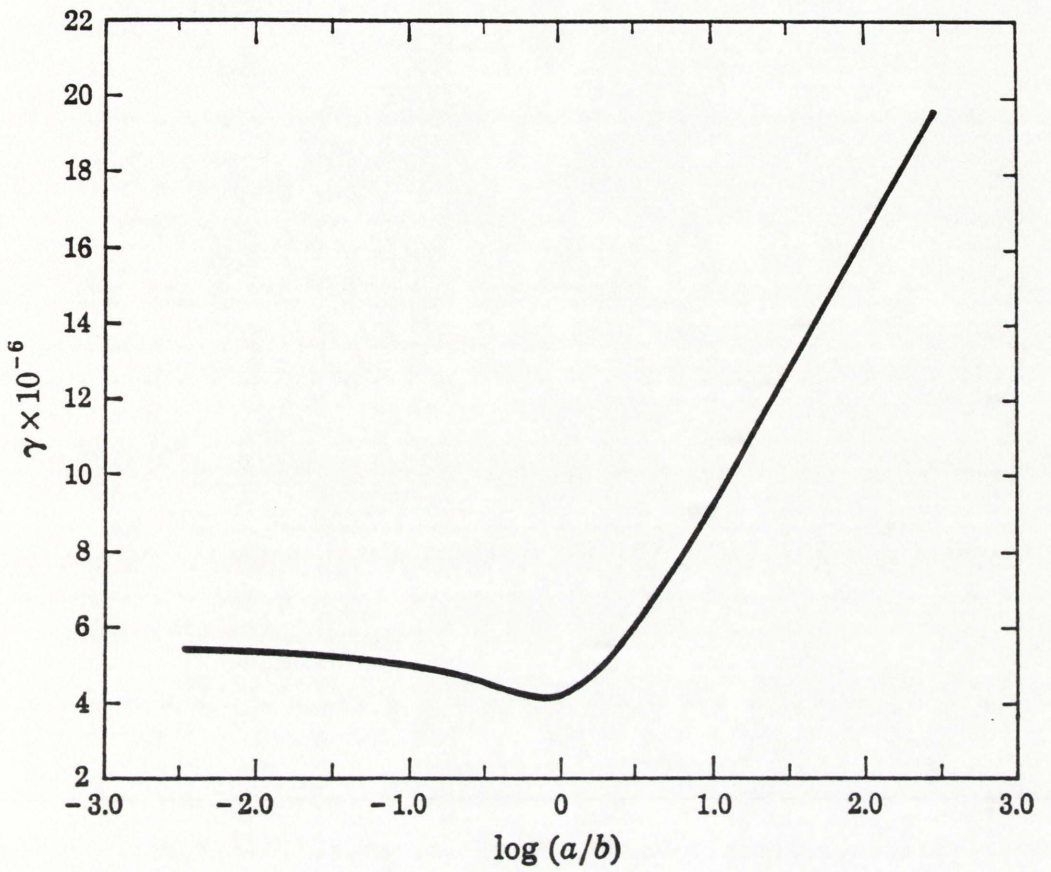
Figure 21. Plot of γ as a function of axial ratio for ellipsoids of revolution (from Martin, 1964)
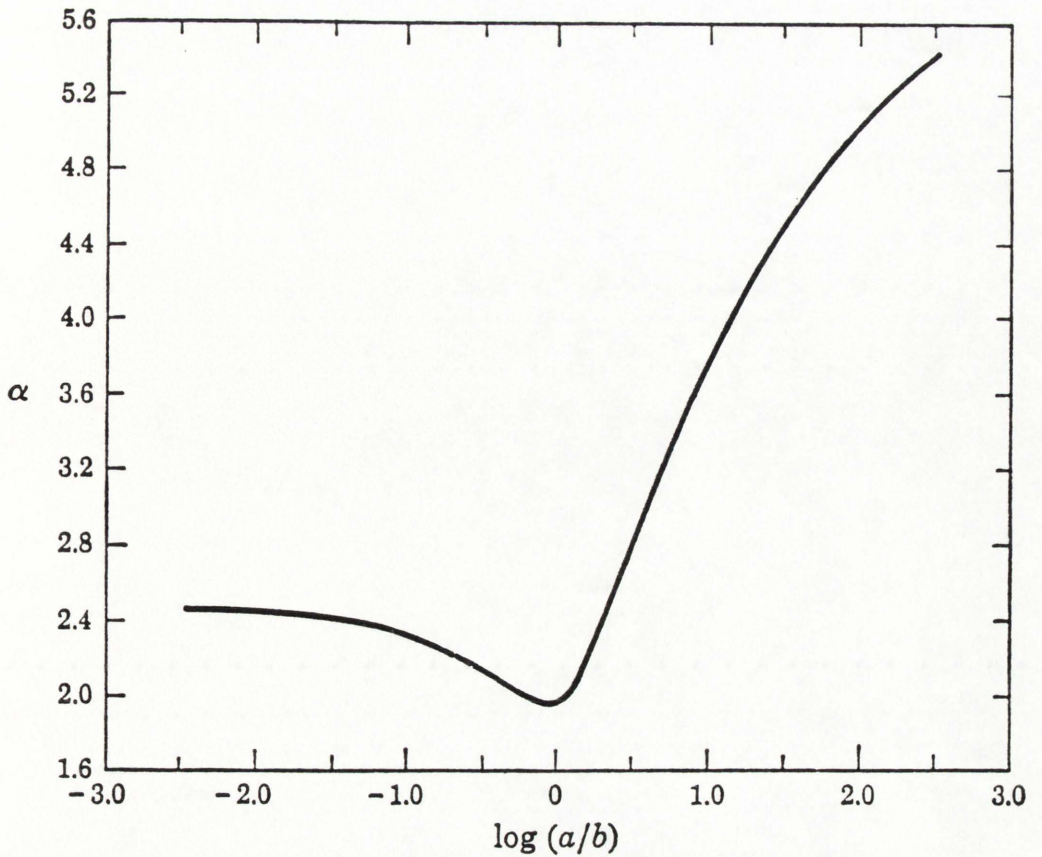
Figure 22. Plot of α as a function of axial ratio for ellipsoids of revolution

67.
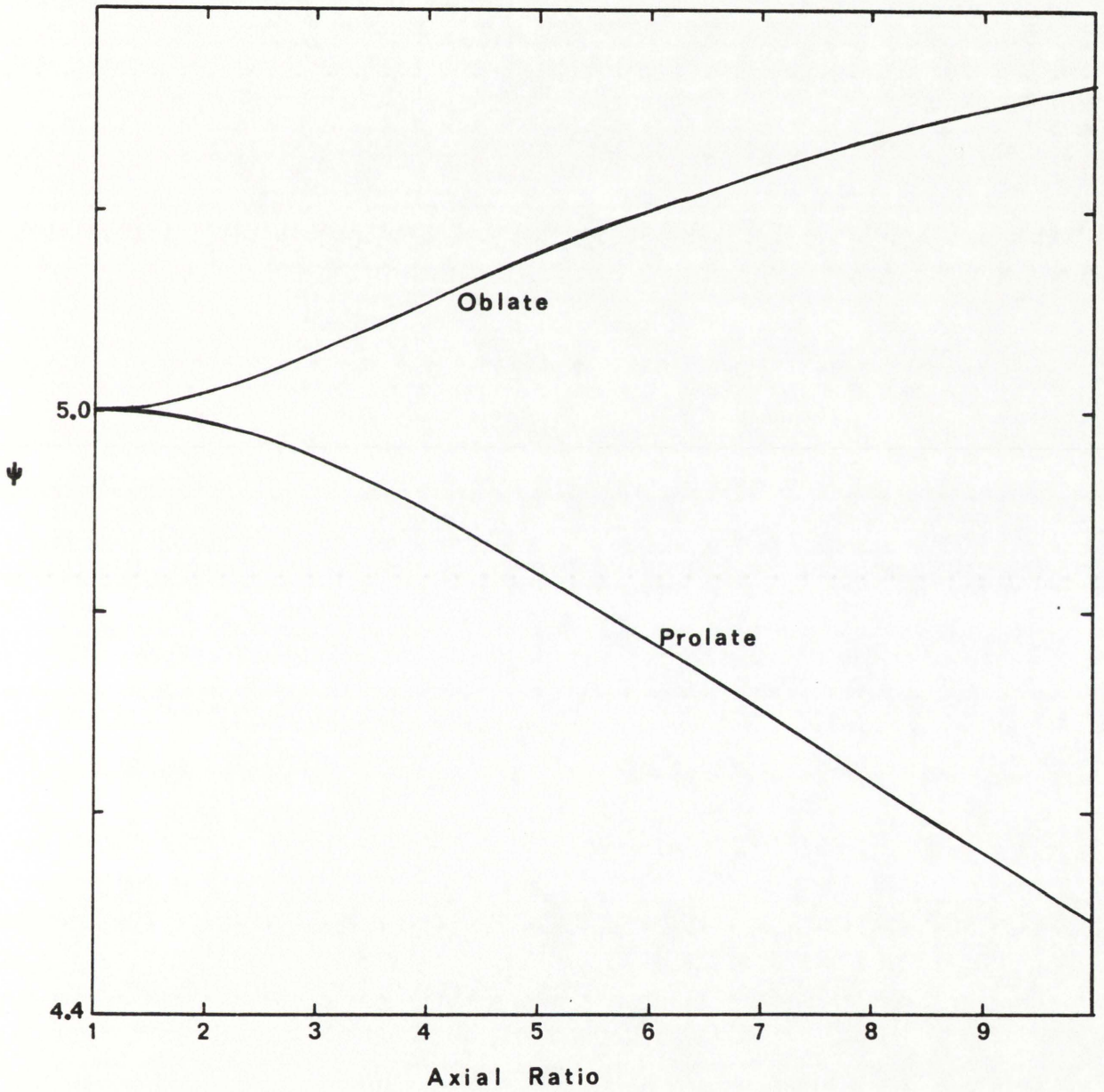
Figure 23. Plot of ψ as a function of axial ratio for ellipsoids
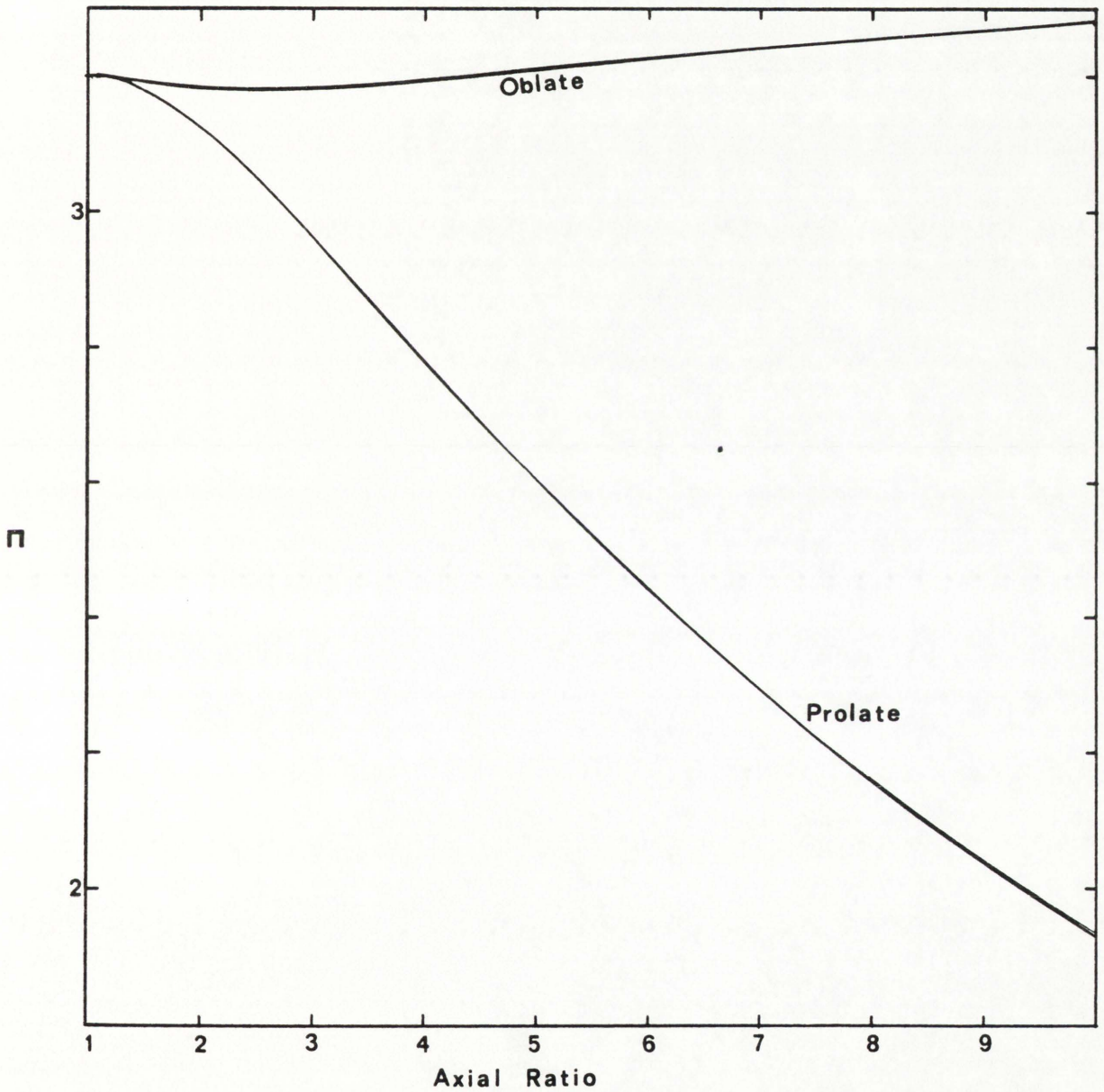
of revolution

Figure 24. Plot of Π as a function of axial ratio for ellipsoids of revolution

C H A P T E R   2

The Viscosity Increment for a Dilute, Newtonian

Suspension of Tri-axial Ellipsoids

2.1. Hydrodynamic Forces and Brownian Motion

Although the forces and torques exerted upon a suspended particle by a fluid are all ultimately of molecular origin, it is convenient to distinguish those that can be explained by continuum hydrodynamics from those, due to molecular fluctuations, that give rise to Brownian motion. If we first completely neglect the Brownian motion, it is clear that, once a steady state has been attained, suspended particles free of any external imposed impressed forces or torques must move in such a way that the net hydrodynamic force and torque, T_H acting upon them are zero, i.e. $T_H = 0$.

Let us consider a steady simple shearing flow (section 1.3.), as in, for example, a simple capillary or Ubbelohde viscometer experiment (Yang, 1961). The motion of the fluid in the neighbourhood of any point can be decomposed into three components; a translational velocity which varies from point to point, an angular velocity which for this type of flow is the same for all points, and a pure straining motion which again is the same for all points. If now a single, neutrally bouyant, rigid ellipsoidal particle is introduced the flow will be disturbed, although at large distances from the ellipsoid the disturbance will tend to zero. We shall assume that the motion of the ellipsoid and of the fluid is such that the Reynold's number (Batchelor, 1967) is very small. Then it is possible on the basis of work by Oberbeck (1876) and Jeffrey (1922) to say what the hydrodynamic forces and torques acting upon the particle are. In particular it is known that the force will be zero when the translational velocity of the particle is the same as the translational velocity of the point in the undisturbed flow at which the point is suspended. The situation for angular velocity is more complicated since two factors come

into play; one gives a torque if the angular velocity of the particle differs from the angular velocity defined by the undisturbed flow (or, equivalently, by the actual flow at infinity), whilst the other gives a torque if the principal axes of the ellipsoid have a different orientation from the principal axes of the straining motion defined by the undisturbed flow. Taken together, these mean that the angular motion of the particle under zero hydrodynamic torque conditions is very complicated (Chwang, 1975) and a complete solution for it is not known.

Turning to the Brownian motion which is in the nature of fluctuations the simplest question we can ask is what is the average velocity and the average angular velocity of the particle? By the average we mean in the first instance the time average, although in practice this will be assumed equal to the volume average taken over an ensemble over a very large number of particles suspended in unit volume (see Batchelor, 1970 for a detailed discussion of various methods of averaging). Ignoring for the moment the hydrodynamic forces, we can answer the question by saying that on average the particle is at rest in the local frame of reference defined by the undisturbed flow. In other words it is on average moving with the translational velocity of the point in the undisturbed flow at which it is suspended and with the angular velocity defined by the undisturbed flow (Kuhn & Kuhn, 1945, Brinkman et al, 1949, Scheraga, 1955).

When we come to consider the combined effect of the hydrodynamic forces and the Brownian motion no problem arises with the translational motion since both effects tend in the same direction - motion with the translational velocity of the flow. But for the angular motion the situation is less simple, the two effects do not have the same tendancy and we must consider a range of possibilities depending on the relative strengths of the two. This range is represented by the Peclet number

$\alpha = G/\theta$ (Brenner, 1972a) where G is the shear rate and θ the mean rotational diffusion coefficient. We shall only be considering the case of overwhelming Brownian motion ($\alpha \to 0$) in which the hydrodynamic effects are completely negligible compared with the Brownian motion effects. Thus we shall take it that on average the particles are rotating with the local angular velocity of the ambient flow; and we may additionally assume that the orientation of the particles will be random. This last fact would not be so if hydrodynamic forces and torques were not negligible for they introduce systematic motions and hence preferred orientations.

2.2.   The Simha Model of Overwhelming Brownian Motion

We consider a homogeneous dilute suspension of identical rigid ellipsoids randomly oriented in an incompressible Newtonian fluid in which they are neutrally buoyant. The ambient flow is taken to be a slow simple shearing flow, whilst the suspended particles are taken to be moving with the velocity and the angular velocity of the ambient flow appropriate to the point at which each is suspended. Near each particle this ambient flow is disturbed but is still taken to be a slow (low Reynold's number) flow so that we may apply the classical results of Jeffrey (1922).

This model, which is taken to be appropriate for the case of over-whelming Brownian motion derives from Simha (1940) although in his original work doubt is left about whether or not the particles are rotating with the local angular velocity of the fluid. An attempt to clear this difficulty is made below (section 2.6.). The key simplifying feature of the model introduced by Simha is that it eliminates the complicated statistical problem presented by the Brownian motion by substituting an assembly of

particles all moving with the average motion. This, together with the assumptions of diluteness and random orientation, allows us to compute the effect of the suspended particles by simply summing their individual effects. The isotropy of the particle distribution in the model means that non-Newtonian behaviour will not appear, and also allows us to use the energy dissipation method of computing the viscosity (Batchelor, 1970, Brenner, 1972b, p93).

The simplifications of the model are achieved, however, at a price. Non-Newtonian and concentration dependent effects, which to the theoretical rheologist are of the greatest interest, have been deliberately discarded; and the model can say nothing about lesser degrees of Brownian motion. In effect we shall be calculating the first term of a series; nevertheless this is of great value to the molecular biologist who can deliberately arrange the conditions of a viscosity experiment so that the model is applicable:

(i) Giesekus (1962) has shown that non-Newtonian normal stress effects are of 2nd order, and can thus be neglected for very low shear rates as in, for example, a capillary viscometer (Yang, 1961);

(ii) Viscosity coefficients are normally extrapolated to 'infinite dilution' i.e. zero concentration-dependent effects, to give the 'intrinsic viscosity' (Van Holde, 1971), related to the viscosity increment by equation (8).

2.3. The Viscosity Increment

We let η be the viscosity measured in an experiment on a dilute suspension of particles in a fluid of viscosity η_o. If ϕ is the volume concentration - the total volume of the particles in unit volume of the suspension - then the viscosity increment ν is defined, from

equation (7), by

$$\frac{\eta}{\eta_0} = 1 + \nu\phi$$

<div align="right">(65)</div>

where, when ν is independent of ϕ, the linear dependence of η/η_0 upon ϕ gives the empirical characteristic of a dilute suspension. From the theoretical point of view however, a dilute suspension is one in which there are no hydrodynamic interactions between the particles and thus one in which each particle independently contributes to the viscosity the same amount it would were it alone present. This contribution for a general ellipsoidal particle was first calculated by Jeffrey (1922) using the simple energy dissipation analysis for averaging over the particle ensemble (Batchelor, 1970) and it is a straightforward matter to extend his results to cover the case of ellipsoids rotating with the local angular velocity of the ambient flow as required by our model.

2.4. The Flow Velocity and Pressure

In order to calculate the additional dissipation of energy caused by introducing the particle into a given flow, we compare that given flow with the consequent disturbed flow within a suitable sphere, S, of radius R, centred on the particle position. We impose two requirements upon S: first, that it is small compared with the scale of spatial variations in the given flow, and thus within it that flow is effectively given as a linear variation of velocity with position; secondly, that it is large compared with the size of the particle, and thus that the disturbed flow will not appreciably differ from the given flow by the time the surface

of S is reached. Naturally, these requirements can only be met when

the particle is, as we have assumed, very much smaller than the scale

of spatial variations in the velocity field of the given flow.

For our purposes then, the disturbed flow may be taken to be the

flow of an incompressible fluid in the region between the rotating

ellipsoidal surface of the particle and the concentric spherical surface

S. On the inner surface we impose the usual no-slip boundary condition,

whilst on S we require the velocity field to be equal to its value in

the original flow. We give the velocity components of the two flows with

respect to rectangular Cartesian axes fixed in the rotating particle so

that its ellipsoidal surface will always be given by

$$\frac{x^2}{a^2} + \frac{y^2}{b^2} + \frac{z^2}{c^2} = 1$$

(66)

The undisturbed flow is given, within S, by

$$u_i^o = g_{ij} \, x_j$$

where g_{ij} are the components of the velocity gradient tensor which are

by our assumptions, independent of position within S. In this equation

and in subsequent equations, the indices range over the values 1,2,3 and

the summation convention is used whereby when an index is repeated within

a term a summation is indicated over the three values of that index.

Using ellipsoidal harmonics, Jeffrey was able to give the flow

velocity and pressure in the region of S for R large, but finite. He gives

the result under the assumption that the angular velocity is such that no

net <u>hydrodynamic</u> torque acts on it, i.e. hydrodynamic effects alone affect

the motion of the particle. In order to consider the Brownian motion we

follow Simha in dropping this restriction whence the flow near S is found,

to leading order, to be

$$u_i = u_i^o - 4\Phi x_i \left(\frac{1}{r^5} - \frac{1}{R^5}\right) + \frac{5\partial\Phi}{\partial x_i} \left(\frac{1}{R^3} - \frac{r^2}{R^5}\right)$$

(67)

In this equation, $\Phi = A_{ij}x_ix_j$, whilst the A_{ij} themselves are coefficients

independent of position but dependent on the g_{ij} and the components, ω_i

of the angular velocity of the particle; their explicit values are given

by Jeffrey (see Table 4 for the relationship between his notation and ours).

We consider the values of the A_{ij} below.

On the assumption that terms of second order in the velocity may be

neglected and that the particle spins are of the same order as the fluid

velocities, the dynamical equation for the fluid reduces to

$$\eta \nabla^2 \underline{u} = \nabla p$$

(68)

from which the pressure, p, can be found. For the disturbed flow we find

the pressure on S to be

$$p = p_o - \frac{50 \eta \Phi}{R^5}$$

(69)

where p_o is a constant.

2.5. The Dissipation of Energy

Assuming a steady state, we can compare the rates of dissipation

of energy within S in the two flows by comparing the corresponding rates

for working of the viscous stresses on the surface S. This rate of

working, dW/dt, is given by

$$\frac{dW}{dt} = \int_S u_i^o \sigma_{ij} n_j \, dS$$

(70)

where

$$\sigma_{ij} = -p\,\delta_{ij} + \eta\left(\frac{\partial u_j}{\partial x_i} + \frac{\partial u_i}{\partial x_j}\right)$$

(71)

are the components of the stress tensor, and

$$n_j = \frac{x_j}{R}$$

(72)

are the components of the unit normal to S.

For the disturbed flow we find

$$\frac{dW}{dt} = \frac{8}{3}\,\pi\eta\,a_{ij}a_{ij}R^3 + \frac{32}{3}\,\pi\,\eta\,A_{ij}g_{ij}$$

(73)

where the $a_{ij} = \frac{1}{2}(g_{ij} + g_{ji})$ are the components of the local distortion in the undisturbed flow. On the other hand, the well-known formula of Stokes gives, for the undisturbed flow

$$\frac{dW}{dt} = \frac{8}{3}\,\pi\eta\,a_{ij}a_{ij}R^3$$

(74)

We thus obtain an expression for Δ , the extra dissipation of energy when the particle is present, namely

$$\Delta = \frac{32}{3}\,\pi\,\eta\,A_{ij}g_{ij}$$

(75)

If we split g_{ij} into its symmetric and skew-symmetric parts, we have

$$\Delta = \frac{32}{3}\,\pi\,\eta\,(A_{ij}a_{ij} + A_{ij}\xi_{ij})$$

(76)

where $\xi_{ij} = \frac{1}{2}(g_{ij} - g_{ji})$. Jeffrey, as a consequence of the dynamical assumption mentioned above, was working with symmetrical A_{ij}, and so naturally obtained only the first term in our expression for Δ; and it appears that Simha, although he removed the restriction on A, failed to find the second term. The consequence of this for his calculation will now be discussed.

2.6. The Particle Rotation

Simha takes the average angular velocity to be zero and on this basis calculates his well known formula for ν (equation 9), a formula which has been shown to give good agreement with observations (Mehl, Oncley & Simha, 1940, Tanford, 1961). A few years later, Saito (1951) using the assumption that the particles should rotate on average with the local undisturbed rotation of the fluid obtained precisely the same result; he suggested that Simha "has committed some errors in calculation" but does not investigate the matter further. Using Jeffrey's notation (Table 4) we have:

$$A_{ij}a_{ij} = (A\underline{a} + B\underline{b} + C\underline{c}) + (F + F')\underline{f} + (G + G)\underline{g} + (H + H')\underline{h}$$

$$\tag{77}$$

$$A_{ij}\xi_{ij} = (F' - F)\xi + (G' - G)\eta + (H' - H)\zeta$$

$$\tag{78}$$

whilst the values of, for example, F and F' are

$$F = \frac{\beta_o \underline{f} - c^2\alpha_o'(\xi - \omega_1)}{2\alpha_o' (b^2\beta_o + c^2\gamma_o)}$$

$$\tag{79}$$

$$F' = \frac{\gamma_0 \underline{f} + b^2 \alpha_0' (\xi - \omega_1)}{2\alpha_0' (b^2 \beta_0 + c^2 \gamma_0)} \qquad (80)$$

In Jeffrey's paper the α_0' etc. in the numerators of the above expressions are misprinted as α_0 etc.

We can thus deduce that

$$(F + F')\underline{f} = \frac{\dfrac{2\alpha_0''}{\alpha_0'} \underline{f}^2 + (b^2 + c^2)\underline{f}^2 + (b^2 - c^2)(\xi - \omega_1)\underline{f}}{2(b^2\beta_0 + c^2\gamma_0)} \qquad (81)$$

$$(F' - F)\xi = \frac{(b^2 - c^2)\underline{f}\xi + (b^2 + c^2)(\xi - \omega_1)\xi}{2(b^2\beta_0 + c^2\gamma_0)} \qquad (82)$$

where we have utilised the various relations between α_0, β_0 etc. that are given by Jeffrey.

Now Simha apparently did not find the $A_{ij} \xi_{ij}$ term and thus would not have had terms like $(F' - F)$ in his calculation. We can see, however, that taking $\omega_1 = 0$ as he apparently did, in the $(F + F')\underline{f}$ term gives the same final result as taking $\omega_1 = \xi$ in the sum of the $(F + F')\underline{f}$ and the $(F' - F)\xi$ terms. Since the same argument applies to the other terms we conclude that Simha's formula (equation 9) although incorrect for $\omega_1 = 0$ on account of the omission of the term $A_{ij} \xi_{ij}$, is, by a lucky coincidence, actually correct if $\omega_1 = \xi$, $\omega_2 = \eta$, $\omega_3 = \zeta$.

It is worth noting that if one does take $\omega_1 = 0$ and includes the $A_{ij} \xi_{ij}$ term, one obtains for spherical particles $\nu = 4$, in contrast to Einsteins (1906, 1911) value of 2.5. The result $\nu = 4$ for $\omega_i = 0$ agrees

with that previously found by Brenner (1970). In all that follows we take the assumption that $\omega_1 = \xi$ etc. i.e. that the particles are on average rotating with the local angular velocity of the fluid.

2.7. The Calculation of ν

To complete our calculation we take, as before, the given flow to be locally a simple shearing flow with shear rate G. The principal axes of any particular particle will not in general coincide with the shear axes but, using the Euler angles to describe relative orientation of the two sets of axes, we can calculate the components g_{ij} relative to the particle axes in terms of G and the Euler angles θ, ϕ and ψ. Hence we can obtain Δ for that particle as a function of these variables; the details can be found at least for a special case in Jeffrey's paper (1922). Since Jeffrey's calculations show that the A_{ij} are linear in the g_{ij}'s, it follows that Δ will involve G^2 as a factor and hence that the total dissipation will be of the form ηG^2 as originally asserted.

To find the total dissipation in unit volume we average the effects of the N particles on the assumption that they are randomly oriented, obtaining

$$\bar{\Delta} = \frac{N}{2\pi} \int_0^{2\pi} \left\{ \frac{1}{4\pi} \int_0^{2\pi} \int_0^{\pi} \Delta(\theta,\phi,\psi) \sin\theta \, d\theta \, d\phi \right\} d\psi$$

(83)

The integrations yield

$$\bar{\Delta} = \frac{32}{3} \pi \eta \, NG^2 Z$$

(84)

where

$$Z = \frac{1}{30} \left(\frac{\alpha''_o + \beta''_o + \gamma''_o}{\beta''_o \gamma''_o + \gamma''_o \alpha''_o + \alpha''_o \beta''_o} \right)$$

$$+ \frac{1}{40} \left[\frac{\beta_o + \gamma_o}{\alpha'_o(b^2\beta_o + c^2\gamma_o)} + \frac{\gamma_o + \alpha_o}{\beta'_o(c^2\gamma_o + a^2\alpha_o)} + \frac{\alpha_o + \beta_o}{\gamma'_o(a^2\alpha_o + b^2\beta_o)} \right] \tag{85}$$

Thus ν is determined from

$$\eta\nu V G^2 = \eta\nu N \frac{4}{3} \pi abc G^2 = \frac{32}{3} \pi\eta N G^2 Z \tag{86}$$

as

$$\nu = \frac{8Z}{abc} \tag{87}$$

Hence on substituting for Z we obtain

$$\nu = \frac{1}{abc} \left\{ \frac{4(\alpha''_o + \beta''_o + \gamma''_o)}{15(\beta''_o\gamma''_o + \gamma''_o\alpha''_o + \alpha''_o\beta''_o)} + \frac{1}{5} \left[\frac{\beta_o + \gamma_o}{\alpha'_o(b^2\beta_o + c^2\gamma_o)} + \right. \right.$$

$$\left. \left. \frac{\gamma_o + \alpha_o}{\beta'_o(c^2\gamma_o + a^2\alpha_o)} + \frac{\alpha_o + \beta_o}{\gamma'_o(a^2\alpha_o + b^2\beta_o)} \right] \right\} \tag{88}$$

where a,b,c are the semi-axes, and the elliptic integrals α_o etc. now depend on a,b and c (Appendix I).

The formula reduces to the Simha-Saito formula (equation 9) when $b=c$, and gives Einstein's value of 2.5 when $a=b=c$. It may be of interest to note that had we followed Simha in taking $\omega_i = 0$ then Z would have contained the following term in addition to those given above,

$$\frac{1}{24} \left\{ \frac{b^2 + c^2}{b^2\beta_o + c^2\gamma_o} + \frac{c^2 + a^2}{c^2\gamma_o + a^2\alpha_o} + \frac{a^2 + b^2}{a^2\alpha_o + b^2\beta_o} \right\}$$

(89)

It is the presence of this added term that gives the value of $\nu = 4$ for spheres rather than the Einstein value $\nu = 2.5$ which is obtained when it is absent. The value of 2.5 has been confirmed experimentally for polystyrene latex spheres by Cheng & Schachman (1955).

2.8. Discussion

An equation similar to (88) was given by Batchelor (1970) on the assumption that the suspended particles, although randomly oriented, moved so that zero __hydrodynamic__ torque acted upon them. His result was

$$\nu = \frac{1}{abc} \left\{ \frac{4(\alpha_o'' + \beta_o'' + \gamma_o'')}{15(\beta_o''\gamma_o'' + \gamma_o''\alpha_o'' + \alpha_o''\beta_o'')} + \frac{2}{5} \left[\frac{1}{\alpha_o'(b^2 + c^2)} + \right. \right.$$

$$\left. \left. \frac{1}{\beta_o'(c^2 + a^2)} + \frac{1}{\gamma_o'(a^2 + b^2)} \right] \right\}$$

(90)

when written in the same notation as we have used before. It does not seem likely that (90) would be applicable to the case of overwhelming Brownian motion since one would need to include the __Brownian torque__ T_B as well as the purely hydrodynamic torque, T_H in satisfying the

condition of zero net torque, i.e.

$$T_B + T_H = 0 \qquad\qquad (91)$$

Random orientation alone is not a sufficient characterisation of overwhelming Brownian motion since one also needs to describe correctly the distribution of the angular velocity. Both (88) and (90) are obtained by methods that avoid the full statistical treatment of the angular motion but as explained earlier we consider the simplified model underlying (88) to be the appropriate one for overwhelming Brownian motion. In effect, formula (88) generalises the Simha-Saito equation for ellipsoids of revolution, whilst (90) generalises formulâe of Jeffrey for ellipsoids of revolution. In general the two formulae give quite different results as can be seen from Figure 25 and Table 5, both of which are for convenience restricted to the case of ellipsoids of revolution. Since (90) does not reduce to the classical Simha-Saito formula the classic experimental evidence on macromolecules which favours the latter (Mehl, et al, 1940, Lauffer, 1942) strengthens the view that (90) is incorrect. More recent experimental evidence is given by Tanford (1961) who allows for particle swelling due to solvation and Table 6 extends his tables to include a comparison with the Jeffrey-Batchelor equation. The table compares the axial ratio inferred from translational diffusion experiments with that inferred from viscometric experiments on the basis first of the Simha-Saito equation and secondly of the Jeffrey-Batchelor equation. Tanford (1961) says "within the accuracy of the measurements, the description of globular proteins in aqueous solution provided by the (Simha-Saito) equation is identical with that provided by (translational)

diffusion". On the other hand we see that the Jeffrey-Batchelor equation gives values of the axial ratio that are consistently too high and outside the expected experimental error bounds. We conclude that (90) is not applicable to the cases of interest to the molecular biologist.

As previously stated, we have avoided the full statistical treatment of the angular motion but have made the assumption of particles being on average at rest in the local referential frame in which they are suspended to be appropriate for the case of overwhelming Brownian motion. Although this has been rigorously proved only for axisymmetric particles (Brenner, 1972), we have made the assumption that it will be a good approximation for general tri-axial ellipsoids, at least for low axial ratios.

Since the derivation of equation (88) a general analysis using the full statistical treatment of the angular motion has been given by Rallison (1978). His results for the case of overwhelming Brownian motion show that to first-order in the shear rate the non-Newtonian stress effects vanish, which is consistent with our assumption of Newtonian behaviour for very low shear rates. He also gives an expression for ν correct to first-order in the shear rate, although not in the form of a simple formula like equation (88), but by using numerical methods Rallison is able to give a plot of ν for various axial ratios; the results are clearly very close to those obtained from equation (88) - compare my Figure 26 with Rallison's Figure 7. However, an exact comparison (personal communication by J.M. Rallison) shows a very slight discrepancy between values from equation (88) and Rallison's procedure, although no difference at levels likely to be experimentally significant for globular particles (i.e. a/b: 1.0 - 3.0, b/c: 1.0 - 3.0) is observed, and the discrepancy is not

apparent within four significant figures for a/b: $1.0 \to 2.0$, b/c: $1.0 \to 2.0$. The values given in Table 7 are therefore definitive.

It has been indicated to us (J.M. Rallison, H. Brenner, private communications of unpublished work) that our formula requires the addition of a very small term related to the deviation from our assumed condition of non-axisymmetric particles rotating on average with the local angular velocity of the fluid:

$$- \frac{1}{5abc} \left\{ \frac{\left[\dfrac{a^2 - b^2}{a^2\alpha_0 + b^2\beta_0} + \dfrac{b^2 - c^2}{b^2\beta_0 + c^2\gamma_0} + \dfrac{c^2 - a^2}{c^2\gamma_0 + a^2\alpha_0} \right]^2}{\left[\dfrac{a^2 + b^2}{a^2\alpha_0 + b^2\beta_0} + \dfrac{b^2 + c^2}{b^2\beta_0 + c^2\gamma_0} + \dfrac{c^2 + a^2}{c^2\gamma_0 + a^2\alpha_0} \right]} \right\} \qquad (88b)$$

The numerical results show our approximation to be extremely accurate for 'globular' particles, as noted above, but for certain particles of higher asymmetry calculations suggest that deviations of up to 1% in ν can arise. It is clear though that our formula provides a good approximation over the entire molecular range. Of particular interest is the fact that the discrepancy tends asymptotically to zero for ellipsoids whose axes are all substantially different in length (i.e. $a \gg b \gg c$ - "tapes").

Table 4. **The relation between the notation used in this study**

and that used by Jeffrey (1922)

$$(A_{ij}) = \begin{pmatrix} A & H & G' \\ H' & B & F \\ G & F' & C \end{pmatrix} \quad ,$$

$$(a_{ij}) = \begin{pmatrix} \underset{\sim}{a} & \underset{\sim}{h} & \underset{\sim}{g} \\ \underset{\sim}{h} & \underset{\sim}{b} & \underset{\sim}{f} \\ \underset{\sim}{g} & \underset{\sim}{f} & \underset{\sim}{c} \end{pmatrix} \quad ,$$

$$(\xi_{ij}) = \begin{pmatrix} 0 & -\zeta & \eta \\ \zeta & 0 & -\zeta \\ -\eta & \xi & 0 \end{pmatrix} \quad .$$

Table 5

ν for an ellipsoid of revolution calculated from the Simha — Saito
equation and the Batchelor — Jeffrey equation

Axial Ratio	Prolate Model		Oblate Model	
	S — S	B — J	S — S	B — J
1.0	2.500	2.500	2.500	2.500
2.0	2.908	2.583	2.854	2.610
3.0	3.685	2.786	3.431	2.868
4.0	4.663	3.077	4.059	3.198
5.0	5.806	3.434	4.708	3.563
6.0	7.099	3.844	5.367	3.947
7.0	8.533	4.302	6.032	4.342
8.0	10.103	4.804	6.700	4.744
9.0	11.804	5.346	7.371	5.151
10.0	13.634	5.928	8.043	5.562

Table 6

Extension of Tanford's Tables ("Physical Chemistry of Macromolecules",
1961, Wiley & Sons, p 359 and 395) to compare the axial ratios
predicted by the Simha-Saito equation and the Batchelor-Jeffrey
equation, using a 0.2 grams/gram solvation for four globular proteins.

		Prolate			Oblate		
		Diffusion	S-S	B-J	Diffusion	S-S	B-J
	υ	a/b	a/b	a/b	a/b	a/b	a/b
Ribonuclease	3.6	2.1	2.9	5.5	2.2	3.4	5.3
β-lactoglobulin	3.6	3.7	2.9	5.5	4.0	3.4	5.3
Serum albumin	4.0	4.9	3.3	6.5	5.0	4.0	6.3
Hemoglobin	3.8	2.1	3.1	6.0	2.2	3.6	5.8

Table 7. Values of ν as a function of (a/b, b/c) for a general tri-axial ellipsoid (a>b>c)

(on the basis of equation 88)

a/b \ b/c	1.0 (Prolate Ellipsoid)	1.1	1.2	1.3	1.4	1.5	1.6	1.7	1.8	1.9	2.0
1.0 (Oblate Ellipsoid)	2.500	2.507	2.524	2.550	2.583	2.620	2.661	2.706	2.753	2.803	2.854
1.1	2.507	2.520	2.544	2.576	2.614	2.656	2.702	2.751	2.803	2.857	2.913
1.2	2.525	2.545	2.575	2.612	2.655	2.703	2.754	2.808	2.865	2.923	2.983
1.3	2.553	2.579	2.615	2.658	2.706	2.579	2.815	2.874	2.935	2.998	3.063
1.4	2.588	2.621	2.662	2.711	2.764	2.822	2.883	2.947	3.013	3.081	3.151
1.5	2.630	2.668	2.716	2.770	2.829	2.892	2.958	3.027	3.098	3.171	3.245
1.6	2.677	2.722	2.775	2.834	2.899	2.967	3.039	3.113	3.189	3.267	3.346
1.7	2.729	2.779	2.839	2.904	2.974	3.047	3.124	3.204	3.285	3.368	3.453
1.8	2.785	2.842	2.907	2.978	3.053	3.132	3.215	3.300	3.386	3.475	3.565
1.9	2.844	2.908	2.978	3.055	3.137	3.222	3.310	3.400	3.492	3.586	3.681
2.0	2.908	2.977	3.054	3.137	3.224	3.315	3.408	3.504	3.602	3.702	3.803
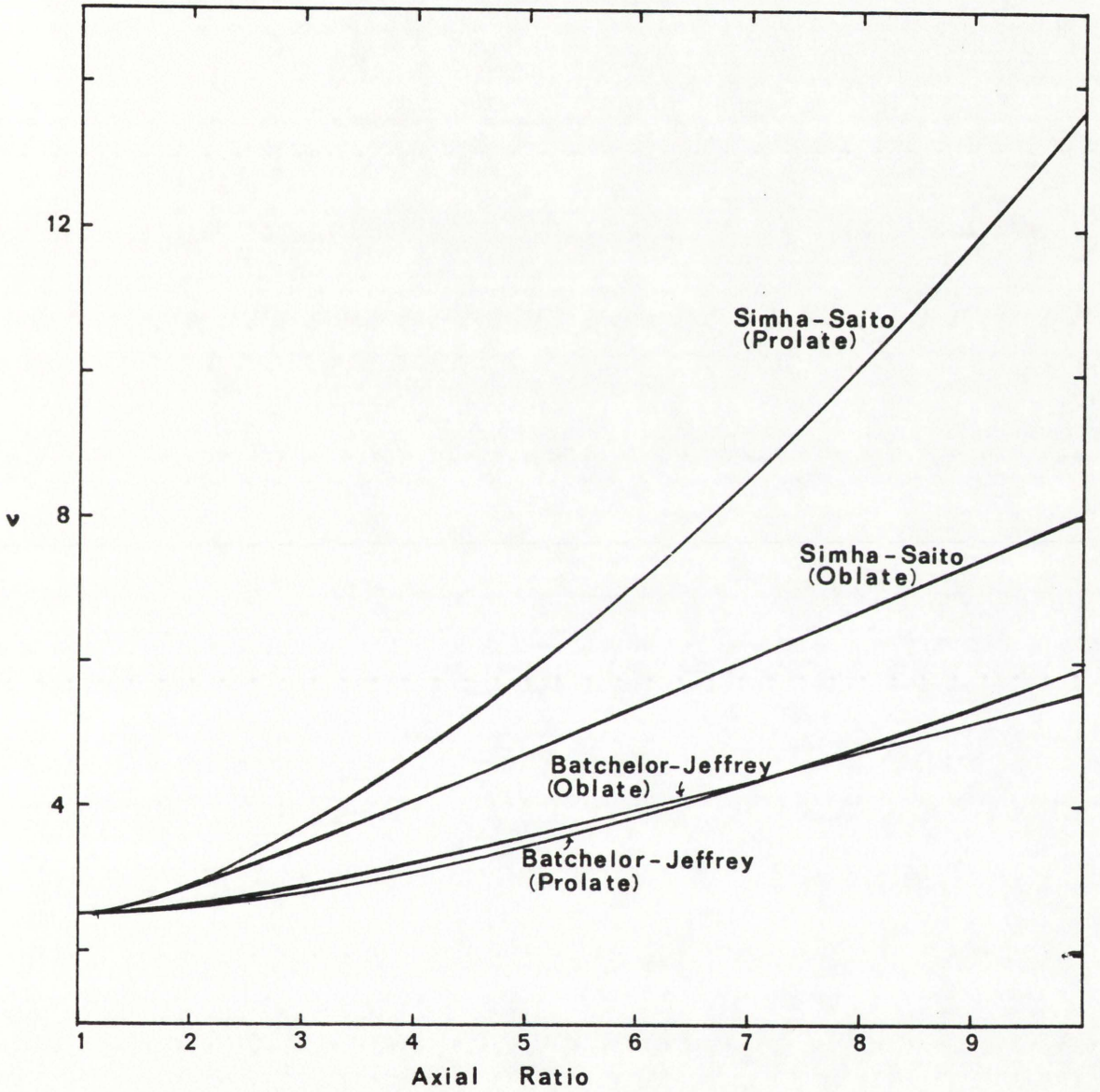
<u>Figure 25.</u> <u>A comparison of the values of ν as a function of axial ratio</u>

<u>predicted by the Simha – Saito and Batchelor – Jeffrey equations</u>

<u>for ellipsoids of revolution</u>
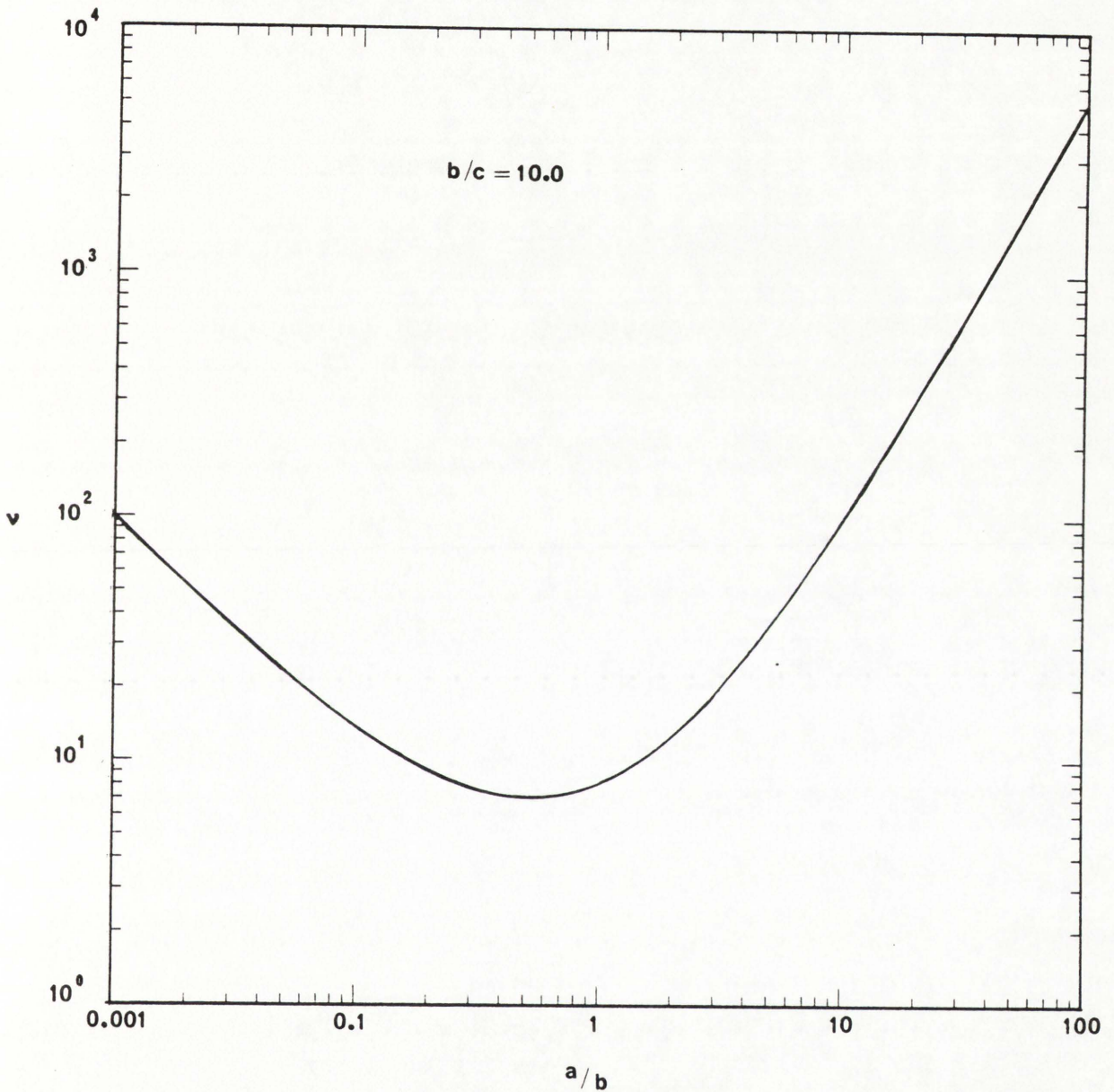
Figure 26. Plot of ν as a function of a/b when b/c = 10.0 (a>b>c) determined from equation (88). This plot agrees very closely with that from the numerical procedure of Rallison (Figure 7, 1978)

N.B. Rallison has c>a>b

C H A P T E R   3

Numerical Inversion Procedures:

The Problem of the Line Solution

3.1 Solution of the Elliptic Integrals

In order to determine the viscosity increment ν that corresponds to a particular value of the axial ratios a/b, b/c, the elliptic integrals α_0 etc. (Appendix I) must be solved. Analytic solutions are not possible but the integrals can be solved numerically with the aid of a high speed computer. The subroutine used for this was the United Kingdom NAG Mk. 6 routine DO1AGF which evaluates a definite integral of the form

$$ I = \int_A^B f(t) dt $$

where A=0, using an interval subdivision strategy developed by Oliver (1972) and based on Clenshaw–Curtis quadrature (1960). Since infinity cannot be used as the upper limit, a finite value of B must be specified. However, a satisfactory value for B can be determined by using successively higher values until the value of the integral converges to a limiting value; in this case a value for B of 10^6 was sufficient. Higher values are also suitable although evaluation of the integral takes longer. The number of interval subdivisions is also specifiable by the user; the maximum number of 50 was used. The routine also estimates the error on the integrals (O'Hara & Smith, 1968). If this error is greater than the maximum allowable error specifiable by the user the routine will stop and print an error message. The maximum allowed absolute error specified was 1.0×10^{-8} ($\equiv .001\%$). The subroutine for evaluating the elliptic integrals can easily be incorporated into a program for evaluating ν for a given value of (a/b, b/c). This is given in Appendix V as Program 1.

3.2. Application to the Crystallographic Dimensions of Myoglobin; Numerical Inversion

The result can be applied to crystallographic data available for

myoglobin. Kendrew et al (1958) gave the dimensions of sperm whale

myoglobin to be 43 x 35 x 23 $\overset{o}{A}$ (Table 3). This corresponds to a general

tri-axial ellipsoid of semi-axes a = 21.5, b = 17.5 and c = 11.5 $\overset{o}{A}$, and

axial ratios a/b = 1.23, b/c = 1.52. Using Program 1 (Appendix V) this

corresponds to a viscosity increment of 2.729. The predicted intrinsic

viscosity can then be found from equation (8):

$$[\eta] = \nu \bar{v}_s \equiv \nu \bar{v} \left(\frac{\bar{v}_s}{\bar{v}} \right)$$

(92)

where $(\bar{v}_s/\bar{v})$ is the swelling ratio (section 1.7.1). By fitting data

of reduced specific viscosity against concentration (Table 8, Figure 27)

I have determined the intrinsic viscosity of myoglobin to be (3.25 $\pm$ .05)

ml/gm, using a weighted least squares analysis (straight line fit).

The concentrations were determined using a high precision auto density

meter (Kratky et al, 1969, 1973) together with a $\bar{v}$ for myoglobin of .741

ml/gm (Theorell, 1934):

$$c_i = \frac{\rho_i - \rho_o}{1 - \bar{v}\rho_o}$$

(93)

where ρ_o is the solvent density and ρ_i the solute densities. Use of the

auto density meter, which is based on the time taken to perform a

preset number of oscillations of a U-tube filled with the sample has

the added advantage that, besides being very accurate, only small amounts

of fluid are required (~1 ml). The experimental arrangement used for

the viscosity and densimetric work is illustrated in Figure 28. The

platinum resistance thermometer shown was used to monitor the sample temperatures to accuracies of .005 degrees and was calibrated by myself. In order that the crystallographic dimensions gives this same value for $[\eta]$, from equation (92), a swelling ratio $(\bar{v}_s/\bar{v})$ of 1.6 is required; alternatively myoglobin is more asymmetric in solution.

In order to determine the actual dimensions of the equivalent tri-axial ellipsoid for myoglobin in solution (or any other macromolecule) from the experimental value for $[\eta]$, the situation is more complicated however. Although equation (88) defines a unique value of ν for a given value of (a/b, b/c), an analytic inversion of (88) to produce an explicit expression for (a/b, b/c) in terms of ν is not available. The inversion must therefore be done numerically by tabulating, or better plotting ν as a function of (a/b, b/c). The same subroutine mentioned in section 3.1. for evaluating the elliptic integrals may be incorporated. A perusal of Table 7 (produced from Program 2) reveals however that a given value of ν does not correspond to a unique value of (a/b, b/c) but to a 'line solution' of possible values of (a/b, b/c). This is clearly illustrated in the contour plot (Figure 29) produced from Program 3 using GHOST graphical facilities where ν is incremented from 2.5 to 7.0 in steps of 0.5. In order to determine a unique solution for (a/b, b/c) and hence the axial dimensions of a macromolecule in solution other hydrodynamic information must be used; we must therefore consider the translational and rotational frictional properties (section 1.2).

3.3. Other Tri-axial Line Solutions

3.3.1. The Translational Frictional Ratio; the β and R Functions

It was previously stated in section 1.4. that although Perrin (1936) had provided an explicit formula for the translational frictional ratio of a general tri-axial ellipsoid in terms of the axial ratios (a/b, b/c), the elliptic integral in equation (12) could only be solved analytically for the special case of ellipsoids of revolution (i.e. two equal axes). However, since the elliptical integral is similar to those for the tri-axial viscosity increment, it too can now be solved numerically using for example the subroutine discussed in section 3.1. A higher value for the upper limit, B was required: 5×10^{7}. A table of values of the Perrin function f/f_{o} ($\equiv$P) for values of a/b and b/c was thus obtained (Table 9). Again, a perusal of the table reveals that a given value of P has a line solution of possible values of (a/b, b/c). However, in principle at least, by combining the line solution for P of a given macromolecule with the line solution for ν, a unique solution for (a/b, b/c) can in principle be found from their intersection. This can be illustrated by assuming a particle of (a/b, b/c) = (1.5, 1.5), calculating the corresponding values for ν and P using Program 1, and then plotting the line solutions using Program 4. Unfortunately Figure 30 reveals that the intersection for accuracies in ν and P to four significant figures is very shallow, and allowing for $\pm$ 1% experimental error in each there is no intersection at all in the 'globular protein' range of the Figure. There is also the additional problem that in order to determine experimentally both ν and P, knowledge is required of the swollen volume in solution.

However, now that ν and P are available for tri-axial ellipsoids, then so should the β and R functions which do not require a knowledge of the swollen volume (equations 45 & 64). I have thus produced tables of these also (Tables 10 & 11); all four tri-axial functions so far mentioned viz ν, P, β and R are plotted in Figure 31 allowing for $\pm$ 1% experimental error in each. There is still no reasonable intersection; the β function is, as expected, seen to be of little practical use as it is very sensitive to experimental error (the β - 1% line is completely off the map area). Of the 4 functions however, the R function is the most useful since it is relatively insensitive to experimental error and the experimental determination does not require a knowledge of the swollen volume (section 1.7.1.). In order to find a unique solution for (a/b, b/c) therefore, this should ideally be combined with a rotational frictional or relaxation tri-axial shape function which should satisfy the following criteria:

(i) provides a suitable intersection with R

(ii) is relatively insensitive to experimental error but sensitive to axial ratio

(iii) is experimentally measurable to a high precision with currently available apparatus and data analytic techniques and

(iv) does not require a knowledge of the swollen volume for its experimental determination.

3.3.2. <u>The Rotational Frictional, Diffusion and Relaxation Line Solutions</u>

For a tri-axial ellipsoid there will be three rotational frictional ratios ζ_i/ζ_0 (i=a,b,c) corresponding to rotation about each of the three axes and hence three rotational diffusion ratios θ_i/θ_0. By analogy with the translational case in the previous section, although Perrin (1934) had

given explicit formula for the ζ_i/ζ_o in terms of (a/b, b/c), - eqn. (25),

the elliptic integrals could only be solved analytically for the

case of ellipsoids of revolution. The integrals can now be solved

numerically, again utilising the routine described in section 3.1 (Programs

1,2 & 4). There is however no experimental technique for determining the

rotational frictional or diffusion coefficients directly; rotational

experiments determine rather relaxation time ratios. For example, the

dielectric dispersion relaxation time ratios are related to the rotational

frictional and diffusion ratios by equations (27). A plot of the

rotational relaxation time ratio line solutions corresponding to (a/b, b/c)

= (1.5, 1.5) is given together with the R function in Figure 32.

Unfortunately, because of the difficulties raised in 1.5.1. resolution of

the dielectric dispersion curve into the 3 relaxation times for a

homogeneous solution of tri-axial ellipsoid particles is impossible in

practice.

Whereas for ellipsoids of revolution there are three fluorescence

anisotropy decay times (equation 42), for general tri-axial ellipsoids,

there will be five (Cantor & Tao, 1971, Small & Isenberg, 1977) related

to the three rotational diffusion coefficients by:

$$\tau_1 = \frac{1}{3(\theta + \theta_1)} \quad ; \quad \tau_2 = \frac{1}{3(\theta + \theta_2)} \quad ; \quad \tau_3 = \frac{1}{3(\theta + \theta_3)}$$

$$\tau_4 = \frac{1}{2(3\theta - \Delta)} \quad ; \quad \tau_5 = \frac{1}{2(3\theta + \Delta)} \tag{94}$$

where $\theta = (\theta_1 + \theta_2 + \theta_3)/3$ is the mean rotational diffusion coefficient,

and Δ is defined by

$$\Delta = (\theta_1^2 + \theta_2^2 + \theta_3^2 - \theta_1\theta_2 - \theta_2\theta_3 - \theta_3\theta_1)^{\frac{1}{2}}$$

The fluorescence anisotropy relaxation time ratios τ_j / τ_o can thus be evaluated (equation 42, where j is now = 1,2,3,4,5); these have been tabulated by Small & Isenberg (1977) and are plotted in Figure 33, for (a/b, b/c) = (1.5, 1.5). Consideration of these functions however, at the moment at least, is purely academic; besides the problems cited in section 1.5.4., the necessary resolution of the decay curve into its four component exponentials (since $\tau_5 \sim \tau_1$) is impossible (Small & Isenberg, 1977). Furthermore, since neither the fluorescence anisotropy decay time ratios nor the dielectric dispersion relaxation time ratios for tri-axial ellipsoids are of apparent use at the moment, the same must be true of their corresponding swelling independent functions, the explicit expressions in terms of axial ratio being obtainable from:

$$\delta_i = \frac{\zeta_o}{\zeta_i} \nu \quad ; \quad \mu_i = \left(\frac{f_o}{f}\right) \left(\frac{\zeta_i}{\zeta_o}\right)^{1/3}$$

$$(95, 96)$$

$$\gamma_i = \left(\frac{f}{f_o}\right)^3 \frac{\rho_o}{\rho_i} \quad ; \quad \varepsilon_i = \nu \frac{\rho_o}{\rho_i}$$

$$(97, 98)$$

$$\kappa_j = \nu \left(\frac{\tau_o}{\tau_j}\right) \quad ; \quad \xi_j = \left(\frac{f}{f_o}\right)^3 \frac{\tau_o}{\tau_j}$$

$$(99, 100)$$

where i=a,b,c and j=1,2,3,4,5. The relations for these functions in terms of experimental parameters have already been given in section 1.7.

Evaluation of the harmonic mean rotational relaxation time ratio in terms of axial ratio for tri-axial ellipsoids we can similarly obtain from

$$\frac{\tau_h}{\tau_o} = \frac{3}{\left(\dfrac{\rho_o}{\rho_a} + \dfrac{\rho_o}{\rho_b} + \dfrac{\rho_o}{\rho_c}\right)}$$

(101)

(Programs 1, 2 & 4, Figure 34). The corresponding swelling independent functions Ψ and Λ determined by combining with the translational frictional ratio and the viscosity increment respectively we can now also obtain from

$$\Psi = \left(\frac{\tau_o}{\tau_h}\right)^{\frac{1}{3}} \left(\frac{f}{f_o}\right)$$

(102)

$$\Lambda = \left(\frac{\tau_o}{\tau_h}\right) \nu$$

(103)

(Programs 1,2 & 4, Figure 34). Unfortunately, these functions are generally very sensitive to experimental error, as Figure 35 illustrates; also the problems in determining the harmonic mean relaxation time raised in 1.5.4. still apply.

3.3.3 Electric Birefringence Decay: the δ_+ and δ_- Functions

In section 1.5.2. we stated that Ridgeway (1966, 1968) has shown that the decay of electric birefringence for a homogeneous suspension of asymmetric macromolecules (e.g. tri-axial ellipsoids) would consist of two exponential terms:

$$\Delta n = \frac{N}{2n_\ell} \left\{ A_+ e^{-6\theta_+ t} + A_- e^{-6\theta_- t} \right\}$$

(32)

where Δn is the birefringence, N the number density of particles in suspension and n_ℓ the refractive index of the suspending medium. A_+ and A_- are complicated functions depending on the initial orientation of the particles and their dielectric and diffusion properties. We may rewrite $NA_\pm / 2n_\ell$ as $A'_\pm$, the 'pre-exponential factors'. Equation (32) then becomes:

$$\Delta n = A'_+ e^{-6\theta_+ t} + A'_- e^{-6\theta_- t}$$

$$(104)$$

θ_+ and θ_- are related to the rotational diffusion constants θ_i (and hence the rotational frictional coefficients since $\zeta_i = kT/\theta_i$) by

$$\theta_\pm = \frac{1}{3} \sum \theta_i \pm \left\{ \left(\frac{1}{3} \sum \theta_i \right)^2 - \frac{1}{3} \sum_i \sum_{i>j} \theta_i \theta_j \right\}^{\frac{1}{2}}$$

$$(105a)$$

$$= \frac{kT}{3} \left\{ \sum_i \frac{1}{\zeta_i} \pm \left(\sum_i \frac{1}{\zeta_i^2} - \sum_i \sum_{i>j} \frac{1}{\zeta_i \zeta_j} \right)^{\frac{1}{2}} \right\}$$

$$(105b)$$

The dimensions of equation (105) are of energy/(volume x viscosity) we therefore 'reduce' it to a function of shape alone:

$$\theta_\pm^{red} \equiv \left(\frac{\eta_o}{kT} \right) V_e \theta_\pm = \frac{abc}{12} \left\{ \left(\frac{1}{\zeta_a''} + \frac{1}{\zeta_b''} + \frac{1}{\zeta_c''} \right) \right.$$

$$\left. \pm \left[\left(\frac{1}{\zeta_a''^2} + \frac{1}{\zeta_b''^2} + \frac{1}{\zeta_c''^2} \right) - \left(\frac{1}{\zeta_a'' \zeta_b''} + \frac{1}{\zeta_b'' \zeta_c''} + \frac{1}{\zeta_c'' \zeta_a''} \right) \right]^{\frac{1}{2}} \right\} \quad (106)$$

where

$$\zeta_a'' = \frac{b^2 + c^2}{b^2 \beta_o + c^2 \gamma_o} \; ; \quad \zeta_b'' = \frac{c^2 + a^2}{c^2 \gamma_o + a^2 \alpha_o} \; ; \quad \zeta_c'' = \frac{a^2 + b^2}{a^2 \alpha_o + b^2 \beta_o} \quad (107)$$

The elliptic integrals α_o etc. are those defined by Jeffrey (1922) and are given in Appendix I.

A plot of the θ_+^{red} and θ_-^{red} functions, together with the R function corresponding to the point (a/b, b/c) = (1.5, 1.5) allowing for $\pm$ 1% experimental error is given in Figure 36. It is seen that the intersections are very reasonable (the θ_+^{red} - R intersection is nearly orthogonal) and the functions are relatively sensitive to axial ratio. However, experimental determination of $\theta_\pm^{red}$ requires of course knowledge of the swollen molecular volume in solution (equation 106). This can be conveniently eliminated however in the standard way by combining (106) either with the viscosity increment (8) or the translational frictional ratio (20b). If for example (106) is combined with the viscosity increment (8), swelling independent $\delta_\pm$ functions are produced (Tables 12, 13, Figure 37):

$$\delta_\pm = 6\theta_\pm^{red} \, \nu \equiv \frac{6}{N_A k} \left(\frac{\eta_o \theta_\pm}{T}\right) [\eta] \, M_r$$

(108)

where [η] is expressed in ml/gm. Alternatively, $\theta_\pm^{red}$ can be combined with the translational frictional ratio (20b) to give swelling independent $\gamma_\pm$ functions (Programs 1,2,4, Figure 38):

$$\gamma_\pm = 6\theta_\pm^{red} \left(\frac{f}{f_o}\right)^3 \equiv \frac{M_r^3 (1 - \bar{v} \rho_o)^3 \theta_\pm}{27 N_A kT \pi^2 \eta_o^2 s^3}$$

(109)

The $\delta_\pm$ and $\gamma_\pm$ functions are new. The $\delta_\pm$ functions are preferred over the $\gamma_\pm$ functions since they require fewer experimental measurements and do not involve squared or cubed terms; hence in principle can be measured more

accurately. It is seen therefore that combination of the R-function

with the $\delta_{\pm}$ functions as a method for determining a unique solution for

the axial ratios (and hence the axial dimensions, if V_e is known from

k_η/k_s - section 1.7.1) of a macromolecule in solution satisfies the

criteria (i), (ii) and (iv) of section 3.3.1. In order for the method to

satisfy criterion (iii) however, there still remains the problem of

resolving the exponential decay term into its 2 component relaxation times

or decay constants (the same is true of course for the $\theta_{\pm}^{red}$ and $\gamma_{\pm}$

functions). To date this has not been possible. We now show that with

a new 'constrained' least squares algorithm using intersection with the

R-curve as the constraint, this is now possible with currently available

experimental precision.

Table 8. Values of reduced specific viscosity for various concentrations of sperm whale myoglobin (0.1M NaCl buffer, pH = 7.1)

Concentration, c (mg/ml)	η_{rel}	η_{sp}/c (ml/gm)
90.2	1.450	4.99
66.1	1.298	4.51
53.3	1.224	4.20
50.2	1.215	4.29
40.7	1.163	4.00
34.4	1.138	4.02
30.5	1.116	3.81
29.6	1.115	3.89
23.2	1.084	3.61
15.5	1.055	3.57
9.7	1.034	3.47
8.1	1.028	3.50

Table 9. Values of P as a function of (a/b, b/c) for a general tri-axial ellipsoid (a>b>c)

a/b \ b/c	1.0 (Prolate Ellipsoid)	1.1	1.2	1.3	1.4	1.5	1.6	1.7	1.8	1.9	2.0
1.0 (Oblate Ellipsoid)	1.000	1.001	1.003	1.006	1.010	1.014	1.019	1.025	1.030	1.036	1.042
1.1	1.001	1.002	1.005	1.009	1.014	1.019	1.024	1.030	1.036	1.042	1.049
1.2	1.003	1.005	1.009	1.013	1.018	1.024	1.030	1.036	1.043	1.049	1.056
1.3	1.006	1.009	1.013	1.018	1.024	1.030	1.037	1.043	1.050	1.057	1.064
1.4	1.010	1.014	1.019	1.024	1.030	1.037	1.044	1.051	1.058	1.065	1.073
1.5	1.015	1.019	1.024	1.031	1.037	1.044	1.051	1.059	1.066	1.074	1.082
1.6	1.020	1.025	1.031	1.037	1.044	1.052	1.059	1.067	1.075	1.083	1.091
1.7	1.026	1.031	1.037	1.044	1.052	1.060	1.068	1.076	1.084	1.092	1.101
1.8	1.031	1.037	1.044	1.052	1.059	1.068	1.076	1.085	1.093	1.102	1.111
1.9	1.038	1.044	1.051	1.059	1.067	1.076	1.085	1.093	1.102	1.111	1.120
2.0	1.044	1.051	1.059	1.067	1.075	1.084	1.093	1.102	1.112	1.121	1.130

Table 10. Values of $\beta \times 10^{-6}$ as a function of (a/b, b/c) for a general triaxial ellipsoid (a>b>c)

a/b \ b/c	1.0 (Prolate Ellipsoid)	1.1	1.2	1.3	1.4	1.5	1.6	1.7	1.8	1.9	2.0
1.0 (Oblate Ellipsoid)	2.111	2.112	2.112	2.113	2.113	2.114	2.115	2.116	2.117	2.117	2.118
1.1	2.112	2.112	2.113	2.113	2.114	2.115	2.116	2.117	2.118	2.118	2.119
1.2	2.112	2.113	2.114	2.114	2.115	2.116	2.117	2.118	2.119	2.120	2.121
1.3	2.113	2.114	2.115	2.116	2.117	2.118	2.119	2.120	2.121	2.122	2.123
1.4	2.114	2.115	2.117	2.118	2.119	2.120	2.121	2.123	2.124	2.125	2.126
1.5	2.116	2.117	2.119	2.120	2.121	2.123	2.124	2.125	2.127	2.128	2.129
1.6	2.118	2.119	2.121	2.123	2.124	2.126	2.127	2.129	2.130	3.131	2.132
1.7	2.120	2.122	2.123	2.125	2.127	2.129	2.130	2.132	2.133	2.135	2.136
1.8	2.122	2.124	2.126	2.128	2.130	2.132	2.134	2.136	2.137	2.139	2.140
1.9	2.124	2.127	2.129	2.131	2.134	2.136	2.138	2.139	2.141	2.143	2.144
2.0	2.127	2.130	3.132	2.135	2.137	2.139	2.141	2.143	2.145	2.147	2.149

Table 11. Values of R as a function of (a/b, b/c) for a general tri-axial ellipsoid (a>b>c)

a/b ＼ b/c	1.0 Prolate Ellipsoid	1.1	1.2	1.3	1.4	1.5	1.6	1.7	1.8	1.9	2.0
1.0 Oblate Ellipsoid	1.600	1.598	1.592	1.583	1.573	1.561	1.548	1.535	1.521	1.507	1.494
1.1	1.598	1.593	1.585	1.575	1.563	1.549	1.536	1.521	1.507	1.493	1.478
1.2	1.592	1.585	1.575	1.563	1.549	1.535	1.520	1.505	1.490	1.475	1.460
1.3	1.582	1.573	1.561	1.548	1.533	1.518	1.502	1.486	1.471	1.455	1.440
1.4	1.570	1.559	1.546	1.531	1.515	1.499	1.483	1.466	1.450	1.435	1.419
1.5	1.556	1.543	1.529	1.513	1.496	1.479	1.462	1.445	1.429	1.413	1.397
1.6	1.540	1.526	1.511	1.494	1.476	1.459	1.441	1.424	1.407	1.391	1.375
1.7	1.524	1.509	1.491	1.474	1.455	1.437	1.419	1.402	1.385	1.368	1.352
1.8	1.507	1.490	1.472	1.453	1.434	1.416	1.398	1.380	1.362	1.346	1.330
1.9	1.489	1.471	1.452	1.433	1.413	1.394	1.376	1.358	1.340	1.324	1.307
2.0	1.471	1.452	1.432	1.412	1.392	1.373	1.354	1.336	1.318	1.302	1.285

Table 12. Values of δ_+ as a function of (a/b, b/c) for a general tri-axial ellipsoid (a>b>c)

a/b \ b/c	1.0 Prolate Ellipsoid	1.1	1.2	1.3	1.4	1.5	1.6	1.7	1.8	1.9	2.0
1.0 Oblate Ellipsoid	2.500	2.541	2.568	2.582	2.588	2.586	2.579	2.568	2.555	2.539	2.522
1.1	2.549	2.577	2.596	2.605	2.606	2.601	2.595	2.279	2.564	2.547	2.529
1.2	2.599	2.624	2.641	2.648	2.648	2.642	2.632	2.619	2.604	2.587	2.570
1.3	2.648	2.675	2.692	2.700	2.700	2.695	2.686	2.674	2.660	2.644	2.627
1.4	2.699	2.729	2.748	2.757	2.759	2.756	2.748	2.737	2.724	2.710	2.694
1.5	2.752	2.785	2.807	2.818	2.823	2.821	2.815	2.806	2.795	2.781	2.767
1.6	2.806	2.844	2.868	2.883	2.890	2.891	2.887	2.880	2.870	2.858	2.845
1.7	2.863	2.905	2.933	2.951	2.961	2.965	2.963	2.958	2.949	2.939	2.927
1.8	2.922	2.968	3.001	3.023	3.036	3.042	3.042	3.039	3.033	3.024	3.014
1.9	2.983	3.035	3.071	3.097	3.113	3.122	3.125	3.124	3.120	3.113	3.104
2.0	3.047	3.103	3.145	3.174	3.194	3.206	3.212	3.213	3.210	3.205	3.198

Table 13. Values of δ as a function of (a/b, b/c) for a general tri-axial ellipsoid (a>b>c)

a/b \ b/c	Prolate Ellipsoid 1.0	1.1	1.2	1.3	1.4	1.5	1.6	1.7	1.8	1.9	2.0
Oblate Ellipsoid 1.0	2.500	2.454	2.413	2.377	2.344	2.314	2.286	2.259	2.235	2.212	2.190
1.1	2.445	2.410	2.372	2.337	2.305	2.274	2.246	2.220	2.195	2.172	2.151
1.2	2.387	2.350	2.313	2.277	2.245	2.214	2.185	2.159	2.134	2.111	2.089
1.3	2.326	2.286	2.248	2.212	2.178	2.147	2.118	2.091	2.066	2.043	2.021
1.4	2.264	2.222	2.183	2.146	2.112	2.081	2.051	2.024	1.999	1.976	1.954
1.5	2.203	2.160	2.119	2.082	2.048	2.016	1.987	1.961	1.936	1.913	1.892
1.6	2.144	2.100	2.059	2.021	1.987	1.956	1.927	1.901	1.877	1.854	1.834
1.7	2.087	2.042	2.001	1.964	1.930	1.899	1.871	1.845	1.822	1.800	1.780
1.8	2.033	1.987	1.946	1.910	1.876	1.846	1.819	1.794	1.771	1.750	1.730
1.9	1.981	1.936	1.895	1.859	1.826	1.797	1.770	1.746	1.724	1.703	1.685
2.0	1.932	1.887	1.847	1.812	1.780	1.751	1.725	1.702	1.680	1.661	1.643

<u>Figure 27.</u> <u>Plot of reduced specific viscosity versus concentration for</u>

<u>sperm whale myoglobin (0.1M NaCl, buffer. pH = 7.1)</u>

The straight line is that due to a weighted least squares fit

to $\dfrac{\eta_{sp}}{c}$ = $[\eta]$ $(1 + k_\eta c)$ where $[\eta]$ = 3.25 ml/gm and k_η = 5.9 ml/gm.

The weight used was $\dfrac{1}{\text{concentration (mg/ml)}}$ (conc. < 40 mg/ml)

$\dfrac{1}{40}$ (conc. ⩾ 40 mg/ml)
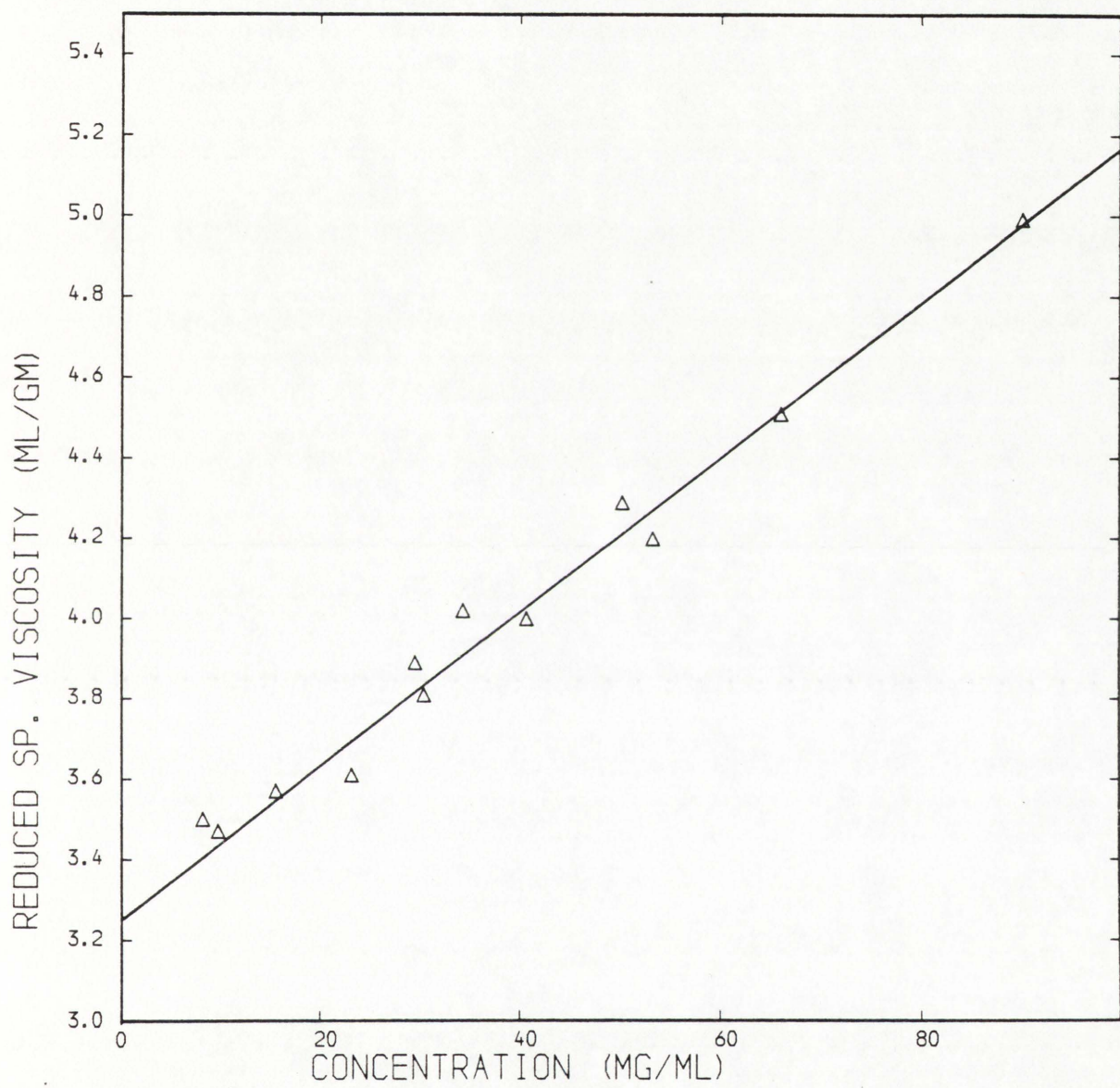
Figure 28. Photograph of the apparatus used for determining solution densities and viscosities. Temperatures were kept constant to within ± 0.01° using a high precision Townson – Mercer constant temperature tank, with a pump attachment to supply the water bath in the precision density meter. These temperatures could be monitored to within ± 0.005° using the platinum resistance thermometer situated directly above the density meter.
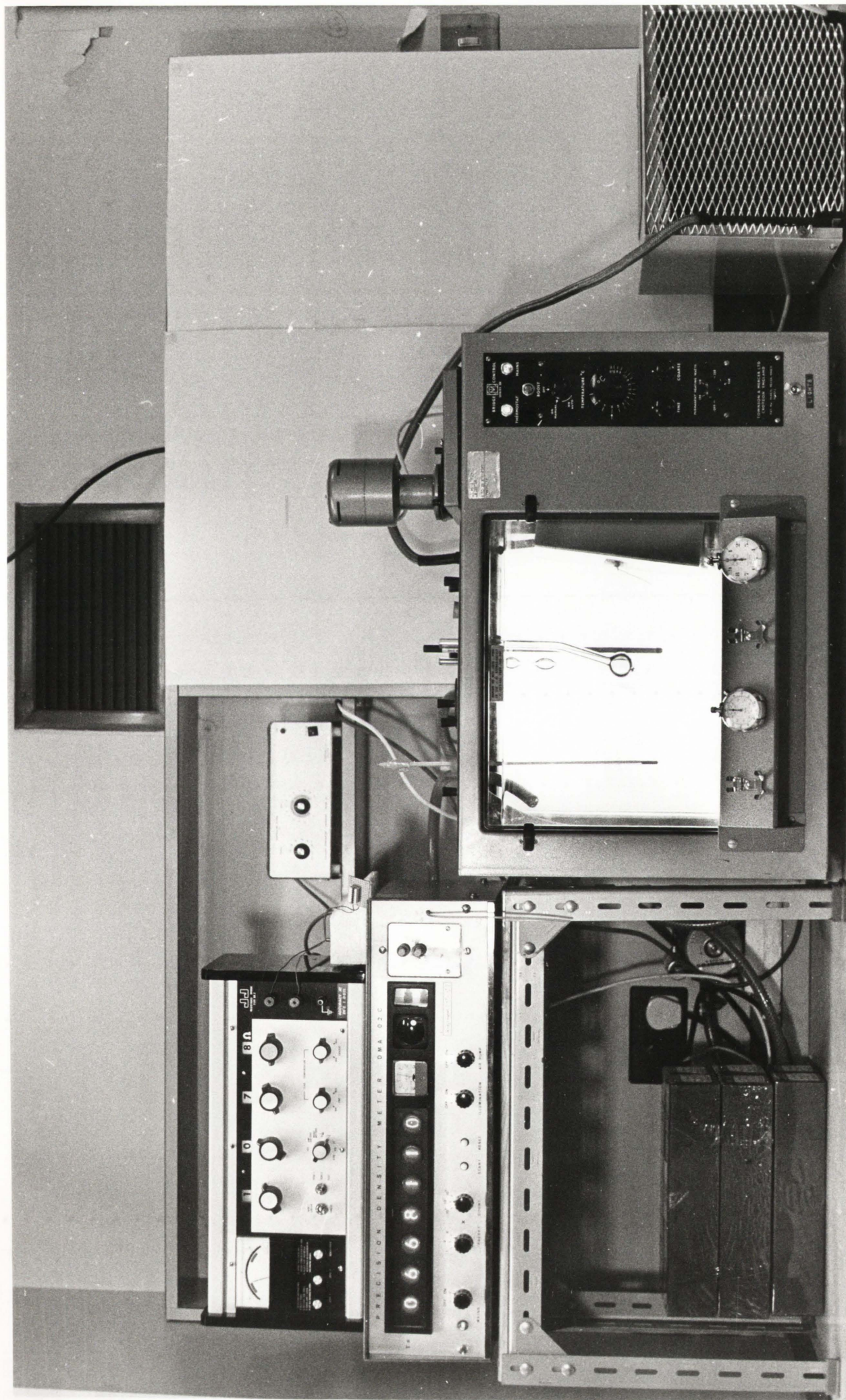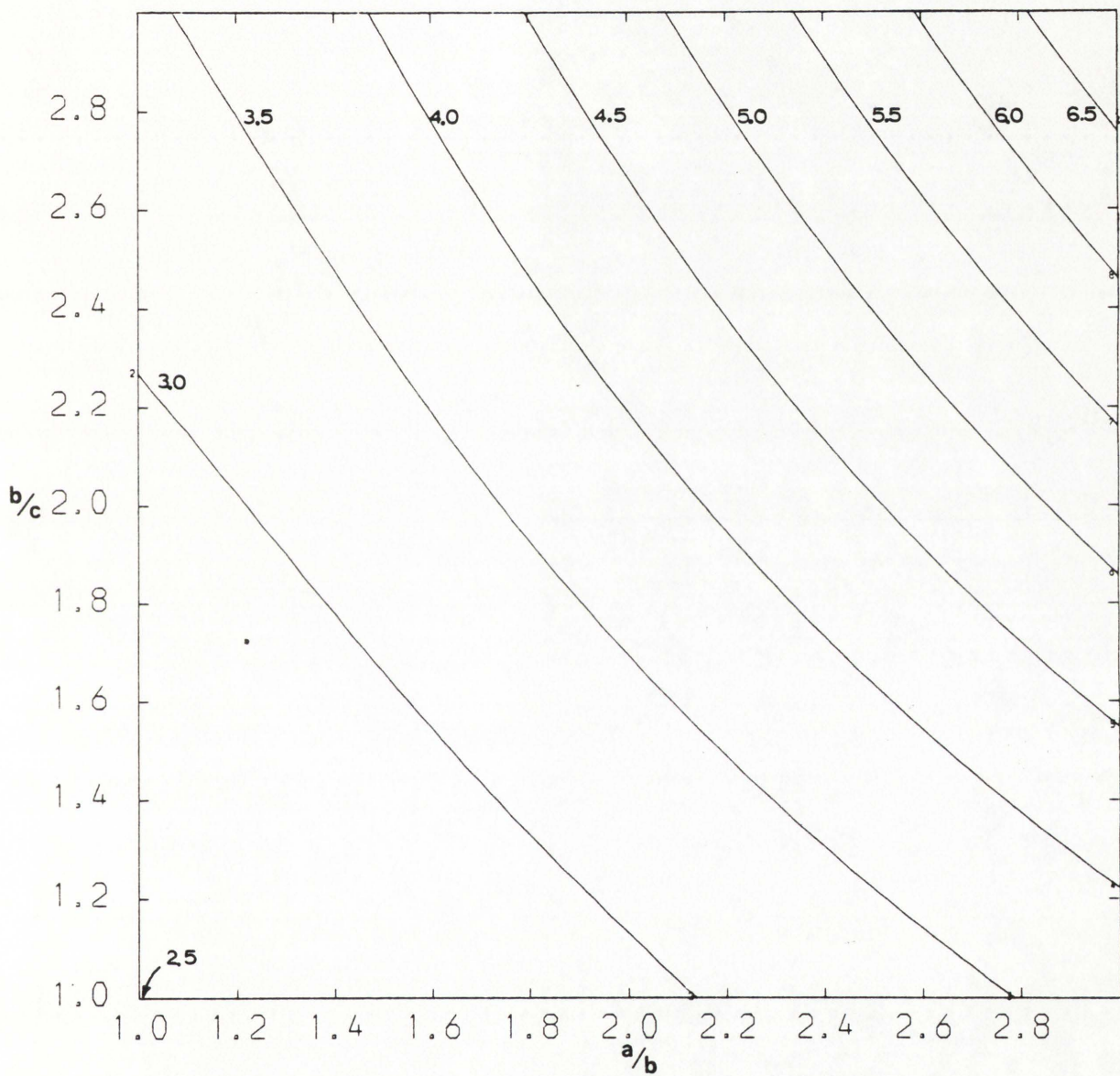
Figure 29. Contour diagram showing curves of constant ν as a function of

the semi-axial ratios a/b, b/c on the basis of equation (88)
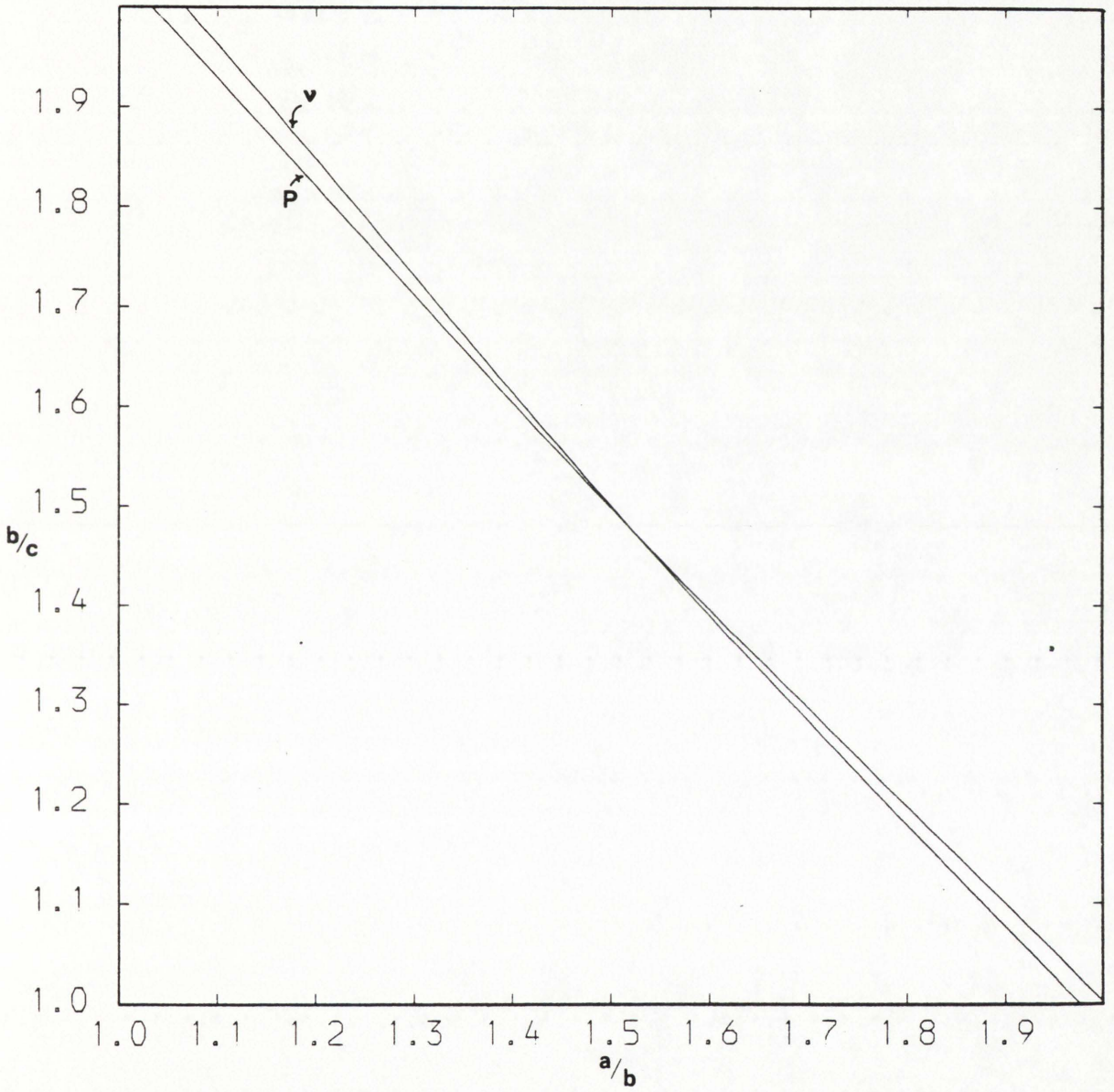
<u>Figure 30.</u> <u>Plots of constant ν and P in the (a/b, b/c) plane corresponding</u>
<u>to a/b = 1.5, b/c = 1.5</u>
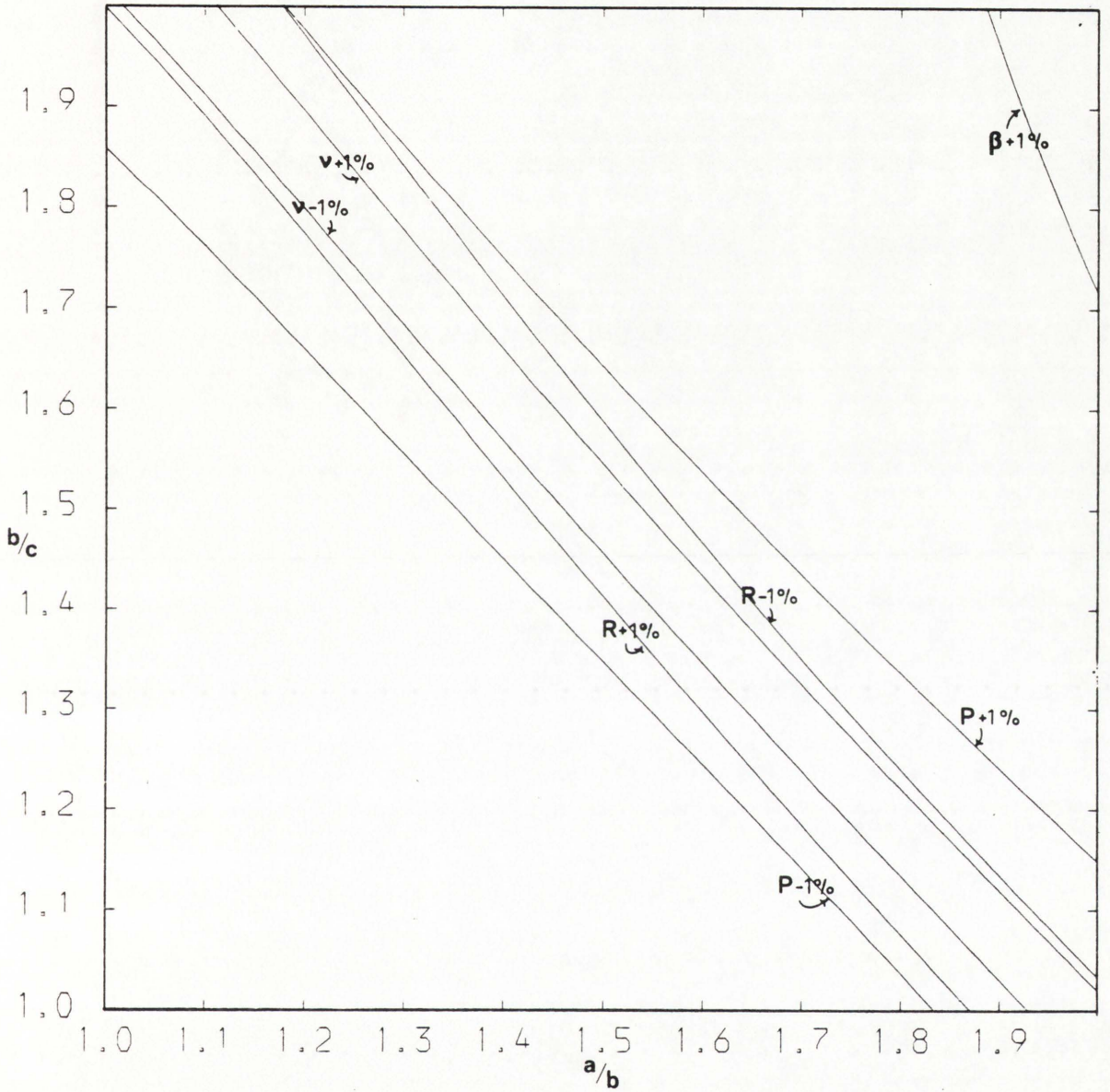
Figure 31. Plots of constant ν, P, β and R, allowing for ± 1% error in
their measured values, in the a/b, b/c plane corresponding
to a/b = 1.5, b/c = 1.5
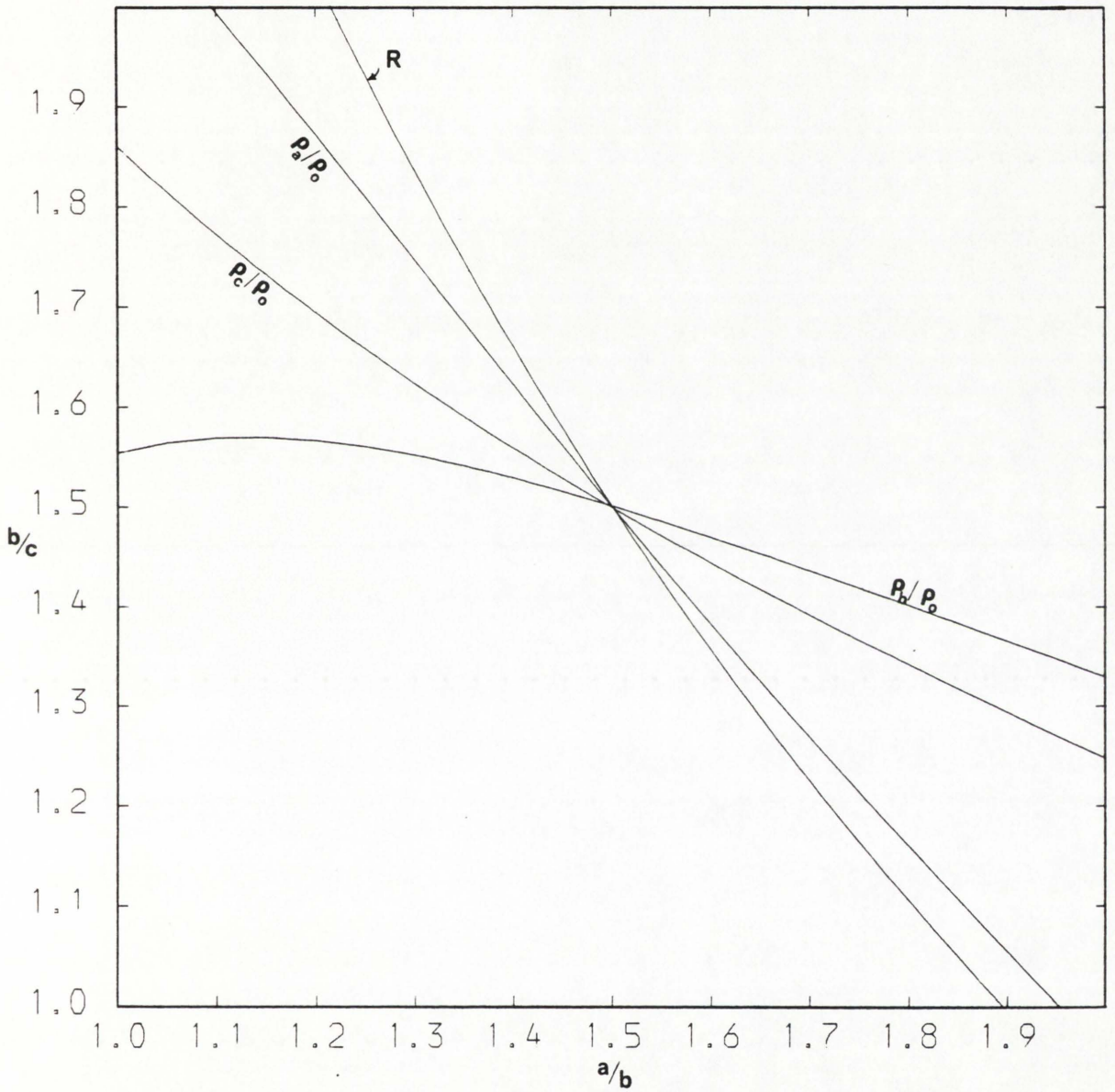
Figure 32.   Plots of constant R and the rotational relaxation time ratios
in the a/b, b/c plane corresponding to a/b = 1.5, b/c = 1.5
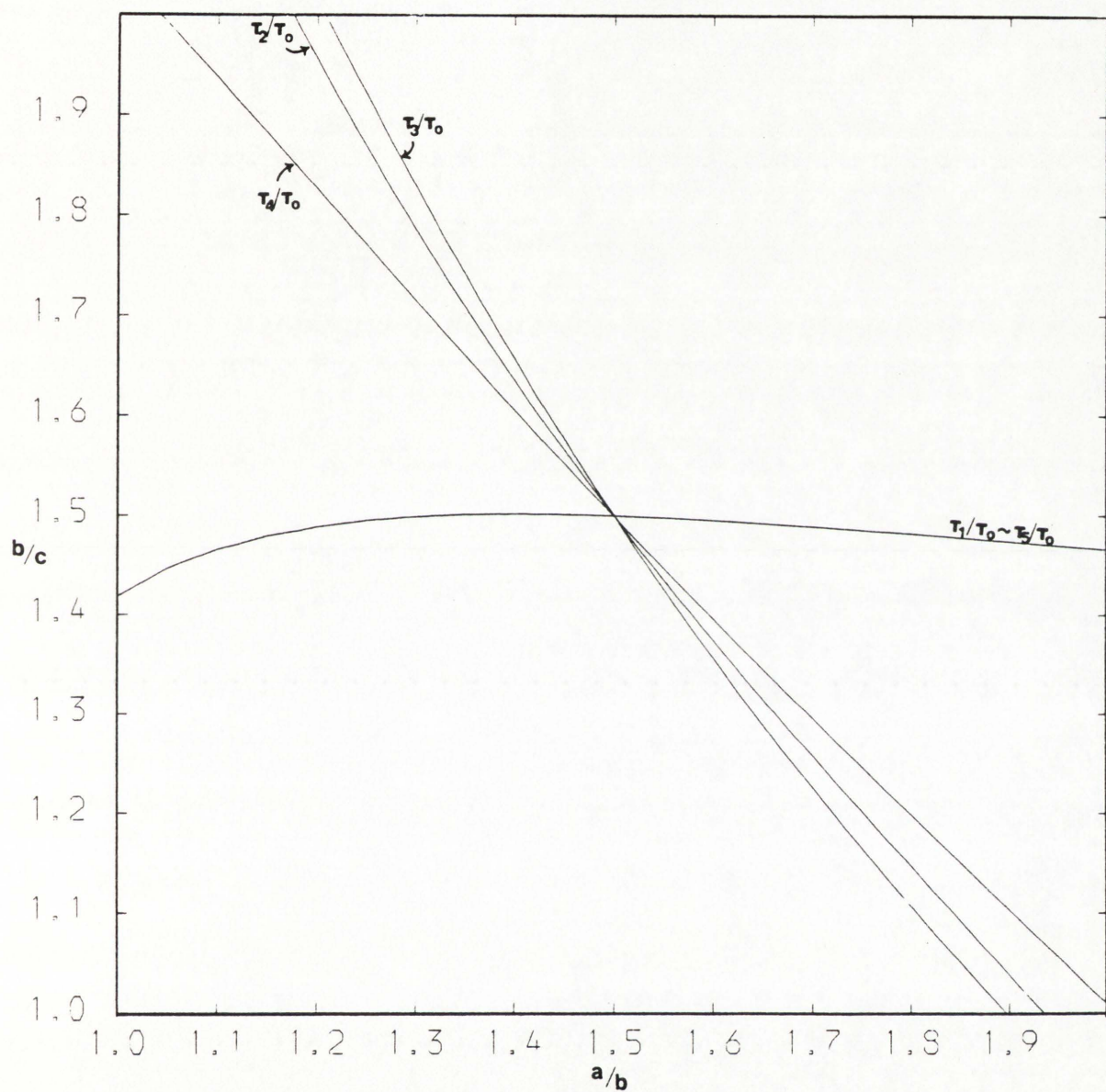
Figure 33. Plots of constant fluorescence anisotropy relaxation time ratios in the a/b, b/c plane corresponding to a/b = 1.5, b/c = 1.5
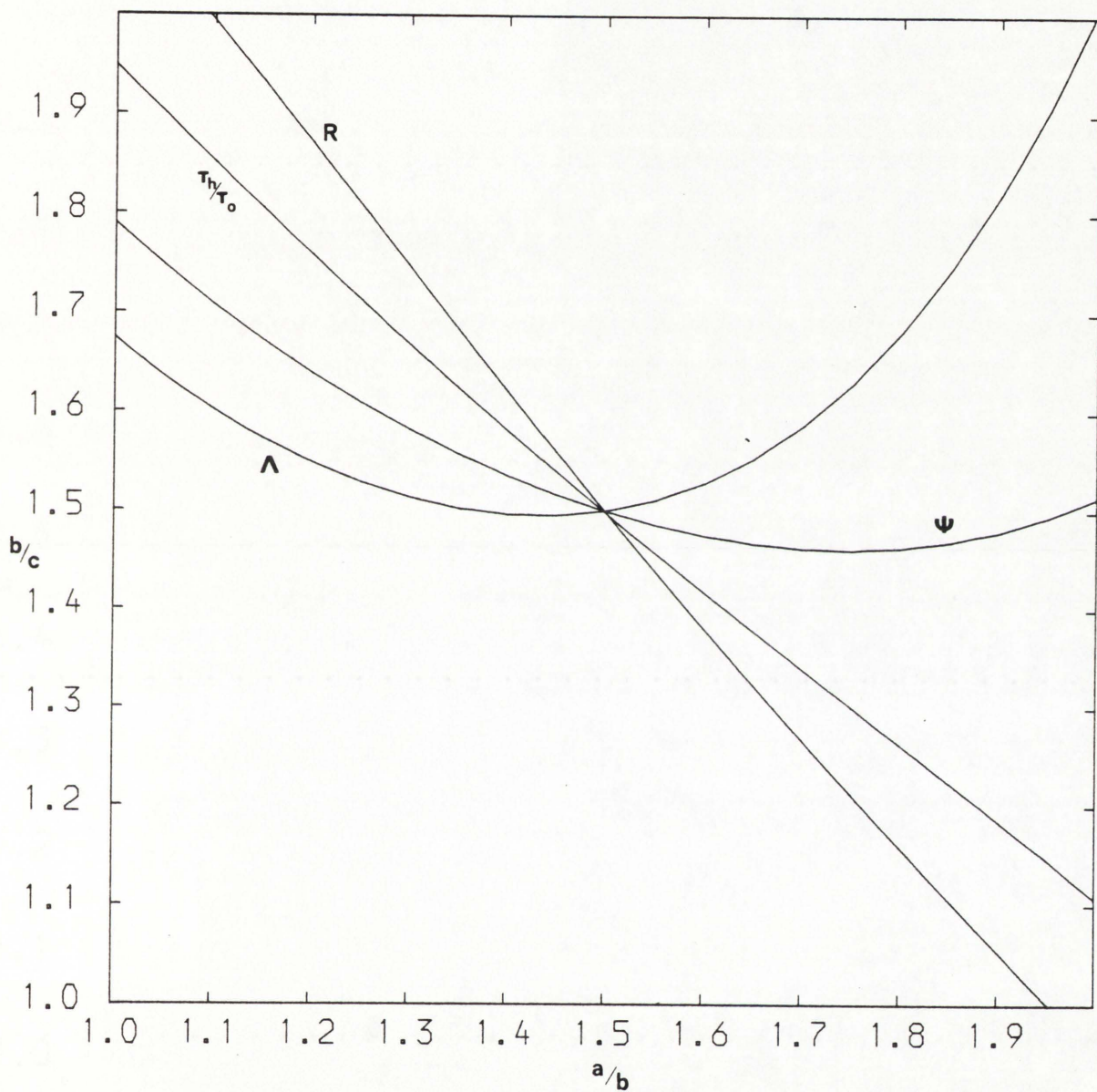
Figure 34. Plots of constant R, Ψ and Λ in the a/b, b/c plane corresponding to a/b = 1.5, b/c = 1.5
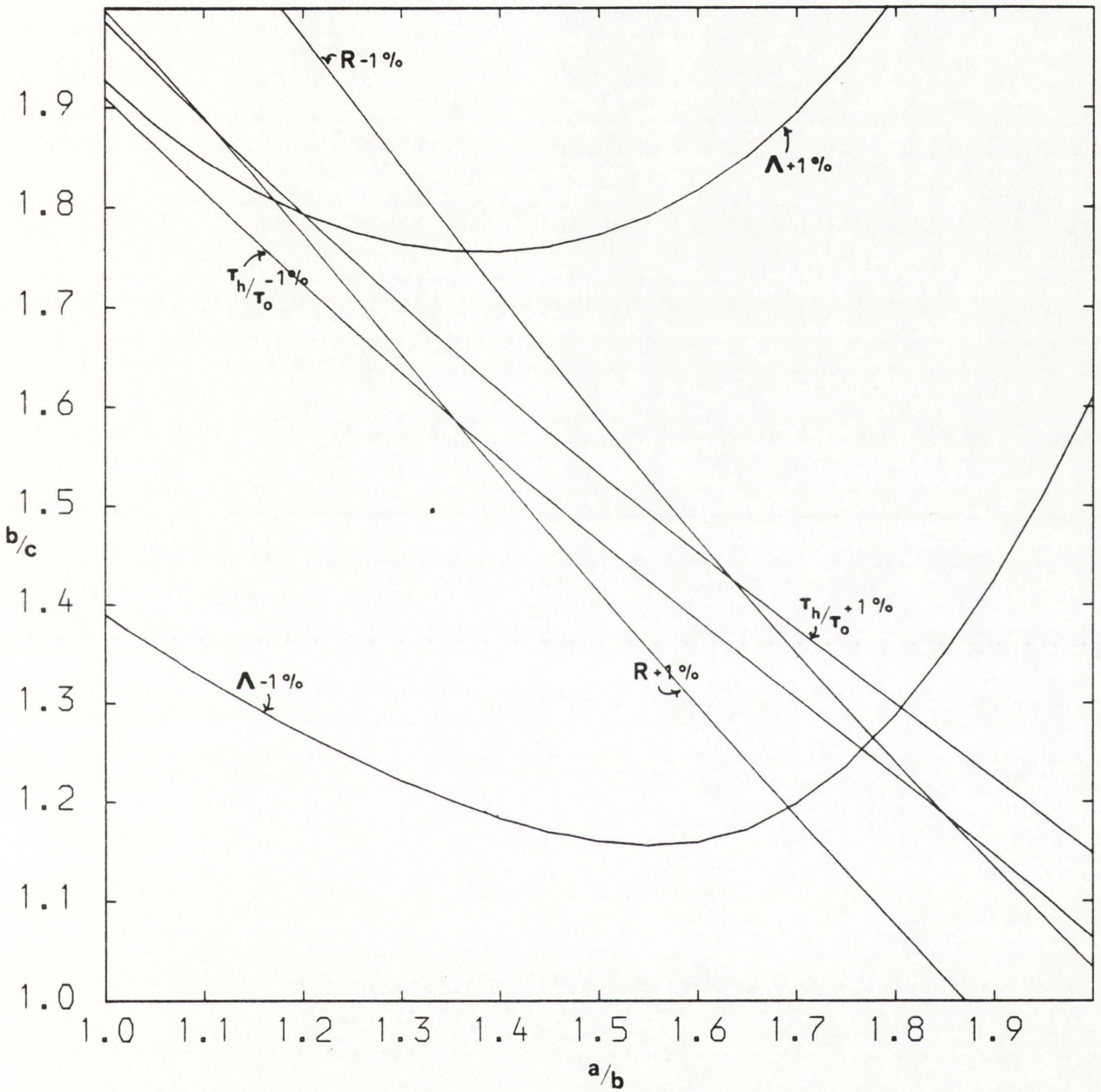
Figure 35. Plots of constant R, Ψ and Λ, allowing for ± 1% error in their measured values, in the a/b, b/c plane corresponding to a/b = 1.5, b/c = 1.5
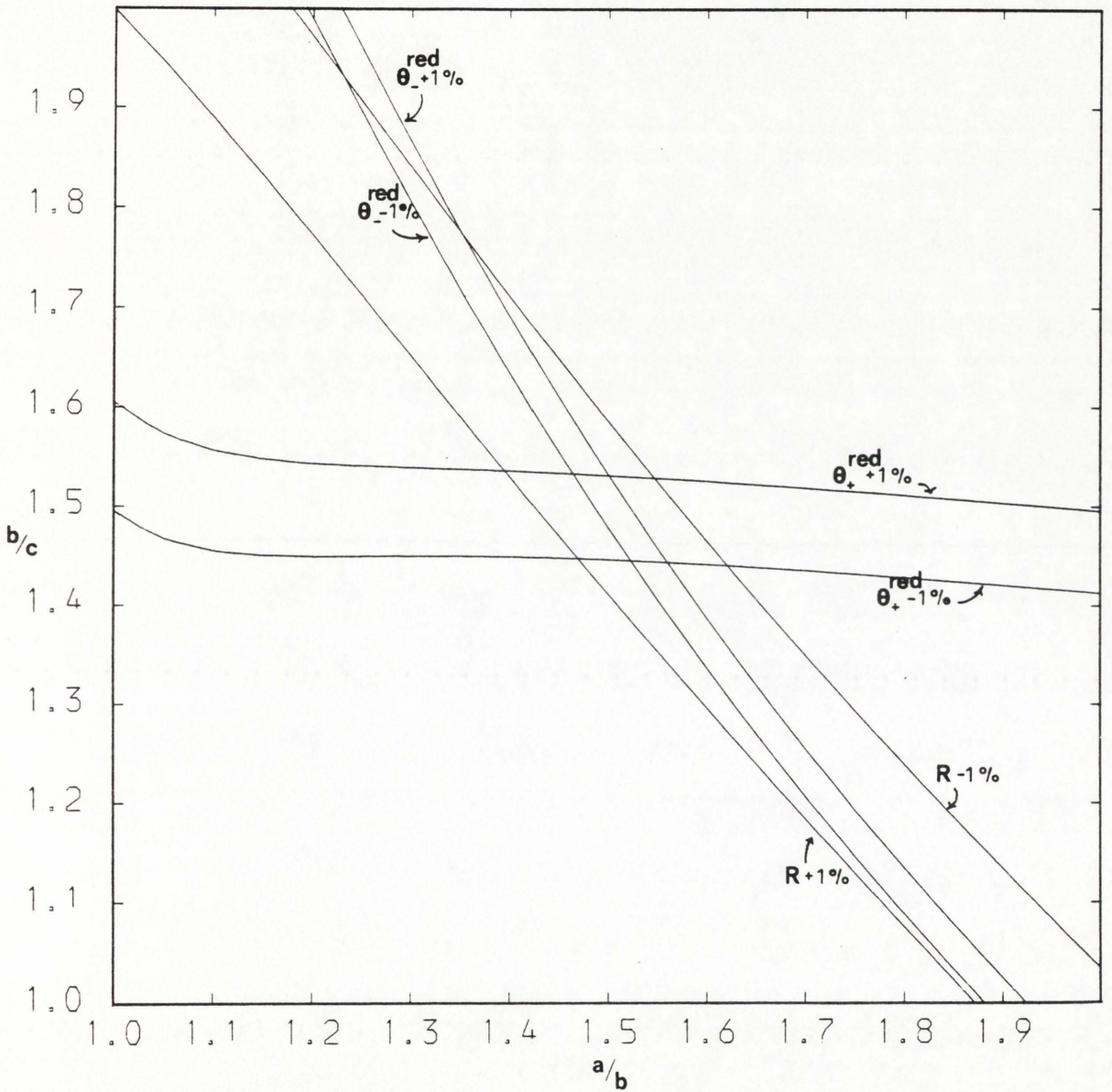
Figure 36. Plots of constant R, θ_+^{red} and θ_-^{red}, allowing for $\pm$ 1% error in their measured values, in the a/b, b/c plane corresponding to a/b = 1.5, b/c = 1.5
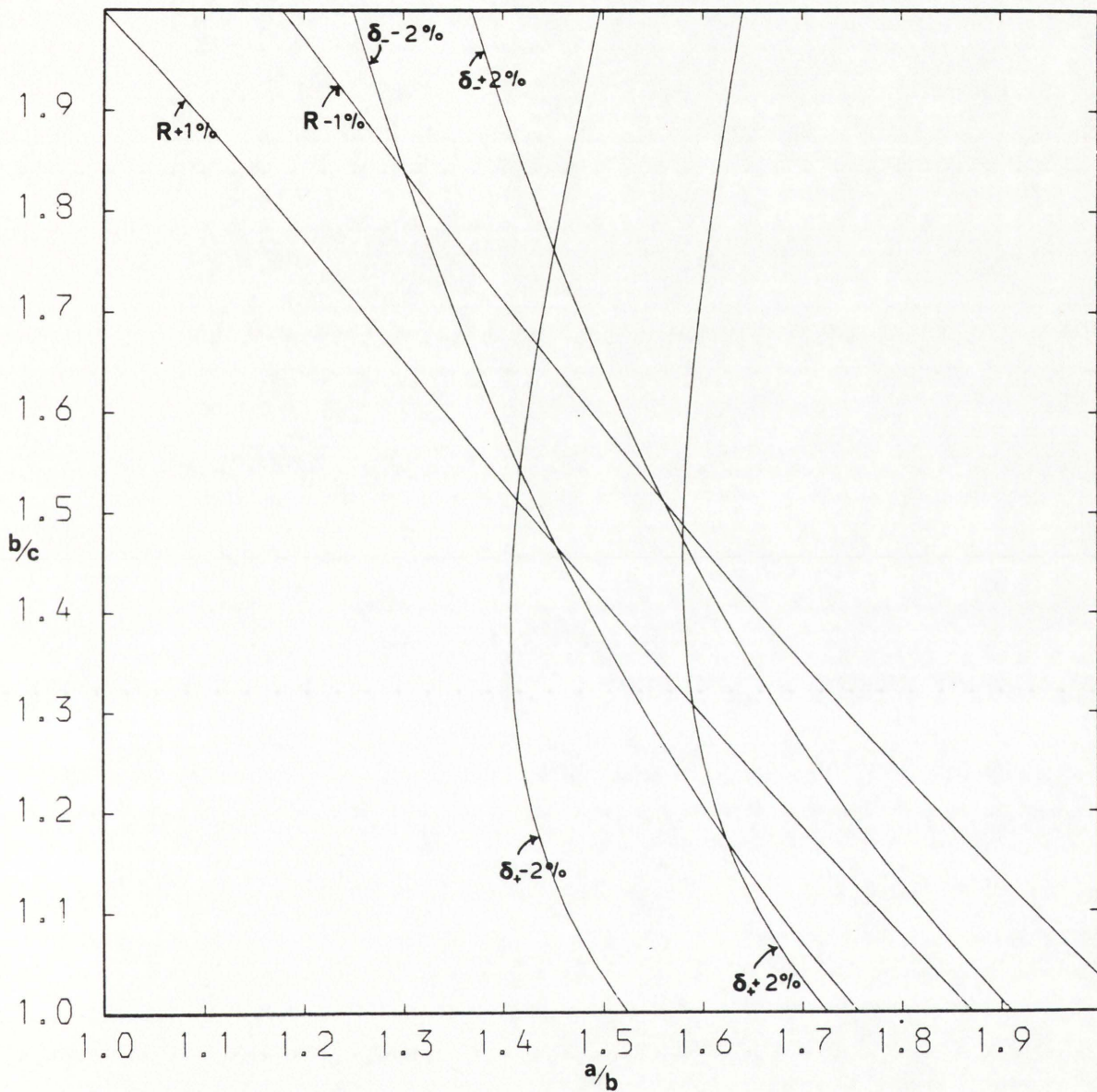
<u>Figure 37.</u> Plots of constant R, δ_+ and δ_-, allowing for $\pm$ 1% measured error

in R and $\pm$ 2% measured error in $\delta_\pm$, in the a/b, b/c plane

corresponding to a/b = 1.5, b/c = 1.5
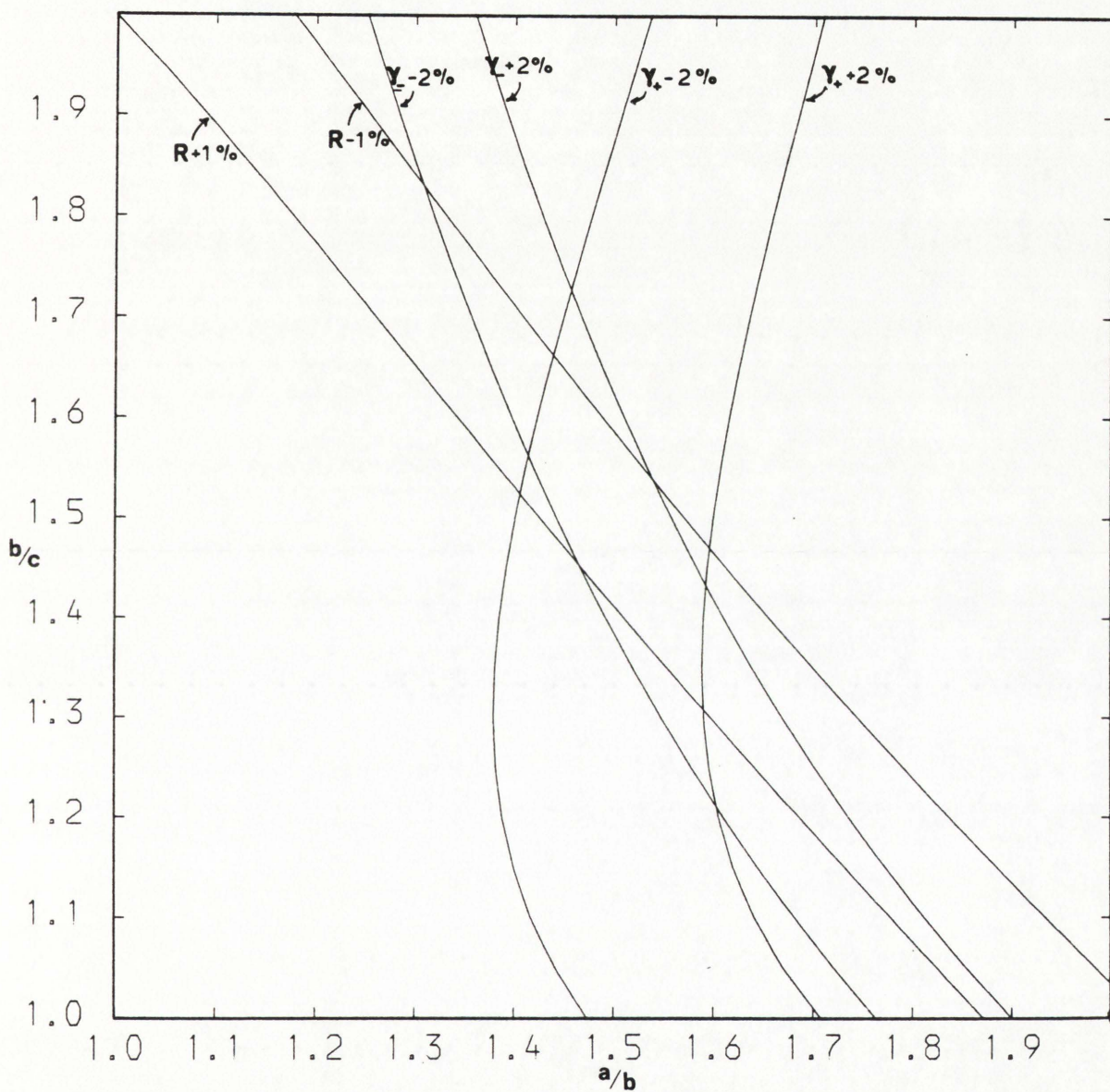
<u>Figure 38.</u> Plots of constant R, γ_+ and γ_-, allowing for $\pm$ 1% measured error

in R and $\pm$ 2% measured error in $\gamma_\pm$, in the a/b, b/c plane

corresponding to a/b = 1.5, b/c = 1.5

C H A P T E R   4

.

Determination of a Stable, Unique Solution by Combining Results

from Viscosity, Sedimentation and Electric Birefringence

4.1 Methods for Analyzing the Decay Curve

Resolution of a 2-term exponential birefringence decay curve into its two component relaxation times or decay constants is notoriously difficult, even for components that differ by several orders of magnitude. The situation is especially difficult for globular macromolecules for which the decay constants will generally not differ by more than $\sim 20\%$ (see below). A recent review of the salient methods currently used for attempting to analyse multi-component exponential decay curves, emphasing these difficulties, has been given by Jost and O'Konski (1978). The three methods that are apparently the most useful are

(1) Graphical Peeling Analysis (O'Konski and Haltner, 1956)

(2) Non-Linear Least Squares Analysis (Wilde, 1964, Powell and Macdonald, 1972, Gill and Murray, 1976)

(3) Fourier Transform Solution of the Laplace Integral Equation (Gardner, Gardner, Laush & Meinke, 1958)

4.1.1. Graphical Peeling Analysis

In this method, the logarithm of the birefringence is plotted as a function of time. For a single term decay this should of course give a straight line. If the plot for a two-term decay can be extended to relatively long times with sufficient signal-to-noise ratio, and if the two terms are not too close, then the limiting slope will give an estimate for the longest relaxation time (or shortest decay constant). This limiting slope can be extrapolated back to zero time and then "subtracted" from the original signal; the slope of the resultant can then be determined and hence the shortest relaxation time found (Figure 39). As might be expected, this method, although rapid, is very approximate and

is of little use for resolving relaxation times of the same order of
magnitude. However it is still useful for indicating the orders of
magnitude of the decay constants which may be used as initial estimates
in non-linear least squares iterative procedures.

4.1.2. Non-Linear Least Squares Iterative Analysis

In this method, the weighted sum of the squares of the residuals
χ^2 is calculated between a set of experimental data points and the
function to be fitted. If x_j represents the value of the j'th
experimental point and $\xi_j(X_m)$ the corresponding computer point for a
given estimate for the X, the number of independent variables, then we
define our 'goodness of fit' parameter, χ^2 , by

$$\chi^2 = \sum_{j=1}^{n} \left(\frac{x_j - \xi_j}{\sigma_j} \right)^2$$

(110)

where σ_j is the standard error in the j'th experimental point. The
best values of the X_m are such that $\partial\chi^2/\partial X_m = 0$, for all the X_m.
For the particular case of electric birefringence, σ_j is approximately
constant for all the x_j (although this is not generally true for photon
counting — e.g. fluorescence depolarization anisotropy — experiments)
and the minimization condition becomes

$$\frac{\partial F}{\partial X_m} = 0$$

(111)

where

$$F = \sum_{j=1}^{n} \{x_j - \xi_j\}^2$$

(111b)

In the case of a two-term birefringence decay, the minimization is said to be 'non-linear' in that the data are to be fitted to a function which is the sum of a product of terms consisting of an adjustable parameter (i.e. a pre-exponential factor) with another function of another adjustable parameter (i.e. a decay constant or relaxation time). In order to evaluate $\partial F/\partial X_m$ for a current estimate for the parameters X_m, the solution either has to be linearized using a Taylor expansion as outlined by Jost & O'Konski, or alternatively, a quadratic or quasi-Newtonian procedure can be employed (Gill & Murray, 1976). In this latter case, the parameters X_m are iterated until the minimum in F is found. Gill & Murray's algorithm is particularly attractive in that upper and lower limits for the variable can be specified and included as external constraints. A problem with the least squares technique however is that the method is very sensitive to subsidiary minima in χ^2 (or F) leading to false 'best parameters', even for data of very high precision. The presence of these subsidiary minima can often be detected by repeating the analysis for a series of different initial guesses of the adjustable parameters.

4.1.3. <u>Fourier Transform Solution of the Laplace Integral Equation</u>

The birefringence $\Delta n(t) \equiv S(t)$ is written as a Stieljes integral:

$$S(t) = \sum_i^n A_i' e^{-6\theta_i t} \equiv \sum_i^n A_i' e^{-\lambda t} = \int_0^\infty \exp(-\lambda t) dh(\lambda)$$

(112)

where $h(\lambda)$ is a step function, $i = +,-$ and $\lambda = 6\theta_i$.

The right hand side of equation (112) can be rewritten in the form of a Laplace Integral:

$$S(t) = \int_0^\infty \exp(-\lambda t) g(\lambda) d\lambda$$

(113)

where $g(\lambda)$ represents a sum of Dirac delta functions. A plot of $g(\lambda)$ versus λ will give a frequency spectrum with peaks; the centre of each peak corresponds to a specific decay constant, and the height of the peak is proportional to the value of the pre-exponential factor A_i. We transform $\lambda = e^{-y}$ and $t = e^x$. Then

$$S(e^x) = \int_{-\infty}^\infty \exp[-e^{(x-y)}] g(e^{-y}) e^{-y} dy$$

(114)

Multiplying by e^x:

$$e^x S(e^x) = \int_{-\infty}^\infty \exp[-e^{(x-y)}] e^{(x-y)} g(e^{-y}) dy$$

(115)

Taking the Fourier Transform of the left hand side of (115)

$$F(\mu) = \frac{1}{\sqrt{2\pi}} \int_{-\infty}^\infty e^x S(e^x) e^{i\mu x} dx$$

(116)

Thus

$$F(\mu) = \frac{1}{\sqrt{2\pi}} \int_{-\infty}^\infty \left\{ \int_{-\infty}^\infty \exp[-e^{(x-y)}] e^{(x-y)} . g(e^{-y}) dy \right\} . \exp[i\mu(s + y)] ds$$

(117)

with s = x - y. Rearranging

$$F(\mu) = \sqrt{\frac{1}{2\pi}} \int_{-\infty}^{\infty} g(e^{-y})\exp(i\mu y)dy. \int_{-\infty}^{\infty} \exp(-e^{s})e^{s}\exp(i\mu s)ds$$

(118)

Now, if we compare equation (113) with equation (114):

$$g(e^{-y})dy \equiv \frac{g(\lambda)}{\lambda} d\lambda$$

(119)

Thus if we obtain $g(e^{-y})$ as a function of y, using equation (119)

this will be equivalent to a plot of $g(\lambda)/\lambda$ as a function of λ .

The right hand side of equation (118) is the product of the Fourier

Transform, $G(\mu)$ of $g(e^{-y})$ and the Fourier Transform, $K(\mu)$ of $\exp(-e^{s})$.

Therefore

$$F(\mu) = \sqrt{2\pi}\ G(\mu)\ K(\mu)$$

(120)

i.e.

$$G(\mu) = \sqrt{\frac{1}{2\pi}}\ \frac{F(\mu)}{K(\mu)}$$

(121)

Taking the inverse Fourier Transform of $G(\mu)$:

$$g(e^{-y}) = \frac{1}{2\pi} \int_{-\infty}^{\infty} \frac{F(\mu)}{K(\mu)}\ e^{-iy\mu}d\mu$$

(122)

$K(\mu)$ can be evaluated analytically in terms of the complex Γ function:

$$K(\mu) = \sqrt{\frac{1}{2\pi}}\ \Gamma(1 + i\mu)$$

(123)

The method therefore has four basic steps:

(i)   Evaluate the Fourier Transform of the data (equation 116)

(ii)   Divide by the complex Γ function (equation 123)

(iii) $g(e^{-y})$ as a function of y is found by using the inverse Fourier

       Transform

(iv)   A plot of $g(\lambda)/\lambda$ is thus obtained as a function of λ

       The advantage of this method is that an initial choice as to the

number of exponential terms to be fitted is not required.

4.1.4.   Other methods of analysis, previously used for deconvoluting

         Fluorescence decay curves

       O'Connor, Ware and Andre (1979) have recently compared methods for

deconvoluting both one and two term exponential fluorescence decay curves

(sections 1.5.4, 3.3.2) – methods which could be equally applicable to

corresponding birefringence decays. The methods chosen were

       (i) Non-Linear Least Squares

       (ii) Method of Moments

       (iii) Laplace Transforms

       (iv) Method of Modulating Functions,

       (v) Exponential series method

       (vi) Fourier Transforms

       They discovered that all six methods were satisfactory for analysing

undistorted one – component data, but that the least squares method was

most suitable when distortions are present. For resolving two closely

spaced terms (9.5ns & 11.5ns) in a 2-term undistorted decay only the least

squares method and the method of modulating functions proved satisfactory.

They thus concluded that the non-linear least squares iterative method

was the technique of preference for the analysis of simple decay laws.

4.2. Choosing the best algorithm: computer simulation

Following the work of Jost & O'Konski (1978) and O'Connor, Ware &

Andre (1979), the non-linear least squares iterative and possibly the

Fourier Transform Solution of the Laplace Integral Equation methods

seemed to be the best available methods for resolving a 2-term

exponential birefringence decay. I attempted to test for myself these

methods by assuming three proteins of known (tri-axial) dimensions and

hence axial ratios (a/b, b/c), assuming a swelling ratio $(\overline{v}_s/\overline{v}) = 1.3$,

and $\overline{v} = .73$ (typical for globular proteins). From these values the

molecular weight, viscosity increment, R-function, $\delta_{\pm}$ functions, intrinsic

viscosity and hence decay constants $\theta_{\pm}$ could be predicted (Table 14). We

then assume pre-exponential factors A'_+, A'_-, of, respectively, 0.07 and 0.05

radians taken from a typical initial birefringence $(\equiv A'_+ + A'_-)$ of 0.12

radians (Krause & O'Konski, 1959) and hence the unperturbed decay curve

for each simulated protein can be given. The actual individual values for

$A'_{\pm}$ are not significant in the analyses, except when they differ by several

orders of magnitude (see section 4.5). One then places simulated

experimental error on each of 100 data points for the curves, using a

computer normal pseudo-random number generator, and, first of all assuming

no errors in the molecular weight or intrinsic viscosity, investigate how

much error in the data points is tolerable, before each algorithm fails to

give back the correct decay constants and hence axial ratios, within

reasonable limits. The algorithms would then be tested for errors in the

intrinsic viscosity and molecular weight. Figure 40 illustrates such a

mock experimental decay curve with 0.1 degree standard error (about the

current available experimental precision — B. Jennings & V. Morris,

private communication) on each of 1000 data points, for Protein 1

[true (a/b, b/c) = (1.5, 1.5)]. In the analyses the pre-exponential

factors $A'_{\pm}$ are of course regarded as unknown variables.

4.3 Non-Linear Least Squares Iterative Method

The quasi-Newtonian quadratic method for minimizing any function

(i.e. in this case, the sum of the squares of the residuals F) given

by Gill & Murray (1976) and incorporated in the UK NAG Mk.VI subroutine

E04JAF was used. In this algorithm the user, besides supplying the

subroutine for calculating the value of F at any point X, has to supply

fixed upper and lower bounds on the independent variables X_1, X_2,

........., X_m. This routine was incorporated in the FORTRAN IV program

given in Appendix IV, as Program 5. This program generated its own

hypothetical decay curve with normal (Gaussian) pseudo-random error

generated on each data point (using NAG routine G05ADF), the amount

specifiable by the user. The program attempted to retrieve the decay

constants, hence the $\delta_{\pm}$ functions (from the user-specified molecular

weight and intrinsic viscosity) and hence the axial ratios (a/b, b/c)

of the general tri-axial ellipsoid. Owing to the problem of the presence

of the danger of the routine falling into subsidiary minima as mentioned

by Jost & O'Konski (1978) — see section 4.1.2. — it was necessary to

repeat the method for a large number (30) of initial guesses. In fact

the program was written to generate its own thirty different initial

guesses by using "DO" loop between user specifiable initial guess limits.

Unfortunately, even data as accurate as .001 degree standard error on

each data point (about 2 orders of magnitude greater than the current

experimental precision) failed to give back the correct (a/b, b/c)

within reasonable limits, and even data of machine accuracy (14

significant figures) did not generate the exact value of (1.5, 1.5),

as Figure 41 illustrates.

4.4. Fourier Transform Solution Method of the Laplace Integral
Equation Method

4.4.1. Cut-off Errors

In order to use this method outlined in section 4.1.3., the

integrals involved in taking the Fourier Transform of the data

(equation 116) and in taking the inverse Fourier Transform (equation 122)

have to be solved numerically. Unfortunately, the integrals extended

from $-\infty$ to $+\infty$; with real data there exists a finite cut-off time, t_0

or equivalently x_0. Cut-off errors tend to increase the height of the

error ripples in the final results. For equation (116), if we choose a

cut-off too short for μ_0 there is a loss of resolution of the component

peaks. On the other hand, if we choose a cut-off in μ_0 too long then

the cut-off at x_0 causes the amplitude of the error ripples to increase;

μ_0 has to be varied therefore to obtain the optimum resolution for a

given data set.

4.4.2. Numerical Integration

Following Gardner et al (1958), each value of S(t) was multiplied

by the current value of t to give $e^x S(e^x)$ (equation 115). Whereas t

ranges from $0 \to \infty$, x ranges from $-\infty$ to $+\infty$, thus we can split the integral

in equation (116) into symmetric and anti-symmetric parts:

$$F(\mu) = \sqrt{\frac{1}{2\pi}} \int_0^{x_0} [S^*(x) + S^*(-x)]e^{i\mu x}dx$$

(124)

Therefore

$$F(\mu) = \sqrt{\frac{1}{2\pi}} \int_0^{x_0} \{[S^*(x) + S^*(-x)]\cos \mu x$$

$$+ i[S^*(x) - S^*(-x)]\sin \mu x \} dx$$

(125)

giving real and imaginary parts for $F(\mu)$, i.e., F_c & F_s. $K(\mu)$ can be similarly split into real & imaginary parts K_c & K_s. Equation (121) thus becomes:

$$G(\mu) = \sqrt{\frac{1}{2\pi}} \frac{F_c + iF_s}{K_c + iK_s} = \frac{(F_i + iF_s)(K_c - iK_s)}{K_c^2 + K_s^2}$$

(126)

and the inverse transform (122) becomes

$$g(e^{-y}) = \frac{1}{2\pi} \int_{-\mu_0}^{\mu_0} \frac{(F_c + iF_s)(K_c + iK_s)}{K_c^2 + K_s^2} (\cos y\mu - i\sin y\mu)d\mu$$

(127)

where μ_0 and $-\mu_0$ are the cut-off values for μ. Since all odd values vanish,

$$g(e^{-y}) = \frac{1}{2\pi} \int_0^{\mu_0} \left\{ \frac{F_cK_c + F_sK_s}{K_c + K_s} \cos y\mu + \frac{F_sK_c - F_cK_s}{K_c + K_s} \sin y\mu \right\} d\mu$$

(128)

The numerical integrations (125) and (128) are solved using the NAG routine DO1GAF. The value of the complex Γ function needed for calculating K_c and K_s was deduced using a routine given by Lucas & Terril (1970). As with the non-linear least squares iterative method, the program (Appendix IV Program 6) generated its own synthetic data using NAG normal pseudo-random number routines GO5ADF & GO5BBF.

4.4.3. Results

The program was firstly checked by applying it to the case first considered by Gardner et al for a single exponential decay, viz.

$$S(t) = 100 \ e^{-0.02t}$$

assuming data of machine accuracy (i.e. no perturbation routine included). The retrieved λ from Figure 42 is .021, in close agreement with Gardner et als value. The data was taken at logarithmic intervals (corresponding to equal linear intervals in x). The algorithm was then applied to the two term exponential decay curve for Protein 2. However, even with data of machine accuracy and taken at logarithmic intervals in t (impossible to obtain in practice for our particular case) the retrieved values for λ_i and hence the decay constants was poor and varied with the cut-off values for μ_o as Figure 43 and Table 15 shows. When normal pseudo-random error of .001 deg was applied to the data points, no resolution was possible for all values of μ_o, as Figure 44 clearly demonstrates. We thus conclude this method to be of little use for our case of interest.

4.5. A new R-Constrained Non-Linear Least Squares Algorithm

Owing to the inadequacy of the other treatments for resolving a two-term exponential birefringence decay into its component relaxation times (or decay constants), particularly for globular proteins (close decay constants), I have now developed a new R-constrained least squares algorithm. If the R-function line solution (3.3.1), which can be found from the ratio of the sedimentation regression coefficient k_s to the intrinsic viscosity [η], is included in the least squares algorithm (4.3) as a constraint, then the problem is effectively reduced from one of four independent variables (θ_+, θ_-, A'_+, A'_-) to one of three (a/b, A'_+, A'_-). The solution is constrained to lie on the R-curve, thus a given estimate for a/b will necessarily give a 'constrained' value for b/c; the computer program can then calculate the values for δ_+ and δ_- corresponding to this estimate, hence the decay constants (using also the values for [η] , M_r – equation 107), the decay curve and finally the sum of the squares of the residuals (SSR) between the computer points and the experimental curve. By iterating along this R-curve for a/b and the two pre-exponential factors A'_+, the best estimate for (a/b, b/c) can be found from the minimum value of the SSR.

The constraint of the R-curve was included in the algorithm (Program 7 of Appendix IV) for the three simulated proteins considered previously by use of the Leicester University Computer Library routine E01LF1, a listing of which is given towards the end of Program 7. The user specifies the coordinates of knots in the curve (see Figures 45, 46 & 47), or alternatively, the whole curve digitised, and the routine interpolates between these points using a cubic polynomial ('spline') fit (K. Brodlie,

private communication). In the main program, normal (Gaussian) random error of 0.1 degrees on each of the 100 linearly separated data points was supplied using the pseudo random number routines mentioned previously. The magnitude of this error corresponds to that expected from current experimental precision (B.R. Jennings, V. Morris, private communication). It was found in pilot runs that the danger of the algorithm falling into subsidiary minima, as present for the unconstrained case (section 4.3.) was no longer significant. The number of initial guesses was thus reduced from thirty to three to save on Computer time; the best estimates were generally the same for all three initial guesses (except those marked with an asterisk in Tables 16, 17 & 18). The values for (a/b, b/c) retrieved did however depend on the cut-off time specified for the decay curve. If there were no error in the data points then very long cut-off times would be desirable, since this region is dominated by the longest relaxation time (or shortest decay constant, θ_-). However, the effect of a given absolute error is more pronounced the lower the birefringence signal.

The optimum cut-off time, and hence the best value for (a/b, b/c) was found by repeating for eight different streams of normal random data, specified by the UK NAG Mk VI routine G05BAF(0.N), where N represents the stream number of the random data; the optimum cut-off time for each decay curve was then determined by finding the best standard deviation of the a/b's from the eight streams for increments of 5ns in the cut-off times. The values for the corresponding best mean value for a/b (and hence b/c) together with the corresponding standard error for the eight streams of data could then be found (Tables 16a, 17a & 18a).

This procedure was then repeated allowing for $\pm1\%$ experimental error

in the R-curves (Tables 16b,c, 17b,c, 18b,c). If the points corresponding

to $<(a/b, b/c)> + \sigma_E$ are joined together for each of the R-curves, and

then those of the $<(a/b, b/c)> - \sigma_E$, regions of allowed values for

(a/b, b/c) could then be found (Figures 48, 49 & 50). The mean values

agree very closely with the true values (Table 19). The algorithm was

then tested for the effect of experimental errors in the intrinsic

viscosity ($\pm$ 1%) and molecular weight ($\pm$1.4%). These were found to be

not significant (Table 20); indeed, the molecular weight can now be found

precisely from the results of sequence analyses. Finally, the algorithm

was tested for different initially assumed values for the pre-exponential

factors A'_+ and A'_- (Table 21). Again, these were found to have no

significant effect on·the results; even for pre-exponential factors

differing by two orders of magnitude, though the retrieved A'_- was poor,

the retrieved a/b was in close agreement with the other values.

Once the value for the axial ratios (a/b, b/c) has been found for a

particular protein, it can be combined with the swollen volume of the

protein, if known, to determine the axial dimensions. In Table 22 a "model

dependent" (section 1.7.1) estimate for V_e has been found for each of the

three simulated proteins we have considered by back substitution of the

mean values of (a/b, b/c) determined from the analysis above into equation

(8) for the viscosity increment, and again the agreement with the initially

assumed values (Table 19) is excellent. If the model dependent values of

V_e are then combined with the values for (a/b, b/c), the semi-axial

dimensions a,b,c for the three proteins considered are found to be ($\overset{o}{A}$):

    Protein 1: 45.00, 29.98, 20.01 (45.0, 30.0, 20.0)

    Protein 2: 42.28, 25.59, 19.61 (42.5, 25.0, 20.0)

    Protein 3: 43.11, 33.58, 19.81 (42.5, 34.0, 20.0)

again, in excellent agreement with the initially assumed (bracketed) values.

4.6. Some Practical Points

In applying these equations and algorithms to real protein and other macromolecular solutions several important factors must be taken into consideration:

(1) Two or more decay constants can also arise if the system is polydisperse. It is therefore essential that the solution be rendered monodisperse by, for example, gel filtration techniques.

(2) It has now been well established that the single exponential decay constant previously resovable from the birefringence decay of monodisperse protein solutions shows a concentration dependence (Riddiford & Jennings, 1967), and it was therefore necessary to determine its value at several concentrations and then extrapolate to infinite dilution. One must naturally assume therefore that the two decay constants for the decay of a monodisperse solution of asymmetric ellipsoids also show a concentration dependence, and hence must be extrapolated to infinite dilution. On the other hand, because of the constraint in our algorithm that they must correspond to δ_+ and δ_- line solutions that intersect with the R-curve, the values for the decay constants are such that they are not the 'true' decay constants for each particular concentration but are closer to the infinite dilution values. Since the extrapolation procedure must therefore be empirical the best estimates for a/b at particular solute concentrations rather than these 'damped' decay constants may be extrapolated to infinite dilution; once the extrapolated value for a/b has been found the corresponding value for b/c can thus also be found from the R-curve.

(3) The requirement on the precision of the electric birefringence apparatus is not only in producing transient decays to a precision of 0.1 degree on each data point but also the availability of response times (i.e. the finite time it takes for the orienting electric pulse to be switched off) of about

an order of magnitude less than that of the faster relaxation time

Adequate response times are now available (Williams, Ham & Wright, 1976)

however with apparatus that uses a laser light source, cable discharge

generator and a memory oscilloscope, giving a response time of ~ 5ns.

(4) In the above analysis it has been shown that greater accuracies in

obtaining the axial ratios can be obtained if the optimum cut-off time

for the decay is found. In our simulations this was achieved by

averaging over several streams of random data; this corresponds in practice

to taking several decays of the same preparation. Different samples of

the same preparation should be used because of the danger of denaturing

the protein by continually pulsing through high electric fields (temp-

erature effects).

(5) It has also been assumed that the R function can be measured to a

precision of ~ $\pm 1\%$. Since s_c values in an s_c versus concentration plot can

be determined to within ~ $\pm .2\%$(Squire, 1978), the k_s value can presumably be

measured to within $\pm 1\%$ (as, from equation 58, it is approximately a

function of (s_c/s) x concentration^{-1}). The intrinsic viscosity [η] can

also be measured to within ~$\pm 1\%$, the limiting factor here being the accuracy

to which the flow times can be measured. The error in R will thus be of

the order of 1% after taking into consideration that any systematic errors

in measuring absolute solute concentrations will cancel in the ratio

$k_s/$[η] (Rowe, 1977).

(6) Finally, it should be pointed out that because of polarisation effects

on the electrodes and also the danger of denaturation due to heating effects

mentioned in (4), solutions of low ionic strength (<0.01M) generally have

to be used. This apparently prevents the investigation of less soluble

materials. On the other hand, an interesting new method is being developed

at Brunel University by Professor B. Jennings and his co-workers in which an ultrasonic field rather than an electric field is used to initially orient the macromolecules before the decay is observed. This "acoustic birefringence" (Ballinger & Jennings, 1979) method does not suffer from the problems of electrode polarisation and denaturation associated with ionic strengths > .01M for the electric birefringence case, allowing the possibility for the investigation of less soluble materials.

Table 14. Assumed and derived characteristics of three hypothetical

globular proteins

Protein	1	2	3
	A S S U M E D V A L U E S		
Characteristic			
a, b, c	45Å,30Å,20Å	42.5Å,25Å,20Å	42.5Å,34Å,20Å
$\bar{v}$	0.730 ml/gm	0.730 ml/gm	0.730 ml/gm
$\bar{v}_s/\bar{v}$	1.3	1.3	1.3
	D E R I V E D V A L U E S		
Characteristic			
$a/b, b/c$	1.50, 1.50	1.70, 1.25	1.25, 1.70
$\bar{v}_s$	0.949 ml/gm	0.949 ml/gm	0.949 ml/gm
swollen molecular volume $V_e = \frac{4\pi abc}{3}$	$1.1309732 \times 10^{-19} cm^3$	$0.89011784 \times 10^{-19} cm^3$	$1.2105602 \times 10^{-19} cm^3$
Anhydrous molecular volume $V \ (=(\bar{v}/\bar{v}_s) V_e)$	$0.8699793 \times 10^{-19} cm^3$	$0.684706 \times 10^{-19} cm^3$	$0.9312001 \times 10^{-19} cm^3$
Molecular weight $M_r \ (=(N_A/\bar{v}) V)$	71,744	56,510	76,853
ν	2.892	2.870	2.840
$[\eta] \ (=N_A V_e \nu/M_r)$	2.75 ml/gm	2.72 ml/gm	2.695 ml/gm
R	1.479	1.482	1.496
$\theta_+^{red}, \theta_-^{red}$	0.163, 0.116	0.171, 0.115	0.155, 0.125
	2.821, 2.016	2.943, 1.982	2.645, 2.125
Decay constants* $\theta_{\pm} = \dfrac{N_A kT}{6\eta_0 \, [\eta] M_r} \delta_{\pm}$	$5.8153835 \times 10^6 sec^{-1}$, $4.1564612 \times 10^6 sec^{-1}$	$7.7660465 \times 10^6 sec^{-1}$, $5.2290121 \times 10^6 sec^{-1}$	$5.1872430 \times 10^6 sec^{-1}$, $4.1674860 \times 10^6 sec^{-1}$
Relaxation times $\tau_{\pm} = 1/6\theta_{\pm}$	28.6596ns, 40.0982ns	21.4609ns, 31.8734ns	32.1301ns, 39.9921ns

* $T = 293K$, $\eta_0 = 0.01$ gm cm^{-1} sec^{-1}

Table 15. Retrieved decay constants for varying values of μ_0

	y_1	y_2	$\lambda_1 = e^{-y_1}$	$\lambda_2 = e^{-y_2}$	$\Theta_+ \times 10^{-6} sec^{-1}$	$\Theta_- \times 10^{-6} sec^{-1}$
11.5	3.13	3.55	0.04372	0.02872	7.286	4.787
11.6	3.00	3.50	0.04979	0.03020	8.292	5.033
11.7	2.94	3.45	0.05287	0.03175	8.811	5.291
12.0	3.14	3.72	0.04328	0.02423	7.214	4.039

True value for $\Theta_+ = 7.7660465 \times 10^6 \ sec^{-1}$

True value for $\Theta_- = 5.2290121 \times 10^6 \ sec^{-1}$

Table 16. Determination of the optimum cut-off time for Protein 1.

True (a/b, b/c) = (1.5, 1.5)

(a) No assumed error in R

Cut-off time	80ns a/b	100ns a/b	110ns a/b	115ns a/b	120ns a/b	140ns a/b
Stream 1	1.580	1.534	1.513	1.503	1.493	1.454
Stream 2	1.946*	1.785	1.692	1.654	1.619	1.497
Stream 3	1.591	1.512	1.483	1.468	1.452	1.392
Stream 4	1.644	1.487	1.425	1.396	1.367	1.249
Stream 5	1.623	1.480	1.426	1.401	1.377	1.287
Stream 6	1.186	1.275	1.303	1.315	1.326	1.364
Stream 7	1.573	1.645	1.678	1.694	1.710	1.772
Stream 8	1.716	1.623	1.590	1.575	1.562	1.514
Mean	1.6074	1.5426	1.5138	1.5008	1.4883	1.4411
σ (SD)	0.209696	0.148967	0.133899	0.132475	0.134402	0.163491
σ (SE)	0.07414	0.05267	0.04734	0.04684	0.04752	0.05780

σ(SD) = Standard Deviation ; σ(SE) = Standard Error

* different answers for different initial guesses

Optimum cut-off time = 115ns

Best estimate for a/b = 1.501 ($\pm$ .047)

Corresponding estimate for b/c = 1.498

(b) +1 % assumed measured error in R

Cut-off time	110ns a/b	115ns a/b	120ns a/b	125ns a/b	130ns a/b	135ns a/b	140ns a/b
Stream 1	1.546	1.534	1.523	1.511	1.500	1.489	1.478
Stream 2	1.837	1.735	1.679	1.633	1.594	1.557	1.522
Stream 3	1.510	1.492	1.474	1.457	1.440	1.423	1.406
Stream 4	1.439	1.406	1.374	1.342	1.310	1.278	1.244
Stream 5	1.442	1.414	1.387	1.361	1.337	1.312	1.289
Stream 6	1.312	1.325	1.340	1.349	1.360	1.370	1.380
Stream 7	1.816	1.871	1.847	1.840	1.878	1.893	1.909
Stream 8	1.643	1.624	1.606	1.590	1.575	1.561	1.548
Mean	1.5681	1.5501	1.5288	1.5104	1.4992	1.4854	1.4720
σ (SD)	0.185700	0.183700	0.174243	0.173033	0.186398	0.195406	0.206181
σ (SE)	0.06565	0.06495	0.06160	0.06118	0.06590	0.06909	0.07290

Optimum cut-off time = 125ns

Best estimate for a/b = 1.510 ($\pm$ .061)

Corresponding estimate for b/c = 1.400

(c) -1% assumed measured error in R

Cut-off time	110ns a/b	115ns a/b	120ns a/b
Stream 1	1.494	1.485	1.476
Stream 2	1.644	1.616	1.588
Stream 3	1.468	1.454	1.440
Stream 4	1.419	1.392	1.366
Stream 5	1.418	1.395	1.373
Stream 6	1.300	1.311	1.321
Stream 7	1.626	1.638	1.649
Stream 8	1.561	1.549	1.537
Mean	1.4913	1.4800	1.4688
σ (SD)	0.115922	0.114924	0.115761
σ (SE)	0.04098	0.04063	0.04093

Optimum cut-off time = 115ns

Best estimate for a/b = 1.480 ($\pm$.041)

Corresponding estimate for b/c = 1.611

Table 17.   Determination of the optimum cut-off time for Protein 2.

True (a/b, b/c) = (1.7, 1.25)

(a) No assumed error in R

| Cut-off time | 85ns | 90ns | 95ns | 100ns | 105ns | 110ns | 120ns |
	a/b	a/b	a/b	a/b	a/b	a/b	a/b
Stream 1	1.709	1.691	1.675	1.659	1.644	1.630	1.603
Stream 2	1.963	1.926	1.872	1.777	1.716	1.666	1.579
Stream 3	1.670	1.645	1.622	1.600	1.578	1.558	1.520
Stream 4	1.602	1.561	1.523	1.486	1.452	1.418	1.351
Stream 5	1.600	1.566	1.534	1.505	1.478	1.453	1.408
Stream 6	1.482	1.496	1.509	1.521	1.533	1.544	1.566
Stream 7	1.924	1.924	1.923	1.923	1.923	1.923	1.922
Stream 8	1.847	1.803	1.771	1.745	1.723	1.703	1.669
Mean	1.7246	1.7015	1.6786	1.6520	1.6309	1.6119	1.5773
σ (SD)	0.170801	0.166408	0.161588	0.154362	0.155373	0.159776	0.173689
σ (SE)	0.06039	0.05883	0.05713	0.05458	0.05493	0.05649	0.06141

Optimum cut-off time = 100ns

Best estimate for a/b = 1.652 ($\pm$.055)

Corresponding estimate for b/c = 1.305

(b) <u>±1 % assumed measured error in R</u>

Cut-off time	75ns a/b	80ns a/b	85ns a/b	90ns a/b	95ns a/b	100ns a/b	105ns a/b
Stream 1	1.856	1.856	1.856	1.820	1.821	1.767	1.834
Stream 2	1.856	1.856	1.856	1.856	1.856	1.856	1.856
Stream 3	1.856	1.821	1.791	1.732	1.691	1.658	1.628
Stream 4	1.843	1.728	1.655	1.599	1.551	1.508	1.467
Stream 5	1.834	1.716	1.655	1.608	1.568	1.532	1.501
Stream 6	1.471	1.492	1.511	1.528	1.544	1.560	1.575
Stream 7	1.856	1.856	1.856	1.856	1.856	1.856	1.856
Stream 8	1.856	1.856	1.856	1.856	1.856	1.856	1.856
Mean	1.8035	1.7726	1.7545	1.7319	1.7179	1.6991	1.6841
σ (SD)	0.134604	0.127668	0.131819	0.135561	0.145962	0.153037	0.163378
σ (SE)	0.04759	0.04514	0.04661	0.04791	0.05161	0.05411	0.05776

Optimum cut-off time = 80ns

Best estimate for a/b = 1.773 ($\pm$.045)

Corresponding estimate for b/c = 1.0875

(c) -1% assumed measured error in R

Cut-off time	80ns a/b	85ns a/b	90ns a/b	95ns a/b	100ns a/b	105ns a/b
Stream 1	1.670	1.656	1.643	1.630	1.617	1.605
Stream 2	1.936[†]	1.861	1.799	1.749	1.705	1.665
Stream 3	1.648	1.628	1.608	1.589	1.570	1.552
Stream 4	1.614	1.576	1.541	1.507	1.475	1.444
Stream 5	1.606	1.573	1.543	1.516	1.490	1.466
Stream 6	1.452	1.466	1.478	1.489	1.499	1.509
Stream 7	1.815	1.842	1.870	1.902	1.936[†]	1.936[†]
Stream 8	1.759	1.737	1.716	1.698	1.681	1.666
Mean	1.6875	1.6674	1.6498	1.6350	1.6216	1.6054
σ (SD)	0.147596	0.137488	0.136111	0.142556	0.153928	0.157728
σ (SE)	0.05218	0.04861	0.04812	0.05040	0.05442	0.05577

[†] Upper limit ($\equiv$ b/c = 1.0)

Optimum cut-off time = 90ns

Best estimate for a/b = 1.650 ($\pm$ .048)

Corresponding estimate for b/c = 1.3905

Table 18. Determination of the optimum cut-off time for Protein 3.

True (a/b, b/c) = (1.25, 1.7)

(a) No assumed error in R

Cut-off time	80ns	100ns	105ns	110ns	115ns	120ns	140ns
	a/b	a/b	a/b	a/b	a/b	a/b	a/b
Stream 1	1.367	1.315	1.303	1.291	1.278	1.266	1.215
Stream 2	1.881	1.587	1.547	1.510	1.476	1.442	1.313
Stream 3	1.388	1.301	1.281	1.263	1.240	1.219	1.119
Stream 4	1.464	1.285	1.244	1.200	1.151	1.089	1.001
Stream 5	1.448	1.278	1.239	1.200	1.157	1.108	1.000
Stream 6	1.000	1.000	1.000	1.000	1.000	1.000	1.000
Stream 7	1.314	1.393	1.409	1.424	1.439	1.453	1.505
Stream 8	1.514	1.421	1.402	1.385	1.370	1.354	1.297
Mean	1.4220	1.3225	1.3031	1.2841	1.2639	1.2414	1.1813
σ (SD)	0.243637	0.165850	0.160554	0.158626	0.161019	0.168224	0.184692
σ (SE)	0.08614	0.05864	0.05676	0.05608	0.05693	0.05948	0.06530

Optimum cut-off time = 110ns

Best estimate for a/b = 1.284 ($\pm$.056)

Corresponding estimate for b/c = 1.695

(b) +1% assumed measured error in R

Cut-off time	105ns	110ns	115ns
	a/b	a/b	a/b
Stream 1	1.319	1.306	1.293
Stream 2	1.618	1.562	1.516
Stream 3	1.294	1.272	1.249
Stream 4	1.247	1.199	1.145
Stream 5	1.245	1.202	1.155
Stream 6	1.000	1.000	1.000
Stream 7	1.444	1.462	1.481
Stream 8	1.431	1.412	1.394
Mean	1.3248	1.3019	1.2791
σ (SD)	0.181404	0.176485	0.178272
σ (SE)	0.06414	0.06240	0.06303

Optimum cut-off time = 110ns.

Best estimate for a/b = 1.302 ($\pm$.062)

Corresponding estimate for b/c = 1.5395

(c) <u>-1% assumed measured error in R</u>

Cut-off time	105ns a/b	110ns a/b	115ns a/b
Stream 1	1.294	1.283	1.271
Stream 2	1.511	1.481	1.452
Stream 3	1.275	1.257	1.238
Stream 4	1.246	1.206	1.163
Stream 5	1.240	1.204	1.165
Stream 6	1.000	1.000	1.000
Stream 7	1.387	1.400	1.413
Stream 8	1.385	1.370	1.355
Mean	1.2923	1.2751	1.2571
$\sigma(SD)$	0.149290	0.147794	0.149222
$\sigma(SE)$	0.05278	0.05225	0.05276

Optimum cut-off time = 110ns

Best estimate for a/b = 1.275 ($\pm$.052)

Corresponding estimate for b/c = 1.764

Table 19. Mean values for the retrieved axial ratios compared

with the real values

	Retrieved $(\frac{a}{b}, \frac{b}{c})$	Real $(\frac{a}{b}, \frac{b}{c})$
Protein 1	(1.501, 1.498)	(1.50, 1.50)
Protein 2	(1.652, 1.305)	(1.70, 1.25)
Protein 3	(1.284, 1.695)	(1.25, 1.70)

Table 20. Effect of experimental errors in the intrinsic viscosity

and molecular weight

(and hence the product $[\eta].M_r$ used in calculating the decay constants

- cf Table 14 and equation 108)

Assumed error in $[\eta]$ = $\pm 1\%$ } total error ~ $\pm 1.7\%$ (calculated
    "   "   " M_r = $\pm 1.4\%$ } from formula given in Paradine & Rivett (1960))

Results are for Protein 1, cut-off time = 115ns, $\pm 0.1°$ standard error

on each of the 100 data points

Stream no. of random data	− 1.7%	No error a/b	+ 1.7%
1	1.493	1.503	1.520
2	1.638	1.654	1.679
3	1.455	1.468	1.487
4	1.374	1.396	1.424
5	1.383	1.401	1.425
6	1.305	1.315	1.333
7	1.695	1.694	1.704
8	1.566	1.575	1.593
mean a/b	1.4886	1.5008	1.5206
σ_{SD}	0.136305	0.132475	0.130253
σ_{SE}	0.04819	0.04684	0.04668

σ_{SD} = standard deviation

σ_{SE} = standard error

Table 21. Effect of using different initially assumed values for the pre-exponential factors $A'_{\pm}$

Protein 1, Cut off time = 100 ns, 0.1 s.e. on each of the 100 data points[*]

Assumed		Retrieved		
A'_+	A'_-	a/b	A'_+	A'_-
0.06	0.06	1.683	0.057	0.064
0.07	0.05	1.674	0.065	0.055
0.09	0.03	1.660	0.083	0.038
0.11	0.01	1.664	0.099	0.021
0.119	0.001	1.644	0.109	0.012

*The data for this table were obtained after the UK NAG Mk VI routines had been updated to Mk VII; the new random number routines corresponding to G05ADF & G05BAF in Mk VI are G05CAF & G05CBF

Table 22. Comparison of model dependent estimates for V_e with

the real values

	Retrieved $(\frac{a}{b}, \frac{b}{c})$	Model-dependent[*] V_e (cm^3)	Real V_e (cm^3) (cf Table 14)
Protein 1	(1.501, 1.498)	1.131×10^{-19}	1.131×10^{-19}
Protein 2	(1.652, 1.305)	0.889×10^{-19}	0.890×10^{-19}
Protein 3	(1.284, 1.695)	1.202×10^{-19}	1.211×10^{-19}

*calculated by determining the value of v corresponding to $(\frac{a}{b}, \frac{b}{c})$

and then back substituting into the equation $v = [\eta] M_r / N_A V_e$,

where $[\eta]$ is in ml/gm
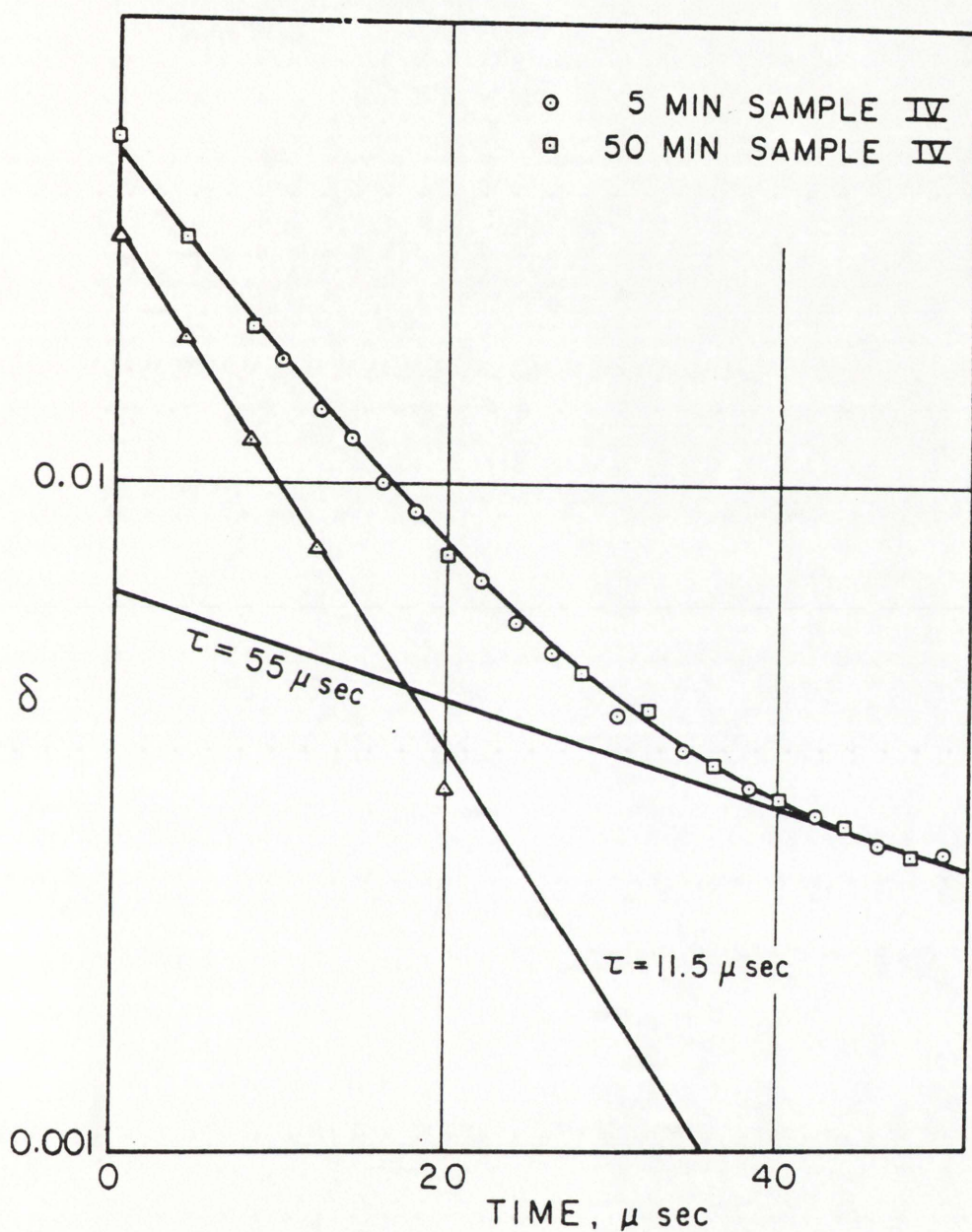
Figure 39. Birefringence decay (expressed in radians) in Helix Pomatia hemocyanin solutions. The triangles represent the difference between the tangential curve (long relaxation time) and the experimental points. (From Pytkowickz & O'Konski, 1959)
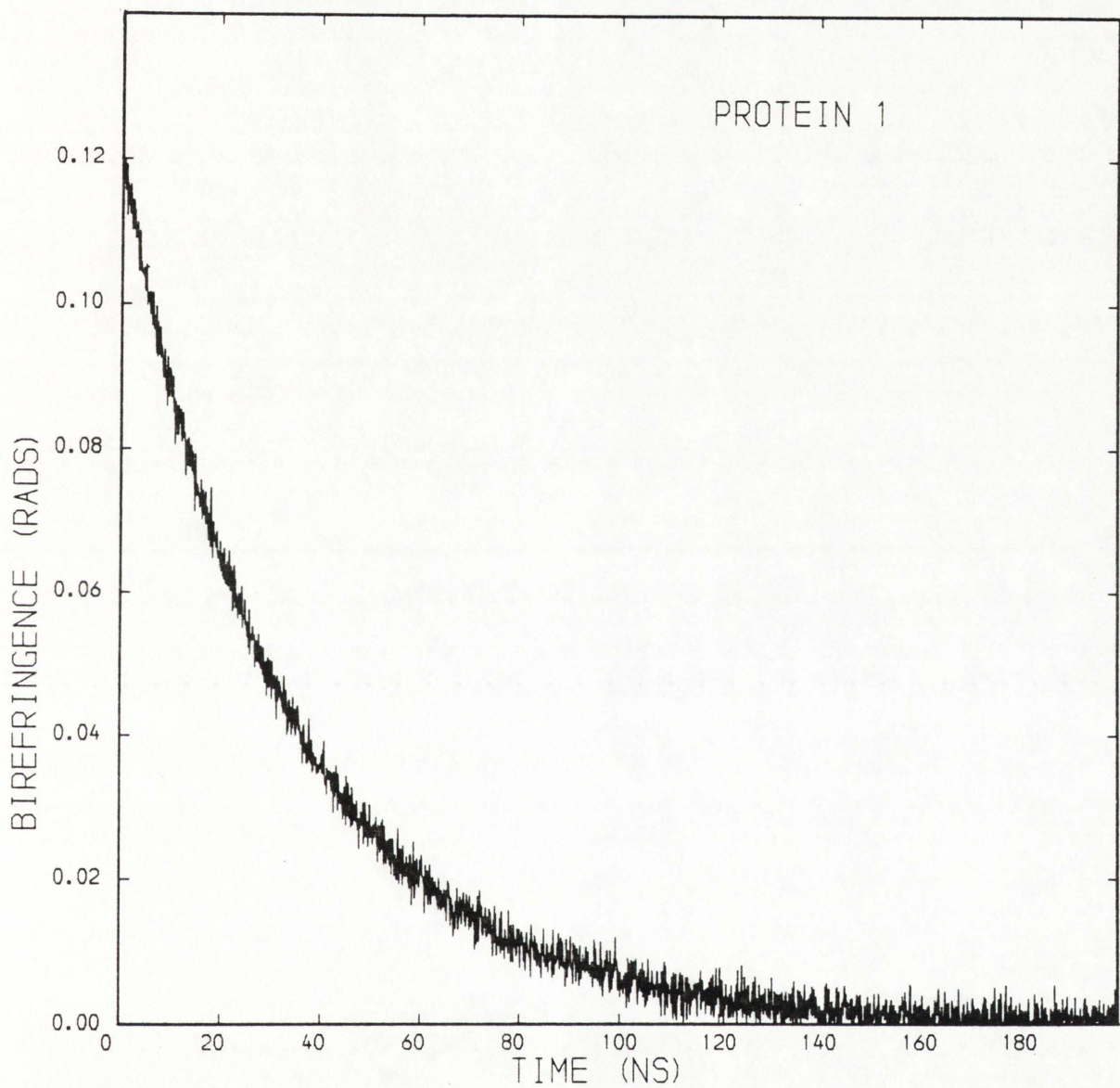
Figure 40. <u>Synthetic two-term exponential electric birefringence decay curve</u>

<u>assuming a standard error of $\pm$ 0.1° on each data point.</u>

Relaxation times assumed: 28.66ns, 40.10ns
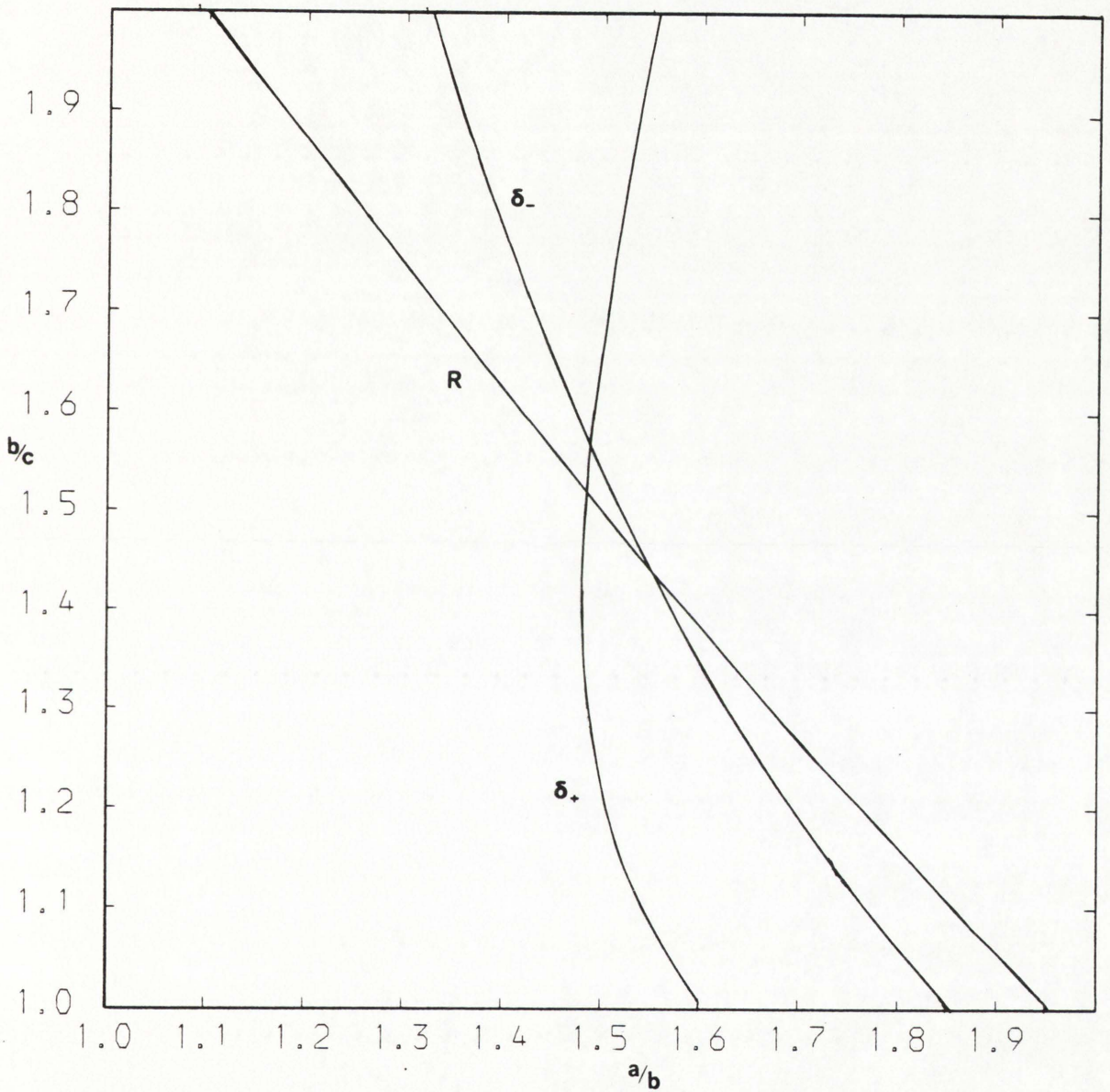
Figure 41. Plot of the R, δ_+ and δ_- values obtained from the non-linear least

squares analysis assuming birefringence data of machine accuracy
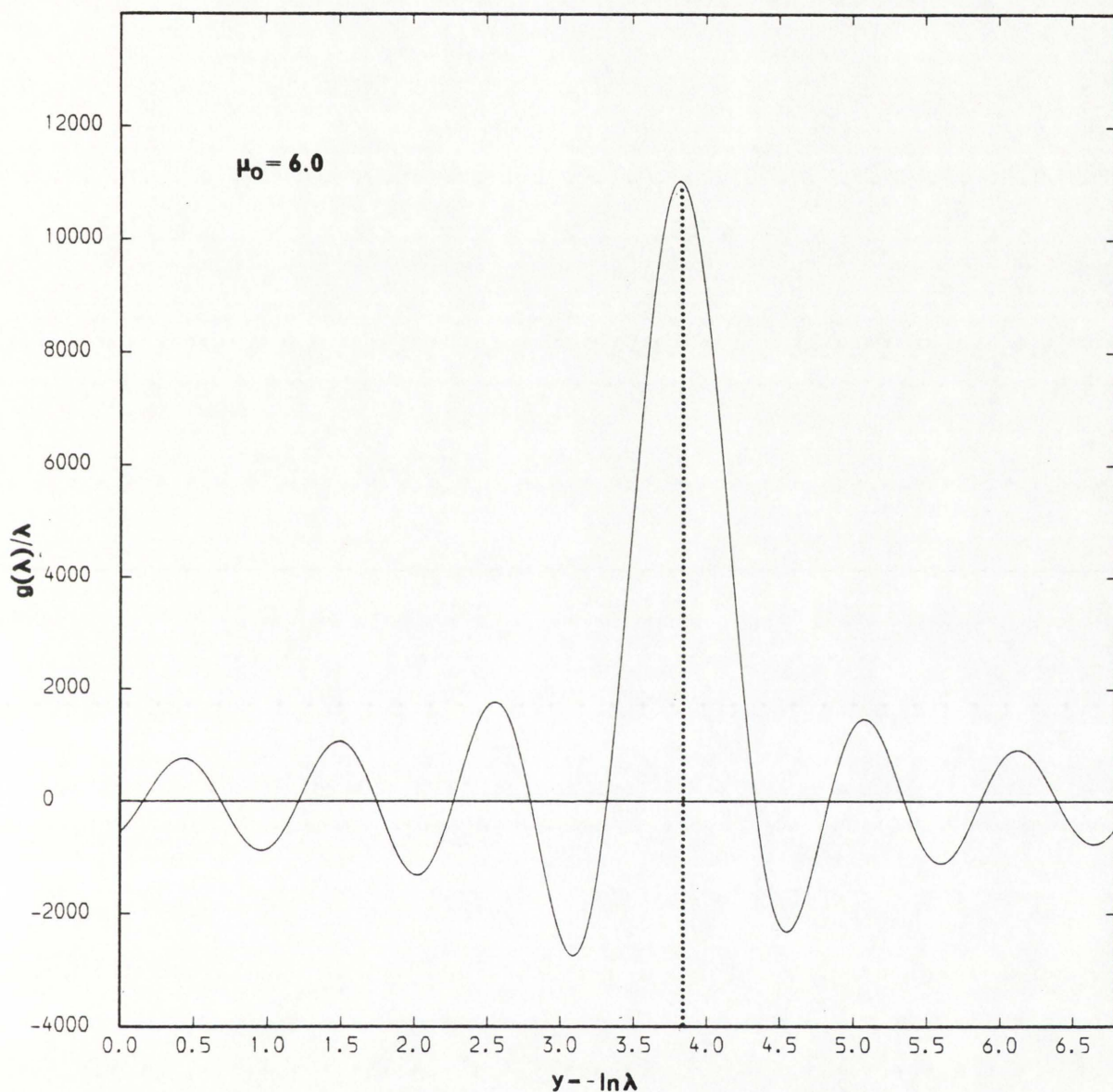
Figure 42. Frequency spectrum of λ (≈ 1/relaxation time) for a single

exponential decay and $\mu_0 = 6.0$, assuming decay data of machine

accuracy (14 figures). The position of the highest peak

corresponds to a value of λ of .021, in agreement with the

initially assumed value of 0.02

Figure 43 (I - VI)

Effect of increasing μ_0 to determine best resolution of the frequency

spectrum corresponding to the decay for Protein 2, for 140 logarithmically

increasing data points of machine accuracy (14 figures)

I

$\mu_o = 6.0$

II

$\mu_o = 8.0$

V $\mu_O = 11.7$

VI $\mu_O = 12.0$
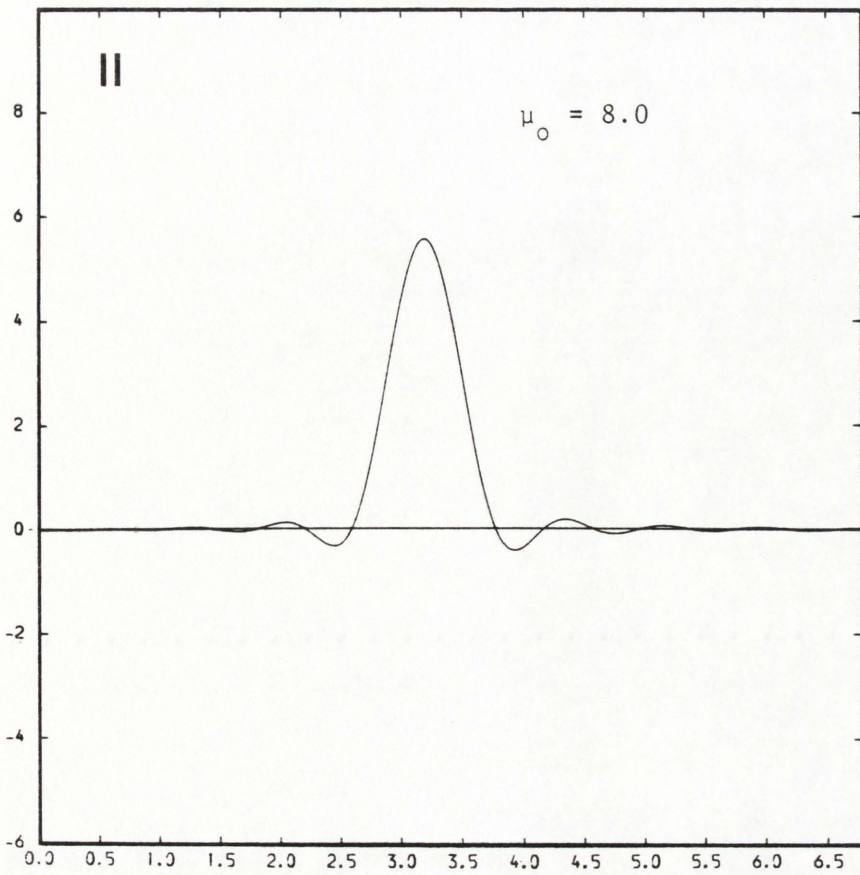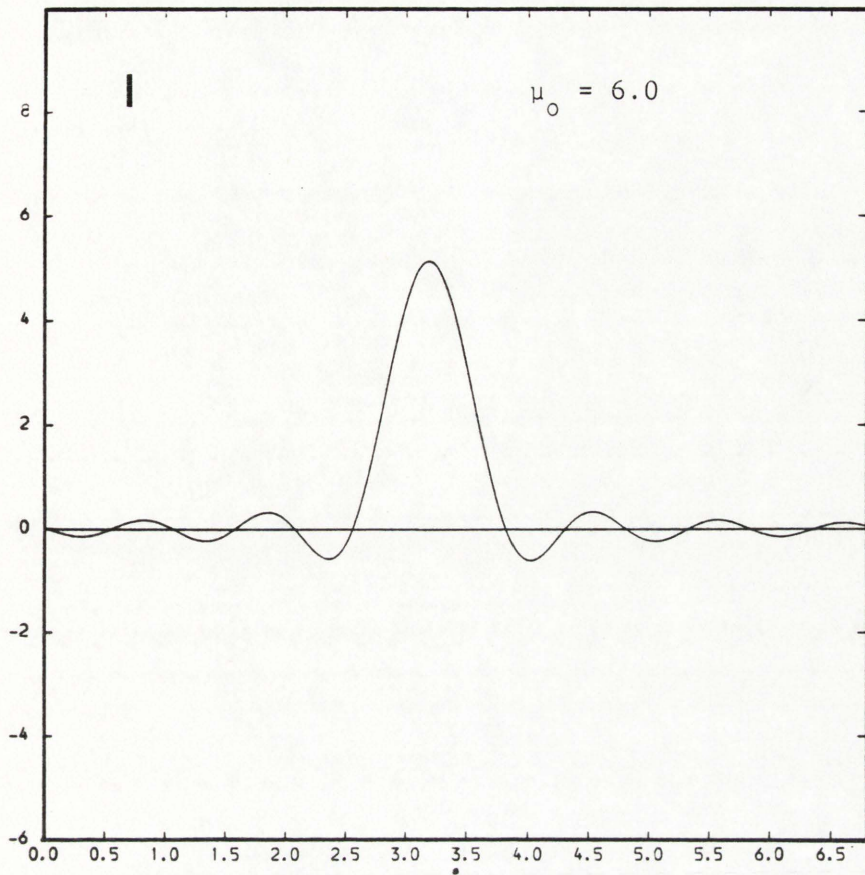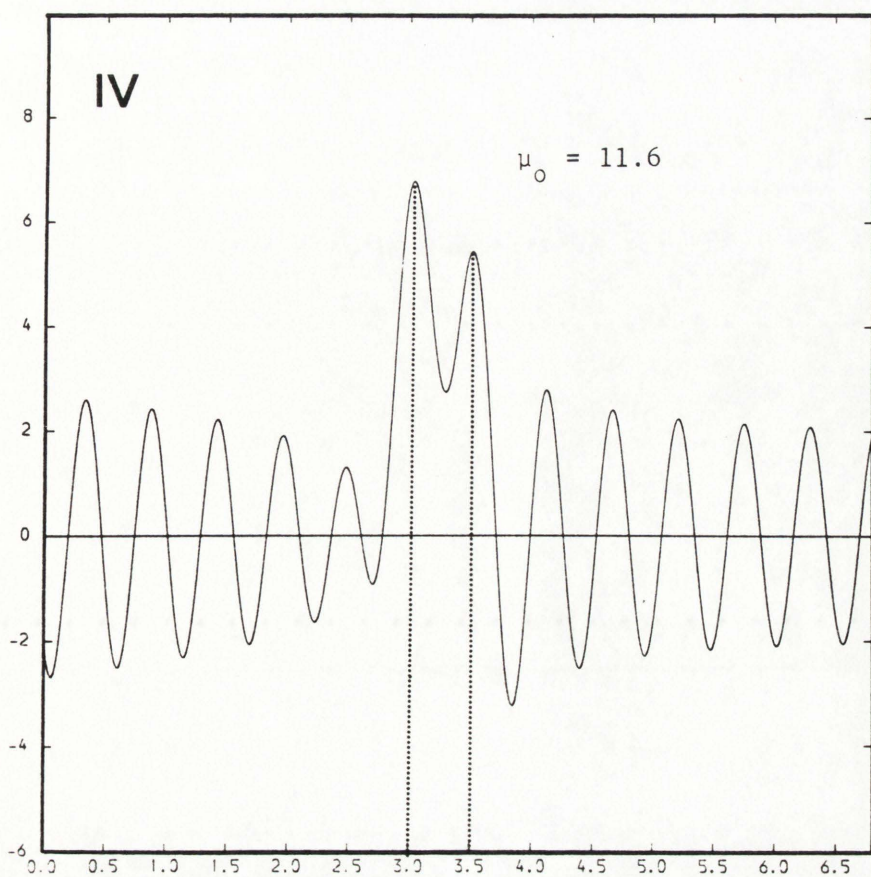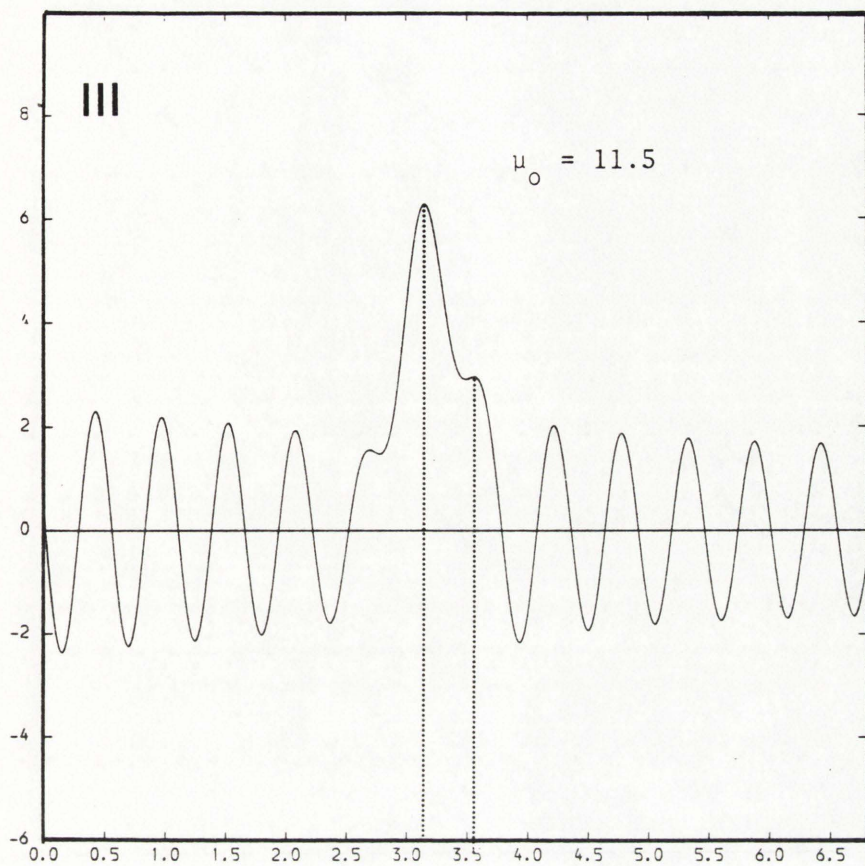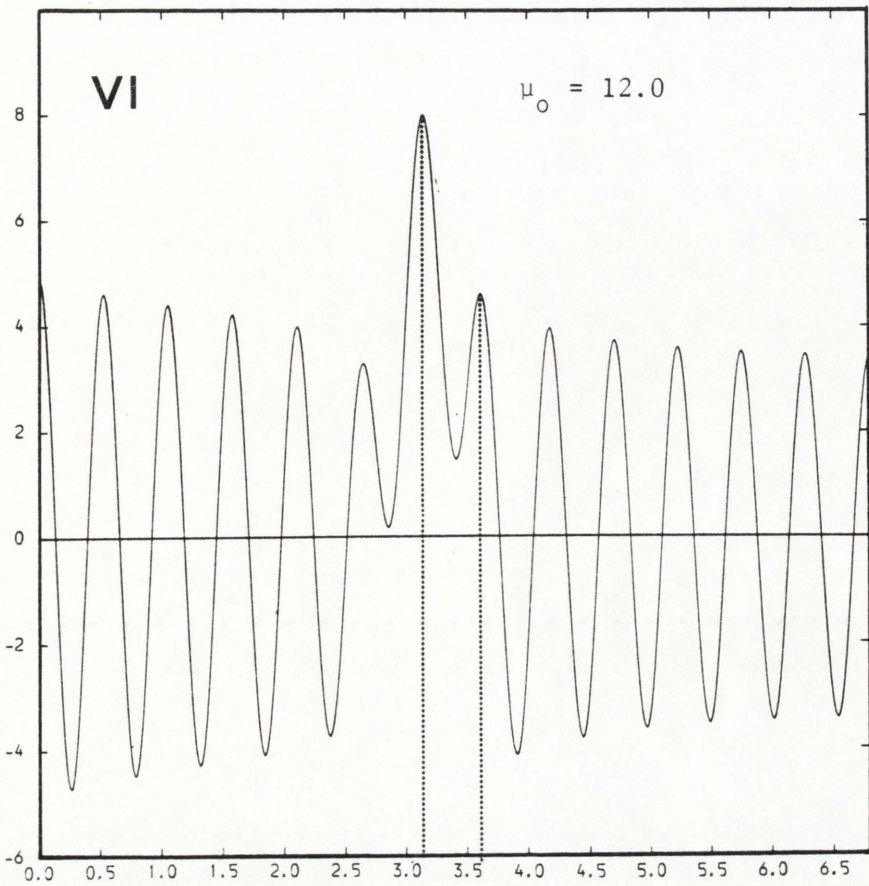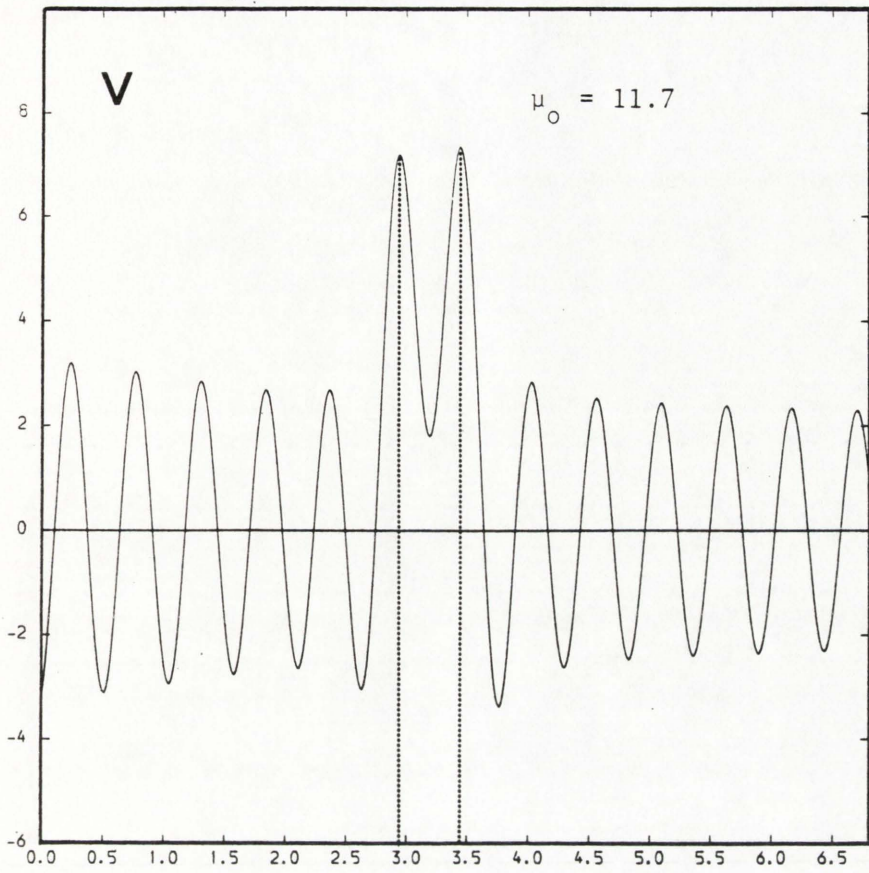
<u>Figur_ 44</u> (I - VI)

As for Figure 43 but for data of .001° standard error on each of the

140 logarithmically increasing data points

I $\mu_o = 6.0$

II $\mu_o = 6.5$

III $\mu_o = 7.0$

IV $\mu_o = 8.0$
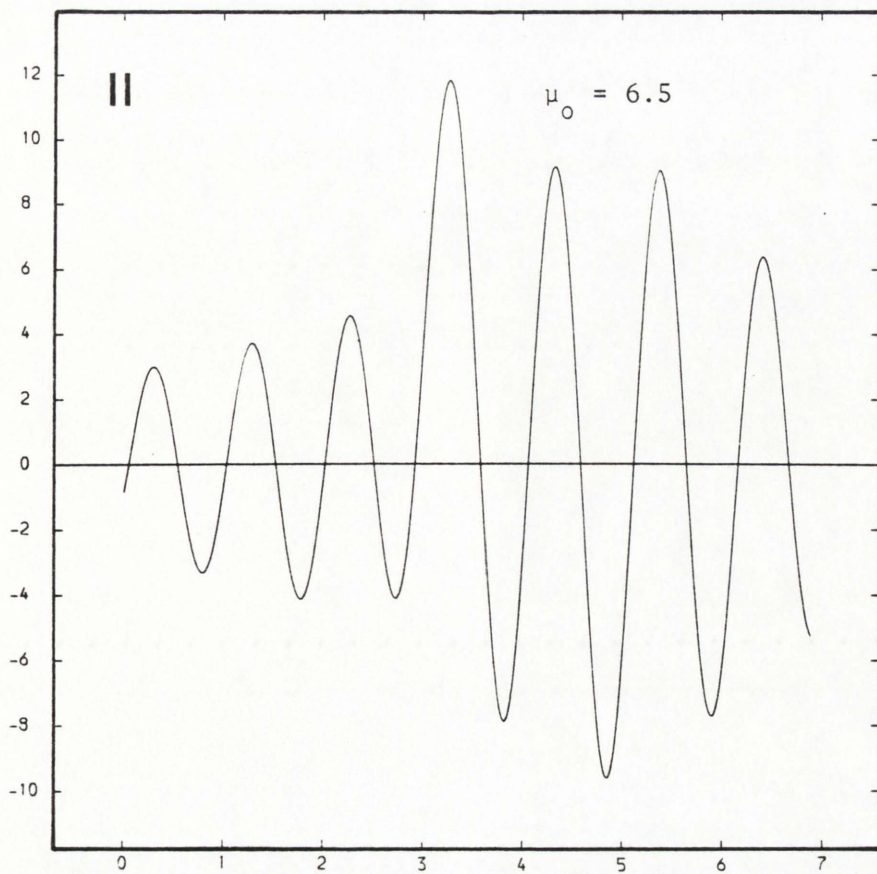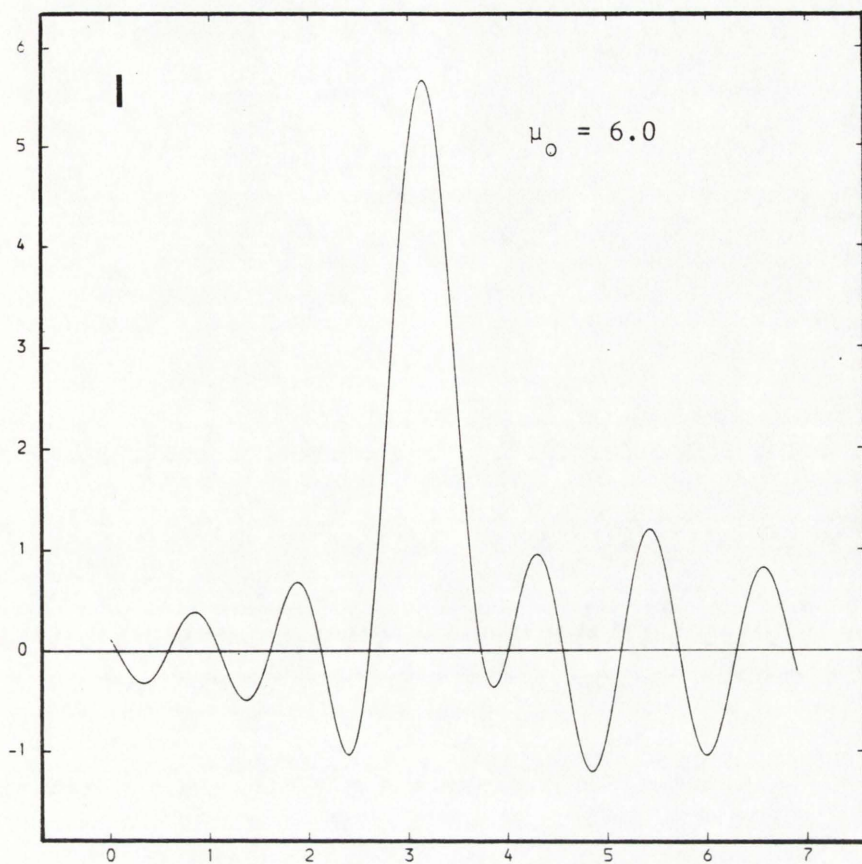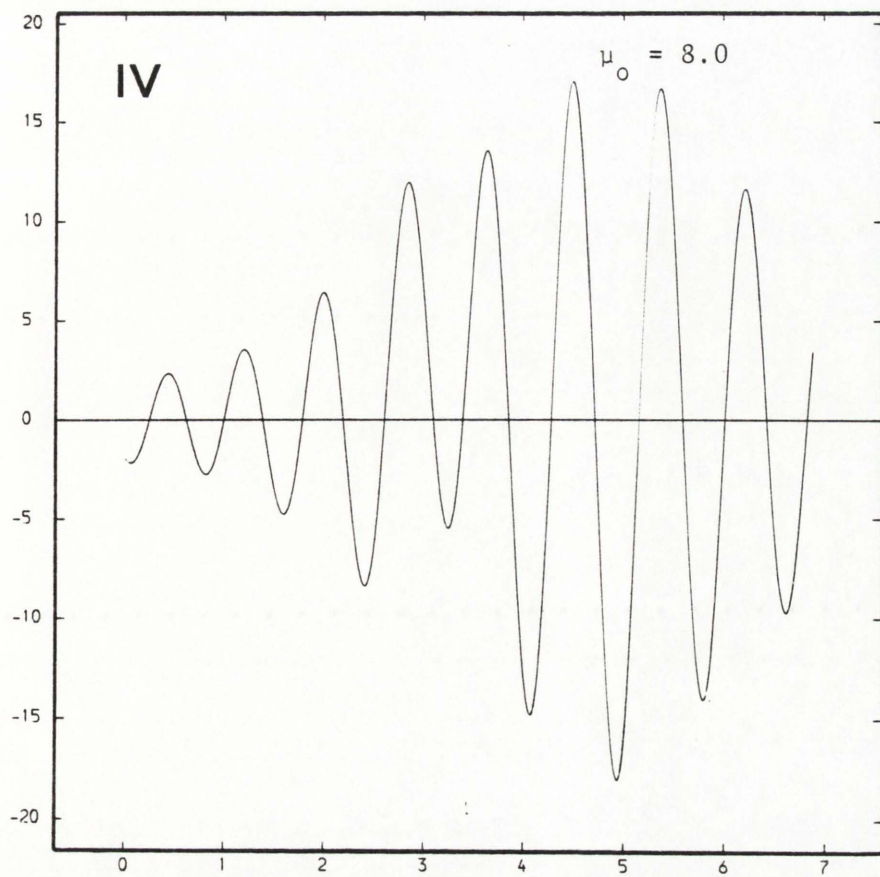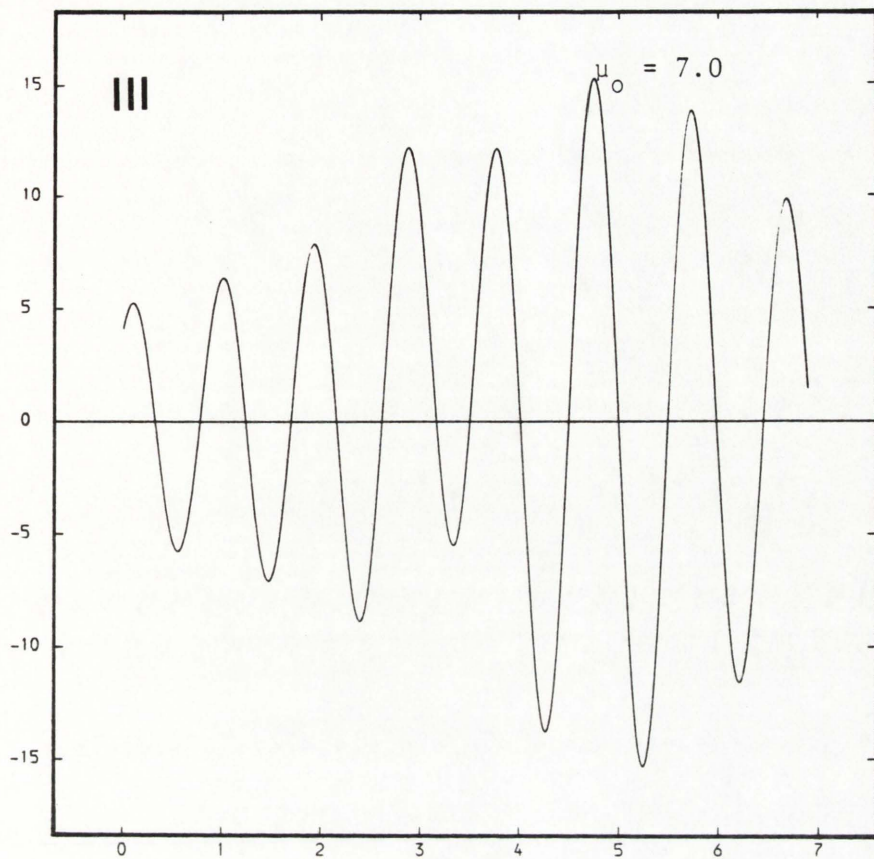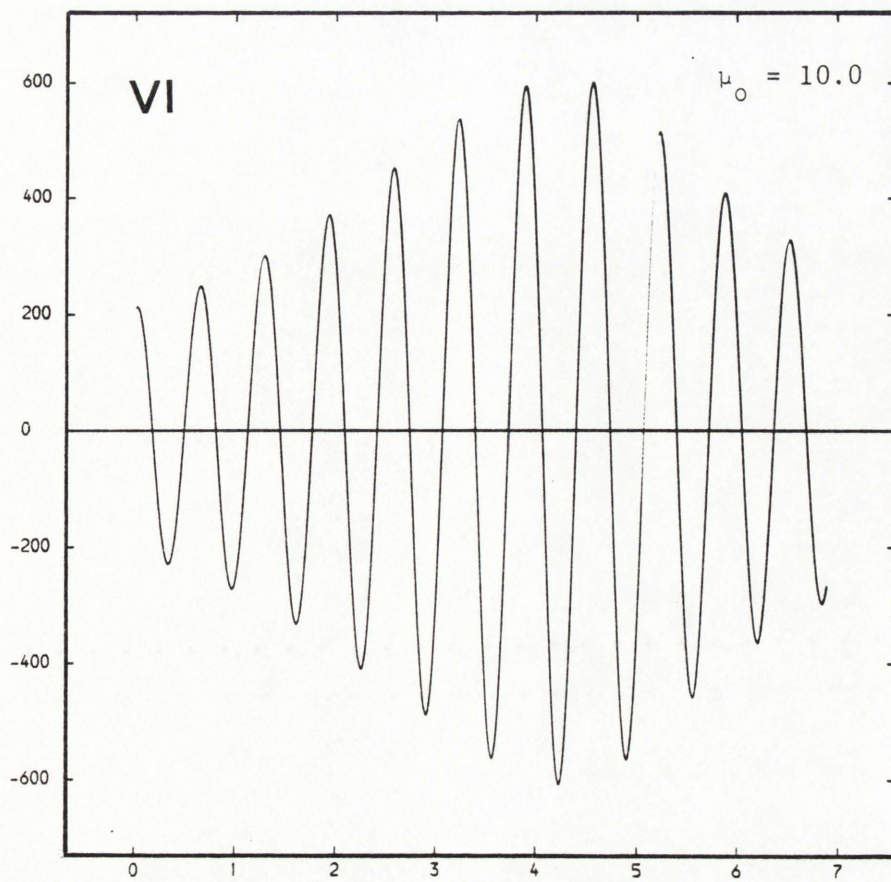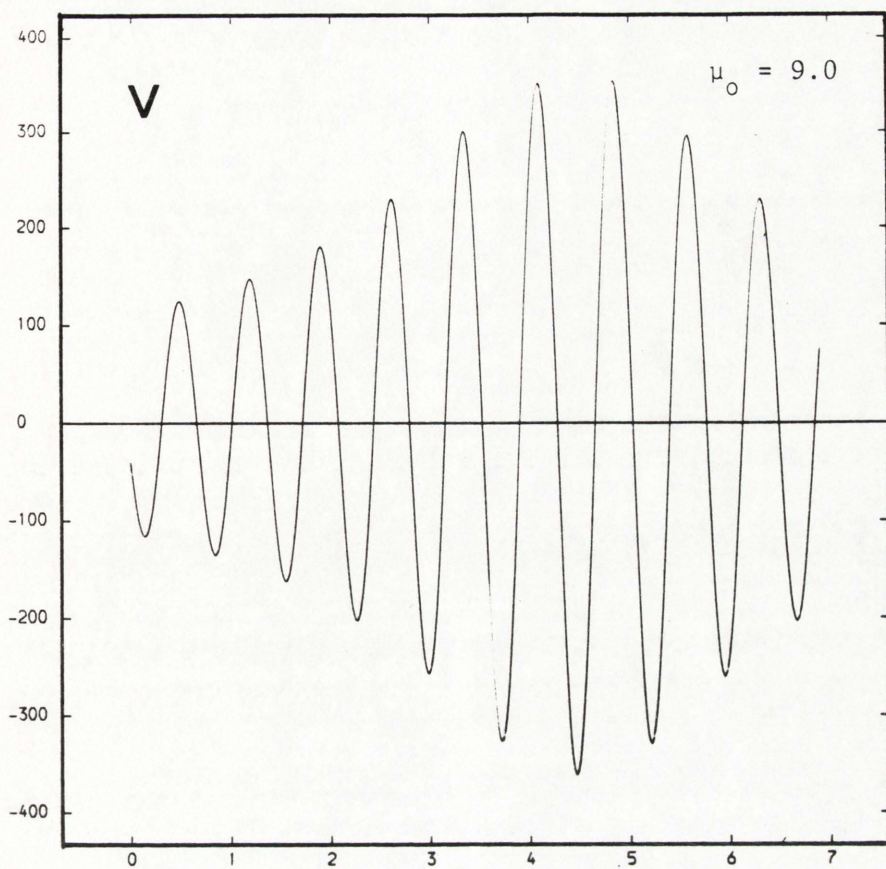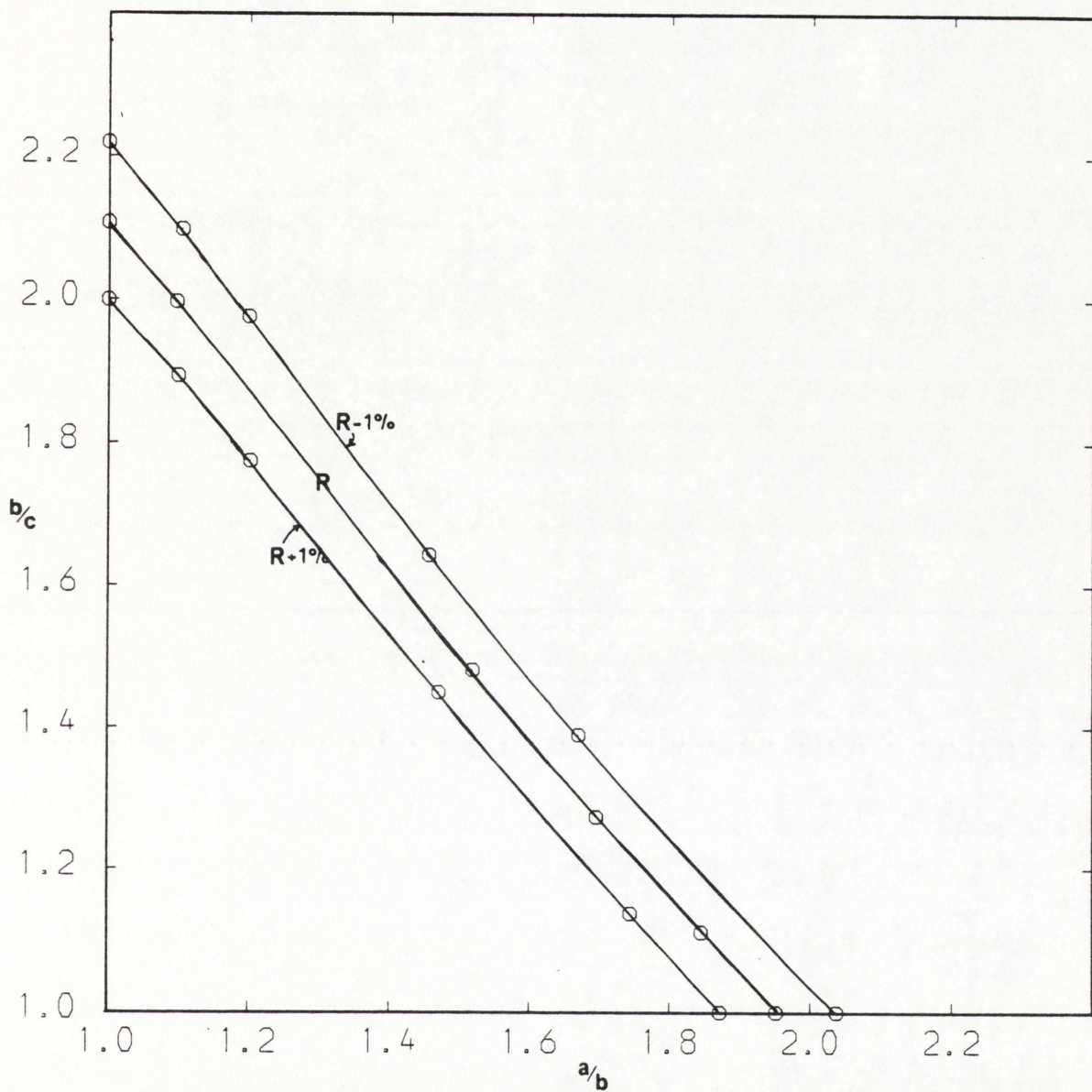
Figure 45. Knots in the R curves for specification in the R – constrained least squares analysis (Program 7) for Protein 1
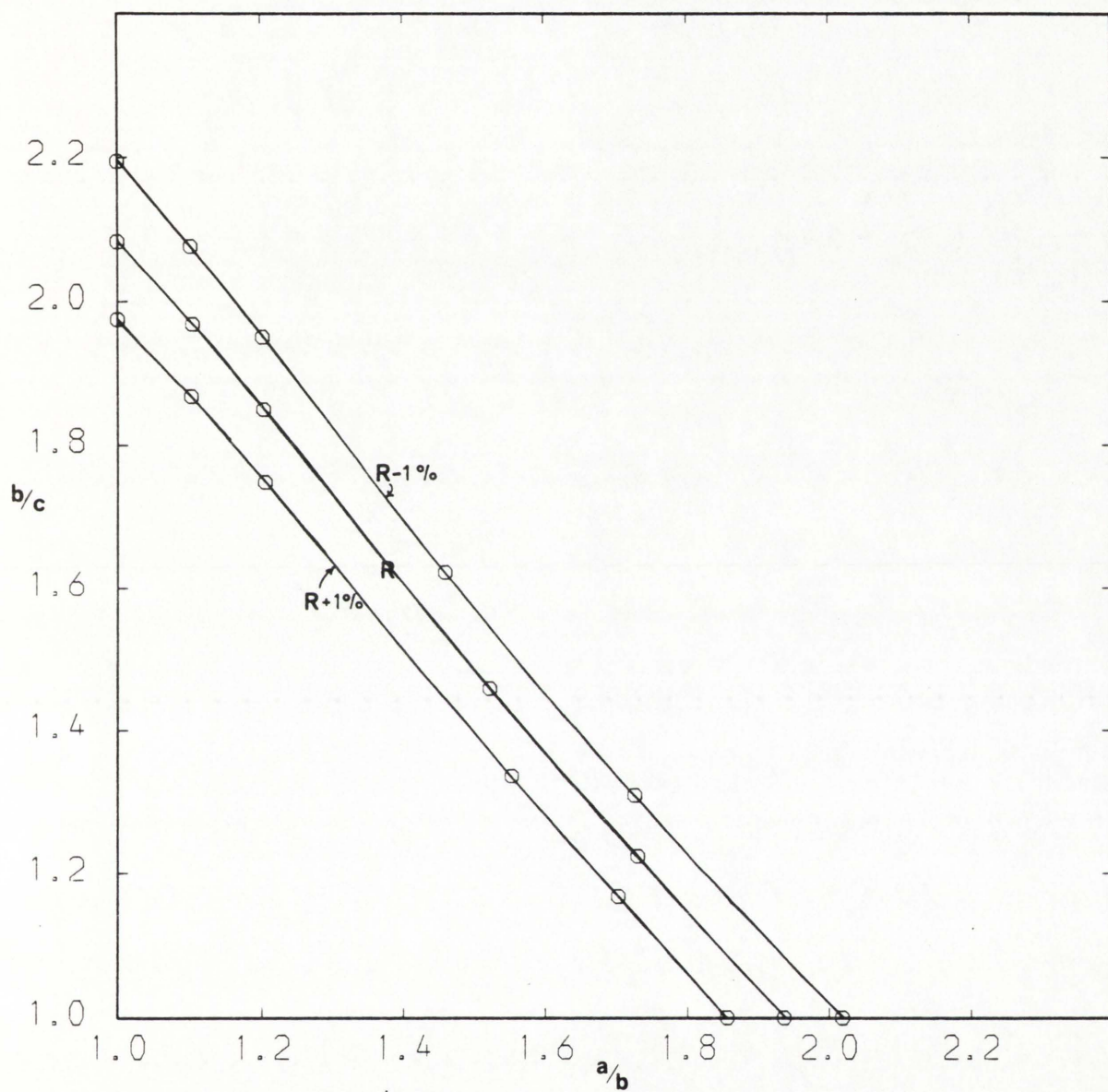
Figure 46. As for Figure 45 but for Protein 2
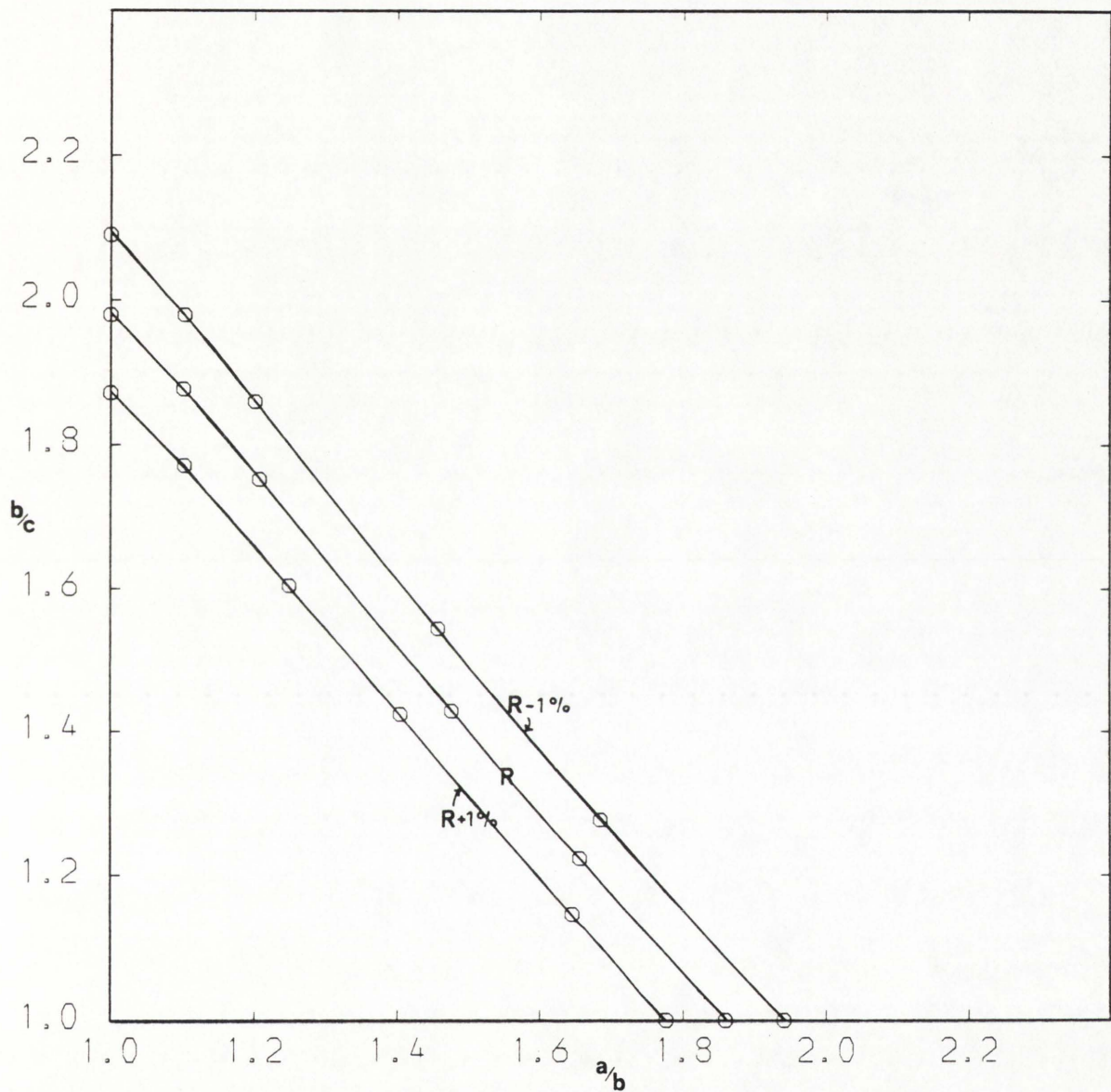
Figure 47. As for Figure 45 but for Protein 3
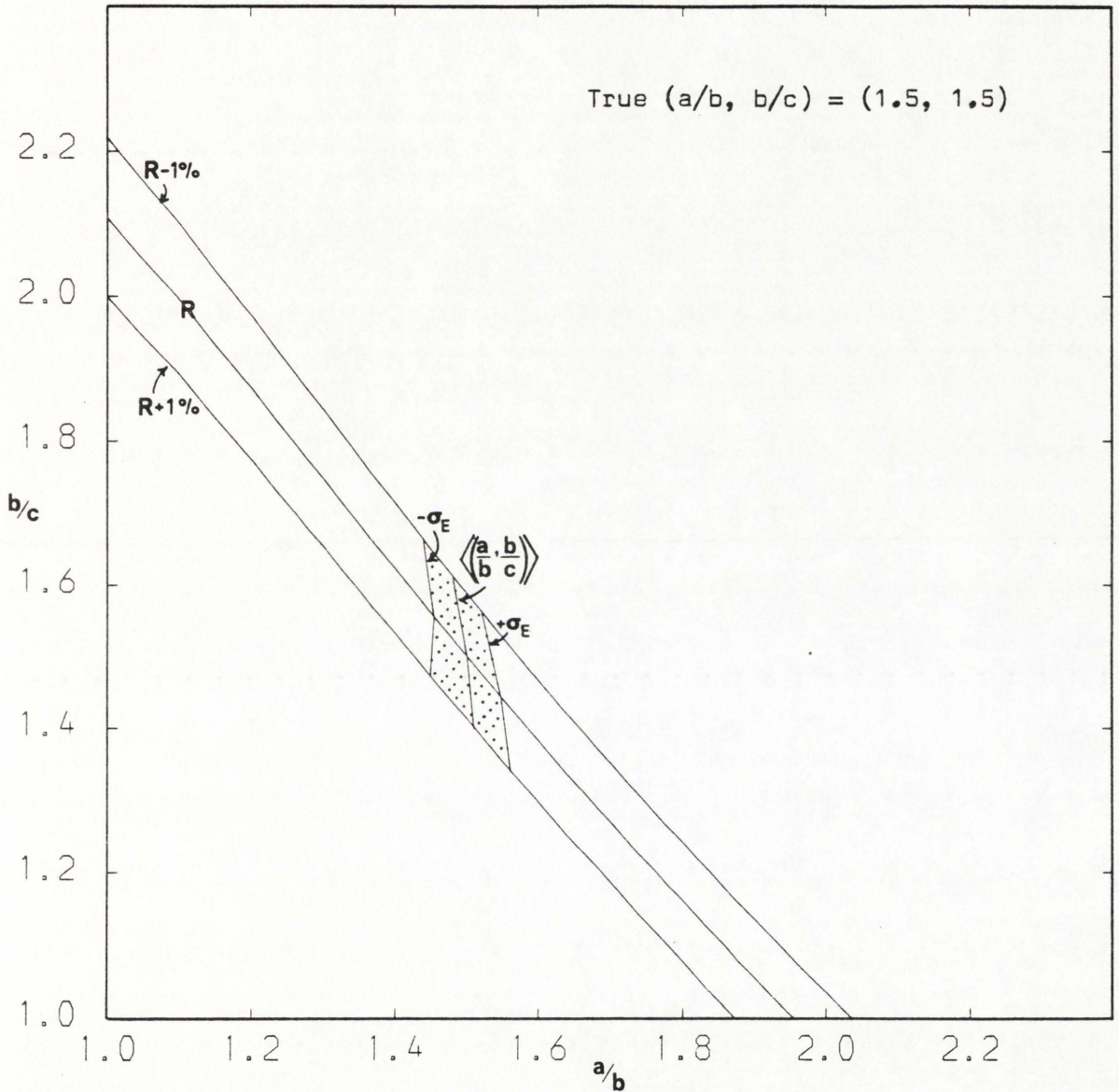
Figure 48. The area marked by dots represents the allowed band of retrieved axial ratios determined using the new R – constrained least squares algorithm for Protein 1. Simulated experimental error of $\pm$ 0.1° standard error on each data point for the electric birefringence decay curve was assumed.
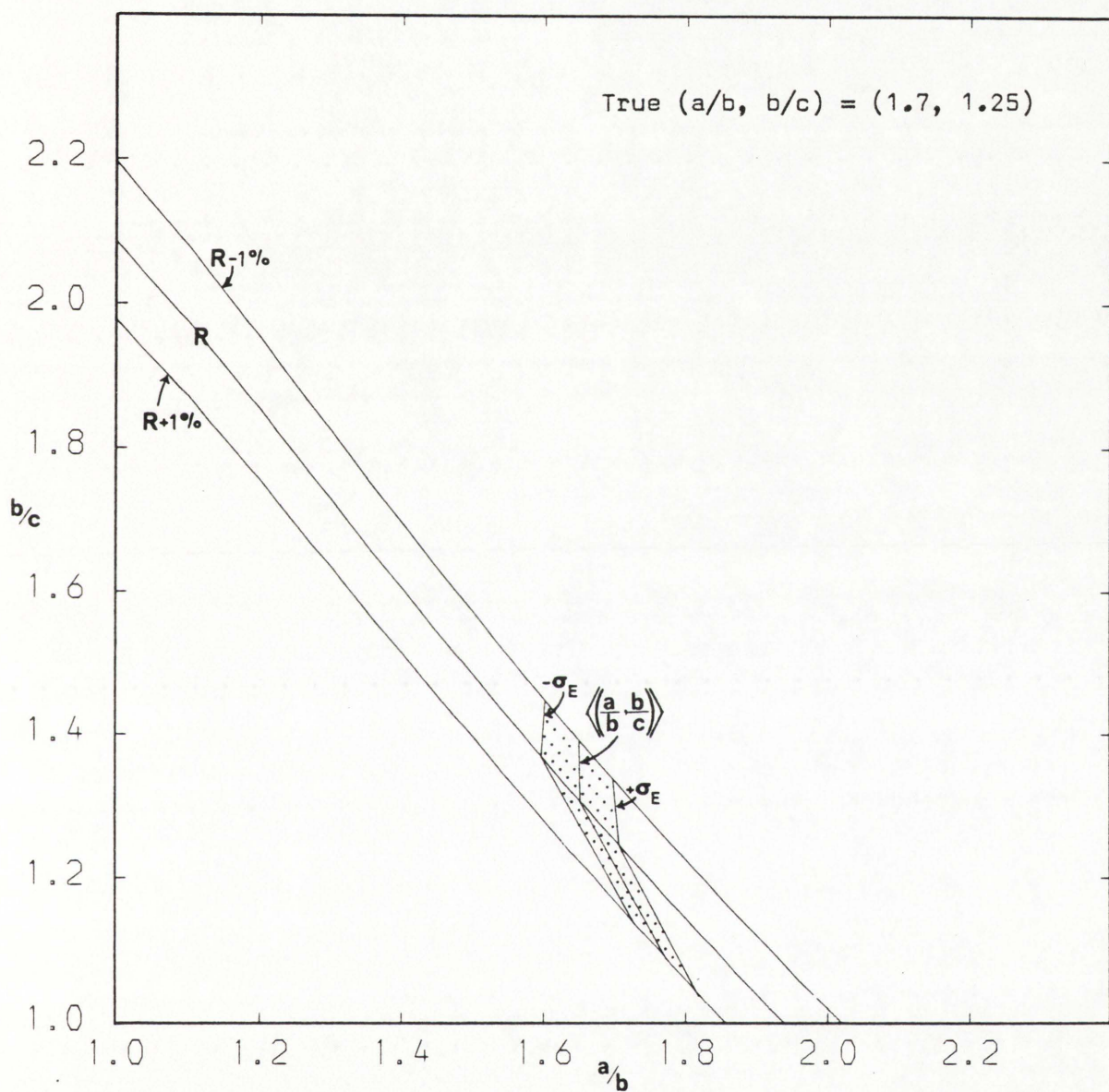
Figure 49. As for Figure 48 but for Protein 2
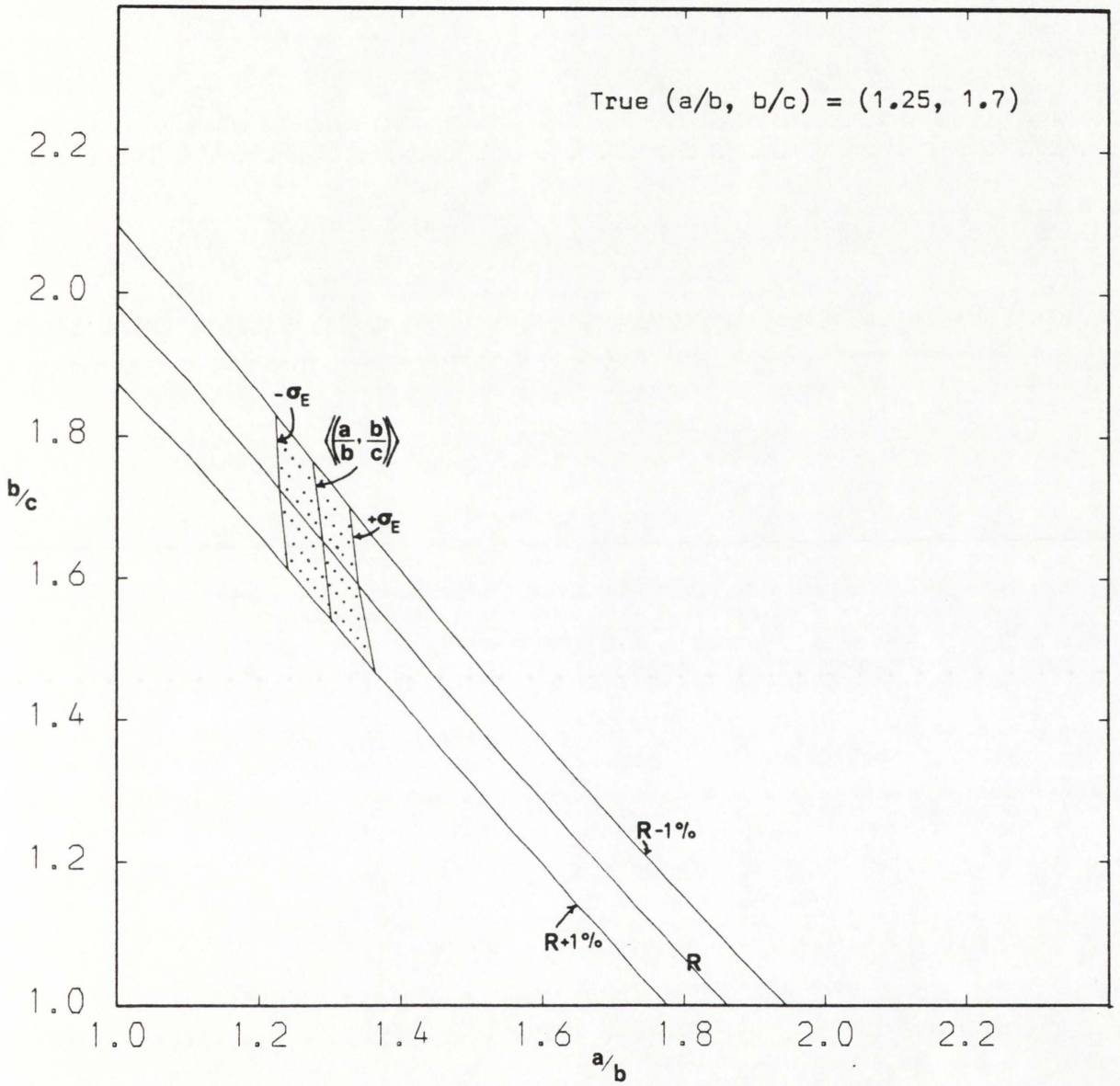
<u>Figure 50.</u>   <u>As for Figure 48 but for Protein 3</u>

C H A P T E R   5

Concluding Remarks

In this study an extensive review of all the possible shape functions available for modelling a biological macromolecule in solution in terms of an ellipsoid model with the restriction of two equal axes has been given, thus updating the classical reviews of Edsall (1953) and Tanford (1961). It was concluded that the most suitable shape parameter (particularly for axial ratios less than 20:1) was the R parameter which can be determined from the ratio of the sedimentation regression coefficient, k_s to the intrinsic viscosity, $[\eta]$ A word of warning should perhaps be given out here in that the k_s value found from fitting sedimentation coefficient versus concentration data either to the general equation (60) or to the approximate linear equation (58), is the value based on particle migration relative to the solvent, whereas the $[\eta]$ values are normally measured to solution density (Tanford, 1955). The value of k_s must therefore be corrected to solution density, and this can be achieved simply by subtracting the value of the partial specific volume, $\bar{v}$ (Rowe, 1977) since this latter can be equated to the reciprocal density of the solute, an assumption reasonably accurate for proteins and possibly for nucleic acids (Pearce et al, 1975). It is also now possible to estimate a value for k_s direct from a knowledge of the sedimentation coefficient, the molecular weight and $\bar{v}$ (Appendix VI).

Despite the availability of the R function for determining the 'equivalent hydrodynamic ellipsoid of revolution' for a structure in solution to a reasonable precision (and also the Π function for prolate ellipsoids - Appendix III), it was clear from a perusal of the crystallographic dimensions given in Table 3 and a comparison of model dependent with model independent estimates for $\bar{v}_s/\bar{v}$ in Table 2, that for many macromolecules the assumption of two equal axes on the ellipsoid model is a poor

approximation to the real structure in solution. This stimulated my
attempts to develop the necessary theoretical and data analysis techniques
so that the restriction of two equal axes could be dispensed with and the
subsequent research has shown that the more general tri-axial ellipsoid
can now, in principle at least, be successfully employed for modelling
biological macromolecules in solution.

The first step was to derive an explicit expression for the viscosity
increment ν for a dilute suspension of general tri-axial ellipsoids in
overwhelming Brownian motion, based on a model first given by Simha (1940)
and improved by Saito (1951) for ellipsoids of revolution. Although the
assumption of the particles rotating on average with the same local angular
velocity of the fluid has only been rigorously proved so far for ellipsoids
of revolution (Brenner, 1972a), it was assumed that this would be a very
close approximation for tri-axial ellipsoids, particularly for low axial
ratios (<3.0, i.e. the globular particle range). After the derivation of
equation (88) a numerical procedure (involving complicated numerical matrix
inversions), but based on a full statistical analysis of the angular motion
was made available by Rallison (1978). It was explained in section 2.8. how
the difference in the results predicted by equation (88) and Rallisons
approach was negligible (<.01%) for the globular particle range mentioned
above, and for some particles of higher asymmetry discrepancies of not more
than 1% arose. Rallison has also given a numerical procedure for
calculating the normal stress coefficients in terms of axial ratio; normal
stress effects are however second order in the shear rate, thus in order
to measure these coefficients it is necessary to use high shear rates.
However, the assumption of overwhelming Brownian motion with respect to
the shear rate ceases to be valid, and hence, unfortunately, the normal
stress coefficients cannot be applied.

It was described how the problem of the line solution (i.e. how a

given value for ν does not uniquely fix a value for the axial ratios

(a/b, b/c)) could be dealt with by combining it graphically with

translational frictional or rotational relaxation line solutions. I

was able to give the R function for tri-axial ellipsoids and also many

other tri-axial functions whose experimental determination did not require

a knowledge of the swollen molecular volume in solution. After a careful

consideration of all these line solutions with regard to giving suitable

intersections, experimental measurability, insensitivity to experimental

error and sensitivity to axial ratio, it was decided that the best approach

for determining a unique solution would be to combine the R line solution

graphically with the δ_+ and δ_- line solutions, the latter to be determined

from the two electric birefringence decay constants and the intrinsic

viscosity.

Unfortunately, this still requires having to resolve the two decay

constants or relaxation times from a two-term exponential birefringence

decay for a homogeneous solution of asymmetric particles. This problem

is notoriously difficult, as reported by Jost & O'Konski (1978) and

O'Connor, Ware & Andre (1979), particularly for close relaxation times (as

applies to globular proteins). The currently best available methods evident

from these studies, viz. the non-linear least squares iterative method and

possibly the Fourier Transform solution of the Laplace Integral equation

method of Gardner et al (1959) were tested by exhaustive computer

simulation to see how much error on the data points each could tolerate

before failing to resolve the decay constants within reasonable limits. The

Fourier method failed, even for data of machine accuracy (14 figures). The

non-linear least squares method was found to be unstable due to the problem

of subsidiary minima located in the iteration procedure, even for data
of two orders of magnitude more precise than that currently available
from the best instrumentation.

The idea of applying the R function line solution as a constraint in
the least squares analysis was then applied to the three simulated decays
thus effectively reducing the problem from one of four independent variables
(the two pre-exponential factors and the two decay constants) to one of
three (two pre-exponential factors and one axial ratio, a/b). The algorithm
was then shown to be very successful for synthetic data corresponding to
that available from current experimental precision. The problem of the
concentration dependence of the decay constants (or equivalently the
relaxation times) was then mentioned, and the necessity for extrapolating
the values for the axial ratios determined at various concentrations to
infinite dilution. The need for extrapolating axial ratios is somewhat
conceptually difficult to envisage at first sight, since one would more
naturally extrapolate the decay constants and then calculate the axial
ratios from them. In the algorithm however, I have included the R value
as the constraint - the R function line solution of possible values of
(a/b, b/c) is the value applicable at _infinite dilution_, thus the decay
constants in the algorithm are constrained to lie on the 'infinite dilution'
curve; hence none of these values are the _true_ values for the decay constants
at each particular solute concentration. Any extrapolation procedure is
therefore empirical, whether it be for the decay constants or for the values
of the axial ratio a/b.

Investigation of the theoretical reasons for the concentration
dependence of the decay constants provides however both an interesting and
important field for further work. It has been described (section 1.7.1. &

Appendix IV) how several important results have arisen from consideration

of the concentration dependence of the 'translational' (i.e. viscosity,

sedimentation and diffusion) transport coefficients: for example, in

producing the R function and making available an estimate of the swollen

volume of a macromolecule in solution independent of any model assumed for

the macromolecule.   The analysis of the concentration dependence of the

decay constants is however much more complicated: Rowe's (1977) theory for

the translational coefficients was derived assuming only hydrodynamic

(i.e. volume flux) concentration effects, viz. solutions of high ionic

strength (>0.1M) and such that electric charge effects (solute-solute

interactions) were not present.   The situation is apparently the reverse

when we come to consider the decay constants: since we are dealing with a

rotary macromolecular property, there should be no solute volume flux

effects on average giving rise to the hydrodynamic concentration effects

considered by Rowe.   On the other hand, the current practical restriction

of low ionic strengths for the electric birefringence probably results in

some solute-solute electric charge effects; the double layer thickness

of charge around a macromolecule in solution is inversely proportional to

the square root of the ionic strength (Guoy, 1910, Chapman, 1913).   For

example, for a macromolecule suspended in a 0.1M NaCl buffer the thickness

of the double layer is ~ 1nm, whereas in a 0.001M NaCl buffer, the thickness

is as high as 10nm (Shaw, 1970).   There is therefore a greater likelihood

of interference between the relaxations of individual macromolecules, the

degree of which one would expect to increase with concentration.

In section 1.6. the techniques of light and low-angle x-ray scattering

were discussed as an alternative to the hydrodynamic techniques, and stated

how Martin (1964) had given formulae relating the radius of gyration to

axial ratio for ellipsoids of revolution. Mendelson and Hartt (1980)

have applied results from low angle x-ray scattering in terms of a

general triaxial ellipsoid model to the regulatory light chains of

scallop myosin, and determined axial dimensions of 16nm x 4.16nm x 1.26nm.

We also mentioned however that the major disadvantage of the scattering

approach was that it is necessary to assume the macromolecule to be of

uniform electron density; this can lead to errors of the order of 3%,

notwithstanding other errors in measurement as the simple calculation

given in Appendix VII for a hypothetical spherical macromolecule with a

cavity (based on the electron microscopy and x-ray diffraction results

for apoferritin - Harrison, 1959) shows.

It is hoped however that the results of the research described here

have now made it possible to determine the gross conformation of biological

macromolecules in solution in terms of a general ellipsoid - independent of

any assumptions concerning the internal homogeneity of the macromolecules -

by combining the results of viscosity, sedimentation and electric (or

acoustic) birefringence. There are some macromolecules however that

apparently will never be modelled by an ellipsoid, even tri-axial.

Bovine serum albumin (BSA) is a typical example; McCammon et al (1975)

have attempted to account for a value for β below the theoretical minimum

of 2.112 x 10^6 (and above the theoretical maximum for R of 1.6 - see Table

2) by assuming its structure to be porous with respect to the solvent, but

found the discrepancy was still far too large. With the availabilty of

the tri-axial ellipsoid model and a comparison with model independent

estimates for the swollen molecular volume, a classification of proteins

into those which do and those which do not behave as hydrodynamic tri-

axial ellipsoids in solution can now be made.

A P P E N D I C E S

Appendix I   Elliptic Integrals used in this study

$$\alpha_o = \int_o^\infty \frac{d\lambda}{(a^2 + \lambda)\Delta} \quad ; \quad \beta_o = \int_o^\infty \frac{d\lambda}{(b^2 + \lambda)\Delta} \quad ; \quad \gamma_o = \int_o^\infty \frac{d\lambda}{(c^2 + \lambda)\Delta}$$

where λ is the positive root of

$$\frac{x^2}{a^2 + \lambda} + \frac{y^2}{b^2 + \lambda} + \frac{z^2}{c^2 + \lambda} = 1$$

and $\Delta = \{(a^2 + \lambda)(b^2 + \lambda)(c^2 + \lambda)\}^{\frac{1}{2}}$.

Also

$$\alpha_o' = \int_o^\infty \frac{d\lambda}{(b^2 + \lambda)(c^2 + \lambda)\Delta} \qquad \alpha_o'' = \int_o^\infty \frac{\lambda d\lambda}{(b^2 + \lambda)(c^2 + \lambda)\Delta}$$

$$\beta_o' = \int_o^\infty \frac{d\lambda}{(c^2 + \lambda)(a^2 + \lambda)\Delta} \qquad \beta_o'' = \int_o^\infty \frac{\lambda d\lambda}{(c^2 + \lambda)(a^2 + \lambda)\Delta}$$

$$\gamma_o' = \int_o^\infty \frac{d\lambda}{(a^2 + \lambda)(b^2 + \lambda)\Delta} \qquad \gamma_o'' = \int_o^\infty \frac{\lambda d\lambda}{(a^2 + \lambda)(b^2 + \lambda)\Delta}$$

Appendix II   Illustration of use of the Λ function (equation 50) by

application to data available for the tryptic subfragments of fibrinogen

It is apparent from Figure 17 that, until the harmonic mean

relaxation time τ_h can be measured to a precision greater than that

currently available ($\sim \pm 3\%$ at best, assuming no significant internal

rotations of the chromophore or segmental rotations of parts of a

macromolecule relative to other parts), use of Λ will generally be

restricted to prolate ellipsoidal particles above an axial ratio of

about three.

Unfortunately, there is at present a lack of reliable steady state

fluorescence depolarization data for macromolecules in this axial range.

Use of the function may however be illustrated by application to data

available for the tryptic fragment of bovine fibrinogen. By using a

steady-state fluorescence - depolarization technique, Johnson & Mihalyi

(1965) reported a harmonic mean relaxation time for fibrinogen of 195 ± 5 ns,

a value lower than the corresponding value for a sphere of the same volume

(299 ns); the value for τ_h of the tryptic subfragment was 178 ns, strongly

suggesting that the tryptic subfragments had rotational freedom within the

fibrinogen molecule. Assuming there is still no further internal rotation

within the subfragment itself, one can combine this result with viscosity

and molecular-weight data obtained previously by Mihalyi & Godfrey (1963).

Taking M_r as 95,000$\pm$2,000, $[\eta]$ as (7.18 ± 0.07) ml.g^{-1} and assuming a

$\pm$ 5 ns standard error in τ_h, Λ is calculated to be 4.74 ± 0.17 where the

method for calculating the standard error in Λ is given by Paradine &

Rivett (1960). This corresponds from Figure 17 to a prolate ellipsoid of

axial ratio 6.8 ± 0.3 consistent with the estimates of the axial ratio

derived from four other hydrodynamic parameters, three of which assume no particle swelling due to solvent association (Table 23). The results from electron microscopy studies suggest however that the subfragments are nearly spherical (Hall & Slayter, 1959); as Mihalyi & Godfrey (1963) have previously stated, this difference is probably too large to be explained by drying effects alone. At least part of this difference can, however, be possibly ascribed to an apparent discrepancy between the viscosity data of their Figure 4 with the sedimentation data of their equation 2; the latter suggests a sedimentation regression coefficient, k_s, of ~ 3.6 (after correction to solution density; Rowe, 1977), whereas the viscosity regression coefficient, k_η, is only ~ 2.5. Rowe (1977) has shown that the ratio k_η/k_s is equal to the swelling ratio $\bar{v}_s/\bar{v}$, where $\bar{v}_s$ is the swollen specific volume in solution. Mihalyi & Godfrey's (1963) data apparently gives a value for the swelling of less than 1, indicating the particle to contract in solution, an unlikely event. Unfortunately, although the pH values of the solutions used for the sedimentation and harmonic mean relaxation time measurements are given and are near (6.5 and 7.1 respectively), that for the viscosity is not given, so this is a possible source of error.

It is hoped that the availability of the new Λ function will encourage the production of more reliable data in order to resolve these difficulties, and also accelerate improvement in the methodology so that τ_h/τ_0 can be measured with much greater precision, enabling application of the Λ function to prolate ellipsoids of axial ratio less than three and also to oblate ellipsoids.

Table 23. Hydrodynamic parameters and axial ratios for the tryptic

subfragments of fibrinogen

Hydrodynamic Parameter	Derived Axial Ratio	Reference
ν*	7.8	Mihalyi & Godfrey (1963)
f / f_0 *	7.1	"
β	9.3	"
τ_h / τ_0 *	5.0	Johnson & Mihalyi (1965)
Λ	6.8	This study

* Assuming no particle swelling due to solvent association

Appendix III   Illustration of use of the Π function (equation 57)

by application to data for hemoglobin

The Π function obtained in section 1.7. can be applied to molecular

covolume and viscosity data available for hemoglobin. The molecular

covolume, U, is related to the 2nd virial coefficient, B employed in

osmometry by $U = 2BM_r^2$. Baghurst et al (1975), using a molecular

weight of 64,500 found   the value of the product BM_r to be 4.8 ml/gm.

Using instead the exact value for the molecular weight found by sequence

analysis to be 64,793, this product becomes 4.78 ml/gm; this gives the

ratio U/M_r to be 9.56 ml/gm. From the plot of reduced specific viscosity

against concentration (Figure 51) an intrinsic viscosity of 2.99 ml/gm

has been determined by a least squares fit to the new universal equation

for transport coefficients at all solute concentrations (see section 1.7.1.

and Appendix IV). The value of Π is calculated to be 3.20, corresponding

to a spherical particle (Figure 24). This is consistent with the findings

of x-ray crystallography (Perutz et al, 1960). The value of ν for a

spherical particle is the Einstein value of 2.5. By back substitution

into equation (8) and using a value for M_r of 64,793 one obtains a value

for V_e of 1.286×10^{-19} cm^3. This corresponds to a Stokes radius of

31.3 $\overset{o}{A}$, in excellent agreement with the result of 32.3 $\overset{o}{A}$ calculated by

Alpert & Banks (1976) from the diffusion coefficient determined by laser

correlation spectroscopy and agrees exactly with the result of 31.3 $\overset{o}{A}$

calculated by Laurent & Killander (1964) from the diffusion coefficient

determined by gel filtration, both groups assuming a hard sphere model.

The Stokes radius can also be found directly from the molecular covolume

and molecular weight assuming a hard sphere model: Baghurst et al (1975)

determined a value of 31.3 $\overset{o}{A}$, again in exact agreement. The corresponding radius of the sphere calculated from the crystallographic dimensions of 64 x 55 x 50 $\overset{o}{A}$ of Perutz et al (1960) is 28.0 $\overset{o}{A}$, indicating hemoglobin to be swollen in solution by approximately 40% (v/v).

If one uses standard errors of ±.03 (≡ 1%) and ± .096 (≡ 1%) in U/M_r respectively, the calculated standard error (Paradine & Rivett, 1960) in Π is ± .045. The maximum error corresponds to an axial ratio of 1.8 for a prolate model but as high as 6.8 for an oblate model, indicating the difficulty in applying Π to macromolecules that are oblatoid.

Figure 51.

Plot of reduced specific viscosity versus concentration for human oxy -
hemoglobin (0.1M KCl, buffer, pH = 6.0).

The curve fitted is that due to a weighted least squares fit to the new
universal equation for the concentration dependence of transport coefficients
(equation 60). The weighting factor used was (1/concentration).
$[\eta] = 2.99$ ml/gm, $k_\eta = 7.8$ ml/gm.
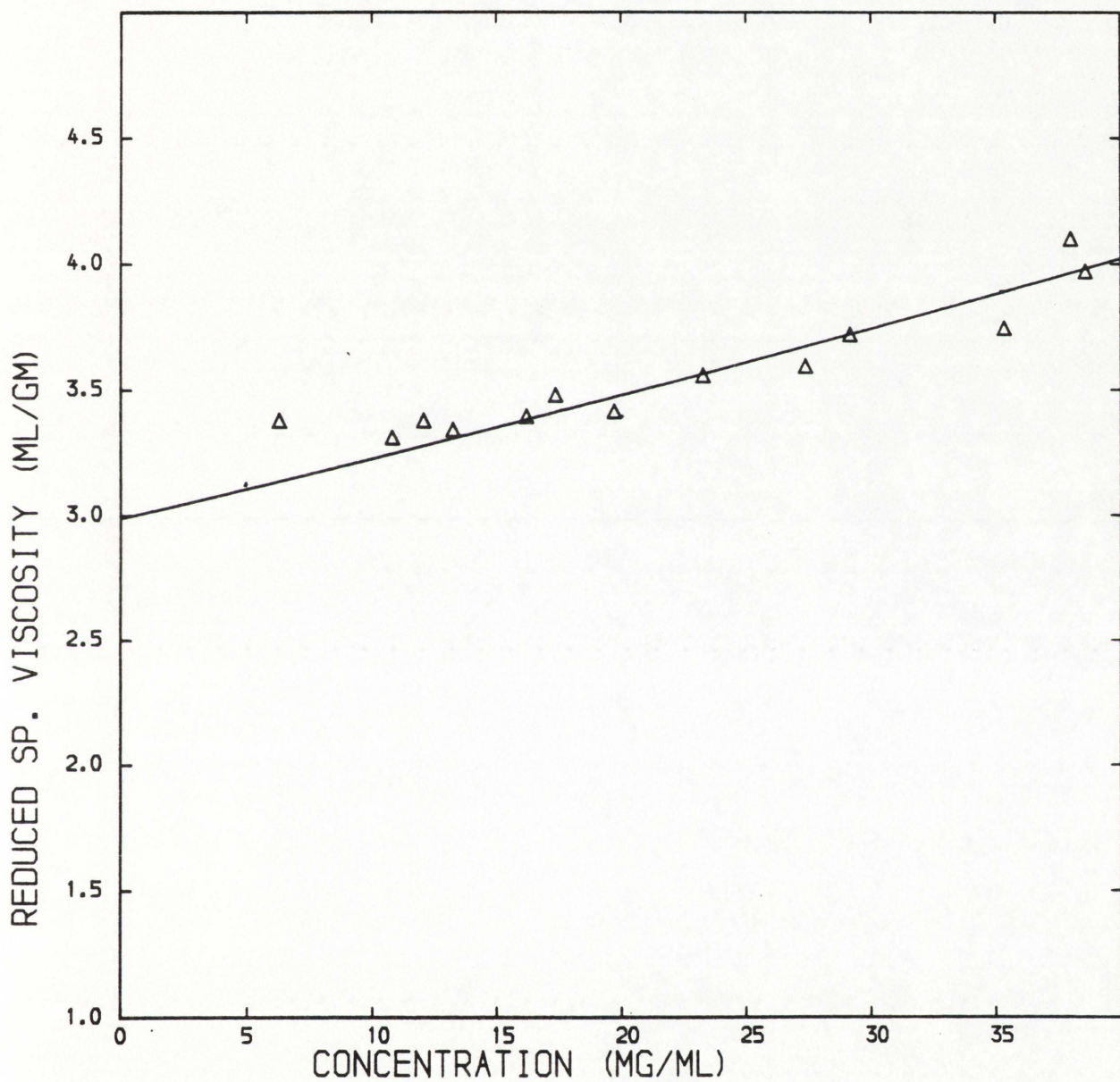
Appendix IV <u>Viscous Flow and Sedimentation of Concentrated Dispersions</u>

<u>of Particles</u> (quoted from A.J. Rowe, mss. in preparation)

The hydrodynamic properties of dispersions of particles in fluids

are quite well described at very high particle dilution, both for simple

models (spheres, ellipsoids, rods) and for more complex models which may

be represented as assemblies of simple models and the appropriate

interaction tensors computed. Restricting outselves to the case of small

particles (Brownian motion dominant) suspended in liquids, the work of

Stokes, Einstein, Perrin, Simha, Broersma and others (for simple models)

and of Kirkwood, Bloomfield and others (for assemblies) enables a

reasonably accurate description to be given of the sedimentation and

viscous flow properties of such suspensions to be given at 'infinite

dilution'.

At real particle concentrations however, no theory has proved

adequate, even for the simplest particle model — the sphere. The need

for such a theory is evident in many fields: in my own field of

Biochemistry it would be useful both for methodological purposes in

characterising macromolecular properties and for the description of

'in vivo' systems, which are generally rather concentrated dispersions

of macromolecular particles. I have been concerned to derive such a

theory, relating the properties of suspensions of particles at real

concentration to their 'infinite dilution' behaviour. In a recent paper

(Rowe, 1977) a first part of such a theory was described: the extension

of this theory to cover the case of high concentrations is now described.

<u>The State of the Problem</u>

It has long been noted that the concentration dependence of

sedimentation and of reduced specific viscosity is finite even at high

dilution, and remains nearly linear over moderate ranges of concentration:

(sedimentation) $s_c = s(1 - k_s c) \sim s(1 + k_s c)^{-1}$

(viscous flow) $\dfrac{\eta_{sp}}{c} = (\dfrac{\eta_{sp}}{c})_{c \to 0} \cdot (1 + k_\eta c)$

A recently derived theory (Rowe, 1977) shows that

$$k = k_s = 2\bar{v} (\dfrac{\bar{v}_s}{\bar{v}} + (f/f_0)^3)$$

for compact particles, where $\bar{v}$ is the partial specific volume of the

particle and f/f_0, the frictional ratio, is a parameter computable for

simple models and for assemblies of sub-units. This theory is thus

applicable to particles of <u>any</u> conformation. The values predicted for

both spheres and other particles agree well with experimental evidence

and with earlier theoretical predictions for spheres (Figure 52, Table 24).

At higher concentrations two further effects must be considered:

(i)   mutually proximity of the particles affects the rate of energy

        dissipation at constant shear (the 'cloud effect' of Burgers).

        In general this poses a many-body problem which is not amenable

        to solution by classical techniques.

(ii)   the critical packing fraction (ϕ_p) will be approached. Semi-

        empirical equations due to Mooney (1951), Dougherty and

        Kreiger (1972) and others describe the viscosity of suspensions

        of spheres in terms of ϕ_p.

<u>A New General Approach</u>

The theory applicable to high dilutions (Rowe, 1977) was based on

the supposition that <u>only</u> a 'frame-of-reference' effect need be considered

in this case. Derived in terms of sedimentation, it is shown that the

latter must be unchanged with concentration in a frame of reference defined by the <u>solvent in return flux</u> (i.e. solvent <u>not</u> transported or convected with the particles). The equation above then follows from the relation between the defined frame of reference and the cell-fixed frame of reference in which measurements are normally made.

To extend this approach to higher concentrations we re-define the problem by considering the system to consist of a large but finite number of volume elements, each element small in comparison to a particle. These volume elements can be classified as elements of disjoint sets V1....V4, shown in a Venn diagram for two particles (Figure 53).

Among interesting properties which may be noticed are that

(i)   Sets V1, V3 can be classified into sub-sets

$v1_1 - v1_n$, $v3_1 - v3_n$, for n particles in the system

(ii) $v1_i \cap v1_j = \Phi$; but $v3_i \cap v3_j \neq \Phi$

(iii) In Newtonian flow, the magnitude of the flow vector of the solvent at any point in the system is defined by the fraction of the volume elements in the vicinity of that point classified as in $V2 \cup V3$ in relation to those in $V4 \cup V2 \cup V3$

(iv) $v1_i \cap V2 \neq \Phi$: more completely V2 is partitioned into the disjoint subsets V2a and V2b, where $v1_i \cap V2a = \Phi$;

$v1_i \cap V2b \neq \Phi$: and ϕ_p, the critical packing volume of the particles, determines the relative number of elements in V2a and V2b { $\phi_p = 1$; $V2a = \Phi$ }.

On the <u>assumptions</u> that n is large, and that the elements in V3 are located randomly in $V3 \cup V4$, then a simple finite probability space

can be constructed, enabling us to calculate the number of elements in

V1....V4, and hence the quantity gc in

$$\frac{s_c}{s} = \frac{\eta_{sp}/c}{(\eta_{sp}/c)_{c \to 0}} = (1 - gc)$$

since $V1 \cup V2 \cup V3 = gc$.

The result is given by

$$\frac{gc - z}{1 - z} = \Phi = (kc - 2c\bar{v}_s) - \sum_{i=2}^{i=\infty}(i - 1)(\Phi^i - \Phi^{i+1})$$

where $z = 2c\bar{v}_s - \dfrac{1}{\phi_p}(c\bar{v}_s)^2(1 - Q)_+$; $Q = (1 - \phi_p)/\phi_p$

which for almost all cases simplifies to

$$gc = \frac{kc - \dfrac{2\phi_p - 1}{\phi_p^2}(c\bar{v}_s)^2}{kc - 2c\bar{v}_s + 1}$$

where $k = k_s$ or k_η ; $\bar{v}_s$ = specific volume of the hydrodynamic particle.

This equation predicts rather accurately the high-shear viscosity of latex spheres over the entire concentration range (Figures 54 - 58). It is applicable only to Newtonian flow, but is free of arbitrary or empirical constants. The treatment used has some affinity with the widely used approach involving transient doublets, triplets, etc. ($i = 2$ in the above summation refers to 'doublet' interaction, etc.), but as no particle model is employed, the results should be general for all particles. The ϕ_p term would often be difficult to estimate, but computer simulation shows that an exact knowledge of ϕ_p is unimportant except at the highest concentrations

Figures 54 – 58 demonstrate the success of the theory in predicting known properties of sedimentation and viscous flow at real concentrations.

Table 24. Various theoretical estimates and a practical estimate for k_2, the second coefficient in the expansion for η_{rel} in terms of Φ (volume fraction)

$$\eta_{rel} = 1 + k_1 \Phi + k_2 \Phi^2 + \ldots\ldots\ldots\ldots$$

Estimate for k_2	Author
7.5	Vand (1948)
9.15	Manley & Mason (modification of Vand) (1954)
7.5	Kynch (1956)
14.1	Gold (1937)
12.6	Simha (modification of Gold) (1952)
7.6	Batchelor & Green (1972)
10.0	Rowe (1977)
'about 10'	Cheng & Schachman data on PSL spheres (1955)

<u>Figure 52.</u>

Empirical data and the equation for transport—concentration dependence (Rowe 1977), at high solute dilution. The equation enables M_r (molecular weight) values to be calculated from s and k_s only. The agreement found between values for M_r computed thus and M_r values from the literature (various methods) is good evidence for the applicability of the equation to a wide range of systems.

Solute	$\dfrac{M_r(s+k_s)}{M_r(lit)}$	Standard error	Symbol
Proteins, nucleic acids, viruses	1.02	0.01	●
Cellulose derivatives in CUAM	1.01	0.09	○
Cellulose derivatives in ACETONE	0.97	0.10	△
Levans (aqueous)	0.99	0.04	□
Poly(methylymacrylate) in ETHYL ACETATE	1.05	0.08	▲
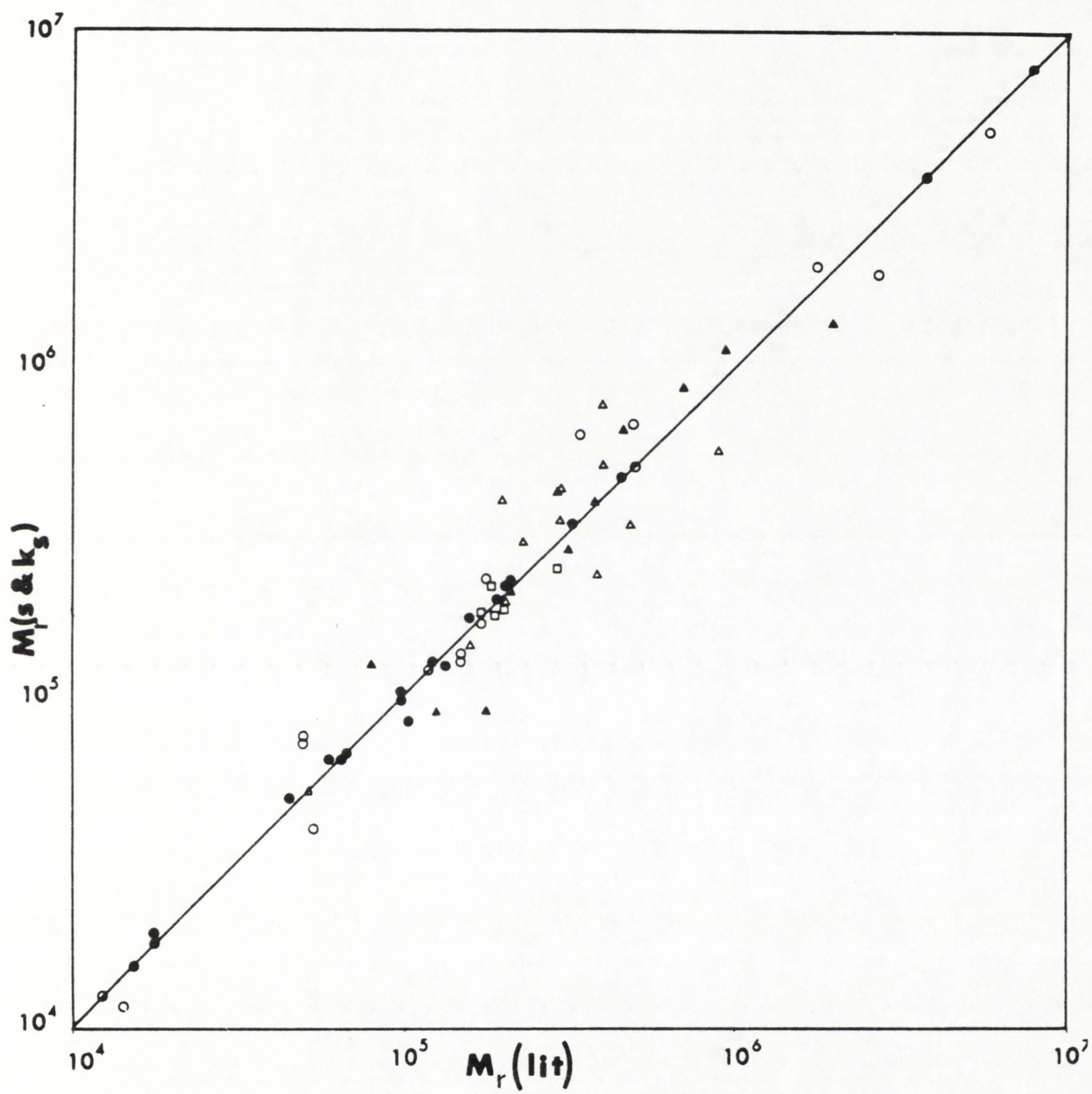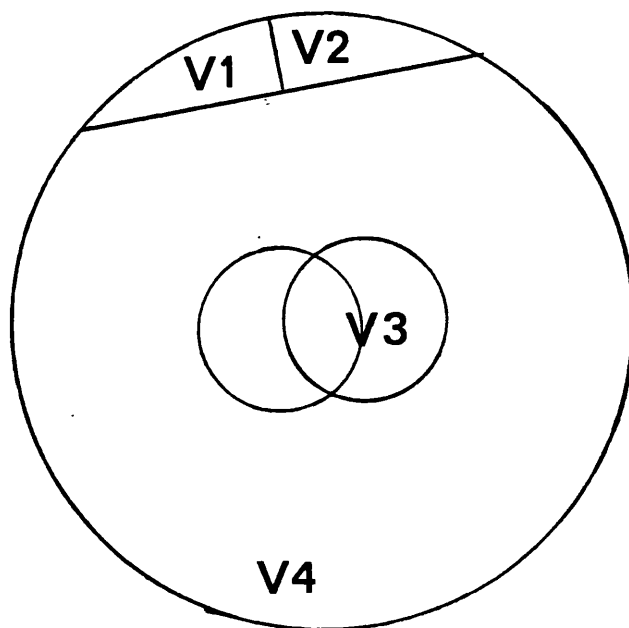
Figure 53. Venn diagram showing the volume elements for two particles
in solution

V1 - particle volume

V2 - particle co-volume

V3 - solvent frictional forward flux

V4 - solvent return volume flux
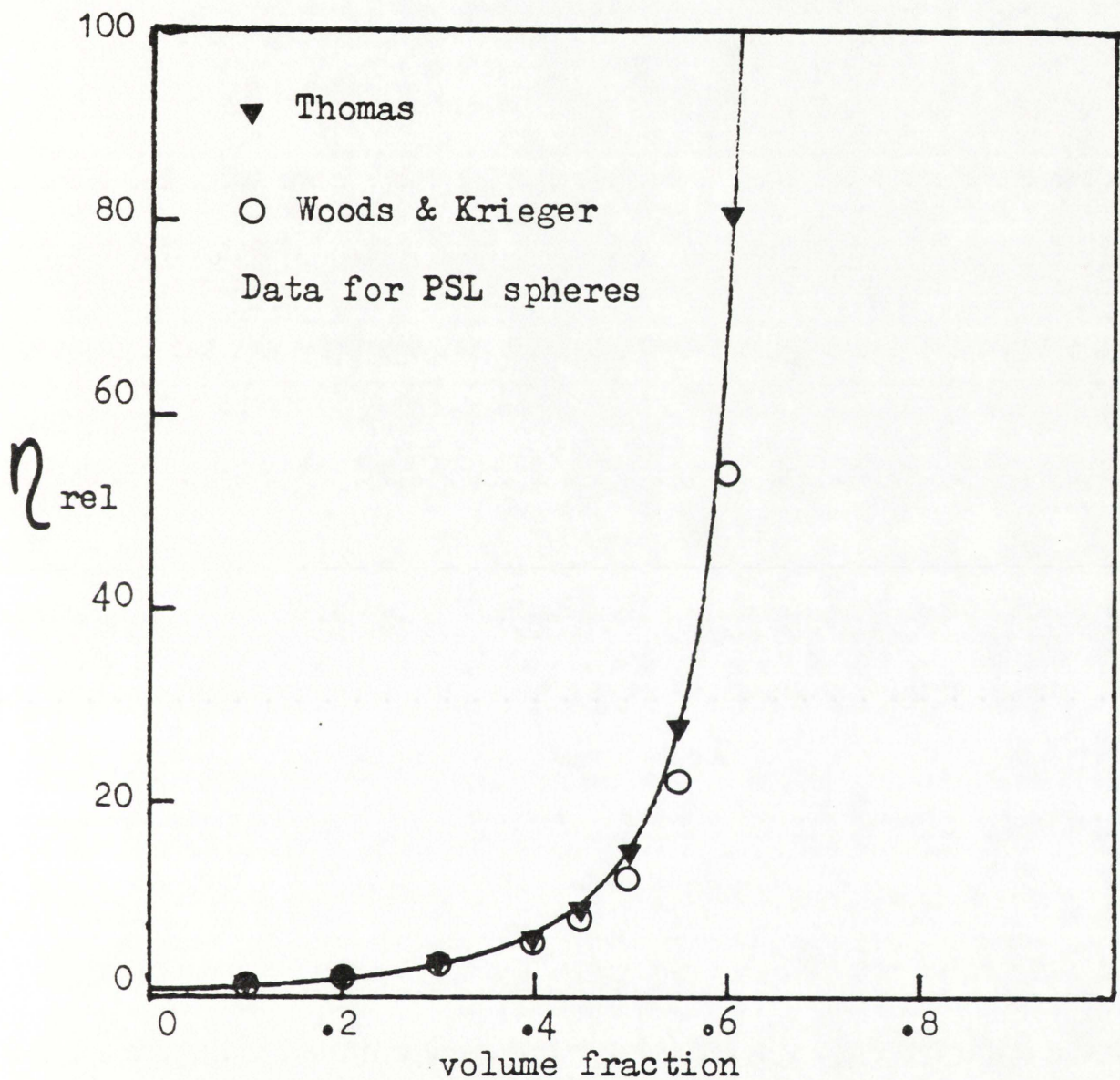
<u>Figure 54.</u> <u>Relative viscosity of spheres as a function of volume fraction.</u>

Predicted line, for $k_\eta = 4$, $\bar{v}_s = 1$, $\phi_p = 0.64$. Experimental

data points are also shown
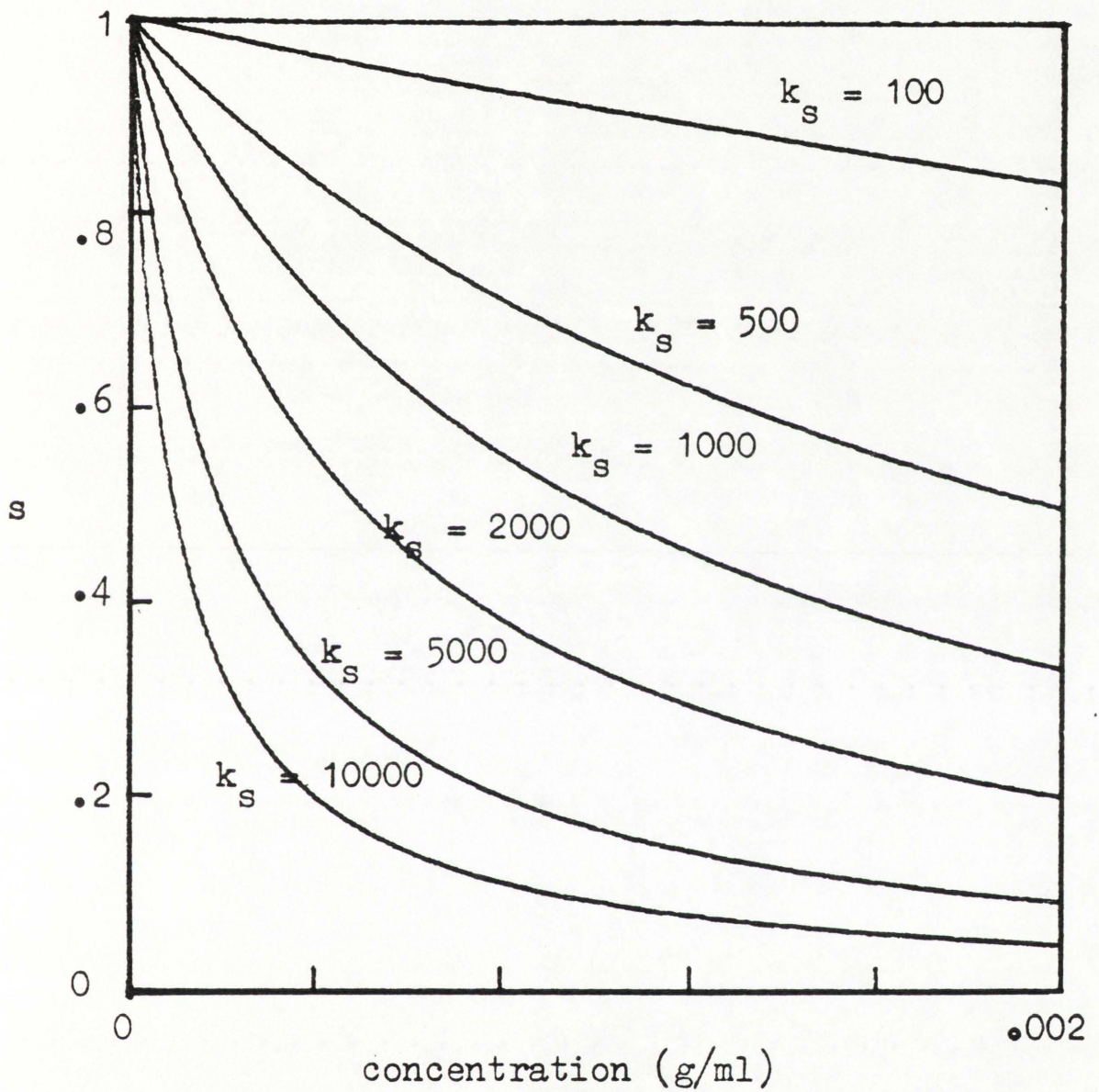
Figure 55. For highly asymmetric particles the sedimentation coefficient
falls very steeply with concentration, to reach a relatively
constant 'plateau' value. Computed curves.
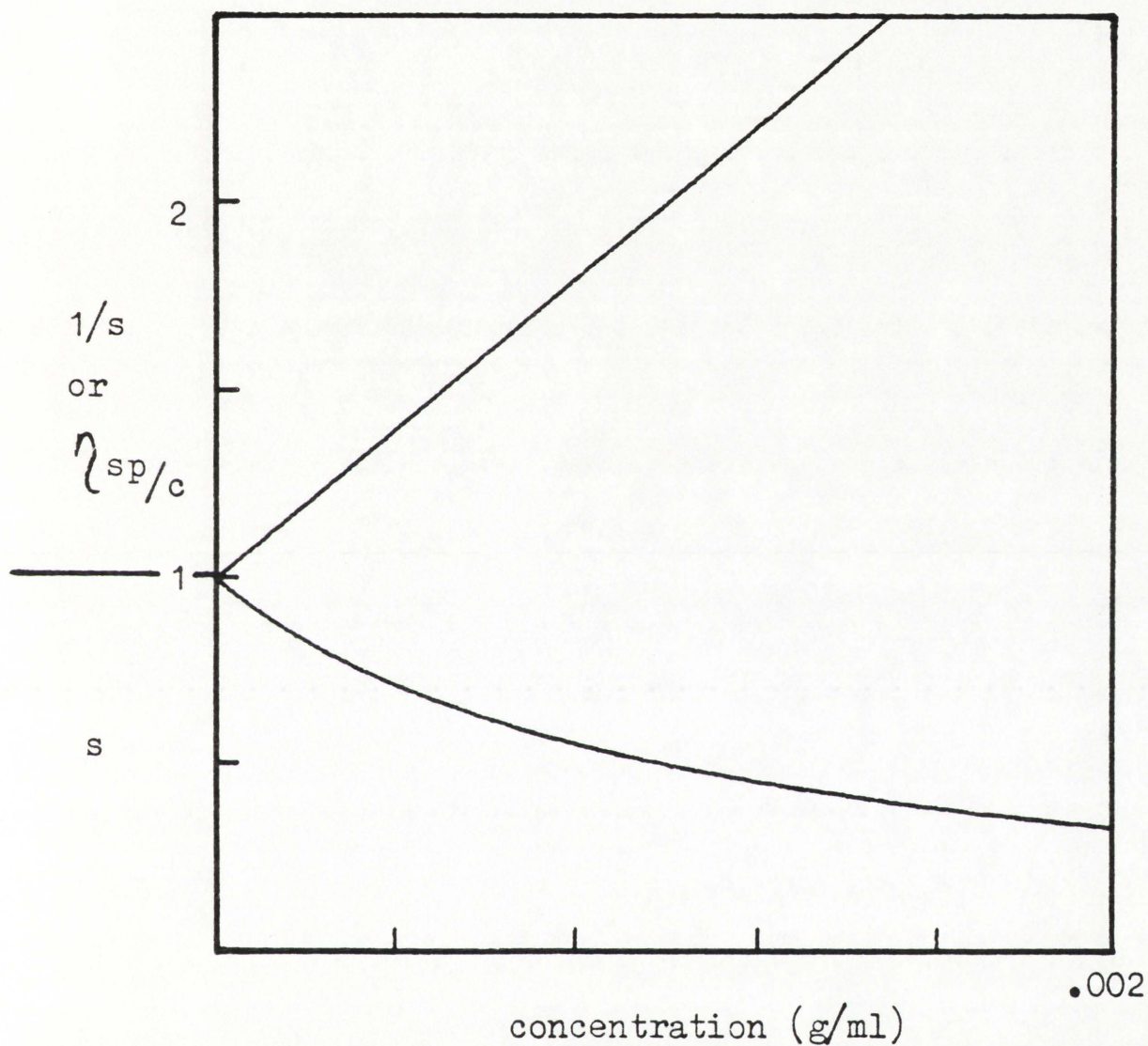
Figure 56. Viscosity/sedimentation coefficients as a function of concentration
for $k_s(k_\eta) = 1000$, $\bar{v}_s = 1$. The 1/s plot is linear, whilst the
direct plot is markedly curved. Computed curves.
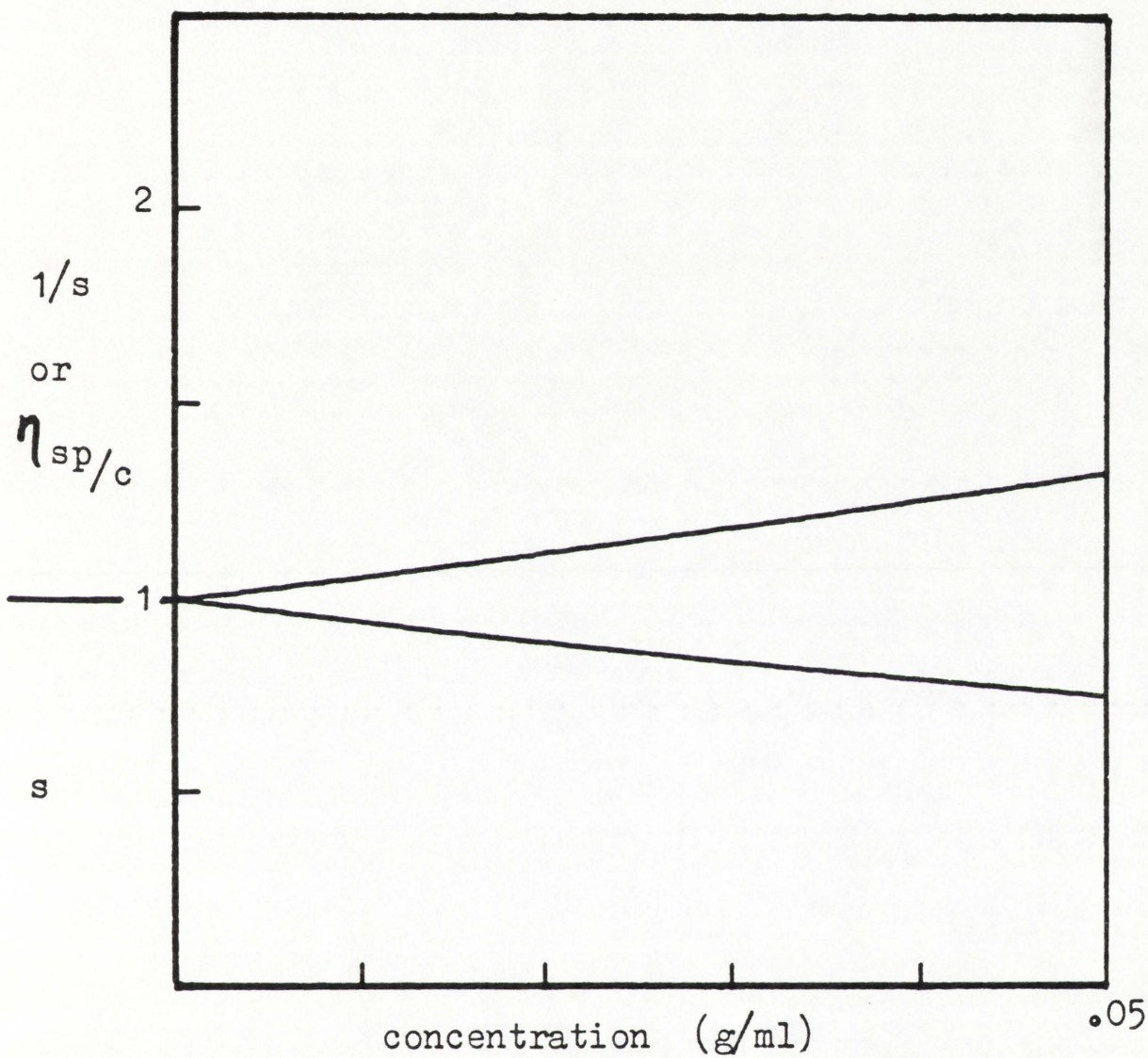
Figure 57. Viscosity/sedimentation coefficients as a function of concentration for k_s (k_η) = 6. Both plots are reasonably linear over this concentration range. Computed curves.

Figure 58. Hydrodynamic data for Bovine serum albumin fitted

using the new general equation for transport at

all solute concentrations

Bovine Serum Albumin
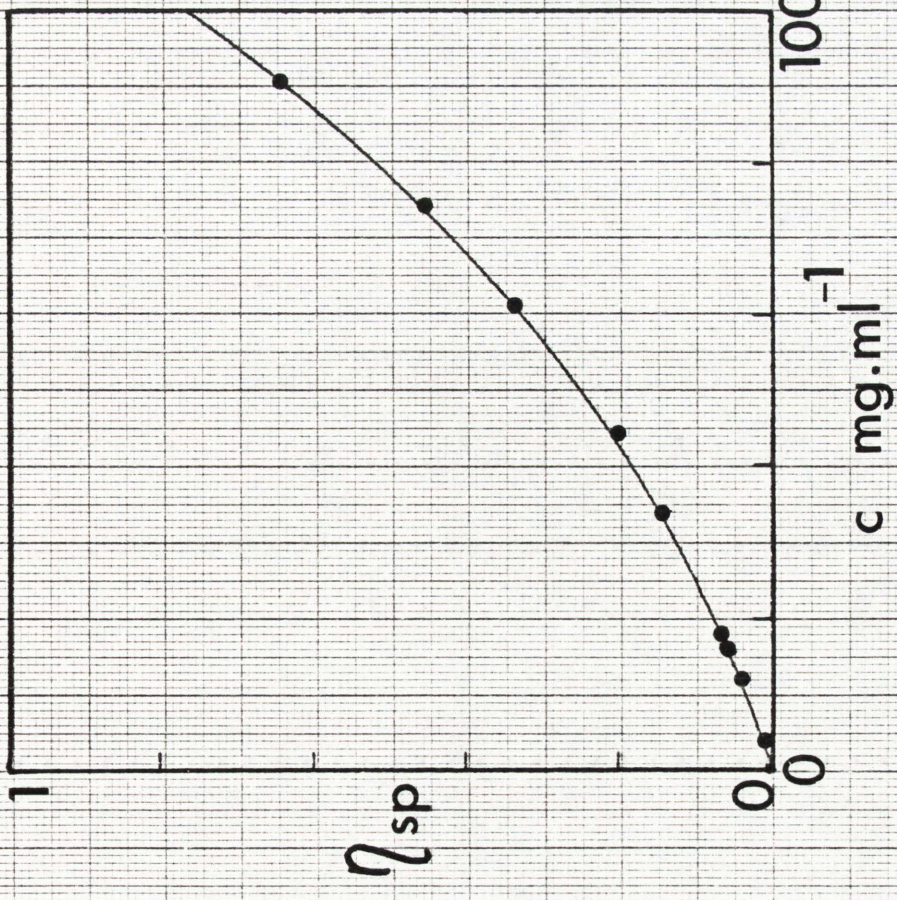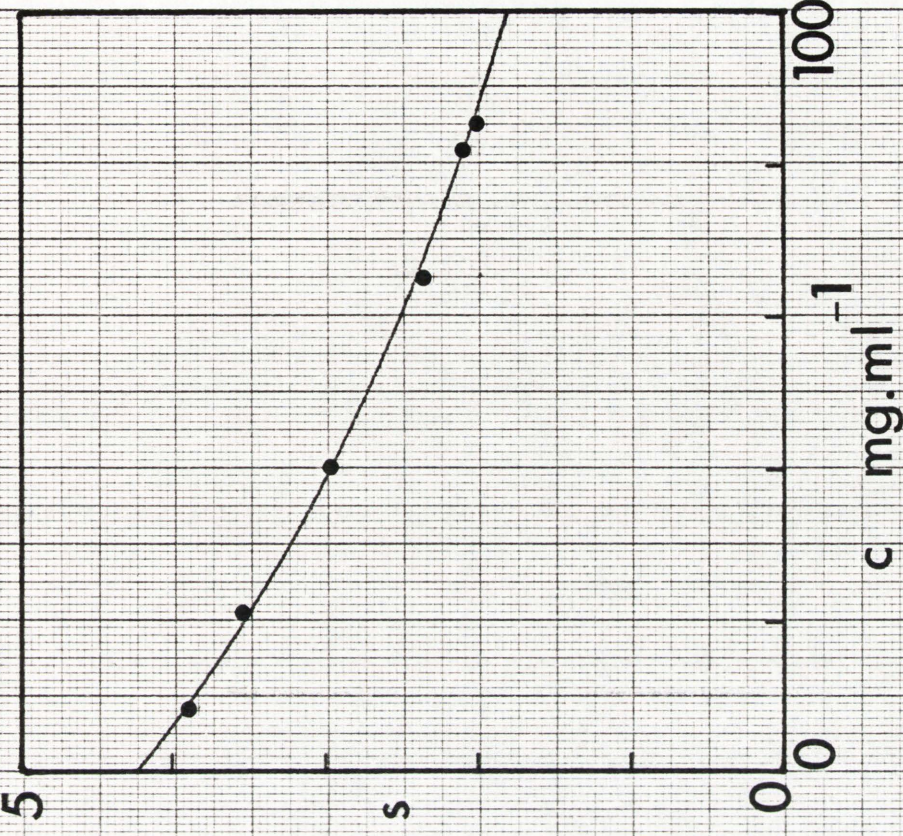
Appendix V   FORTRAN IV computer programs

Program 1:   Evaluates values of the various hydrodynamic shape functions
for tri-axial ellipsoids for a user specifiable value of
the axial ratios (a/b, b/c)

Program 2:   Produces tables of these functions for axial ratios between
1.0 and 2.0 in steps of 0.1

Program 3:   Produces a contour map of ν in the (a/b, b/c) plane for
axial ratios between 1.0 and 3.0

Program 4:   Produces plots of the various tri-axial functions in the
(a/b, b/c) plane corresponding to the point (1.5, 1.5).
Several plots allow for arbitrary errors in measurement

Program 5:   Non-linear least squares iterative method for resolving a 2-
term exponential birefringence decay. This program (and the
following two) produces its own synthetic data

Program 6:   Fourier Transform solution of the Laplace Integral Equation
method

Program 7:   R-constrained non-linear least squares iterative method

Function	Computer Symbol
a/b	A/B
b/c	B/C
ν	NU, S
f/f_o ($\equiv P$)	F
ζ_a/ζ_o	CA, CA/CO
ζ_b/ζ_o	CB, CB/CO
ζ_c/ζ_o	CC, CC/CO
ϱ_a/ϱ_o	RHOA, RHOA/RHOO
ϱ_b/ϱ_o	RHOB, RHOB/RHOO
ϱ_c/ϱ_o	RHOC, RHOC/RHOO
β	BETA
R	R
δ_a	DELTAA, DELTA(A)
δ_b	DELTAB, DELTA(B)
δ_c	DELTAC, DELTA(C)
γ_a	GAMMAA, GAMMA(A)
γ_b	GAMMAB, GAMMA(B)
γ_c	GAMMAC, GAMMA(C)
μ_a	MUA, MU(A)
μ_b	MUB, MU(B)
μ_c	MUC, MU(C)
τ_h/τ_o	TAU, TAU/TAUO
Ψ	PSI
Λ	LAMBDA
θ_+^{red}	TPLS, THETA+, Z
θ_-^{red}	TMNS, THETA-, U

Function	Computer Symbol
δ_+	DPLS, DELTA+, V
δ_-	DMNS, DELTA-, W
γ_+	GPLS, GAMMA+
γ_-	GMNS, GAMMA-
τ_1/τ_0	T1
τ_2/τ_0	T2
τ_3/τ_0	T3
τ_4/τ_0	T4
τ_5/τ_0	T5
θ_+	THPLUS
θ_-	THMNUS

```
C     ***.*******************************************************************
C         THIS PROGRAM GENERATES VALUES OF THE VARIOUS HYDRODYNAMIC
C         SHAPE FUNCTIONS FOR A USER SPECIFIABLE VALUE OF THE AXIAL
C         RATIOS A/B (=N1) & B/C (=N2)
C     ***********************************************************************
      PROGRAM MAIN(INPUT,OUTPUT,TAPE2=INPUT,TAPE3=OUTPUT)
      COMMON/PARAM/A,C,NN
      EXTERNAL FUN
      DIMENSION ALPHA(10)
      REAL NU,M,O,P
      REAL MUA,MUB,MUC,PSI,N1,N2,RHOA,RHOB,RHOC
C ENTER AS DATA AT THE FOOT OF THE PROGRAM (A/B, B/C)
      READ(2,*)N1,N2
      NN=0
C     COMPUTE THE ELLIPTIC INTEGRALS
      DO45 K=1,10
      A=N1
      B=1.0
      C=1.0/N2
      NN=NN+1
C     SET LIMITS FOR NUMERICAL INTEGRATION (THESE LIMITS
C     BELOW HAVE BEEN PREVIOUSLY TESTED FOR CONVERGENCE)
      AA=0.0
      BB=1000000
      IF(NN.EQ.10)BB=500000000
      MAXDIV=50
      EPS=1.0E-08
      ACC=0.0
      IFAIL=0
C     CALL U.K. "NAG" LIBRARY ROUTINE FOR NUMERICAL EVALUATION
C     OF THE INTEGRALS "ALPHA" GIVEN IN THE SUBROUTINE BELOW
      CALL D01AGF(AA,BB,FUN,MAXDIV,EPS,ACC,ANS,ERROR,NOFUN,IFAIL)
      ALPHA(NN)=ANS
   45 CONTINUE
      B=1.0
C     NOW COMPUTE THE FUNCTION VALUES USING THE STORED INTEGRAL VALUES
      NU=(1.0/(A*B*C))*((4.0/15.0)*((ALPHA(7)+ALPHA(8)
     + +ALPHA(9))/(ALPHA(8)*ALPHA(9)+ALPHA(9)*ALPHA
     + (7)+ALPHA(7)*ALPHA(8)))+(1.0/5.0)*(((ALPHA(2)
     + +ALPHA(3))/(ALPHA(4)*(B*B*ALPHA(2)+C*C*ALPHA(3)
     + )))+((ALPHA(3)+ALPHA(1))/(ALPHA(5)*(C*C*ALPHA(3)
     + +A*A*ALPHA(1))))+((ALPHA(1)+ALPHA(2))/(ALPHA(6)
     + *(A*A*ALPHA(1)+B*B*ALPHA(2))))))
      M=(B*B+C*C)/(B*B*ALPHA(2)+C*C*ALPHA(3))
      O=(C*C+A*A)/(C*C*ALPHA(3)+A*A*ALPHA(1))
      P=(A*A+B*B)/(A*A*ALPHA(1)+B*B*ALPHA(2))
      TPLS=((A*B*C)/(12.0))*((((1.0/M)+(1.0/O)+(1.0/P
     + ))+((((1.0/M**2.0)+(1.0/O**2.0)+(1.0/P**2.0))-
     + ((1.0/(M*O))+(1.0/(O*P))+(1.0/(P*M
     + ))))**0.5))
      TMNS=((A*B*C)/(12.0))*((((1.0/M)+(1.0/O)+(1.0/P
     + ))-((((1.0/M**2.0)+(1.0/O**2.0)+(1.0/P**2.0))-
     + ((1.0/(M*O))+(1.0/(O*P))+(1.0/(P*M
     + ))))**0.5))
      DPLS=6.0*TPLS*NU
      DMNS=6.0*TMNS*NU
      F=2.0/((((A*B*C)**(1.0/3.0))*ALPHA(10))
      R=2.0*(1.0+(F**3.0))/NU
      BETA=(1.0/1000000.0)*(((6.0249**(1.0/3.0))*(10.0**(23.0/3.0
     +)))/((16200.0*3.141592654*3.141592654)**(1.0/3.0)))*(NU
     +**(1.0/3.0)))/F
      CA=(2.0/(3.0*A*B*C))*M
      CB=(2.0/(3.0*A*B*C))*O
      CC=(2.0/(3.0*A*B*C))*P
      RHOA=2.0/((1.0/CB)+(1.0/CC))
      RHOB=2.0/((1.0/CC)+(1.0/CA))
      RHOC=2.0/((1.0/CA)+(1.0/CB))
      DELA=NU/CA
      DELB=NU/CB
      DELC=NU/CC
      TAU=3.0/((1.0/CA)+(1.0/CB)+(1.0/CC))
      PSI=F*((1.0/TAU)**(1.0/3.0))
      V=NU/TAU
      ZZ=(1.0/2.0)*(F**3.0)
      GAMMAA=ZZ*((1.0/CB)+(1.0/CC))
      GAMMAB=ZZ*((1.0/CC)+(1.0/CA))
      GAMMAC=ZZ*((1.0/CA)+(1.0/CB))
      MUA=(CA**(1.0/3.0))/F
      MUB=(CB**(1.0/3.0))/F
      MUC=(CC**(1.0/3.0))/F
      GPLS=6.0*TPLS*(F**3.0)
```

```
      GMNS=6.0*TMNS*(F**3.0)
      X1=0.5*((1.0/RHOB)+(1.0/RHOC)-(1.0/RHOA))
      X2=0.5*((1.0/RHOC)+(1.0/RHOA)-(1.0/RHOB))
      X3=0.5*((1.0/RHOA)+(1.0/RHOB)-(1.0/RHOC))
      X4=(X1+X2+X3)/3.0
      X5=((X1**2.0)+(X2**2.0)+(X3**2.0)-(X1*X2)-(X2*X3)-(X3*X1))
     +**0.5
      T1=1.0/(X4+X1)
      T2=1.0/(X4+X2)
      T3=1.0/(X4+X3)
      T4=3.0/((6.0*X4)-(2.0*X5))
      T5=3.0/((6.0*X4)+(2.0*X5))
      WRITE(3,97)
  97 FORMAT( "      ")
      WRITE(3,98)
  98 FORMAT( "      ")
      WRITE(3,99)A,1/C
  99 FORMAT( 5X," A/B    "F7.2,"    B/C  ",F7.2)
      WRITE(3,100)NU
 100 FORMAT( 5X," NU  ",F10.5)
      WRITE(3,106)F
 106 FORMAT( 5X,"  F  ",F10.5)
      WRITE(3,101)TPLS
 101 FORMAT( 5X," THETA+   ",F15.5)
      WRITE(3,102)TMNS
 102 FORMAT( 5X," THETA-   ",F15.5)
      WRITE(3,103)DPLS
 103 FORMAT( 5X," DELTA+   ",F15.5)
      WRITE(3,104)DMNS
 104 FORMAT( 5X," DELTA-   ",F15.5)
      WRITE(3,105)R
 105 FORMAT( 5X,"   R  ",F15.5)
      WRITE(3,107)BETA
 107 FORMAT( 5X," BETA  ",F15.5)
      WRITE(3,202)
 202 FORMAT( 5X,"THE 3 ROTATIONAL FRICTIONAL RATIOS:")
      WRITE(3,108)CA
 108 FORMAT( 5X,"  CA  ",F15.5)
      WRITE(3,109)CB
 109 FORMAT( 5X,"  CB  ",F15.5)
      WRITE(3,110)CC
 110 FORMAT( 5X,"  CC  ",F15.5)
      WRITE(3,203)
 203 FORMAT( 5X,"THE 3 ROTATIONAL RELAXATION TIME RATIOS:")
      WRITE(3,111)RHOA
 111 FORMAT( 5X,"  RHOA  ",F15.5)
      WRITE(3,112)RHOB
 112 FORMAT( 5X,"  RHOB  ",F15.5)
      WRITE(3,113)RHOC
 113 FORMAT( 5X,"  RHOC  ",F15.5)
      WRITE(3,114)DELA
 114 FORMAT( 5X," DELTAA  ",F15.5)
      WRITE(3,115)DELB
 115 FORMAT( 5X," DELTAB  ",F15.5)
      WRITE(3,116)DELC
 116 FORMAT( 5X," DELTAC  ",F15.5)
      WRITE(3,204)
 204 FORMAT( 5X,"THE HARMONIC MEAN RELAXATION TIME RATIO:")
      WRITE(3,117)TAU
 117 FORMAT( 5X,"  TAU  ",F15.5)
      WRITE(3,118)PSI
 118 FORMAT( 5X,"  PSI  ",F15.5)
      WRITE(3,119)V
 119 FORMAT( 5X,"LAMBDA ",F15.5)
      WRITE(3,120)GAMMAA
 120 FORMAT( 5X,"GAMMAA ",F15.5)
      WRITE(3,121)GAMMAB
 121 FORMAT( 5X,"GAMMAB ",F15.5)
      WRITE(3,122)GAMMAC
 122 FORMAT( 5X,"GAMMAC ",F15.5)
      WRITE(3,123)MUA
 123 FORMAT( 5X,"  MUA  ",F15.5)
      WRITE(3,124)MUB
 124 FORMAT( 5X,"  MUB  ",F15.5)
      WRITE(3,125)MUC
 125 FORMAT( 5X,"  MUC  ",F15.5)
      WRITE(3,126)GPLS
 126 FORMAT( 5X,"GAMMA+ ",F15.5)
      WRITE(3,127)GMNS
 127 FORMAT( 5X, "GAMMA- ",F15.5)
      WRITE(3,201)
```

```
201 FORMAT( 5X,"FLUORESCENCE ANISOTROPY RELAXATION TIME RATIOS:")
    WRITE(3,130)T1
130 FORMAT( 5X,"    T1    ",F15.5)
    WRITE(3,131)T2
131 FORMAT( 5X,"    T2    ",F15.5)
    WRITE(3,132)T3
132 FORMAT( 5X,"    T3    ",F15.5)
    WRITE(3,133)T4
133 FORMAT( 5X,"    T4    ",F15.5)
    WRITE(3,134)T5
134 FORMAT( 5X,"    T5    ",F15.5)
    STOP
    END
```

```
C
C
C
    REAL FUNCTION FUN(X)
    COMMON/PARAM/A,C,NN
    B=1.0
    GOTO(10,20,30,40,50,60,70,80,90,100),NN
 10 FUN=1/((A*A+X)**1.5*(B*B+X)**0.5*(C*C+X)**0.5)
    RETURN
 20 FUN=1/((A*A+X)**0.5*(B*B+X)**1.5*(C*C+X)**0.5)
    RETURN
 30 FUN=1/((A*A+X)**0.5*(B*B+X)**0.5*(C*C+X)**1.5)
    RETURN
 40 FUN=1/((A*A+X)**0.5*(B*B+X)**1.5*(C*C+X)**1.5)
    RETURN
 50 FUN=1/((A*A+X)**1.5*(B*B+X)**0.5*(C*C+X)**1.5)
    RETURN
 60 FUN=1/((A*A+X)**1.5*(B*B+X)**1.5*(C*C+X)**0.5)
    RETURN
 70 FUN=X/((A*A+X)**0.5*(B*B+X)**1.5*(C*C+X)**1.5)
    RETURN
 80 FUN=X/((A*A+X)**1.5*(B*B+X)**0.5*(C*C+X)**1.5)
    RETURN
 90 FUN=X/((A*A+X)**1.5*(B*B+X)**1.5*(C*C+X)**0.5)
    RETURN
100 FUN=1.0/(((A*A+X)*(B*B+X)*(C*C+X))**0.5)
    RETURN
    END
```

Program 1 Results

```
A/B        1.50     B/C        1.50
NU         2.89170
  F        1.04410
 THETA+                .16261
 THETA-                .11622
 DELTA+               2.82127
 DELTA-               2.01645
     R               1.47887
 BETA                2.12334
THE 3 ROTATIONAL FRICTIONAL RATIOS:
    CA                .89762
    CB               1.39800
    CC               1.47041
THE 3 ROTATIONAL RELAXATION TIME RATIOS:
   RHOA               1.43329
   RHOB               1.11474
   RHOC               1.09327
   DELTAA             3.22152
   DELTAB             2.06846
   DELTAC             1.96660
THE HARMONIC MEAN RELAXATION TIME RATIO:
   TAU                1.19548
   PSI                 .98378
LAMBDA                2.41886
GAMMAA                 .79414
GAMMAB               1.02107
GAMMAC               1.04112
   MUA                 .92389
   MUB                1.07092
   MUC                1.08910
GAMMA+               1.11051
GAMMA-                 .79372
FLUORESCENCE ANISOTROPY RELAXATION TIME RATIOS:
    T1                1.02536
    T2                1.28883
    T3                1.31877
    T4                1.43405
    T5                1.02497
```

Program 2

```
****************************************************************
   THIS PROGRAM COMPUTES TABLES OF THE VISCOSITY INCREMENT NU,
   THE TRANSLATIONAL FRICTIONAL RATIO (F/F0), THE ROTATIONAL
   FRICTIONAL RATIOS( CA/C0, CB/C0, CC/C0 ), THE ROTATIONAL
   RELAXATION TIME RATIOS(RHOA/RHO0, RHOB/RHO0, RHOC/RHO0), THE
   HARMONIC MEAN RELAXATION TIME RATIO( TAU/TAU0 ), THE RIDGEWAY
   ELECTRIC BIREFRINGENCE DECAY CONSTANTS( THETA+, THETA-), AND
   THEIR CORRESPONDING SWELLING - INDEPENDENT FUNCTIONS:
   R, BETA, DELTAA, DELTAB, DELTAC, GAMMAA, GAMMAB, GAMMAC,
   MUA, MUB, MUC, PSI, DELTA+, DELTA-, GAMMA+ AND GAMMA-
   AS FUNCTIONS OF THE AXIAL RATIOS A/B, B/C, IN THE RANGE 1.0 TO
   2.0 IN STEPS OF 0.1, FOR A GENERAL TRIAXIAL ELLIPSOID PARTICLE
   MODEL. ( THE SUBSCRIPT "0" REFERS TO THE CORRESPONDING COEFFICIENT
   FOR A SPHERE OF EQUAL VOLUME )
****************************************************************
      PROGRAM MAIN(INPUT,OUTPUT,TAPE2=INPUT,TAPE3=OUTPUT)
      COMMON/PARAM/A,C,NN
      EXTERNAL FUN
      DIMENSION ALPHA(10,11,11),NU(11,11),F(11,11),R(11,11),H(1)
     + ,BETA(11,11),CA(11,11),CB(11,11),CC(11,11),M(11,11),O(11,11)
     + ,P(11,11),TPLS(11,11),TMNS(11,11),RHOA(11,11),RHOB(11,11)
     + ,RHOC(11,11),TAU(11,11),PSI(11,11),DELA(11,11),DELB(11,11)
     + ,DELC(11,11),GAMMAA(11,11),GAMMAB(11,11),GAMMAC(11,11),MUA(11,11)
     + ,MUB(11,11),MUC(11,11),DPLS(11,11),DMNS(11,11),GPLS(11,11)
     + ,GMNS(11,11),Y(11),Z(11),ZZ(11,11)
      REAL NU,M,O,P,MUA,MUB,MUC,PSI
      COMPUTE THE ELLIPTIC INTEGRALS
      NN=0
      DO45 K=1,10
      A=0.9
      NN=NN+1
      DO40 I=1,11
      A=A+0.1
      C=1.0/0.9
      DO30 N=1,11
      C=C/(1.0+0.1*C)
      SET LIMITS FOR NUMERICAL INTEGRATION (THESE LIMITS
      BELOW HAVE BEEN PREVIOUSLY TESTED FOR CONVERGENCE)
      AA=0.0
      BB=1000000
      IF(NN.EQ.10)BB=500000000
      MAXDIV=50
      EPS=1.0E-08
      ACC=0.0
      IFAIL=0
      CALL U.K. "NAG" LIBRARY ROUTINE FOR NUMERICAL EVALUATION
      OF THE INTEGRALS "ALPHA" GIVEN IN THE SUBROUTINE BELOW
      CALL D01AGF(AA,BB,FUN,MAXDIV,EPS,ACC,ANS,ERROR,NOFUN,IFAIL)
      ALPHA(NN,I,N)=ANS
   30 CONTINUE
   40 CONTINUE
   45 CONTINUE
      B=1.0
      A=0.9
      DO80 J=1,11
      A=A+0.1
      Y(J)=A
      C=1.0/0.9
      DO70 N=1,11
      C=C/(1.0+0.1*C)
      Z(N)=1/C
      NOW COMPUTE THE FUNCTION VALUES USING THE STORED INTEGRAL VALUES
      NU(J,N)=(1.0/(A*B*C))*((4.0/15.0)*((ALPHA(7,J,N)+ALPHA(3,J,N)
     + +ALPHA(9,J,N))/(ALPHA(8,J,N)*ALPHA(9,J,N)+ALPHA(9,J,N)*ALPHA
     + (7,J,N)+ALPHA(7,J,N)*ALPHA(8,J,N)))+(1.0/5.0)*(((ALPHA(2,J,N)
     + +ALPHA(3,J,N))/(ALPHA(4,J,N)*(B*B*ALPHA(2,J,N)+C*C*ALPHA(3,J,N)
     + )))+((ALPHA(3,J,N)+ALPHA(1,J,N))/(ALPHA(5,J,N)*(C*C*ALPHA(3,J,N)
     + +A*A*ALPHA(1,J,N))))+((ALPHA(1,J,N)+ALPHA(2,J,N))/(ALPHA(6,J,N)
     + *(A*A*ALPHA(1,J,N)+B*B*ALPHA(2,J,N))))))
      F(J,N)=2.0/(((A*B*C)**(1.0/3.0))*ALPHA(10,J,N))
      R(J,N)=2.0*(1.0+(F(J,N)**3.0))/NU(J,N)
      BETA(J,N)=(1.0/1000000.0)*(((6.0249**(1.0/3.0))*(10.0**(23.0/3.0
     + )))/((16200.0*3.141592654*3.141592654)**(1.0/3.0)))*(NU(J,N)
     + **(1.0/3.0))/F(J,N)
      M(J,N)=(B*B+C*C)/(B*B*ALPHA(2,J,N)+C*C*ALPHA(3,J,N))
      O(J,N)=(C*C+A*A)/(C*C*ALPHA(3,J,N)+A*A*ALPHA(1,J,N))
      P(J,N)=(A*A+B*B)/(A*A*ALPHA(1,J,N)+B*B*ALPHA(2,J,N))
      TPLS(J,N)=((A*B*C)/(12.0))*((((1.0/M(J,N))+(1.0/O(J,N))+(1.0/P(J,
     + N)))+(((1.0/M(J,N)**2.0)+(1.0/O(J,N)**2.0)+(1.0/P(J,N)**2.0))-
```

```
      + ((1.0/(M(J,N)*O(J,N)))+(1.0/(O(J,N)*P(J,N)))+(1.0/(P(J,N)*M(J,
      + N)))))**0.5))
        TMNS(J,N)=((A*B*C)/(12.0))*((((1.0/M(J,N))+(1.0/O(J,N))+(1.0/P(J,
      + N)))-(((1.0/M(J,N)**2.0)+(1.0/O(J,N)**2.0)+(1.0/P(J,N)**2.0))-
      + ((1.0/(M(J,N)*O(J,N)))+(1.0/(O(J,N)*P(J,N)))+(1.0/(P(J,N)*M(J,
      + N)))))**0.5))
        CA(J,N)=(2.0/(3.0*A*B*C))*M(J,N)
        CB(J,N)=(2.0/(3.0*A*B*C))*O(J,N)
        CC(J,N)=(2.0/(3.0*A*B*C))*P(J,N)
        RHOA(J,N)=2.0/((1.0/CB(J,N))+(1.0/CC(J,N)))
        RHOB(J,N)=2.0/((1.0/CA(J,N))+(1.0/CC(J,N)))
        RHOC(J,N)=2.0/((1.0/CA(J,N))+(1.0/CB(J,N)))
        DELA(J,N)=NU(J,N)/CA(J,N)
        DELB(J,N)=NU(J,N)/CB(J,N)
        DELC(J,N)=NU(J,N)/CC(J,N)
        TAU(J,N)=3.0/((1.0/CA(J,N))+(1.0/CB(J,N))+(1.0/CC(J,N)))
        PSI(J,N)=F(J,N)*((1.0/TAU(J,N))**(1.0/3.0))
        ZZ(J,N)=(1.0/2.0)*(F(J,N)**3.0)
        GAMMAA(J,N)=ZZ(J,N)*((1.0/CB(J,N))+(1.0/CC(J,N)))
        GAMMAB(J,N)=ZZ(J,N)*((1.0/CA(J,N))+(1.0/CC(J,N)))
        GAMMAC(J,N)=ZZ(J,N)*((1.0/CA(J,N))+(1.0/CB(J,N)))
        MUA(J,N)=(CA(J,N)**(1.0/3.0))/F(J,N)
        MUB(J,N)=(CB(J,N)**(1.0/3.0))/F(J,N)
        MUC(J,N)=(CC(J,N)**(1.0/3.0))/F(J,N)
        DPLS(J,N)=6.0*TPLS(J,N)*NU(J,N)
        DMNS(J,N)=6.0*TMNS(J,N)*NU(J,N)
        GPLS(J,N)=6.0*TPLS(J,N)*(F(J,N)**3.0)
        GMNS(J,N)=6.0*TMNS(J,N)*(F(J,N)**3.0)
   70 CONTINUE
   80 CONTINUE
C     THE PROGRAM NOW WRITES OUT THE COMPUTED VALUES IN TABLE FORM
      WRITE(3,600)
  600 FORMAT( " ")
      PRINT(3,60)
   60 FORMAT( "1   A/B     B/C    NU     F/FO     R      BETA")
      DO71 J=1,11
      DO72 N=1,11
      WRITE(3,73)Y(J),Z(N),NU(J,N),F(J,N),R(J,N),BETA(J,N)
   73 FORMAT( 2F7.1,4F8.3)
   72 CONTINUE
   71 CONTINUE
      WRITE(3,610)
  610 FORMAT(" ")
      PRINT(3,61)
   61 FORMAT( "1    A/B     B/C   CA/CO   CB/CO    CC/CO")
      DO74 J=1,11
      DO75 N=1,11
      WRITE(3,76)Y(J),Z(N),CA(J,N),CB(J,N),CC(J,N)
   76 FORMAT( 2F7.1,3F8.3)
   75 CONTINUE
   74 CONTINUE
      WRITE(3,620)
  620 FORMAT( " ")
      PRINT(3,62)
   62 FORMAT( "1    A/B     B/C RHOA/RHOO RHOB/RHOO RHOC/RHOO")
      DO81 J=1,11
      DO82 N=1,11
      WRITE(3,83)Y(J),Z(N),RHOA(J,N),RHOB(J,N),RHOC(J,N)
   83 FORMAT( 2F7.1,3F9.3)
   82 CONTINUE
   81 CONTINUE
      WRITE(3,630)
  630 FORMAT( " ")
      PRINT(3,63)
   63 FORMAT( "1    A/B     B/C  DELTA(A) DELTA(B) DELTA(C)")
      DO84 J=1,11
      DO85 N=1,11
      WRITE(3,86)Y(J),Z(N),DELA(J,N),DELB(J,N),DELC(J,N)
   86 FORMAT( 2F7.1,3F8.3)
   85 CONTINUE
   84 CONTINUE
      WRITE(3,640)
  640 FORMAT( " ")
      PRINT(3,64)
   64 FORMAT( "1    A/B     B/C  GAMMA(A) GAMMA(B) GAMMA(C)")
      DO91 J=1,11
      DO92 N=1,11
      WRITE(3,93)Y(J),Z(N),GAMMAA(J,N),GAMMAB(J,N),GAMMAC(J,N)
   93 FORMAT( 2F7.1,3F8.3)
   92 CONTINUE
   91 CONTINUE
```

```
      WRITE(3,650)
  650 FORMAT( " ")
      PRINT(3,65)
   65 FORMAT( "1    A/B      B/C     MU(A)    MU(B)    MU(C)")
      DO94 J=1,11
      DO95 N=1,11
      WRITE(3,96)Y(J),Z(N),MUA(J,N),MUB(J,N),MUC(J,N)
   96 FORMAT( 2F7.1,3F8.3)
   95 CONTINUE
   94 CONTINUE
      WRITE(3,660)
  660 FORMAT( " ")
      PRINT(3,66)
   66 FORMAT( "1    A/B      B/C  THETA+   THETA-   TAU/TAUO  PSI")
      DO101 J=1,11
      DO102 N=1,11
      WRITE(3,103)Y(J),Z(N),TPLS(J,N),TMNS(J,N),TAU(J,N),PSI(J,N)
  103 FORMAT( 2F7.1,4F8.3)
  102 CONTINUE
  101 CONTINUE
      WRITE(3,670)
  670 FORMAT( " ")
      PRINT(3,67)
   67 FORMAT( "1    A/B      B/C    DELTA+    DELTA-")
      DO104 J=1,11
      DO105 N=1,11
      WRITE(3,106)Y(J),Z(N),DPLS(J,N),DMNS(J,N)
  106 FORMAT( 2F7.1,2F8.3)
  105 CONTINUE
  104 CONTINUE
      WRITE(3,680)
  680 FORMAT( " ")
      PRINT(3,68)
   68 FORMAT( "1    A/B      B/C    GAMMA+    GAMMA-")
      DO111 J=1,11
      DO112 N=1,11
      WRITE(3,113)Y(J),Z(N),GPLS(J,N),GMNS(J,N)
  113 FORMAT( 2F7.1,2F8.3)
  112 CONTINUE
  111 CONTINUE
      WRITE(3,690)
  690 FORMAT( " ")
      DO114 J=1,11
      DO115 N=1,11
  115 CONTINUE
  114 CONTINUE
      STOP
      END



C
C
C

      REAL FUNCTION FUN(X)
      COMMON/PARAM/A,C,NN
      B=1.0
      GOTO(10,20,30,40,50,60,70,80,90,100),NN
   10 FUN=1/((A*A+X)**1.5*(B*B+X)**0.5*(C*C+X)**0.5)
      RETURN
   20 FUN=1/((A*A+X)**0.5*(B*B+X)**1.5*(C*C+X)**0.5)
      RETURN
   30 FUN=1/((A*A+X)**0.5*(B*B+X)**0.5*(C*C+X)**1.5)
      RETURN
   40 FUN=1/((A*A+X)**0.5*(B*B+X)**1.5*(C*C+X)**1.5)
      RETURN
   50 FUN=1/((A*A+X)**1.5*(B*B+X)**0.5*(C*C+X)**1.5)
      RETURN
   60 FUN=1/((A*A+X)**1.5*(B*B+X)**1.5*(C*C+X)**0.5)
      RETURN
   70 FUN=X/((A*A+X)**0.5*(B*B+X)**1.5*(C*C+X)**1.5)
      RETURN
   80 FUN=X/((A*A+X)**1.5*(B*B+X)**0.5*(C*C+X)**1.5)
      RETURN
   90 FUN=X/((A*A+X)**1.5*(B*B+X)**1.5*(C*C+X)**0.5)
      RETURN
  100 FUN=1.0/(((A*A+X)*(B*B+X)*(C*C+X))**0.5)
      RETURN
      END
```

A/B	B/C	NU	F/F0	R	BETA
1.0	1.0	2.500	1.000	1.600	2.112
1.0	1.1	2.507	1.001	1.598	2.112
1.0	1.2	2.524	1.003	1.592	2.113
1.0	1.3	2.550	1.006	1.583	2.113
1.0	1.4	2.583	1.010	1.572	2.114
1.0	1.5	2.620	1.014	1.560	2.115
1.0	1.6	2.661	1.019	1.548	2.115
1.0	1.7	2.706	1.025	1.534	2.116
1.0	1.8	2.753	1.030	1.521	2.117
1.0	1.9	2.803	1.036	1.507	2.118
1.0	2.0	2.854	1.042	1.493	2.118
1.1	1.0	2.507	1.001	1.598	2.112
1.1	1.1	2.520	1.002	1.593	2.112
1.1	1.2	2.544	1.005	1.585	2.113
1.1	1.3	2.576	1.009	1.574	2.114
1.1	1.4	2.614	1.014	1.562	2.115
1.1	1.5	2.656	1.019	1.549	2.115
1.1	1.6	2.702	1.024	1.535	2.116
1.1	1.7	2.751	1.030	1.521	2.117
1.1	1.8	2.803	1.036	1.507	2.118
1.1	1.9	2.857	1.042	1.492	2.119
1.1	2.0	2.913	1.049	1.478	2.120
1.2	1.0	2.525	1.003	1.591	2.113
1.2	1.1	2.545	1.005	1.584	2.113
1.2	1.2	2.575	1.009	1.574	2.114
1.2	1.3	2.612	1.013	1.562	2.115
1.2	1.4	2.655	1.018	1.549	2.116
1.2	1.5	2.703	1.024	1.535	2.117
1.2	1.6	2.754	1.030	1.520	2.118
1.2	1.7	2.808	1.036	1.505	2.119
1.2	1.8	2.865	1.043	1.490	2.120
1.2	1.9	2.923	1.049	1.475	2.120
1.2	2.0	2.983	1.056	1.460	2.121
1.3	1.0	2.553	1.006	1.582	2.114
1.3	1.1	2.579	1.009	1.573	2.114
1.3	1.2	2.615	1.013	1.561	2.115
1.3	1.3	2.658	1.018	1.547	2.116
1.3	1.4	2.706	1.024	1.533	2.118
1.3	1.5	2.759	1.030	1.518	2.119
1.3	1.6	2.815	1.037	1.502	2.120
1.3	1.7	2.874	1.043	1.486	2.121
1.3	1.8	2.935	1.050	1.471	2.122
1.3	1.9	2.998	1.057	1.455	2.123
1.3	2.0	3.063	1.064	1.440	2.124
1.4	1.0	2.588	1.010	1.569	2.115
1.4	1.1	2.621	1.014	1.559	2.116
1.4	1.2	2.662	1.019	1.545	2.117
1.4	1.3	2.711	1.024	1.531	2.118
1.4	1.4	2.764	1.030	1.515	2.120
1.4	1.5	2.822	1.037	1.499	2.121
1.4	1.6	2.883	1.044	1.482	2.122
1.4	1.7	2.947	1.051	1.466	2.123
1.4	1.8	3.013	1.058	1.450	2.124
1.4	1.9	3.081	1.065	1.434	2.125
1.4	2.0	3.151	1.073	1.419	2.126
1.5	1.0	2.630	1.015	1.555	2.116
1.5	1.1	2.668	1.019	1.543	2.118
1.5	1.2	2.716	1.024	1.528	2.119
1.5	1.3	2.770	1.031	1.512	2.121
1.5	1.4	2.829	1.037	1.496	2.122
1.5	1.5	2.892	1.044	1.479	2.123
1.5	1.6	2.958	1.051	1.462	2.125
1.5	1.7	3.027	1.059	1.445	2.126
1.5	1.8	3.098	1.066	1.429	2.127
1.5	1.9	3.171	1.074	1.413	2.128
1.5	2.0	3.245	1.082	1.397	2.129
1.6	1.0	2.677	1.020	1.540	2.118
1.6	1.1	2.722	1.025	1.526	2.120
1.6	1.2	2.775	1.031	1.510	2.121
1.6	1.3	2.834	1.037	1.493	2.123
1.6	1.4	2.899	1.044	1.476	2.125
1.6	1.5	2.967	1.052	1.458	2.126
1.6	1.6	3.039	1.059	1.441	2.128
1.6	1.7	3.113	1.067	1.423	2.129
1.6	1.8	3.189	1.075	1.407	2.130
1.6	1.9	3.267	1.083	1.390	2.132
1.6	2.0	3.346	1.091	1.374	2.133
1.7	1.0	2.729	1.026	1.524	2.120
1.7	1.1	2.779	1.031	1.508	2.122
1.7	1.2	2.839	1.037	1.491	2.124
1.7	1.3	2.904	1.044	1.473	2.126
1.7	1.4	2.974	1.052	1.455	2.128
1.7	1.5	3.047	1.060	1.437	2.129
1.7	1.6	3.124	1.068	1.419	2.131

1.7	1.7	3.204	1.076	1.402	2.132
1.7	1.8	3.285	1.084	1.384	2.134
1.7	1.9	3.368	1.092	1.368	2.135
1.7	2.0	3.453	1.101	1.352	2.137
1.8	1.0	2.785	1.031	1.506	2.123
1.8	1.1	2.842	1.037	1.490	2.125
1.8	1.2	2.907	1.044	1.472	2.127
1.8	1.3	2.978	1.052	1.453	2.129
1.8	1.4	3.053	1.059	1.434	2.131
1.8	1.5	3.132	1.068	1.415	2.133
1.8	1.6	3.215	1.076	1.397	2.134
1.8	1.7	3.300	1.085	1.379	2.136
1.8	1.8	3.386	1.093	1.362	2.138
1.8	1.9	3.475	1.102	1.345	2.139
1.8	2.0	3.565	1.111	1.329	2.141
1.9	1.0	2.844	1.038	1.489	2.125
1.9	1.1	2.908	1.044	1.471	2.127
1.9	1.2	2.978	1.051	1.452	2.130
1.9	1.3	3.055	1.059	1.432	2.132
1.9	1.4	3.137	1.067	1.413	2.134
1.9	1.5	3.222	1.076	1.394	2.136
1.9	1.6	3.310	1.085	1.375	2.138
1.9	1.7	3.400	1.093	1.357	2.140
1.9	1.8	3.492	1.102	1.340	2.142
1.9	1.9	3.586	1.111	1.323	2.143
1.9	2.0	3.681	1.120	1.307	2.145
2.0	1.0	2.908	1.044	1.470	2.128
2.0	1.1	2.977	1.051	1.451	2.130
2.0	1.2	3.054	1.059	1.432	2.133
2.0	1.3	3.137	1.067	1.412	2.135
2.0	1.4	3.224	1.075	1.392	2.138
2.0	1.5	3.315	1.084	1.372	2.140
2.0	1.6	3.408	1.093	1.354	2.142
2.0	1.7	3.504	1.102	1.335	2.144
2.0	1.8	3.602	1.112	1.318	2.146
2.0	1.9	3.702	1.121	1.301	2.148
2.0	2.0	3.803	1.130	1.285	2.149

A/B	B/C	CA/C0	CB/C0	CC/C0
1.0	1.0	1.000	1.000	1.000
1.0	1.1	.986	.986	1.040
1.0	1.2	.983	.983	1.081
1.0	1.3	.988	.988	1.121
1.0	1.4	.998	.998	1.162
1.0	1.5	1.013	1.013	1.203
1.0	1.6	1.032	1.032	1.244
1.0	1.7	1.054	1.054	1.286
1.0	1.8	1.078	1.078	1.327
1.0	1.9	1.104	1.104	1.368
1.0	2.0	1.132	1.132	1.410
1.1	1.0	.964	1.025	1.025
1.1	1.1	.952	1.020	1.067
1.1	1.2	.950	1.026	1.110
1.1	1.3	.955	1.038	1.153
1.1	1.4	.966	1.056	1.196
1.1	1.5	.981	1.078	1.240
1.1	1.6	1.000	1.103	1.283
1.1	1.7	1.021	1.132	1.327
1.1	1.8	1.045	1.162	1.370
1.1	1.9	1.071	1.195	1.414
1.1	2.0	1.099	1.229	1.458
1.2	1.0	.934	1.058	1.058
1.2	1.1	.923	1.062	1.103
1.2	1.2	.922	1.075	1.148
1.2	1.3	.928	1.095	1.194
1.2	1.4	.939	1.120	1.240
1.2	1.5	.955	1.150	1.286
1.2	1.6	.973	1.182	1.332
1.2	1.7	.995	1.217	1.378
1.2	1.8	1.019	1.254	1.425
1.2	1.9	1.044	1.293	1.471
1.2	2.0	1.072	1.333	1.518
1.3	1.0	.909	1.097	1.097
1.3	1.1	.899	1.110	1.146
1.3	1.2	.899	1.131	1.194
1.3	1.3	.905	1.159	1.243
1.3	1.4	.917	1.191	1.292
1.3	1.5	.933	1.227	1.341
1.3	1.6	.951	1.266	1.390
1.3	1.7	.973	1.308	1.439
1.3	1.8	.997	1.351	1.488
1.3	1.9	1.022	1.397	1.538
1.3	2.0	1.049	1.443	1.587
1.4	1.0	.887	1.143	1.143
1.4	1.1	.879	1.164	1.194
1.4	1.2	.879	1.193	1.246
1.4	1.3	.886	1.228	1.298
1.4	1.4	.898	1.267	1.350
1.4	1.5	.914	1.310	1.402
1.4	1.6	.933	1.356	1.455
1.4	1.7	.954	1.404	1.507
1.4	1.8	.978	1.454	1.560
1.4	1.9	1.003	1.506	1.612
1.4	2.0	1.030	1.559	1.665
1.5	1.0	.869	1.193	1.193
1.5	1.1	.862	1.222	1.248
1.5	1.2	.862	1.259	1.304
1.5	1.3	.870	1.301	1.359
1.5	1.4	.882	1.348	1.415
1.5	1.5	.898	1.398	1.470
1.5	1.6	.917	1.451	1.526
1.5	1.7	.938	1.506	1.582
1.5	1.8	.961	1.563	1.638
1.5	1.9	.987	1.621	1.694
1.5	2.0	1.013	1.681	1.751
1.6	1.0	.853	1.248	1.248
1.6	1.1	.846	1.285	1.307
1.6	1.2	.848	1.330	1.366
1.6	1.3	.855	1.379	1.425
1.6	1.4	.868	1.433	1.485
1.6	1.5	.884	1.490	1.544
1.6	1.6	.903	1.550	1.604
1.6	1.7	.924	1.612	1.663
1.6	1.8	.947	1.676	1.723
1.6	1.9	.972	1.741	1.783
1.6	2.0	.999	1.807	1.843
1.7	1.0	.839	1.307	1.307
1.7	1.1	.833	1.352	1.370
1.7	1.2	.835	1.404	1.433
1.7	1.3	.843	1.461	1.496
1.7	1.4	.855	1.523	1.559
1.7	1.5	.871	1.587	1.623
1.7	1.6	.890	1.654	1.686

1.7	1.7	.912	1.723	1.750
1.7	1.8	.935	1.793	1.814
1.7	1.9	.960	1.865	1.877
1.7	2.0	.986	1.939	1.941
1.8	1.0	.827	1.370	1.370
1.8	1.1	.822	1.423	1.437
1.8	1.2	.824	1.483	1.504
1.8	1.3	.832	1.547	1.571
1.8	1.4	.845	1.616	1.639
1.8	1.5	.861	1.687	1.706
1.8	1.6	.880	1.762	1.774
1.8	1.7	.901	1.838	1.842
1.8	1.8	.924	1.915	1.910
1.8	1.9	.949	1.995	1.978
1.8	2.0	.975	2.075	2.046
1.9	1.0	.816	1.436	1.436
1.9	1.1	.811	1.497	1.507
1.9	1.2	.814	1.564	1.579
1.9	1.3	.822	1.637	1.650
1.9	1.4	.835	1.713	1.722
1.9	1.5	.851	1.792	1.794
1.9	1.6	.870	1.873	1.866
1.9	1.7	.892	1.957	1.938
1.9	1.8	.915	2.042	2.011
1.9	1.9	.939	2.128	2.083
1.9	2.0	.965	2.216	2.155
2.0	1.0	.807	1.505	1.505
2.0	1.1	.802	1.574	1.581
2.0	1.2	.805	1.650	1.657
2.0	1.3	.814	1.730	1.733
2.0	1.4	.826	1.813	1.810
2.0	1.5	.843	1.900	1.886
2.0	1.6	.862	1.989	1.963
2.0	1.7	.883	2.080	2.040
2.0	1.8	.906	2.172	2.116
2.0	1.9	.931	2.266	2.193
2.0	2.0	.957	2.361	2.270

A/B	B/C	RHOA/RHOO	RHOB/RHOO	RHOC/RHOO
1.0	1.0	1.000	1.000	1.000
1.0	1.1	1.013	1.013	.986
1.0	1.2	1.030	1.030	.983
1.0	1.3	1.050	1.050	.988
1.0	1.4	1.074	1.074	.998
1.0	1.5	1.100	1.100	1.013
1.0	1.6	1.128	1.128	1.032
1.0	1.7	1.158	1.158	1.054
1.0	1.8	1.189	1.189	1.078
1.0	1.9	1.222	1.222	1.104
1.0	2.0	1.256	1.256	1.132
1.1	1.0	1.025	.993	.993
1.1	1.1	1.043	1.006	.985
1.1	1.2	1.066	1.024	.986
1.1	1.3	1.092	1.045	.995
1.1	1.4	1.122	1.069	1.009
1.1	1.5	1.153	1.095	1.027
1.1	1.6	1.187	1.124	1.049
1.1	1.7	1.222	1.154	1.074
1.1	1.8	1.258	1.186	1.101
1.1	1.9	1.295	1.219	1.130
1.1	2.0	1.334	1.253	1.160
1.2	1.0	1.058	.992	.992
1.2	1.1	1.082	1.005	.988
1.2	1.2	1.111	1.023	.993
1.2	1.3	1.143	1.044	1.005
1.2	1.4	1.177	1.069	1.022
1.2	1.5	1.214	1.096	1.043
1.2	1.6	1.253	1.125	1.068
1.2	1.7	1.293	1.156	1.095
1.2	1.8	1.334	1.188	1.124
1.2	1.9	1.376	1.222	1.155
1.2	2.0	1.419	1.256	1.188
1.3	1.0	1.097	.994	.994
1.3	1.1	1.128	1.008	.994
1.3	1.2	1.162	1.026	1.002
1.3	1.3	1.199	1.048	1.017
1.3	1.4	1.239	1.072	1.036
1.3	1.5	1.281	1.100	1.060
1.3	1.6	1.325	1.130	1.086
1.3	1.7	1.370	1.161	1.116
1.3	1.8	1.417	1.194	1.147
1.3	1.9	1.464	1.228	1.180
1.3	2.0	1.512	1.263	1.215
1.4	1.0	1.143	.999	.999
1.4	1.1	1.179	1.013	1.002
1.4	1.2	1.219	1.031	1.012
1.4	1.3	1.262	1.053	1.029
1.4	1.4	1.307	1.079	1.051
1.4	1.5	1.355	1.107	1.077
1.4	1.6	1.404	1.137	1.105
1.4	1.7	1.454	1.168	1.136
1.4	1.8	1.505	1.202	1.169
1.4	1.9	1.558	1.237	1.204
1.4	2.0	1.611	1.272	1.240
1.5	1.0	1.193	1.006	1.006
1.5	1.1	1.235	1.020	1.011
1.5	1.2	1.281	1.038	1.024
1.5	1.3	1.330	1.061	1.043
1.5	1.4	1.381	1.086	1.066
1.5	1.5	1.433	1.115	1.093
1.5	1.6	1.488	1.145	1.123
1.5	1.7	1.543	1.178	1.156
1.5	1.8	1.600	1.212	1.190
1.5	1.9	1.657	1.247	1.227
1.5	2.0	1.715	1.283	1.264
1.6	1.0	1.248	1.014	1.014
1.6	1.1	1.296	1.028	1.021
1.6	1.2	1.348	1.046	1.035
1.6	1.3	1.402	1.069	1.056
1.6	1.4	1.458	1.095	1.081
1.6	1.5	1.517	1.124	1.109
1.6	1.6	1.576	1.155	1.141
1.6	1.7	1.637	1.188	1.175
1.6	1.8	1.699	1.223	1.210
1.6	1.9	1.762	1.258	1.248
1.6	2.0	1.825	1.295	1.287
1.7	1.0	1.307	1.022	1.022
1.7	1.1	1.361	1.036	1.031
1.7	1.2	1.418	1.055	1.047
1.7	1.3	1.479	1.078	1.069
1.7	1.4	1.541	1.105	1.095
1.7	1.5	1.605	1.134	1.125
1.7	1.6	1.670	1.165	1.158

1.7	1.7	1.736	1.199	1.192
1.7	1.8	1.803	1.234	1.229
1.7	1.9	1.871	1.270	1.268
1.7	2.0	1.940	1.308	1.307
1.8	1.0	1.370	1.032	1.032
1.8	1.1	1.430	1.045	1.042
1.8	1.2	1.493	1.065	1.059
1.8	1.3	1.559	1.088	1.082
1.8	1.4	1.627	1.115	1.109
1.8	1.5	1.697	1.144	1.140
1.8	1.6	1.768	1.176	1.173
1.8	1.7	1.840	1.210	1.209
1.8	1.8	1.913	1.246	1.247
1.8	1.9	1.986	1.283	1.286
1.8	2.0	2.060	1.321	1.327
1.9	1.0	1.436	1.041	1.041
1.9	1.1	1.502	1.055	1.052
1.9	1.2	1.572	1.074	1.071
1.9	1.3	1.644	1.098	1.095
1.9	1.4	1.718	1.125	1.123
1.9	1.5	1.793	1.155	1.154
1.9	1.6	1.870	1.187	1.188
1.9	1.7	1.948	1.221	1.225
1.9	1.8	2.026	1.257	1.263
1.9	1.9	2.105	1.295	1.303
1.9	2.0	2.185	1.334	1.345
2.0	1.0	1.505	1.050	1.050
2.0	1.1	1.577	1.064	1.063
2.0	1.2	1.653	1.084	1.082
2.0	1.3	1.731	1.107	1.107
2.0	1.4	1.812	1.135	1.135
2.0	1.5	1.893	1.165	1.168
2.0	1.6	1.976	1.198	1.203
2.0	1.7	2.059	1.233	1.240
2.0	1.8	2.144	1.269	1.279
2.0	1.9	2.229	1.307	1.320
2.0	2.0	2.314	1.346	1.362

A/B	B/C	DELTA(A)	DELTA(B)	DELTA(C)
1.0	1.0	2.500	2.500	2.500
1.0	1.1	2.541	2.541	2.410
1.0	1.2	2.568	2.568	2.336
1.0	1.3	2.582	2.582	2.274
1.0	1.4	2.588	2.588	2.222
1.0	1.5	2.586	2.586	2.178
1.0	1.6	2.579	2.579	2.139
1.0	1.7	2.568	2.568	2.105
1.0	1.8	2.555	2.555	2.075
1.0	1.9	2.539	2.539	2.048
1.0	2.0	2.522	2.522	2.024
1.1	1.0	2.601	2.446	2.446
1.1	1.1	2.648	2.470	2.362
1.1	1.2	2.679	2.481	2.292
1.1	1.3	2.697	2.482	2.234
1.1	1.4	2.706	2.475	2.185
1.1	1.5	2.707	2.464	2.143
1.1	1.6	2.702	2.449	2.106
1.1	1.7	2.694	2.431	2.074
1.1	1.8	2.682	2.412	2.046
1.1	1.9	2.667	2.392	2.020
1.1	2.0	2.651	2.371	1.998
1.2	1.0	2.704	2.387	2.387
1.2	1.1	2.757	2.397	2.308
1.2	1.2	2.793	2.395	2.242
1.2	1.3	2.815	2.385	2.188
1.2	1.4	2.827	2.370	2.141
1.2	1.5	2.831	2.351	2.102
1.2	1.6	2.829	2.330	2.067
1.2	1.7	2.822	2.308	2.037
1.2	1.8	2.812	2.285	2.010
1.2	1.9	2.799	2.261	1.987
1.2	2.0	2.784	2.238	1.966
1.3	1.0	2.809	2.326	2.326
1.3	1.1	2.868	2.323	2.251
1.3	1.2	2.909	2.311	2.190
1.3	1.3	2.936	2.293	2.139
1.3	1.4	2.951	2.272	2.095
1.3	1.5	2.958	2.248	2.058
1.3	1.6	2.959	2.223	2.025
1.3	1.7	2.954	2.197	1.997
1.3	1.8	2.945	2.172	1.972
1.3	1.9	2.934	2.147	1.950
1.3	2.0	2.920	2.122	1.930
1.4	1.0	2.916	2.264	2.264
1.4	1.1	2.981	2.252	2.194
1.4	1.2	3.028	2.232	2.136
1.4	1.3	3.059	2.208	2.088
1.4	1.4	3.078	2.181	2.047
1.4	1.5	3.088	2.154	2.012
1.4	1.6	3.091	2.126	1.982
1.4	1.7	3.089	2.099	1.955
1.4	1.8	3.082	2.072	1.932
1.4	1.9	3.072	2.046	1.911
1.4	2.0	3.060	2.021	1.892
1.5	1.0	3.026	2.203	2.203
1.5	1.1	3.097	2.183	2.137
1.5	1.2	3.149	2.157	2.083
1.5	1.3	3.185	2.128	2.038
1.5	1.4	3.208	2.098	2.000
1.5	1.5	3.222	2.068	1.967
1.5	1.6	3.227	2.039	1.938
1.5	1.7	3.227	2.010	1.913
1.5	1.8	3.222	1.983	1.891
1.5	1.9	3.214	1.956	1.871
1.5	2.0	3.204	1.931	1.854
1.6	1.0	3.137	2.144	2.144
1.6	1.1	3.215	2.117	2.082
1.6	1.2	3.273	2.087	2.031
1.6	1.3	3.313	2.055	1.989
1.6	1.4	3.341	2.023	1.953
1.6	1.5	3.358	1.991	1.922
1.6	1.6	3.366	1.960	1.895
1.6	1.7	3.369	1.931	1.871
1.6	1.8	3.366	1.903	1.851
1.6	1.9	3.360	1.877	1.832
1.6	2.0	3.351	1.852	1.816
1.7	1.0	3.251	2.087	2.087
1.7	1.1	3.336	2.055	2.029
1.7	1.2	3.399	2.021	1.981
1.7	1.3	3.445	1.987	1.941
1.7	1.4	3.476	1.953	1.907
1.7	1.5	3.497	1.920	1.878
1.7	1.6	3.509	1.889	1.853

1.7	1.7	3.514	1.860	1.831
1.7	1.8	3.513	1.832	1.811
1.7	1.9	3.509	1.806	1.794
1.7	2.0	3.501	1.781	1.779
1.8	1.0	3.366	2.033	2.033
1.8	1.1	3.459	1.997	1.978
1.8	1.2	3.528	1.960	1.933
1.8	1.3	3.579	1.924	1.895
1.8	1.4	3.615	1.889	1.863
1.8	1.5	3.639	1.856	1.836
1.8	1.6	3.654	1.825	1.812
1.8	1.7	3.662	1.796	1.792
1.8	1.8	3.664	1.768	1.773
1.8	1.9	3.661	1.742	1.757
1.8	2.0	3.655	1.718	1.743
1.9	1.0	3.484	1.981	1.981
1.9	1.1	3.584	1.942	1.929
1.9	1.2	3.660	1.904	1.887
1.9	1.3	3.716	1.867	1.851
1.9	1.4	3.757	1.831	1.821
1.9	1.5	3.785	1.798	1.796
1.9	1.6	3.803	1.767	1.773
1.9	1.7	3.813	1.738	1.754
1.9	1.8	3.818	1.710	1.737
1.9	1.9	3.817	1.685	1.722
1.9	2.0	3.813	1.662	1.708
2.0	1.0	3.604	1.932	1.932
2.0	1.1	3.712	1.891	1.883
2.0	1.2	3.794	1.851	1.843
2.0	1.3	3.856	1.814	1.810
2.0	1.4	3.901	1.778	1.781
2.0	1.5	3.933	1.745	1.757
2.0	1.6	3.955	1.714	1.736
2.0	1.7	3.968	1.685	1.718
2.0	1.8	3.975	1.658	1.702
2.0	1.9	3.977	1.634	1.688
2.0	2.0	3.975	1.611	1.675

A/B	B/C	GAMMA(A)	GAMMA(B)	GAMMA(C)
1.0	1.0	1.000	1.000	1.000
1.0	1.1	.990	.990	1.016
1.0	1.2	.980	.980	1.026
1.0	1.3	.970	.970	1.031
1.0	1.4	.959	.959	1.032
1.0	1.5	.949	.949	1.031
1.0	1.6	.939	.939	1.027
1.0	1.7	.929	.929	1.021
1.0	1.8	.919	.919	1.015
1.0	1.9	.910	.910	1.008
1.0	2.0	.901	.901	1.000
1.1	1.0	.978	1.009	1.009
1.1	1.1	.966	1.001	1.023
1.1	1.2	.953	.993	1.030
1.1	1.3	.941	.984	1.033
1.1	1.4	.929	.974	1.032
1.1	1.5	.917	.965	1.029
1.1	1.6	.905	.956	1.024
1.1	1.7	.894	.947	1.017
1.1	1.8	.884	.937	1.010
1.1	1.9	.874	.929	1.002
1.1	2.0	.864	.920	.994
1.2	1.0	.954	1.017	1.017
1.2	1.1	.939	1.011	1.029
1.2	1.2	.925	1.004	1.034
1.2	1.3	.911	.996	1.036
1.2	1.4	.897	.988	1.034
1.2	1.5	.885	.980	1.029
1.2	1.6	.872	.971	1.023
1.2	1.7	.861	.963	1.016
1.2	1.8	.850	.954	1.008
1.2	1.9	.840	.946	1.000
1.2	2.0	.830	.938	.991
1.3	1.0	.928	1.025	1.025
1.3	1.1	.912	1.020	1.035
1.3	1.2	.896	1.015	1.039
1.3	1.3	.881	1.008	1.039
1.3	1.4	.867	1.001	1.036
1.3	1.5	.853	.994	1.031
1.3	1.6	.840	.986	1.025
1.3	1.7	.829	.978	1.018
1.3	1.8	.817	.970	1.009
1.3	1.9	.807	.962	1.001
1.3	2.0	.797	.954	.992
1.4	1.0	.902	1.032	1.032
1.4	1.1	.884	1.029	1.041
1.4	1.2	.867	1.025	1.044
1.4	1.3	.851	1.020	1.044
1.4	1.4	.837	1.014	1.041
1.4	1.5	.823	1.007	1.035
1.4	1.6	.810	1.000	1.029
1.4	1.7	.798	.993	1.021
1.4	1.8	.787	.986	1.013
1.4	1.9	.777	.978	1.005
1.4	2.0	.767	.971	.996
1.5	1.0	.876	1.039	1.039
1.5	1.1	.857	1.038	1.047
1.5	1.2	.839	1.036	1.050
1.5	1.3	.823	1.032	1.050
1.5	1.4	.808	1.027	1.046
1.5	1.5	.794	1.021	1.041
1.5	1.6	.781	1.015	1.035
1.5	1.7	.769	1.008	1.027
1.5	1.8	.758	1.001	1.019
1.5	1.9	.748	.994	1.011
1.5	2.0	.739	.987	1.002
1.6	1.0	.850	1.047	1.047
1.6	1.1	.831	1.048	1.055
1.6	1.2	.813	1.047	1.058
1.6	1.3	.796	1.044	1.057
1.6	1.4	.781	1.040	1.054
1.6	1.5	.767	1.035	1.048
1.6	1.6	.754	1.029	1.042
1.6	1.7	.742	1.023	1.035
1.6	1.8	.731	1.017	1.027
1.6	1.9	.721	1.010	1.019
1.6	2.0	.712	1.003	1.010
1.7	1.0	.825	1.055	1.055
1.7	1.1	.805	1.058	1.063
1.7	1.2	.787	1.058	1.066
1.7	1.3	.770	1.056	1.065
1.7	1.4	.755	1.053	1.062
1.7	1.5	.741	1.049	1.057
1.7	1.6	.729	1.044	1.051

1.7	1.7	.717	1.038	1.044
1.7	1.8	.706	1.032	1.036
1.7	1.9	.697	1.026	1.029
1.7	2.0	.688	1.020	1.020
1.8	1.0	.801	1.064	1.064
1.8	1.1	.781	1.068	1.072
1.8	1.2	.763	1.070	1.075
1.8	1.3	.746	1.069	1.075
1.8	1.4	.731	1.067	1.072
1.8	1.5	.717	1.064	1.068
1.8	1.6	.705	1.059	1.062
1.8	1.7	.693	1.054	1.055
1.8	1.8	.683	1.049	1.048
1.8	1.9	.674	1.043	1.040
1.8	2.0	.665	1.037	1.032
1.9	1.0	.778	1.073	1.073
1.9	1.1	.758	1.079	1.081
1.9	1.2	.739	1.082	1.085
1.9	1.3	.723	1.082	1.085
1.9	1.4	.708	1.081	1.083
1.9	1.5	.695	1.079	1.079
1.9	1.6	.682	1.075	1.074
1.9	1.7	.671	1.070	1.067
1.9	1.8	.661	1.065	1.060
1.9	1.9	.652	1.060	1.053
1.9	2.0	.643	1.054	1.045
2.0	1.0	.756	1.083	1.083
2.0	1.1	.736	1.090	1.092
2.0	1.2	.717	1.095	1.096
2.0	1.3	.701	1.096	1.097
2.0	1.4	.687	1.096	1.095
2.0	1.5	.673	1.094	1.092
2.0	1.6	.661	1.091	1.087
2.0	1.7	.651	1.087	1.081
2.0	1.8	.641	1.083	1.074
2.0	1.9	.632	1.078	1.067
2.0	2.0	.624	1.072	1.060

A/B	B/C	MU(A)	MU(B)	MU(C)
1.0	1.0	1.000	1.000	1.000
1.0	1.1	.995	.995	1.012
1.0	1.2	.991	.991	1.023
1.0	1.3	.990	.990	1.033
1.0	1.4	.989	.989	1.041
1.0	1.5	.990	.990	1.048
1.0	1.6	.991	.991	1.055
1.0	1.7	.993	.993	1.061
1.0	1.8	.995	.995	1.067
1.0	1.9	.998	.998	1.072
1.0	2.0	1.000	1.000	1.076
1.1	1.0	.987	1.007	1.007
1.1	1.1	.981	1.004	1.019
1.1	1.2	.978	1.003	1.030
1.1	1.3	.976	1.003	1.039
1.1	1.4	.975	1.005	1.047
1.1	1.5	.975	1.007	1.055
1.1	1.6	.976	1.009	1.061
1.1	1.7	.978	1.012	1.067
1.1	1.8	.980	1.015	1.072
1.1	1.9	.982	1.018	1.077
1.1	2.0	.984	1.022	1.081
1.2	1.0	.975	1.016	1.016
1.2	1.1	.969	1.015	1.028
1.2	1.2	.965	1.015	1.038
1.2	1.3	.963	1.017	1.047
1.2	1.4	.962	1.020	1.055
1.2	1.5	.962	1.023	1.062
1.2	1.6	.962	1.027	1.068
1.2	1.7	.963	1.030	1.074
1.2	1.8	.965	1.034	1.079
1.2	1.9	.967	1.038	1.084
1.2	2.0	.969	1.042	1.088
1.3	1.0	.963	1.025	1.025
1.3	1.1	.956	1.026	1.037
1.3	1.2	.952	1.028	1.047
1.3	1.3	.950	1.031	1.056
1.3	1.4	.949	1.035	1.063
1.3	1.5	.948	1.039.	1.070
1.3	1.6	.949	1.044	1.077
1.3	1.7	.950	1.048	1.082
1.3	1.8	.951	1.053	1.087
1.3	1.9	.953	1.057	1.092
1.3	2.0	.955	1.062	1.096
1.4	1.0	.951	1.035	1.035
1.4	1.1	.945	1.037	1.046
1.4	1.2	.940	1.041	1.056
1.4	1.3	.938	1.045	1.065
1.4	1.4	.936	1.050	1.073
1.4	1.5	.936	1.055	1.080
1.4	1.6	.936	1.060	1.086
1.4	1.7	.937	1.066	1.091
1.4	1.8	.938	1.071	1.096
1.4	1.9	.939	1.076	1.101
1.4	2.0	.941	1.081	1.105
1.5	1.0	.940	1.045	1.045
1.5	1.1	.934	1.049	1.056
1.5	1.2	.929	1.054	1.066
1.5	1.3	.926	1.059	1.075
1.5	1.4	.925	1.065	1.082
1.5	1.5	.924	1.071	1.089
1.5	1.6	.924	1.077	1.095
1.5	1.7	.924	1.082	1.101
1.5	1.8	.925	1.088	1.105
1.5	1.9	.927	1.094	1.110
1.5	2.0	.928	1.099	1.114
1.6	1.0	.930	1.056	1.056
1.6	1.1	.923	1.061	1.067
1.6	1.2	.918	1.067	1.076
1.6	1.3	.915	1.073	1.085
1.6	1.4	.913	1.080	1.092
1.6	1.5	.912	1.086	1.099
1.6	1.6	.912	1.092	1.105
1.6	1.7	.913	1.099	1.110
1.6	1.8	.913	1.105	1.115
1.6	1.9	.915	1.111	1.119
1.6	2.0	.916	1.116	1.123
1.7	1.0	.920	1.066	1.066
1.7	1.1	.913	1.073	1.077
1.7	1.2	.908	1.080	1.087
1.7	1.3	.905	1.087	1.095
1.7	1.4	.903	1.094	1.103
1.7	1.5	.901	1.101	1.109
1.7	1.6	.901	1.108	1.115

1.7	1.7	.901	1.114	1.120
1.7	1.8	.902	1.121	1.125
1.7	1.9	.903	1.127	1.129
1.7	2.0	.904	1.133	1.133
1.8	1.0	.910	1.077	1.077
1.8	1.1	.903	1.084	1.088
1.8	1.2	.898	1.092	1.097
1.8	1.3	.894	1.100	1.105
1.8	1.4	.892	1.108	1.113
1.8	1.5	.891	1.115	1.119
1.8	1.6	.890	1.122	1.125
1.8	1.7	.891	1.129	1.130
1.8	1.8	.891	1.136	1.135
1.8	1.9	.892	1.142	1.139
1.8	2.0	.893	1.149	1.143
1.9	1.0	.901	1.087	1.087
1.9	1.1	.893	1.096	1.098
1.9	1.2	.888	1.104	1.108
1.9	1.3	.885	1.113	1.116
1.9	1.4	.882	1.121	1.123
1.9	1.5	.881	1.129	1.129
1.9	1.6	.880	1.137	1.135
1.9	1.7	.880	1.144	1.140
1.9	1.8	.881	1.151	1.145
1.9	1.9	.881	1.157	1.149
1.9	2.0	.882	1.164	1.153
2.0	1.0	.892	1.098	1.098
2.0	1.1	.884	1.107	1.109
2.0	1.2	.879	1.116	1.118
2.0	1.3	.875	1.125	1.126
2.0	1.4	.873	1.134	1.133
2.0	1.5	.871	1.142	1.140
2.0	1.6	.870	1.150	1.145
2.0	1.7	.870	1.158	1.150
2.0	1.8	.870	1.165	1.155
2.0	1.9	.871	1.172	1.159
2.0	2.0	.872	1.178	1.163

A/B	B/C	THETA+	THETA-	TAU/TAUO	PSI
1.0	1.0	.167	.167	1.000	1.000
1.0	1.1	.169	.163	1.004	1.000
1.0	1.2	.170	.159	1.014	.998
1.0	1.3	.169	.155	1.029	.997
1.0	1.4	.167	.151	1.047	.995
1.0	1.5	.165	.147	1.069	.992
1.0	1.6	.162	.143	1.094	.989
1.0	1.7	.158	.139	1.121	.986
1.0	1.8	.155	.135	1.150	.983
1.0	1.9	.151	.132	1.180	.980
1.0	2.0	.147	.128	1.211	.977
1.1	1.0	.170	.163	1.004	1.000
1.1	1.1	.170	.159	1.011	.999
1.1	1.2	.170	.155	1.024	.997
1.1	1.3	.169	.151	1.042	.995
1.1	1.4	.166	.147	1.064	.993
1.1	1.5	.163	.143	1.089	.990
1.1	1.6	.160	.139	1.117	.987
1.1	1.7	.156	.134	1.147	.984
1.1	1.8	.152	.131	1.178	.981
1.1	1.9	.149	.127	1.211	.978
1.1	2.0	.145	.123	1.245	.975
1.2	1.0	.172	.158	1.013	.999
1.2	1.1	.172	.154	1.023	.998
1.2	1.2	.171	.150	1.040	.996
1.2	1.3	.169	.145	1.061	.994
1.2	1.4	.166	.141	1.085	.991
1.2	1.5	.163	.137	1.113	.988
1.2	1.6	.159	.132	1.143	.985
1.2	1.7	.155	.128	1.175	.982
1.2	1.8	.152	.124	1.209	.979
1.2	1.9	.148	.120	1.244	.976
1.2	2.0	.144	.117	1.281	.972
1.3	1.0	.173	.152	1.026	.998
1.3	1.1	.173	.148	1.040	.996
1.3	1.2	.172	.143	1.059	.994
1.3	1.3	.169	.139	1.082	.992
1.3	1.4	.166	.134	1.109	.989
1.3	1.5	.163	.130	1.139	.986
1.3	1.6	.159	.125	1.172	.983
1.3	1.7	.155	.121	1.206	.980
1.3	1.8	.151	.117	1.242	.977
1.3	1.9	.147	.114	1.279	.974
1.3	2.0	.143	.110	1.318	.971
1.4	1.0	.174	.146	1.043	.996
1.4	1.1	.174	.141	1.059	.995
1.4	1.2	.172	.137	1.080	.993
1.4	1.3	.170	.132	1.106	.991
1.4	1.4	.166	.127	1.135	.988
1.4	1.5	.163	.123	1.167	.985
1.4	1.6	.159	.119	1.201	.982
1.4	1.7	.155	.114	1.238	.979
1.4	1.8	.151	.111	1.276	.976
1.4	1.9	.147	.107	1.315	.972
1.4	2.0	.143	.103	1.356	.969
1.5	1.0	.174	.140	1.061	.995
1.5	1.1	.174	.135	1.079	.994
1.5	1.2	.172	.130	1.103	.992
1.5	1.3	.170	.125	1.130	.989
1.5	1.4	.166	.121	1.161	.987
1.5	1.5	.163	.116	1.195	.984
1.5	1.6	.159	.112	1.232	.981
1.5	1.7	.155	.108	1.270	.978
1.5	1.8	.150	.104	1.310	.975
1.5	1.9	.146	.101	1.351	.972
1.5	2.0	.142	.097	1.393	.969
1.6	1.0	.175	.134	1.081	.994
1.6	1.1	.174	.129	1.101	.993
1.6	1.2	.172	.124	1.126	.991
1.6	1.3	.170	.119	1.156	.988
1.6	1.4	.166	.114	1.189	.986
1.6	1.5	.162	.110	1.224	.983
1.6	1.6	.158	.106	1.262	.980
1.6	1.7	.154	.102	1.302	.977
1.6	1.8	.150	.098	1.344	.974
1.6	1.9	.146	.095	1.386	.971
1.6	2.0	.142	.091	1.430	.969
1.7	1.0	.175	.127	1.102	.993
1.7	1.1	.174	.122	1.124	.992
1.7	1.2	.172	.117	1.151	.990
1.7	1.3	.169	.113	1.182	.988
1.7	1.4	.166	.108	1.216	.985
1.7	1.5	.162	.104	1.253	.983
1.7	1.6	.158	.100	1.293	.980

1.7	1.7	.154	.096	1.334	.977
1.7	1.8	.150	.092	1.377	.974
1.7	1.9	.145	.089	1.422	.972
1.7	2.0	.141	.086	1.467	.969
1.8	1.0	.175	.122	1.124	.992
1.8	1.1	.174	.117	1.147	.991
1.8	1.2	.172	.112	1.175	.990
1.8	1.3	.169	.107	1.207	.988
1.8	1.4	.166	.102	1.243	.985
1.8	1.5	.162	.098	1.282	.983
1.8	1.6	.158	.094	1.323	.980
1.8	1.7	.154	.091	1.366	.978
1.8	1.8	.149	.087	1.410	.975
1.8	1.9	.145	.084	1.456	.972
1.8	2.0	.141	.081	1.503	.970
1.9	1.0	.175	.116	1.146	.992
1.9	1.1	.174	.111	1.170	.991
1.9	1.2	.172	.106	1.199	.989
1.9	1.3	.169	.101	1.233	.988
1.9	1.4	.165	.097	1.270	.986
1.9	1.5	.162	.093	1.310	.983
1.9	1.6	.157	.089	1.352	.981
1.9	1.7	.153	.086	1.396	.978
1.9	1.8	.149	.082	1.442	.976
1.9	1.9	.145	.079	1.489	.973
1.9	2.0	.141	.076	1.538	.971
2.0	1.0	.175	.111	1.168	.991
2.0	1.1	.174	.106	1.193	.991
2.0	1.2	.172	.101	1.224	.990
2.0	1.3	.169	.096	1.258	.988
2.0	1.4	.165	.092	1.296	.986
2.0	1.5	.161	.088	1.337	.984
2.0	1.6	.157	.084	1.381	.982
2.0	1.7	.153	.081	1.426	.979
2.0	1.8	.149	.078	1.473	.977
2.0	1.9	.144	.075	1.522	.975
2.0	2.0	.140	.072	1.571	.972

A/B	B/C	DELTA+	DELTA-
1.0	1.0	2.500	2.500
1.0	1.1	2.541	2.454
1.0	1.2	2.568	2.413
1.0	1.3	2.582	2.377
1.0	1.4	2.588	2.344
1.0	1.5	2.586	2.314
1.0	1.6	2.579	2.286
1.0	1.7	2.568	2.259
1.0	1.8	2.555	2.235
1.0	1.9	2.539	2.212
1.0	2.0	2.522	2.190
1.1	1.0	2.549	2.446
1.1	1.1	2.577	2.410
1.1	1.2	2.596	2.372
1.1	1.3	2.605	2.337
1.1	1.4	2.606	2.305
1.1	1.5	2.601	2.274
1.1	1.6	2.592	2.246
1.1	1.7	2.579	2.220
1.1	1.8	2.564	2.195
1.1	1.9	2.547	2.172
1.1	2.0	2.529	2.151
1.2	1.0	2.599	2.387
1.2	1.1	2.624	2.350
1.2	1.2	2.641	2.313
1.2	1.3	2.648	2.277
1.2	1.4	2.648	2.245
1.2	1.5	2.642	2.214
1.2	1.6	2.632	2.185
1.2	1.7	2.619	2.159
1.2	1.8	2.604	2.134
1.2	1.9	2.587	2.111
1.2	2.0	2.570	2.089
1.3	1.0	2.648	2.326
1.3	1.1	2.675	2.286
1.3	1.2	2.692	2.248
1.3	1.3	2.700	2.212
1.3	1.4	2.700	2.178
1.3	1.5	2.695	2.147
1.3	1.6	2.686	2.118
1.3	1.7	2.674	2.091
1.3	1.8	2.660	2.066
1.3	1.9	2.644	2.043
1.3	2.0	2.627	2.021
1.4	1.0	2.699	2.264
1.4	1.1	2.729	2.222
1.4	1.2	2.748	2.183
1.4	1.3	2.757	2.146
1.4	1.4	2.759	2.112
1.4	1.5	2.756	2.081
1.4	1.6	2.748	2.051
1.4	1.7	2.737	2.024
1.4	1.8	2.724	1.999
1.4	1.9	2.710	1.976
1.4	2.0	2.694	1.954
1.5	1.0	2.752	2.203
1.5	1.1	2.785	2.160
1.5	1.2	2.807	2.119
1.5	1.3	2.818	2.082
1.5	1.4	2.823	2.048
1.5	1.5	2.821	2.016
1.5	1.6	2.815	1.987
1.5	1.7	2.806	1.961
1.5	1.8	2.795	1.936
1.5	1.9	2.781	1.913
1.5	2.0	2.767	1.892
1.6	1.0	2.806	2.144
1.6	1.1	2.844	2.100
1.6	1.2	2.868	2.059
1.6	1.3	2.883	2.021
1.6	1.4	2.890	1.987
1.6	1.5	2.891	1.956
1.6	1.6	2.887	1.927
1.6	1.7	2.880	1.901
1.6	1.8	2.870	1.877
1.6	1.9	2.858	1.854
1.6	2.0	2.845	1.834
1.7	1.0	2.863	2.087
1.7	1.1	2.905	2.042
1.7	1.2	2.933	2.001
1.7	1.3	2.951	1.964
1.7	1.4	2.961	1.930
1.7	1.5	2.965	1.899
1.7	1.6	2.963	1.871

1.7	1.7	2.958	1.845
1.7	1.8	2.949	1.822
1.7	1.9	2.939	1.800
1.7	2.0	2.927	1.780
1.8	1.0	2.922	2.033
1.8	1.1	2.968	1.987
1.8	1.2	3.001	1.946
1.8	1.3	3.023	1.910
1.8	1.4	3.036	1.876
1.8	1.5	3.042	1.846
1.8	1.6	3.042	1.819
1.8	1.7	3.039	1.794
1.8	1.8	3.033	1.771
1.8	1.9	3.024	1.750
1.8	2.0	3.014	1.730
1.9	1.0	2.983	1.981
1.9	1.1	3.035	1.936
1.9	1.2	3.071	1.895
1.9	1.3	3.097	1.859
1.9	1.4	3.113	1.826
1.9	1.5	3.122	1.797
1.9	1.6	3.125	1.770
1.9	1.7	3.124	1.746
1.9	1.8	3.120	1.724
1.9	1.9	3.113	1.703
1.9	2.0	3.104	1.685
2.0	1.0	3.047	1.932
2.0	1.1	3.103	1.887
2.0	1.2	3.145	1.847
2.0	1.3	3.174	1.812
2.0	1.4	3.194	1.780
2.0	1.5	3.206	1.751
2.0	1.6	3.212	1.725
2.0	1.7	3.213	1.702
2.0	1.8	3.210	1.680
2.0	1.9	3.205	1.661
2.0	2.0	3.198	1.643

A/B	B/C	GAMMA+	GAMMA-
1.0	1.0	1.000	1.000
1.0	1.1	1.016	.981
1.0	1.2	1.026	.965
1.0	1.3	1.031	.949
1.0	1.4	1.032	.935
1.0	1.5	1.031	.922
1.0	1.6	1.027	.910
1.0	1.7	1.021	.898
1.0	1.8	1.015	.888
1.0	1.9	1.008	.878
1.0	2.0	1.000	.868
1.1	1.0	1.020	.978
1.1	1.1	1.030	.963
1.1	1.2	1.037	.947
1.1	1.3	1.039	.932
1.1	1.4	1.039	.918
1.1	1.5	1.035	.905
1.1	1.6	1.030	.893
1.1	1.7	1.024	.881
1.1	1.8	1.017	.871
1.1	1.9	1.009	.861
1.1	2.0	1.001	.851
1.2	1.0	1.038	.954
1.2	1.1	1.048	.938
1.2	1.2	1.053	.922
1.2	1.3	1.055	.907
1.2	1.4	1.053	.893
1.2	1.5	1.050	.880
1.2	1.6	1.044	.867
1.2	1.7	1.038	.855
1.2	1.8	1.030	.844
1.2	1.9	1.023	.834
1.2	2.0	1.015	.825
1.3	1.0	1.057	.928
1.3	1.1	1.066	.911
1.3	1.2	1.072	.895
1.3	1.3	1.073	.879
1.3	1.4	1.072	.865
1.3	1.5	1.068	.851
1.3	1.6	1.063	.838
1.3	1.7	1.057	.826
1.3	1.8	1.049	.815
1.3	1.9	1.042	.805
1.3	2.0	1.034	.795
1.4	1.0	1.075	.902
1.4	1.1	1.085	.884
1.4	1.2	1.091	.867
1.4	1.3	1.093	.851
1.4	1.4	1.092	.836
1.4	1.5	1.089	.822
1.4	1.6	1.084	.809
1.4	1.7	1.078	.797
1.4	1.8	1.071	.786
1.4	1.9	1.064	.776
1.4	2.0	1.056	.766
1.5	1.0	1.094	.876
1.5	1.1	1.105	.857
1.5	1.2	1.111	.839
1.5	1.3	1.114	.823
1.5	1.4	1.113	.808
1.5	1.5	1.111	.794
1.5	1.6	1.106	.781
1.5	1.7	1.101	.769
1.5	1.8	1.094	.758
1.5	1.9	1.087	.748
1.5	2.0	1.080	.738
1.6	1.0	1.113	.850
1.6	1.1	1.125	.831
1.6	1.2	1.132	.812
1.6	1.3	1.135	.796
1.6	1.4	1.136	.781
1.6	1.5	1.133	.767
1.6	1.6	1.130	.754
1.6	1.7	1.125	.742
1.6	1.8	1.119	.731
1.6	1.9	1.112	.721
1.6	2.0	1.105	.712
1.7	1.0	1.132	.825
1.7	1.1	1.145	.805
1.7	1.2	1.154	.787
1.7	1.3	1.158	.770
1.7	1.4	1.159	.755
1.7	1.5	1.157	.741
1.7	1.6	1.154	.729

1.7	1.7	1.149	.717
1.7	1.8	1.144	.706
1.7	1.9	1.138	.697
1.7	2.0	1.131	.688
1.8	1.0	1.151	.801
1.8	1.1	1.166	.781
1.8	1.2	1.176	.762
1.8	1.3	1.181	.746
1.8	1.4	1.182	.731
1.8	1.5	1.182	.717
1.8	1.6	1.179	.705
1.8	1.7	1.175	.693
1.8	1.8	1.170	.683
1.8	1.9	1.164	.674
1.8	2.0	1.158	.665
1.9	1.0	1.172	.778
1.9	1.1	1.188	.758
1.9	1.2	1.198	.739
1.9	1.3	1.204	.723
1.9	1.4	1.207	.708
1.9	1.5	1.207	.695
1.9	1.6	1.205	.682
1.9	1.7	1.201	.671
1.9	1.8	1.197	.661
1.9	1.9	1.191	.652
1.9	2.0	1.185	.643
2.0	1.0	1.192	.756
2.0	1.1	1.210	.736
2.0	1.2	1.221	.717
2.0	1.3	1.229	.701
2.0	1.4	1.232	.687
2.0	1.5	1.233	.673
2.0	1.6	1.231	.661
2.0	1.7	1.229	.651
2.0	1.8	1.224	.641
2.0	1.9	1.219	.632
2.0	2.0	1.214	.624

Program 3

```
C
C
C      *******************************************************
C      THIS PROGRAM PRODUCES A CONTOUR MAP OF THE VISCOSITY
C      INCREMENT OVER THE AXIAL RANGE A/B, B/C 1.0 TO 3.0, IN
C      STEPS OF 0.5 OF THE FUNCTION FROM NU=2.5 TO NU=7.0
C      *******************************************************
C
       PROGRAM MAIN(INPUT,OUTPUT,TAPE2=INPUT,TAPE3=OUTPUT)
       COMMON/PARAM/A,C,NN
       EXTERNAL FUN
       DIMENSION ALPHA(10,21,21),NU(21,21),H(10)
       REAL NU
       NN=0
C      COMPUTE THE ELLIPTIC INTEGRALS
       DO45 K=1,10
       A=0.9
       NN=NN+1
       DO40 I=1,21
       A=A+0.1
       C=1.0/0.9
       DO30 N=1,21
       C=C/(1.0+0.1*C)
C      SET LIMITS FOR NUMERICAL INTEGRATION (THESE LIMITS
C      BELOW HAVE BEEN PREVIOUSLY TESTED FOR CONVERGENCE)
       AA=0.0
       BB=1000000
       IF(NN.EQ.10)BB=500000000
       MAXDIV=50
       EPS=1.0E-08
       ACC=0.0
       IFAIL=0
C      CALL U.K. "NAG" LIBRARY ROUTINE FOR NUMERICAL EVALUATION
C      OF THE INTEGRALS "ALPHA" GIVEN IN THE SUBROUTINE BELOW
       CALL D01AGF(AA,BB,FUN,MAXDIV,EPS,ACC,ANS,ERROR,NOFUN,IFAIL)
       ALPHA(NN,I,N)=ANS
   30  CONTINUE
   40  CONTINUE
   45  CONTINUE
       B=1.0
       A=0.9
       DO80 J=1,21
       A=A+0.1
       C=1.0/0.9
       DO70 N=1,21
       C=C/(1.0+0.1*C)
C      NOW COMPUTE THE FUNCTION VALUES USING THE STORED INTEGRAL VALUES
       NU(J,N)=(1.0/(A*B*C))*((4.0/15.0)*((ALPHA(7,J,N)+ALPHA(8,J,N)
     + +ALPHA(9,J,N))/(ALPHA(8,J,N)*ALPHA(9,J,N)+ALPHA(9,J,N)*ALPHA
     + (7,J,N)+ALPHA(7,J,N)*ALPHA(8,J,N)))+(1.0/5.0)*(((ALPHA(2,J,N)
     + +ALPHA(3,J,N))/(ALPHA(4,J,N)*(B*B*ALPHA(2,J,N)+C*C*ALPHA(3,J,N)
     + )))+((ALPHA(3,J,N)+ALPHA(1,J,N))/(ALPHA(5,J,N)*(C*C*ALPHA(3,J,N)
     + +A*A*ALPHA(1,J,N))))+((ALPHA(1,J,N)+ALPHA(2,J,N))/(ALPHA(6,J,N)
     + *(A*A*ALPHA(1,J,N)+B*B*ALPHA(2,J,N))))))
   70  CONTINUE
   80  CONTINUE
C
C      CALL CONTOUR PLOTTING ROUTINE
C
       CALL PAPER(1)
       H(1)=2.5
       H(2)=3.0
       H(3)=3.5
       H(4)=4.0
       H(5)=4.5
       H(6)=5.0
       H(7)=5.5
       H(8)=6.0
       H(9)=6.5
       H(10)=7.0
       CALL MAP(1.0,3.0,1.0,3.0)
       CALL SCALES
       CALL BORDER
       CALL CONTRL(NU,1,21,21,1,21,21,H,1,10)
       CALL GREND
       STOP
       END
```

```
C
C
C
      REAL FUNCTION FUN(X)
      COMMON/PARAM/A,C,NN
      B=1.0
      GOTO(10,20,30,40,50,60,70,80,90,100),NN
   10 FUN=1/((A*A+X)**1.5*(B*B+X)**0.5*(C*C+X)**0.5)
      RETURN
   20 FUN=1/((A*A+X)**0.5*(B*B+X)**1.5*(C*C+X)**0.5)
      RETURN
   30 FUN=1/((A*A+X)*-0.5*(B*B+X)**0.5*(C*C+X)**1.5)
      RETURN
   40 FUN=1/((A*A+X)**0.5*(B*B+X)**1.5*(C*C+X)**1.5)
      RETURN
   50 FUN=1/((A*A+X)**1.5*(B*B+X)**0.5*(C*C+X)**1.5)
      RETURN
   60 FUN=1/((A*A+X)**1.5*(B*B+X)**1.5*(C*C+X)**0.5)
      RETURN
   70 FUN=X/((A*A+X)**0.5*(B*B+X)**1.5*(C*C+X)**1.5)
      RETURN
   80 FUN=X/((A*A+X)**1.5*(B*B+X)**0.5*(C*C+X)**1.5)
      RETURN
   90 FUN=X/((A*A+X)**1.5*(B*B+X)**1.5*(C*C+X)**0.5)
      RETURN
  100 FUN=1.0/(((A*A+X)*(B*B+X)*(C*C+X))**0.5)
      RETURN
      END
```

```
C
C
C      ************************************************************
C      THIS PROGRAM GIVES PLOTS OF THE LINE SOLUTIONS OF THE
C      VARIOUS TRIAXIAL SHAPE FUNCTIONS ( AS TABULATED IN THE
C      PREVIOUS PROGRAM) FOR AXIAL RATIOS A/B = B/C = 1.5, IN
C      ORDER TO DETERMINE THE BEST COMBINATION FOR PRODUCING
C      A UNIQUE SOLUTION.
C      ************************************************************
C
       PROGRAM MAIN(INPUT,OUTPUT,TAPE2=INPUT,TAPE3=OUTPUT)
       COMMON/PARAM/A,C,NN
       EXTERNAL FUN
       DIMENSION ALPHA(10,21,21),NU(21,21),F(21,21),R(21,21),H(1)
     + ,BETA(21,21),CA(21,21),CB(21,21),CC(21,21),M(21,21),O(21,21)
     + ,P(21,21),TPLS(21,21),TMNS(21,21),RHOA(21,21),RHOB(21,21)
     + ,RHOC(21,21),TAU(21,21),PSI(21,21),DELA(21,21),DELB(21,21)
     + ,DELC(21,21),GAMMAA(21,21),GAMMAB(21,21),GAMMAC(21,21),MUA(21,21)
     + ,MUB(21,21),MUC(21,21),DPLS(21,21),DMNS(21,21),GPLS(21,21)
     + ,GMNS(21,21),V(21,21)
     + ,X1(21,21),X2(21,21),X3(21,21),X4(21,21),X5(21,21)
     + ,T1(21,21),T2(21,21),T3(21,21),T4(21,21),T5(21,21)
       REAL NU,M,O,P,MUA,MUB,MUC,PSI
C      COMPUTE THE ELLIPTIC INTEGRALS
       NN=0
       DO45 K=1,10
       A=0.95
       NN=NN+1
       DO40 I=1,21
       A=A+0.05
       C=1.0/0.95
       DO30 N=1,21
       C=C/(1.0+0.05*C)
C      SET LIMITS FOR NUMERICAL INTEGRATION (THESE LIMITS
C      BELOW HAVE BEEN PREVIOUSLY TESTED FOR CONVERGENCE)
       AA=0.0
       BB=1000000
       IF(NN.EQ.10)BB=500000000
       MAXDIV=50
       EPS=1.0E-08
       ACC=0.0
       IFAIL=0
C      CALL U.K. "NAG" LIBRARY ROUTINE FOR NUMERICAL EVALUATION
C      OF THE INTEGRALS "ALPHA" GIVEN IN THE SUBROUTINE BELOW
       CALL D01AGF(AA,BB,FUN,MAXDIV,EPS,ACC,ANS,ERROR,NOFUN,IFAIL)
       ALPHA(NN,I,N)=ANS
    30 CONTINUE
    40 CONTINUE
    45 CONTINUE
       B=1.0
       A=0.95
       DO80 J=1,21
       A=A+0.05
       C=1.0/0.95
       DO70 N=1,21
       C=C/(1.0+0.05*C)
C      NOW COMPUTE THE FUNCTION VALUES USING THE STORED INTEGRAL VALUES
       NU(J,N)=(1.0/(A*B*C))*((4.0/15.0)*((ALPHA(7,J,N)+ALPHA(8,J,N)
     + +ALPHA(9,J,N))/(ALPHA(8,J,N)*ALPHA(9,J,N)+ALPHA(9,J,N)*ALPHA
     + (7,J,N)+ALPHA(7,J,N)*ALPHA(8,J,N)))+(1.0/5.0)*(((ALPHA(2,J,N)
     + +ALPHA(3,J,N))/(ALPHA(4,J,N)*(B*B*ALPHA(2,J,N)+C*C*ALPHA(3,J,N)
     + )))+((ALPHA(3,J,N)+ALPHA(1,J,N))/(ALPHA(5,J,N)*(C*C*ALPHA(3,J,N)
     + +A*A*ALPHA(1,J,N))))+((ALPHA(1,J,N)+ALPHA(2,J,N))/(ALPHA(6,J,N)
     + *(A*A*ALPHA(1,J,N)+B*B*ALPHA(2,J,N))))))
       F(J,N)=2.0/((((A*B*C)**(1.0/3.0))*ALPHA(10,J,N))
       R(J,N)=2.0*(1.0+(F(J,N)**3.0))/NU(J,N)
       BETA(J,N)=(1.0/1000000.0)*(((6.0249**(1.0/3.0))*(10.0**(23.0/3.0
     + )))/((16200.0*3.141592654*3.141592654)**(1.0/3.0)))*(NU(J,N)
     + **(1.0/3.0))/F(J,N)
       M(J,N)=(B*B+C*C)/(B*B*ALPHA(2,J,N)+C*C*ALPHA(3,J,N))
       O(J,N)=(C*C+A*A)/(C*C*ALPHA(3,J,N)+A*A*ALPHA(1,J,N))
       P(J,N)=(A*A+B*B)/(A*A*ALPHA(1,J,N)+B*B*ALPHA(2,J,N))
       TPLS(J,N)=((A*B*C)/(12.0))*((((1.0/M(J,N))+(1.0/O(J,N))+(1.0/P(J,
     + N)))+((((1.0/M(J,N)**2.0)+(1.0/O(J,N)**2.0)+(1.0/P(J,N)**2.0))-
     + ((1.0/(M(J,N)*O(J,N)))+(1.0/(O(J,N)*P(J,N)))+(1.0/(P(J,N)*M(J,
     + N)))))**0.5))
       TMNS(J,N)=((A*B*C)/(12.0))*((((1.0/M(J,N))+(1.0/O(J,N))+(1.0/P(J,
     + N)))-((((1.0/M(J,N)**2.0)+(1.0/O(J,N)**2.0)+(1.0/P(J,N)**2.0))-
     + ((1.0/(M(J,N)*O(J,N)))+(1.0/(O(J,N)*P(J,N)))+(1.0/(P(J,N)*M(J,
     + N)))))**0.5))
       CA(J,N)=(2.0/(3.0*A*B*C))*M(J,N)
       CB(J,N)=(2.0/(3.0*A*B*C))*O(J,N)
```

```
      CC(J,N)=(2.0/(3.0*A*B*C))*P(J,N)
      RHOA(J,N)=2.0/(((1.0/CB(J,N))+(1.0/CC(J,N)))
      RHOB(J,N)=2.0/(((1.0/CA(J,N))+(1.0/CC(J,N)))
      RHOC(J,N)=2.0/(((1.0/CA(J,N))+(1.0/CB(J,N)))
      DELA(J,N)=NU(J,N)/CA(J,N)
      DELB(J,N)=NU(J,N)/CB(J,N)
      DELC(J,N)=NU(J,N)/CC(J,N)
      TAU(J,N)=3.0/((1.0/CA(J,N))+(1.0/CB(J,N))+(1.0/CC(J,N)))
      PSI(J,N)=F(J,N)*((1.0/TAU(J,N))**(1.0/3.0))
      V(J,N)=NU(J,N)/TAU(J,N)
      X1(J,N)=0.5*((1.0/RHOB(J,N))+(1.0/RHOC(J,N))-(1.0/RHOA(J,N)))
      X2(J,N)=0.5*((1.0/RHOC(J,N))+(1.0/RHOA(J,N))-(1.0/RHOB(J,N)))
      X3(J,N)=0.5*((1.0/RHOA(J,N))+(1.0/RHOB(J,N))-(1.0/RHOC(J,N)))
      X4(J,N)=(X1(J,N)+X2(J,N)+X3(J,N))/3.0
      X5(J,N)=((X1(J,N)**2.0)+(X2(J,N)**2.0)+(X3(J,N)**2.0)-(X1(J,N)*X2
     +(J,N))-(X2(J,N)*X3(J,N))-(X3(J,N)*X1(J,N)))**0.5
      T1(J,N)=1.0/(X4(J,N)+X1(J,N))
      T2(J,N)=1.0/(X4(J,N)+X2(J,N))
      T3(J,N)=1.0/(X4(J,N)+X3(J,N))
      T4(J,N)=3.0/((6.0*X4(J,N))-(2.0*X5(J,N)))
      T5(J,N)=3.0/((6.0*X4(J,N))+(2.0*X5(J,N)))
      GAMMAA(J,N)=(1.0/2.0)*(F(J,N)**3.0)*((1.0/CB(J,N))+(1.0/CC(J,N)))
      GAMMAB(J,N)=(1.0/2.0)*(F(J,N)**3.0)*((1.0/CA(J,N))+(1.0/CC(J,N)))
      GAMMAC(J,N)=(1.0/2.0)*(F(J,N)**3.0)*((1.0/CA(J,N))+(1.0/CB(J,N)))
      MUA(J,N)=(CA(J,N)**(1.0/3.0))/F(J,N)
      MUB(J,N)=(CB(J,N)**(1.0/3.0))/F(J,N)
      MUC(J,N)=(CC(J,N)**(1.0/3.0))/F(J,N)
      DPLS(J,N)=6.0*TPLS(J,N)*NU(J,N)
      DMNS(J,N)=6.0*TMNS(J,N)*NU(J,N)
      GPLS(J,N)=6.0*TPLS(J,N)*(F(J,N)**3.0)
      GMNS(J,N)=6.0*TMNS(J,N)*(F(J,N)**3.0)
   70 CONTINUE
   80 CONTINUE
      CALL PAPER(1)
      CALL MAP(1.0,2.0,1.0,2.0)
      CALL SCALSI(0.1,0.1)
      CALL GPSTOP(21)
      CALL BORDER
      CALL CSPACE(0.0,0.0001,0.0,0.0001)
C
C
C     (I)PLOT OF VISCOSITY INCREMENT AND PERRIN TRANSLATIONAL
C         FRICTIONAL FUNCTION
C
      H(1)=2.892
      CALL CONTRL(NU,1,21,21,1,21,21,H,1,1)
      CALL REDPEN
      H(1)=1.044
      CALL CONTRL(F,1,21,21,1,21,21,H,1,1)
C
C
C     (II)PLOT OF THE TRANSLATIONAL FUNCTIONS: THE VISCOSITY INCREMENT
C         THE PERRIN FUNCTION, THE BETA FUNCTION AND THE R FUNCTION, ALL
C         WITH +/-1% ASSUMED EXPERIMENTAL ERROR
C
      CALL FRAME
      CALL BLKPEN
      CALL BORDER
      CALL CSPACE(0.0,1.0,0.0,1.0)
      CALL SCALSI(0.1,0.1)
      CALL CSPACE(0.0,0.0001,0.0,0.0001)
      H(1)=2.92092
      CALL CONTRL(NU,1,21,21,1,21,21,H,1,1)
      H(1)=2.86308
      CALL CONTRL(NU,1,21,21,1,21,21,H,1,1)
      H(1)=2.14423
      CALL REDPEN
      CALL CONTRL(BETA,1,21,21,1,21,21,H,1,1)
      H(1)=2.10177
      CALL CONTRL(BETA,1,21,21,1,21,21,H,1,1)
      H(1)=1.05444
      CALL GRNPEN
      CALL CONTRL(F,1,21,21,1,21,21,H,1,1)
      H(1)=1.03356
      CALL CONTRL(F,1,21,21,1,21,21,H,1,1)
      H(1)=1.49379
      CALL BROKEN(4,8,8,8)
      CALL CONTRL(R,1,21,21,1,21,21,H,1,1)
      H(1)=1.46421
      CALL CONTRL(R,1,21,21,1,21,21,H,1,1)
C
C     (III)PLOT OF THE R FUNCTION AND ROTATIONAL RELAXATION
C          TIME RATIOS
```

```
C
          CALL FRAME
          CALL FULL
          CALL BLKPEN
          CALL BORDER
          CALL CSPACE(0.0,1.0,0.0,1.0)
          CALL SCALSI(0.1,0.1)
          CALL CSPACE(0.0,0.0001,0.0,0.0001)
          H(1)=1.479
          CALL CONTRL(R,1,21,21,1,21,21,H,1,1)
          H(1)=1.433
          CALL CONTRL(RHOA,1,21,21,1,21,21,H,1,1)
          H(1)=1.115
          CALL REDPEN
          CALL CONTRL(RHOB,1,21,21,1,21,21,H,1,1)
          H(1)=1.093
          CALL GRNPEN
          CALL CONTRL(RHOC,1,21,21,1,21,21,H,1,1)
C
C      (IV)PLOT OF THE R FUNCTION WITH +/- 1% ASSUMED ERROR AND THE
C          ROTATIONAL RELAXATION TIME RATIOS WITH +/-2% ASSUMED ERROR
C
C
C      (IV)PLOT OF THE R FUNCTION, HARMONIC MEAN RELAXATION TIME
C          RATIO (TH/T0) THE PSI & LAMBDA FUNCTIONS
C
          CALL FRAME
          CALL BLKPEN
          CALL BORDER
          CALL CSPACE(0.0,1.0,0.0,1.0)
          CALL SCALSI(0.1,0.1)
          CALL CSPACE(0.0,0.0001,0.0,0.0001)
          H(1)=1.479
          CALL CONTRL(R,1,21,21,1,21,21,H,1,1)
          H(1)=1.195
          CALL CONTRL(TAU,1,21,21,1,21,21,H,1,1)
          H(1)=.98378
          CALL REDPEN
          CALL CONTRL(PSI,1,21,21,1,21,21,H,1,1)
          H(1)=2.41886
          CALL GRNPEN
          CALL CONTRL(V,1,21,21,1,21,21,H,1,1)
C
C      (V)PLOT OF THE R FUNCTION (+/-1%) , THE HARMONIC MEAN
C          RELAXATION TIME RATIO (+/-1%) AND THE PSI FUNCTION
C          (+/- 2%) & THE LAMBDA FUNCTION (+/- 2%)
          CALL FRAME
          CALL BLKPEN
          CALL BORDER
          CALL CSPACE(0.0,1.0,0.0,1.0)
          CALL SCALSI(0.1,0.1)
          CALL CSPACE(0.0,0.0001,0.0,0.0001)
          H(1)=1.49379
          CALL CONTRL(R,1,21,21,1,21,21,H,1,1)
          H(1)=1.46421
          CALL CONTRL(R,1,21,21,1,21,21,H,1,1)
          H(1)=1.20695
          CALL CONTRL(TAU,1,21,21,1,21,21,H,1,1)
          H(1)=1.18305
          CALL CONTRL(TAU,1,21,21,1,21,21,H,1,1)
          H(1)=1.0034556
          CALL REDPEN
          CALL CONTRL(PSI,1,21,21,1,21,21,H,1,1)
          H(1)=0.9641044
          CALL CONTRL(PSI,1,21,21,1,21,21,H,1,1)
          CALL GRNPEN
          H(1)=2.4672372
          CALL CONTRL(V,1,21,21,1,21,21,H,1,1)
          H(1)=2.3704828
          CALL CONTRL(V,1,21,21,1,21,21,H,1,1)
C
C      (VI)PLOT OF R (+/-1%), DELTA1 (+/-1%), DELTA2 (+/-1%)
C      AND DELTA3 (+/-1%)
          CALL FRAME
          CALL BLKPEN
          CALL BORDER
          CALL CSPACE(0.0,1.0,0.0,1.0)
          CALL SCALSI(0.1,0.1)
          CALL CSPACE(0.0,0.0001,0.0,0.0001)
          H(1)=1.49379
```

```
        CALL CONTRL(R,1,21,21,1,21,21,H,1,1)
        H(1)=1.46421
        CALL CONTRL(R,1,21,21,1,21,21,H,1,1)
        H(1)=3.2849
        CALL CONTRL(DELA,1,21,21,1,21,21,H,1,1)
        H(1)=3.1560802
        CALL CONTRL(DELA,1,21,21,1,21,21,H,1,1)
        H(1)=2.110
        CALL REDPEN
        CALL CONTRL(DELB,1,21,21,1,21,21,H,1,1)
        H(1)=2.072
        CALL CONTRL(DELB,1,21,21,1,21,21,H,1,1)
        H(1)=2.006
        CALL GRNPEN
        CALL CONTRL(DELC,1,21,21,1,21,21,H,1,1)
        H(1)=1.928
        CALL CONTRL(DELC,1,21,21,1,21,21,H,1,1)
C
C       (VII)PLOT OF THE R, GAMMAA, GAMMAB AND GAMMAC FUNCTIONS
C
        CALL FRAME
        CALL BLKPEN
        CALL BORDER
        CALL CSPACE(0.0,1.0,0.0,1.0)
        CALL SCALSI(0.1,0.1)
        CALL CSPACE(0.0,0.0001,0.0,0.0001)
        H(1)=1.479
        CALL CONTRL(R,1,21,21,1,21,21,H,1,1)
        H(1)=0.795
        CALL CONTRL(GAMMAA,1,21,21,1,21,21,H,1,1)
        H(1)=1.022
        CALL REDPEN
        CALL CONTRL(GAMMAB,1,21,21,1,21,21,H,1,1)
        H(1)=1.042
        CALL GRNPEN
        CALL CONTRL(GAMMAC,1,21,21,1,21,21,H,1,1)
C
C       (VIII)PLOT OF R (+/-1%), GAMMAA (+/-1%), GAMMAB (+/-1%)
C       AND GAMMAC (+/-1%)
C
        CALL FRAME
        CALL BLKPEN
        CALL BORDER
        CALL CSPACE(0.0,1.0,0.0,1.0)
        CALL SCALSI(0.1,0.1)
        CALL CSPACE(0.0,0.0001,0.0,0.0001)
        H(1)=1.49379
        CALL CONTRL(R,1,21,21,1,21,21,H,1,1)
        H(1)=1.46421
        CALL CONTRL(R,1,21,21,1,21,21,H,1,1)
        H(1)=.81498
        CALL CONTRL(GAMMAA,1,21,21,1,21,21,H,1,1)
        H(1)=.78302
        CALL CONTRL(GAMMAA,1,21,21,1,21,21,H,1,1)
        H(1)=1.04244
        CALL REDPEN
        CALL CONTRL(GAMMAB,1,21,21,1,21,21,H,1,1)
        H(1)=1.00156
        CALL CONTRL(GAMMAB,1,21,21,1,21,21,H,1,1)
        CALL GRNPEN
        H(1)=1.06284
        CALL CONTRL(GAMMAC,1,21,21,1,21,21,H,1,1)
        H(1)=1.02116
        CALL CONTRL(GAMMAC,1,21,21,1,21,21,H,1,1)
C
C       (IX)PLOT OF THE R ,MUA, MUB AND MUC FUNCTIONS
C
        CALL FRAME
        CALL BLKPEN
        CALL BORDER
        CALL CSPACE(0.0,1.0,0.0,1.0)
        CALL SCALSI(0.1,0.1)
        CALL CSPACE(0.0,0.0001,0.0,0.0001)
        H(1)=1.479
        CALL CONTRL(R,1,21,21,1,21,21,H,1,1)
        H(1)=.924
        CALL CONTRL(MUA,1,21,21,1,21,21,H,1,1)
        CALL REDPEN
        H(1)=1.071
        CALL CONTRL(MUB,1,21,21,1,21,21,H,1,1)
```

```
        CALL GRNPEN
        H(1)=1.089
        CALL CONTRL(MUC,1,21,21,1,21,21,H,1,1)

C
C       (X)PLOT OF R (+/-1%), MUA (+/-1%), MUB (+/-1%)
C       AND MUC (+/-1%)
C
        CALL FRAME
        CALL BLKPEN
        CALL BORDER
        CALL CSPACE(0.0,1.0,0.0,1.0)
        CALL SCALSI(0.1,0.1)
        CALL CSPACE(0.0,0.0001,0.0,0.0001)
        H(1)=1.49379
        CALL CONTRL(R,1,21,21,1,21,21,H,1,1)
        H(1)=1.46421
        CALL CONTRL(R,1,21,21,1,21,21,H,1,1)
        H(1)=.94248
        CALL CONTRL(MUA,1,21,21,1,21,21,H,1,1)
        H(1)=.90552
        CALL CONTRL(MUA,1,21,21,1,21,21,H,1,1)
        H(1)=1.90242
        CALL REDPEN
        CALL CONTRL(MUB,1,21,21,1,21,21,H,1,1)
        H(1)=1.04958
        CALL CONTRL(MUB,1,21,21,1,21,21,H,1,1)
        H(1)=1.11078
        CALL GRNPEN
        CALL CONTRL(MUC,1,21,21,1,21,21,H,1,1)
        H(1)=1.06722
        CALL CONTRL(MUC,1,21,21,1,21,21,H,1,1)

C
C       (XI)PLOT OF THE R, REDUCED THETA+ AND REDUCED
C       THETA - FUNCTIONS
C
        CALL FRAME
        CALL BLKPEN
        CALL BORDER
        CALL CSPACE(0.0,1.0,0.0,1.0)
        CALL SCALSI(0.1,0.1)
        CALL CSPACE(0.0,0.0001,0.0,0.0001)
        H(1)=1.479
        CALL CONTRL(R,1,21,21,1,21,21,H,1,1)
        CALL REDPEN
        H(1)=.163
        CALL CONTRL(TPLS,1,21,21,1,21,21,H,1,1)
        CALL GRNPEN
        H(1)=.116
        CALL CONTRL(TMNS,1,21,21,1,21,21,H,1,1)

C
C       (XII)PLOT OF THE R(+/-1%), REDUCED THETA+ (+/-1%)
C       AND REDUCED THETA- (+/-1%) FUNCTIONS
        CALL FRAME
        CALL BLKPEN
        CALL BORDER
        CALL CSPACE(0.0,1.0,0.0,1.0)
        CALL SCALSI(0.1,0.1)
        CALL CSPACE(0.0,0.0001,0.0,0.0001)
        H(1)=1.49379
        CALL CONTRL(R,1,21,21,1,21,21,H,1,1)
        H(1)=1.46421
        CALL CONTRL(R,1,21,21,1,21,21,H,1,1)
        CALL REDPEN
        H(1)=.16463
        CALL CONTRL(TPLS,1,21,21,1,21,21,H,1,1)
        H(1)=.16137
        CALL CONTRL(TPLS,1,21,21,1,21,21,H,1,1)
        CALL GRNPEN
        H(1)=.11716
        CALL CONTRL(TMNS,1,21,21,1,21,21,H,1,1)
        H(1)=.11484
        CALL CONTRL(TMNS,1,21,21,1,21,21,H,1,1)

C
C       (XIII)PLOT OF THE R, DELTA+ AND DELTA- FUNCTIONS
C
```

```
      CALL FRAME
      CALL BLKPEN
      CALL BORDER
      CALL CSPACE(0.0,1.0,0.0,1.0)
      CALL SCALSI(0.1,0.1)
      CALL CSPACE(0.0,0.0001,0.0,0.0001)
      H(1)=1.479
      CALL CONTRL(R,1,21,21,1,21,21,H,1,1)
     CALL REDPEN
      H(1)=2.821
      CALL CONTRL(DPLS,1,21,21,1,21,21,H,1,1)
     CALL GRNPEN
      H(1)=2.016
     CALL CONTRL(DMNS,1,21,21,1,21,21,H,1,1)
C
C
C     (XIV)PLOT OF R (;/-1%), DELTA+ (+/-2%) AND DELTA- (+/-2%)
C
C
      CALL FRAME
      CALL BLKPEN
      CALL BORDER
      CALL CSPACE(0.0,1.0,0.0,1.0)
      CALL SCALSI(0.1,0.1)
      CALL CSPACE(0.0,0.0001,0.0,0.0001)
      H(1)=1.49379
      CALL CONTRL(R,1,21,21,1,21,21,H,1,1)
      H(1)=1.46421
      CALL CONTRL(R,1,21,21,1,21,21,H,1,1)
     CALL REDPEN
      H(1)=2.87742
      CALL CONTRL(DPLS,1,21,21,1,21,21,H,1,1)
      H(1)=2.76458
      CALL CONTRL(DPLS,1,21,21,1,21,21,H,1,1)
     CALL GRNPEN
      H(1)=2.05632
      CALL CONTRL(DMNS,1,21,21,1,21,21,H,1,1)
      H(1)=1.97568
      CALL CONTRL(DMNS,1,21,21,1,21,21,H,1,1)
C
C
C     (XV)PLOT OF THE R, GAMMA+ AND GAMMA- FUNCTIONS
C
C
      CALL FRAME
      CALL BLKPEN
      CALL BORDER
      CALL CSPACE(0.0,1.0,0.0,1.0)
      CALL SCALSI(0.1,0.1)
      CALL CSPACE(0.0,0.0001,0.0,0.0001)
      H(1)=1.479
      CALL CONTRL(R,1,21,21,1,21,21,H,1,1)
     CALL REDPEN
      H(1)=1.111
     CALL CONTRL(GPLS,1,21,21,1,21,21,H,1,1)
     CALL GRNPEN
     CALL CONTRL(GMNS,1,21,21,1,21,21,H,1,1)
C
C
C     (XVI)PLOT OF R(+/-1%), GAMMA+ (+/-2%) AND GAMMA- (+/-2%)
C
      CALL FRAME
      CALL BLKPEN
      CALL BORDER
      CALL CSPACE(0.0,1.0,0.0,1.0)
      CALL SCALSI(0.1,0.1)
      CALL CSPACE(0.0,0.0001,0.0,0.0001)
      H(1)=1.49379
      CALL CONTRL(R,1,21,21,1,21,21,H,1,1)
      H(1)=1.46421
      CALL CONTRL(R,1,21,21,1,21,21,H,1,1)
      CALL REDPEN
      H(1)=1.13322
      CALL CONTRL(GPLS,1,21,21,1,21,21,H,1,1)
      H(1)=1.08878
      CALL CONTRL(GPLS,1,21,21,1,21,21,H,1,1)
      CALL GRNPEN
      H(1)=.80988
      CALL CONTRL(GMNS,1,21,21,1,21,21,H,1,1)
      H(1)=.77812
```

```
      CALL CONTRL(GMNS,1,21,21,1,21,21,H,1,1)
C
C
C      (XVII)PLOT OF THE 5 FLUORESCENCE ANISOTROPY RELAXATION TIME
C      RATIOS
C
      CALL FRAME
      CALL BLKPEN
      CALL BORDER
      CALL CSPACE(0.0,1.0,0.0,1.0)
      CALL SCALSI(0.1,0.1)
      CALL CSPACE(0.0,0.0001,0.0,0.0001)
      H(1)=1.02536
      CALL CONTRL(T1,1,21,21,1,21,21,H,1,1)
      H(1)=1.28883
      CALL REDPEN
      CALL CONTRL(T2,1,21,21,1,21,21,H,1,1)
      CALL GRNPEN
      H(1)=1.31877
      CALL CONTRL(T3,1,21,21,1,21,21,H,1,1)
      CALL BROKEN(4,8,8,8)
      H(1)=1.43405
      CALL CONTRL(T4,1,21,21,1,21,21,H,1,1)
      CALL BLKPEN
      H(1)=1.02497
      CALL CONTRL(T5,1,21,21,1,21,21,H,1,1)
      STOP
      END




C
C
C
      REAL FUNCTION FUN(X)
      COMMON/PARAM/A,C,NN
      B=1.0
      GOTO(10,20,30,40,50,60,70,80,90,100),NN
   10 FUN=1/((A*A+X)**1.5*(B*B+X)**0.5*(C*C+X)**0.5)
      RETURN
   20 FUN=1/((A*A+X)**0.5*(B*B+X)**1.5*(C*C+X)**0.5)
      RETURN
   30 FUN=1/((A*A+X)**0.5*(B*B+X)**0.5*(C*C+X)**1.5)
      RETURN
   40 FUN=1/((A*A+X)**0.5*(B*B+X)**1.5*(C*C+X)**1.5)
      RETURN
   50 FUN=1/((A*A+X)**1.5*(B*B+X)**0.5*(C*C+X)**1.5)
      RETURN
   60 FUN=1/((A*A+X)**1.5*(B*B+X)**1.5*(C*C+X)**0.5)
      RETURN
   70 FUN=X/((A*A+X)**0.5*(B*B+X)**1.5*(C*C+X)**1.5)
      RETURN
   80 FUN=X/((A*A+X)**1.5*(B*B+X)**0.5*(C*C+X)**1.5)
      RETURN
   90 FUN=X/((A*A+X)**1.5*(B*B+X)**1.5*(C*C+X)**0.5)
      RETURN
  100 FUN=1.0/(((A*A+X)*(B*B+X)*(C*C+X))**0.5)
      RETURN
      END
```

Program 5

```
C
C  NON-LINEAR LEAST SQUARES METHOD USING AN ALGORITHM OF GILL AND
C  MURRAY (1976)
C
C  GAMMA = BIREFRINGENCE (RADS), F = SUM OF SQUARES OF THE RESIDUALS
C  DPLS = DELTA+, DMNS = DELTA-
C  X(1) = CURRENT INITIAL GUESS FOR THETA+
C  X(2) =       "        "        "     "    -
C  X(3) =       "        "        "     "  A'+
C  X(4) =       "        "        "     "  A'-
C  X1 = CURRENT ESTIMATE FOR THETA+
C  X2 =       "        "        "     -
C  X3 =       "        "        "  A'+
C  X4 =       "        "        "  A'-
C
C  *******************************
C  LINEAR TIME INCREASE, 100PTS.
C  .001 DEGREES S.E.
C
C  RANDOM NUMBER RUN 50
C
C     *************************************************
C        PROTEIN 3
C
C     *************************************************
       PROGRAM MAIN(INPUT,OUTPUT,TAPE2=INPUT,TAPE3=OUTPUT)
       COMMON/PARAM/GAMMA(101),T(101),R(101)
       REAL BL(4),BU(4),X(4),F,W(54)
       REAL Q1,Q2,Q3,Q4,Q5
       INTEGER IBOUND,IFAIL,J,LIW,LW,N
       INTEGER IW(6)
       P=-1.0
       DO21 I=1,101
       P=P+1.0
       R(I)=P
       T(I)=R(I)*1.0E-09
    21 CONTINUE
       WRITE(3,32)
    32 FORMAT("    TIME(NS)    GAMMA")
C  G05BBF REINITIALIZES THE STREAM OF THE RANDOM NUMBERS
       CALL G05BBF
C  CALCULATE THE UNPERTURBED DECAY CURVE
       DO50 I=1,101
       GAMMA(I)=0.07*EXP(-T(I)*6.0*5.187243E06)+
      +0.05*EXP(-T(I)*6.0*4.167486E06)
C  NOW PERTURB EACH OF THE 160 DATA POINTS USING A NORMAL PSEUDO-RANDOM
C  NUMBER GENERATOR G05ADF
       GAMMA(I)=GAMMA(I)+((0.1*1.74555E-04)*G05ADF(Y))
       WRITE(3,33)R(I),GAMMA(I)
    33 FORMAT( F10.5,F8.5)
    50 CONTINUE
       N=4
       IBOUND=0
       Q1=1.0
C  DO THE MINIMIZATION FOR 30 INITIAL GUESSES TO ATTEMPT TO AVOID
C  SUBSIDIARY MINIMA
       DO10 I=1,30
C  CALL RECTANGULAR PSEUDO RANDOM NUMBER ROUTINE G05AAF
       Z=G05AAF(X)
       X(1)=4.0+2.0*Z
       X(2)=3.0+2.0*Z
       X(3)=6.0+2.0*Z
       X(4)=4.0+2.0*Z
       BL(1)=4.0
       BL(2)=3.0
       BL(3)=6.0
       BL(4)=4.0
       BU(1)=6.0
       BU(2)=5.0
       BU(3)=8.0
       BU(4)=6.0
       LIW=6
       LW=54
       IFAIL=1
       CALL E04JAF(N,IBOUND,BL,BU,X,F,IW,LIW,W,LW,IFAIL)
       IF(IFAIL.NE.0)WRITE(3,100)IFAIL
       IF(IFAIL.EQ.1)GOTO 20
   100 FORMAT("ERROR EXIT TYPE",I3,"SEE ROUTINE MANUAL")
       WRITE(3,110)F
       WRITE(3,120)(X(J),J=1,4)
   110 FORMAT( " FUNCTION VALUE ON EXIT IS",F15.12)
```

```
120 FORMAT( " THETA+",F10.7," THETA-",F10.7,"A ",F7.4,
    + " A- ",F7.4)
     IF(Q1.LE.F)GOTO 30
     Q1=F
     Q2=X(1)
     Q3=X(2)
     Q4=X(3)
     Q5=X(4)
 30 CONTINUE
    WRITE(3,130)
130 FORMAT( " ")
    WRITE(3,140)
140 FORMAT( " ")
 10 CONTINUE
    DPLS=0.50996303*Q2
    DMNS=0.50996303*Q3
    WRITE(3,141)
141 FORMAT( " ")
    WRITE(3,142)
142 FORMAT( " ")
    WRITE(3,143)
143 FORMAT( " ")
    WRITE(3,145)
145 FORMAT( " ")
    WRITE(3,150)Q1
150 FORMAT( " BEST LEAST SQUARES VALUE = ",F15.12)
    WRITE(3,160)Q2
160 FORMAT( "       THETA+ = ",F10.7)
    WRITE(3,170)Q3
170 FORMAT( "       THETA- = ",F10.7)
    WRITE(3,180)Q4
180 FORMAT( "          A'+ = ",F7.4)
    WRITE(3,190)Q5
190 FORMAT( "          A'- = ",F7.4)
    WRITE(3,200)DPLS
200 FORMAT( "       DELTA+ = ",F10.7)
    WRITE(3,210)DMNS
210 FORMAT( "       DELTA- = ",F10.7)
 20 STOP
    END




C SUBROUTINE FOR CALCULATING THE SUM OF SQUARES OF THE RESIDUALS FOR THE
C CURRENT ESTIMATES OF THE ADJUSTABLE PARAMETERS
    SUBROUTINE FUNCT1(N,XC,FC)
    COMMON/PARAM/GAMMA(101),T(101),R(101)
    EXTERNAL FUN
    REAL Q,FC
    INTEGER N
    REAL XC(N)
    REAL X1,X2,X3,X4
    X1=XC(1)
    X2=XC(2)
    X3=XC(3)
    X4=XC(4)
    FC=0.0
    DO75 I=1,101
    Q=(GAMMA(I)-(0.01*X3*EXP(-6.0E06*X1*T(I))+0.01*X4
   + *EXP(-6.0E06*X2*T(I))))**2.0
    FC=FC+Q
 75 CONTINUE
    RETURN
    END
```

Program 6

```
C
C
C FOURIER TRANSFORM SOLUTION OF THE LAPLACE INTEGRAL EQUATION METHOD OF
C GARDNER, GARDNER, LAUSH AND MEINKE (1959)
C
C S = BIREFRINGENCE (RADS), GM = INTEGRAND OF EQUATION    , G = G(EXP(-Y))
C T = TIME (SEC), R = TIME (NS), EC AND ES ARE THE ERROR ESTIMATES IN FC
C AND FS RESPECTIVELY DUE TO THE NUMERICAL INTEGRATION IN EQN. 125
C AND ER IS THE ERROR ESTIMATE DUE TO THE NUMERICAL INTEGRATION IN
C EQN. 128
C
C *******************************************
C LOGARITHMIC TIME INCREASE, 140 DATA PTS.
C .001 DEGREES S.E.
C
C RANDOM NUMBER RUN 2
C
C     ****************************
C      PROTEIN 2
C
C     ****************************
      PROGRAM MAIN(INPUT,OUTPUT,TAPE2=INPUT,TAPE3=OUTPUT)
      EXTERNAL FUNXN
      REAL MMU(66),KC(66),KS(66),FC(66),FS(66),GM(66),MU
      REAL YYY,G(690),Y(690),EC(66),ES(66)
      INTEGER N,I,IFAIL
      INTEGER L
      REAL X(141),S(141),R(141),T(141),YC(141),YS(141)
      COMPLEX Z,C,K,CGAMMA
      P=-7.1
      DO21 I=1,141
      P=P+.1
      WRITE(3,500)
  500 FORMAT( " ")
      X(I)=P
      T(I)=(1.0E-09)*EXP(X(I))
      R(I)=T(I)*1.0E09
   21 CONTINUE
      WRITE(3,32)
   32 FORMAT( "   TIME(NS)     X       S(T) = S(EXP(-X))")
      WRITE(3,501)
  501 FORMAT( " ")
      WRITE(3,502)
  502 FORMAT( "*****************************************")
      WRITE(3,503)
  503 FORMAT( " ")
C G05BBF REINITIALIZES THE STREAM OF THE RANDOM NUMBERS
      CALL G05BBF
      DO50 I=1,141
C CALCULATE THE UNPERTURBED DECAY CURVE
      S(I)=0.07*EXP(-T(I)*4.6596278E07)+
     +0.05*EXP(-T(I)*3.137407E07)
C NOW PERTURB EACH OF THE 140 DATA PTS USING A NORMAL PSEUDO-RANDOM
C NUMBER GENERATOR
      S(I)=S(I)+((0.1*1.74555E-04)*G05ADF(Y))
      WRITE(3,33)R(I),X(I),S(I)
   33 FORMAT( F10.5,F6.2,F8.5)
   50 CONTINUE
      DO47 L=1,20
      WRITE(3,504)
  504 FORMAT( " ")
   47 CONTINUE
C THE NEXT PART OF THE PROGRAM EVALUATES THE FOURIER TRANSFORM OF THE DATA
      MU=-.1
      WRITE(3,99)
   99 FORMAT( "          MU          KC              KS")
      WRITE(3,505)
  505 FORMAT( " ")
      WRITE(3,506)
  506 FORMAT( " ***********************************************************")
      WRITE(3,507)
  507 FORMAT( " ")
      DO010 J=1,66
      MU=MU+.1
      MMU(J)=MU
      DO51 I=1,141
      YC(I)=(EXP(X(I)))*S(I)*COS(MU*X(I))
      YS(I)=(EXP(X(I)))*S(I)*SIN(MU*X(I))
      Y(I)=CMPLX(YC(I),YS(I))
   51 CONTINUE
      N=141
      IFAIL=1
```

```
C CALL NUMERICAL INTEGRATION ROUTINE FROM THE UK NAG LIBRARY (MK 6)
      CALL D01GAF(X,YC,N,ANS,ER,IFAIL)
      FC(J)=((1.0/(2.0*3.141593))**0.5)*ANS
      EC(J)=((1.0/(2.0*3.141593))**0.5)*ER
      CALL D01GAF(X,YS,N,ANS,ER,IFAIL)
      FS(J)=((1.0/(2.0*3.141593))**0.5)*ANS
      ES(J)=((1.0/(2.0*3.141593))**0.5)*ER
C EVALUATE THE COMPLEX GAMMA FUNCTION FOR THE CURRENT VALUE OF MU USING
C THE SUBROUTINE BELOW
      Z=CMPLX(1.0,MU)
      C=CGAMMA(Z)
C DETERMINE THE EULER INTEGRAL OF THE COMPLEX GAMMA FUNCTION (EQN. 123 )
      K=((1.0/(2.0*3.141593))**0.5)*C
      KC(J)=REAL(K)
      KS(J)=AIMAG(K)
      C=CGAMMA(Z)
      WRITE(3,101)MU,K
  101 FORMAT( 7X,1F8.2,2E15.7)
   10 CONTINUE
      DO49 L=1,20
      WRITE(3,509)
  509 FORMAT( " ")
   49 CONTINUE
      WRITE(3,90)
   90 FORMAT( "        MU        FC          (ERR)          FS
     +     (ERR)")
      WRITE(3,510)
  510 FORMAT( " ")
      WRITE(3,511)
  511 FORMAT( "******************************************************
     +*********")
      WRITE(3,512)
  512 FORMAT( " ")
      DO38 J=1,66
      WRITE(3,91)MMU(J),FC(J),EC(J),FS(J),ES(J)
   91 FORMAT( 1X,1F8.2,4E14.7)
   38 CONTINUE
      DO52 L=1,20
      WRITE(3,513)
  513 FORMAT( " ")
   52 CONTINUE
      WRITE(3,93)
   93 FORMAT( "          Y          G(EXP(-Y))          ERROR")
      WRITE(3,514)
  514 FORMAT( " ")
      WRITE(3,515)
  515 FORMAT( " *******************************************************")
      WRITE(3,516)
  516 FORMAT( " ")
      YYY=-.01
      DO31 M=1,690
      YYY=YYY+.01
      Y(M)=YYY
      DO29 J=1,66
C DIVIDE THE FOURIER TRANSFORM OF THE DATA BY THE EULER INTEGRAL FOR THE
C COMPLEX GAMMA FUNCTION
      GM(J)=(((((FC(J)*KC(J))+(FS(J)*KS(J)))*COS(YYY*MMU(J)))/((KC(J)
     +*KC(J))
     ++(KS(J)*KS(J)))+(((((FS(J)*KC(J))-(FC(J)*KS(J)))*SIN(YYY*MMU(J)))/
     +((KC(J)*KC(J))+(KS(J)*KS(J)))))
   29 CONTINUE
      NN=66
C NOW G(EXP(-Y)) AS A FUNCTION OF Y IS FOUND FROM THE INVERSE FOURIER
C TRANSFORM USING THE SAME NUMERICAL INTEGRATION ROUTINE
      CALL D01GAF(MMU,GM,NN,ANS,ER,IFAIL)
      G(M)=(1.0/3.141593)*ANS
      ER=(1.0/3.141593)*ER
      WRITE(3,290)YYY,G(M),ER
      IF(IFAIL)241,261,241
  241 WRITE(3,289)
  261 CONTINUE
  290 FORMAT(/3X,F7.2,4X,1E15.7,4X,1E15.7)
  289 FORMAT(/28H LESS THAN 4 POINTS SUPPLIED)
   31 CONTINUE
C HENCE A PLOT OF G(EXP(-Y)) AGAINST Y IS OBTAINED
      CALL PAPER(1)
      CALL MAP(0.0,0.0,0.0,0.0)
      CALL CURVEO(Y,G,1,690)
      CALL SCALES
      CALL BORDER
      CALL GRAPHF(FUNXN)
```

```
      CALL GREND
      STOP
      END




C

      FUNCTION FUNXN(X)
      FUNXN=0.0
      RETURN
      END
```

```
C
C SUBROUTINE FOR CALCULATING THE COMPLEX GAMMA FUNCTION C = CGAMMA(Z) FOR
C THE CURRENT VALUE OF MU. THIS SUBROUTINE IS THAT GIVEN BY LUCAS AND
C TERRILL (1970)
      COMPLEX FUNCTION CGAMMA(Z)
      COMPLEX Z,ZM,T,TT,SUM,TERM,DEN,PI,A
      DIMENSION C(12)
      LOGICAL REFLEX
C SET IOUT FOR PROPER OUTPUT CHANNEL OF COMPUTER SYSTEM FOR
C ERROR MESSAGES
      IOUT=3
      PI=(3.141593,0.0)
      X=REAL(Z)
      Y=AIMAG(Z)
C TOL = LIMIT OF PRECISION OF COMPUTER SYSTEM IN SINGLE PRECISION
      TOL=1.0E-07
      REFLEX=.TRUE.
C DETERMINE WHETHER Z IS TOO CLOSE TO A POLE
C CHECK WHETHER TOO CLOSE TO ORIGIN
      IF(X.GE.TOL) GO TO 20
C FIND THE NEAREST POLE AND COMPUTE DISTANCE TO IT
      XDIST=X-INT(X-.5)
      ZM=CMPLX(XDIST,Y)
      IF(CABS(ZM).GE.TOL)GOTO 10
C IF Z IS TOO CLOSE TO A POLE, PRINT ERROR MESSAGE AND RETURN
C WITH CGAMMA=(1.E7,0.F0)
      WRITE (IOUT,900)Z
      CGAMMA=(1.E7,0.E0)
      RETURN
C FOR REAL(Z) NEGATIVE EMPLOY THE REFLECTION FORMULA
C      GAMMA(Z)=PI(SINPI*Z)*GAMMA(1-Z))
C AND COMPUTE GAMMA(1-Z). NOTE REFLEX IS A TAG TO INDICATE THAT
C THIS RELATION MUST BE USED LATER.
   10 IF(X.GE.0.0)GOTO 20
      REFLEX=.FALSE.
      Z=(1.0,0.0)-Z
      X=1.0-X
      Y=-Y
C IF Z IS NOT TOO CLOSE TO A POLE, MAKE REAL(Z)>10 AND ARG(Z)<PI/4
   20 M=0
   40 IF(X.GE.10.)GOTO 50
      X=X+1.0
      M=M+1
      GOTO 40
   50 IF(ABS(Y).LT.X)GOTO 60
      X=X+1.0
      M=M+1
      GOTO 50
   60 T=CMPLX(X,Y)
      TT=T*T
      DEN=T
```

```
C COEFFICIENTS IN STIRLING'S APPROXIMATION FOR LN(GAMMA(T))
      C(1)=1./12.
      C(2)=-1./360.
      C(3)=1./1260.
      C(4)=-1./1680.
      C(5)=1./1188.
      C(6)=-691./36060.
      C(7)=1./156.
      C(8)=-3617./122400.
      C(9)=43867./244188.
      C(10)=-174611./125400.
      C(11)=77683./5796.
      SUM=(T-(.5,0.0))*CLOG(T)-T*CMPLX(.5*ALOG(2.*3.14159),0.0)
      J=1
   70 TERM=C(J)/DEN
C TEST REAL AND IMAGINARY PARTS OF LN(GAMMA(Z))SEPARATELY FOR
C CONVERGENCE. IF Z IS REAL SKIP IMAGINARY PART OF CHECK.
      IF(ABS(REAL(TERM)/REAL(SUM)).GE.TOL)GOTO 80
      IF(Y.EQ.0.0)GOTO 100
      IF(ABS(AIMAG(TERM)/AIMAG(SUM)).LT.TOL)GOTO 100
   80 SUM=SUM+TERM
      J=J+1
      DEN=DEN*TT
C TEST FOR CONVERGENCE
      IF(J.EQ.12)GOTO 90
      GOTO 70
C STIRLINGS SERIES DID NOT CONVERGE. PRINT ERROR MESSAGE AND
C PROCEDE
   90 WRITE(IOUT,910)Z
C RECURSION RELATION USED TO OBTAIN LN(GAMMA(Z))
C         LN(GAMMA(Z))=LN(GAMMA(Z+M)/(Z*(Z+1)*...*(Z+M-1)))
C                     =LN(GAMMA(Z+M)-LN(Z)-LN(Z+1)-...-LN(Z+M-1)
  100 IF(M.EQ.0)GOTO 120
      DO110 I=1,M
      A=CMPLX(I*1.-1.,0.0)
  110 SUM=SUM-CLOG(Z+A)
C CHECK TO SEE IF REFLECTION FORMULA SHOULD BE USED
  120 IF(REFLEX)GOTO 130
      SUM=CLOG(PI/CSIN(PI*Z))-SUM
      Z=(1.0,0.0)-Z
  130 CGAMMA=CEXP(SUM)
      RETURN
  900 FORMAT(1X,2F14.7,10X,49HARGUMENT OF GAMMA FUNCTION IS TOO CLOSE TO
     + A POLE)
  910 FORMAT(44H ERROR - STIRLING'S SERIES HAS NOT CONVERGED/14X,4H7    ,
     +2E14.7)
      END
```

Program 7

```
C
C R-CONSTRAINED NON-LINEAR LEAST SQUARES METHOD (HARDING)
C
C GAMMA = BIREFRINGENCE (RADS), FC = SUM OF SQUARES OF THE RESIDUALS
C X(1) = CURRENT INITIAL GUESS FOR A/B
C X(2) =      "      "     "    "    "    A+
C X(3) =      "      "     "    "    "    A-
C ON EXIT, X(1), X(2), X(3) CONTAIN THE BEST ESTIMATES FOR THESE PARAMETERS
C XC(1) = A = CURRENT ESTIMATE FOR A/B
C D = 1/C = VALUE OF B/C                   CORRESPONDING TO THIS ESTIMATE
C     S   =   "     "   VISCOSITY INCREMENT     "      "     "   "   "
C     V   =   "     "        DELTA+             "      "     "   "   "
C     W   =   "     "        DELTA-             "      "     "   "   "
C  THPLUS =   "     "        THETA+             "      "     "   "   "
C  THMNUS =   "     "        THETA-             "      "     "   "   "
C XC(2) = CURRENT ESTIMATE FOR A+
C XC(3) =      "      "     "    A-
C AA1,AA2,....AA6 ARE THE A/B COORDINATES FOR 6 PTS ON THE R-CURVE
C AD1,AD2,....AD6   "    "   B/C      "      "    "   "   "   "    "
C THE VALUE FOR B/C CORRESPONDING TO THE CURRENT ESTIMATE FOR A/B CAN THEN
C BE FOUND USING A CUBIC POLYNOMIAL INTERPOLATION PROCEDURE BETWEEN THE
C SIX GIVEN POINTS.THIS IS DONE USING A LIBRARY ROUTINE E01LF1
C
C ************
C  PROTEIN 1
C ************
C LINEAR TIME INCREASE, 100PTS.
C CUT OFF TIME: 100NS
C STREAM OF RANDOM NUMBERS: 3
C 0.1 DEG STANDARD ERROR ON EACH DATA PT.
C
      PROGRAM MAIN(INPUT,OUTPUT,TAPE2=INPUT,TAPE3=OUTPUT)
      COMMON/PARAM/GAMMA(101),T(101),A,C,D,NN,AA(6),AD(6)
      REAL R(101)
      REAL AA1,AA2,AA3,AA4,AA5,AA6,AD1,AD2,AD3,AD4,AD5,AD6
      REAL BL(3),BU(3),X(3),F,W(39)
      INTEGER IBOUND,IFAIL,J,LIW,LW,N
      INTEGER IW(5)
      REAL Q1,Q2,Q3,Q4
      WRITE(3,37)
   37 FORMAT(" PROTEIN 1,   0.1 DEG. STANDARD ERROR")
      WRITE(3,38)
   38 FORMAT("
     + 100NS, 100PTS")
      WRITE(3,39)
   39 FORMAT("
     +STREAM 3")
      P=-1.1
      DO21 I=1,101
      P=P+1.1
      R(I)=P
      T(I)=R(I)*1.0E-09
      R(I)=T(I)*1.0E09
   21 CONTINUE
C G05BAF(0.X) SPECIFIES THE XTH STREAM OF THE RANDOM NUMBERS
      CALL G05BAF(0.3)
      DO50 I=1,101
C CALCULATE THE UNPERTURBED DECAY CURVE
      GAMMA(I)=0.07*EXP(-T(I)*6.0*5.815383E06)+
     +0.05*EXP(-T(I)*6.0*4.1564612E06)
C NOW PERTURB EACH OF THE 100 DATA POINTS USING A NORMAL PSEUDO RANDOM
C NUMBER GENERATOR G05ADF
      GAMMA(I)=GAMMA(I)+((1.74555E-03)*G05ADF(Y))
   50 CONTINUE
C READ IN THE VALUES FOR THE LOWER LIMITS FOR THE INITIAL GUESSES OF THE
C A/B, A+, A- (X100), THE LOWER AND UPPER LIMITS FOR THE COMPUTER ESTIMATES
C THE COORDINATES OF THE A/B VALUES AND THEN THE COORDINATES OF THE B/C
C FOR THE R-CURVE TO WHICH THESE ESTIMATES ARE CONSTRAINED
      READ(2,*)XX1,XX2,XX3,BBL1,BBL2,BBL3,BBU1,BBU2,BBU3,
     +AA1,AA2,AA3,AA4,AA5,AA6,AD1,AD2,AD3,AD4,AD5,AD6
        AA(1)=AA1
        AA(2)=AA2
        AA(3)=AA3
        AA(4)=AA4
        AA(5)=AA5
        AA(6)=AA6
        AD(1)=AD1
        AD(2)=AD2
        AD(3)=AD3
        AD(4)=AD4
        AD(5)=AD5
```

```
      AD(6)=AD6
      N=3
      IBOUND=0
      Q1=1.0
      DO10 I=1,3
      Z=G05AAF(X)
      X(1)=XX1+0.2*Z
      X(2)=XX2+2.0*Z
      X(3)=XX3+2.0*Z
      BL(1)=BBL1
      BL(2)=BBL2
      BL(3)=BBL3
      BU(1)=BBU1
      BU(2)=BBU2
      BU(3)=BBU3
      LIW=5
      LW=39
      IFAIL=1
      CALL E04JAF(N,IBOUND,BL,BU,X,F,IW,LIW,W,LW,IFAIL)
      IF(IFAIL.NE.0)WRITE(3,100)IFAIL
      IF(IFAIL.EQ.1)GOTO 20
100   FORMAT("ERROR EXIT TYPE",I3,"SEE ROUTINE MANUAL")
      X(2)=X(2)*.01
      X(3)=X(3)*.01
      WRITE(3,110)F
      WRITE(3,120)(X(1),X(2),X(3))
110   FORMAT( " FUNCTION VALUE ON EXIT IS",F15.12)
120   FORMAT( " A/B= ",F8.5," A+=",F15.12,
     +" A-=",F15.12)
      IF(Q1.LE.F)GOTO 30
      Q1=F
      Q2=X(1)
      Q3=X(2)
      Q4=X(3)
30    CONTINUE
      WRITE(3,130)
130   FORMAT( " ")
      WRITE(3,140)
140   FORMAT( " ")
10    CONTINUE
      WRITE(3,150)Q1
150   FORMAT( " BEST LEAST SQUARES VALUE = ",F15.12)
      WRITE(3,160)Q2
160   FORMAT( "                          A / B = ",F8.5)
      WRITE(3,170)Q3
170   FORMAT( "                          B / C = ",F8.5)
      WRITE(3,180)Q3
180   FORMAT( "                          A+ = ",F7.4)
      WRITE(3,190)Q4
190   FORMAT( "                          A- = ",F7.4)
20    STOP
      END
```

```
C
C
C
C     SUBROUTINE FOR CALCULATING THE SUM OF THE SQUARES OF THE RESIDUALS FOR
C     CURRENT ESTIMATES OF A/B, A+ AND A-
C     KB = BOLTZMANNS CONSTANT, NA = AVOGADROS NUMBER
C
      SUBROUTINE FUNCT1(N,XC,FC)
      COMMON/PARAM/GAMMA(101),T(101),A,C,D,NN,AA(6),AD(6)
      EXTERNAL FUN
      REAL Q,FC
      INTEGER N
      DIMENSION ALPHA(9)
      REAL XC(N)
      REAL X2,X3
      REAL THPLUS,THMNUS,TEMP,ETA,M,O,P,KB,NA,MW
      NN=0
      A=XC(1)
      NM=6
      IEXIT=0
C CALL LIBRARY ROUTINE FOR THE CUBIC POLYNOMIAL FIT TO THE R-CURVE POINTS
C A LISTING OF THIS IS GIVEN BELOW
      CALL E01LF1(NM,AA,AD,A,D,IEXIT)
      C=1.0/D
      B=1.0
      DO45 K=1,9
      AZ=0.0
      BZ=1000000
      NN=NN+1
      MAXDIV=50
      EPS=1.0E-08
      ACC=0.0
      IFAIL=0
      CALL D01AGF(AZ,BZ,FUN,MAXDIV,EPS,ACC,ANS,ERROR,NOFUN,IFAIL)
      ALPHA(NN)=ANS
   45 CONTINUE
      S=(1.0/(A*B*C))*((4.0/15.0)*((ALPHA(7)+ALPHA(8)
     + +ALPHA(9))/(ALPHA(8)*ALPHA(9)+ALPHA(9)*ALPHA
     + (7)+ALPHA(7)*ALPHA(8)))+(1.0/5.0)*(((ALPHA(2)
     + +ALPHA(3))/(ALPHA(4)*(B*B*ALPHA(2)+C*C*ALPHA(3)
     + )))+((ALPHA(3)+ALPHA(1))/(ALPHA(5)*(C*C*ALPHA(3)
     + +A*A*ALPHA(1))))+((ALPHA(1)+ALPHA(2))/(ALPHA(6)
     + *(A*A*ALPHA(1)+B*B*ALPHA(2))))))
      M=(B*B+C*C)/(B*B*ALPHA(2)+C*C*ALPHA(3))
      O=(C*C+A*A)/(C*C*ALPHA(3)+A*A*ALPHA(1))
      P=(A*A+B*B)/(A*A*ALPHA(1)+B*B*ALPHA(2))
      Z=((A*B*C)/(12.0))*(((((1.0/M)+(1.0/O)+(1.0/P
     + ))-(((1.0/M**2.0)+(1.0/O**2.0)+(1.0/P**2.0))-
     + ((1.0/(M*O))+(1.0/(O*P))+(1.0/(P*M
     + )))))**0.5))
      U=((A*B*C)/(12.0))*(((((1.0/M)+(1.0/O)+(1.0/P
     + ))+(((1.0/M**2.0)+(1.0/O**2.0)+(1.0/P**2.0))-
     + ((1.0/(M*O))+(1.0/(O*P))+(1.0/(P*M
     + )))))**0.5))
      V=6.0*U*S
      W=6.0*Z*S
C     ENTER INTRINSIC VISCOSITY
      ETA=2.746
C     ENTER TEMPERATURE
      TEMP=293.0
C     ENTER MOLECULAR WEIGHT
      MW=71744.0
      KB=1.38046E-16
      NA=6.0248E23
      THPLUS=(NA*KB*100.0/6.0)*(TEMP/(ETA*MW))*V
      THMNUS=(NA*KB*100.0/6.0)*(TEMP/(ETA*MW))*W
      X2=XC(2)
      X3=XC(3)
      FC=0.0
      DO75 I=1,101
      Q=(GAMMA(I)-(0.01*X2*EXP(-6.0*THPLUS*T(I))+0.01*X3*EXP
     + (-6.0*THMNUS*T(I))))**2.0
      FC=FC+Q
   75 CONTINUE
      RETURN
      END
```

```
C LEICESTER UNIVERSITY COMPUTER LIBRARY SUBROUTINE FOR A CUBIC
C POLYNOMIAL FIT TO A SET OF POINTS (K. BRODLIE)
C
      SUBROUTINE E01LF1(N,AX,AY,X,Y,IEXIT)
      DIMENSION AX(N),AY(N)
C   CHECK DATA POINTS ARE MONOTONICALLY INCREASING
      IEXIT=1
      DO 5 I=2,N
      IF(AX(I).LE.AX(I-1))RETURN
    5 CONTINUE
C   CHECK THAT X IS A VALID POINT
      IEXIT=2
      IF((AX(1)-X)*(AX(N)-X).GT.0)RETURN
C   LOCATE INTERVAL IN WHICH X LIES -
C         AX(J-1).LT.X.LE.AX(J)
      IEXIT=0
      Y=AY(1)
      IF(X.EQ.AX(1))RETURN
      DO 10 I=2,N
      J=I
      IF(X.LE.AX(I))GOTO 20
   10 CONTINUE
   20 CONTINUE
      Y=AY(J)
      IF(X.EQ.AX(J))RETURN
C   ESTIMATE SLOPE AT AX(J-1)
      CALL E011A(N,AX,AY,J-1,G1)
C   ESTIMATE SLOPE AT AX(J)
      CALL E011A(N,AX,AY,J,G2)
C   CONSTRUCT INTERPOLATING CUBIC POLYNOMIAL IN INTERVAL
      D=AY(J-1)
      C=G1
      H=AX(J)-AX(J-1)
      S=(AY(J)-AY(J-1))/H
      B=(3.0*S-2.0*G1-G2)/H
      A=(G1+G2-2.0*S)/H/H
C   EVALUATE POLYNOMIAL AT POINT
      H=X-AX(J-1)
      Y=((A*H+B)*H+C)*H+D
      RETURN
      END
      SUBROUTINE E011A(N,AX,AY,J,G)
      DIMENSION AX(N),AY(N)
C   CALCULATE SLOPES ON EITHER SIDE OF DATA POINT
      JM1=J-1
      JP1=J+1
      IF(J.NE.1)GO TO 20
C   END-POINT IS DIFFERENT
      H1=AX(2)-AX(1)
      S1=2.0*(AY(2)-AY(1))/H1-(AY(3)-AY(2))/(AX(3)-AX(2))
      GO TO 30
   20 CONTINUE
      H1=AX(J)-AX(J-1)
      S1=(AY(J)-AY(JM1))/H1
   30 CONTINUE
      IF(J.NE.N)GO TO 40
C   END-POINT IS DIFFERENT
      H2=AX(N)-AX(N-1)
      S2=2.0*(AY(N)-AY(N-1))/H2-(AY(N-1)-AY(N-2))/(AX(N-1)-AX(N-2))
      GO TO 50
   40 CONTINUE
      H2=AX(JP1)-AX(J)
      S2=(AY(JP1)-AY(J))/H2
   50 CONTINUE
      S12=S1*S2
C   IF DATA IS NOT MONOTONIC SET SLOPE TO ZERO
      IF(S12.GT.0.0)GO TO 10
      G=0.0
      RETURN
   10 CONTINUE
C   WHEN DATA IS MONOTONIC USE WEIGHTED AVERAGE OF NORMAL SLOPES
      T1=2.0*H1+H2
      T2=H1+2.0*H2
      T=(T1*S2+T2*S1)/(3.0*(H1+H2))
      G=S12/T
      RETURN
      END
```

```
C
C
C SUBROUTINE FOR CALCULATING THE ELLIPTIC INTEGRALS USED FOR DETERMINING
C THE S VALUE FROM THE CURRENT GUESS FOR A/B

      REAL FUNCTION FUN(Y)
      COMMON/PARAM/GAMMA(101),T(101),A,C,D,NN,AA(6),AD(6)
      B=1.0
      GOTO(10,20,30,40,50,60,70,80,90),NN
   10 FUN=1.0/((A*A+Y)**1.5*(B*B+Y)**0.5*(C*C+Y)**0.5)
      RETURN
   20 FUN=1.0/((A*A+Y)**0.5*(B*B+Y)**1.5*(C*C+Y)**0.5)
      RETURN
   30 FUN=1.0/((A*A+Y)**0.5*(B*B+Y)**0.5*(C*C+Y)**1.5)
      RETURN
   40 FUN=1.0/((A*A+Y)**0.5*(B*B+Y)**1.5*(C*C+Y)**1.5)
      RETURN
   50 FUN=1.0/((A*A+Y)**1.5*(B*B+Y)**0.5*(C*C+Y)**1.5)
      RETURN
   60 FUN=1.0/((A*A+Y)**1.5*(B*B+Y)**1.5*(C*C+Y)**0.5)
      RETURN
   70 FUN=Y/((A*A+Y)**0.5*(B*B+Y)**1.5*(C*C+Y)**1.5)
      RETURN
   80 FUN=Y/((A*A+Y)**1.5*(B*B+Y)**0.5*(C*C+Y)**1.5)
      RETURN
   90 FUN=Y/((A*A+Y)**1.5*(B*B+Y)**1.5*(C*C+Y)**0.5)
      RETURN
      END
```

Results:

PROTEIN 1, 0.1 DEG. ABSOLUTE ERROR

110NS, 100PTS
STREAM3

FUNCTION VALUE ON EXIT IS .000399962998
A/B= 1.48309 A+= .070458728408 A-= .048831535604

FUNCTION VALUE ON EXIT IS .000399962998
A/B= 1.48309 A+= .070458845275 A-= .048831534073

FUNCTION VALUE ON EXIT IS .00399962998
A/B= 1.48309 A+= .070458881237 A-= .048831534081

BEST LEAST SQUARES VALUE = .000399962998
                  A / B = 1.48309
                     A+ = .0707
                     A- = .0488

Appendix VI   Use of M_r, $\bar{v}$ and s to determine k_s

Rowe (1977) has shown that

$$M_r = N_A \left[\frac{6\pi\eta_o s}{(1 - \bar{v}\rho_o)} \right]^{3/2} \cdot \left[\left(\frac{3\bar{v}}{4\pi} \right) \left(\frac{k_s}{2\bar{v}} - \frac{\bar{v}_s}{\bar{v}} \right) \right]^{1/2}$$

This can be rearranged to give

$$k_s = 2\bar{v} \left[\frac{4\pi}{3\bar{v}} \cdot \frac{M_r^2}{N_A^2} \left(\frac{1 - \bar{v}\rho_o}{6\pi\eta_o s} \right)^3 + \frac{\bar{v}_s}{\bar{v}} \right]$$

An estimate for $\bar{v}_s/\bar{v}$ is required, thus this equation would normally be used as a check for internal consistency between values for sedimentation and viscosity parameters, since $\bar{v}_s/\bar{v} = k_\eta / k_s$.

Appendix VII   Comparison of the radius of gyration for a sphere of

uniform mass with that for a sphere of the same mass but with a spherical

cavity

The radius of gyration, R_G of a sphere of uniform mass and radius

R is given by:

$$R_G^{\ 2} = \int_0^R 4\pi r^4\,dr \bigg/ \int_0^R 4\pi r^2\,dr \qquad = \quad \frac{3}{5}R^2 \qquad \text{(i)}$$

(Tanford, p 306, 1961). The radius of gyration of a spherical shell of

uniform mass with radius R_2 and with a centrally placed spherical cavity

of radius R_1 is given by:

$$R_G^{\ 2} = \int_{R_1}^{R_2} 4\pi r^4\,dr \bigg/ \int_{R_1}^{R_2} 4\pi r^2\,dr \qquad = \quad \frac{3}{5}\left(\frac{R_2^{\ 5} - R_1^{\ 5}}{R_2^{\ 3} - R_1^{\ 3}}\right) \qquad \text{(ii)}$$

The results of electron microscopy and x-ray diffraction (Harrison,

1959, Farrant, 1954, Kuff & Dalton, 1957, Labaw & Wycoff, 1957) suggest

that apoferritin consists of twenty four sub-units, each of molecular

weight 20,000, arranged in the form of a spherical shell of diameter

109 $\overset{o}{A}$. If we take the radius of the hollow to be 18.5 $\overset{o}{A}$, and the outer

radius of the shell to be 54.5 $\overset{o}{A}$, R_G is calculated using formula (ii) to

be 43.0 $\overset{o}{A}$. The radius of gyration, had the same mass been concentrated

into a uniform sphere of density identical to the shell would have been

41.6 $\overset{o}{A}$, using formula (i); i.e. a discrepancy of $\sim 3.4\%$

BIBLIOGRAPHY

Alexander, A.E. and Johnson, P. (1949)

'Colloid Science', Volume 2, Oxford University Press

Alpert, S.S. and Banks, G. (1976)

Biophysical Chem. 4, 287

Baghurst, P.A., Nichol, L.W., Ogston, A.G., Winzor, D.J. (1975)

Biochem. J. 147, 575

Ballinger, K.W.A. and Jennings, B.R. (1979)

Nature 282, 699

Batchelor, G.K. (1967)

'An Introduction to Fluid Mechanics', Cambridge University Press

Batchelor, G.K. (1970)

J. Fluid Mech. 41, 545

Batchelor, G.K. and Green, J.T. (1972)

J. Fluid Mech. 56, 375

Beeman, W.W., Koesberg, P., Anderegg, J.W. and Webb, M.B. (1957)

in 'Handbuck der Physik', (Flugge, S. ed.), 32, 321, Springer-Verlagg

(Berlin)

Benoit, H. (1951)

Ann. Physik. 6, 561

Berne, P.J. and Pecora, R. (1974)

Ann. Rev. Phys. Chem. 25, 233

Blake, C.C.F. (1975)

Essays in Biochem. II, 37

Blake, C.C.F., Geisow, M.J. and Oatley, S.J. (1978)

J. Mol. Biol. 121, 339

Blake, C.C.F., Koenig, D.F., Mair, G.A., North, A.C.T., Phillips, D.C.

and Sarma, V.R. (1965)

Nature 206, 757

Bloomfield, V.A., Dalton, W.O. and Van Holde, K.E. (1967)

Biopolymers 5, 135

Bresler and Talmud (1944)

CR Acad. Sci. URSS, 43, 310

Brinkman, H.C., Hermans, J.J., Oosterhoff, L.J., Overbeek, J. Th. G.,

Polder, D., Staverman, A.J. and Wiebenga, E.H. (1949)

Proc. Int. Rheol. Congress (Schveningen) II, 77

Brenner, H. (1970)

J. Coll. Int. Sci. 32, 141

Brenner, H. (1972a)

Chem. Eng. Sci. 27, 1069

Brenner, H. (1972b)

Progr. Heat and Mass Transfer 5, 93

Cantor, C.R. and Tao, T. (1971)

Proc. Nucl. Acid Res. 2, 31

Cerf, R. and Scheraga, H.A. (1952)

Chem. Revs. 51, 185

Chapman, P.F. (1913)

Phil. Mag. 25, 475

Cheng, P.Y. and Schachman, H.K. (1955)

J. Polymer Sci. 16, 19

Chu, B. (1974)

'Laser Light Scattering', Academic, New York

Chwang, A.T. (1975)

J. Fluid Mech. 72, 17

Clenshaw, C.W. and Curtis, A.R. (1960)

Num. Math. 2, 197

Creeth, J.M. and Knight, C.G. (1965)

Biochim. Biophys. Acta 102, 549

Cummings, H.Z. and Pike, E.R. (1973)

(eds.) 'Photon Correlation and Light Beating Spectroscopy', Plenum,

New York

Dickerson, R.E. and Geiss, I. (1969)

'The Structure and Action of Proteins', Benjamin, California

Dougherty, J. and Kreiger, I.M. (1972)

in Kreiger, Adv. Colloid Sci. 3, 111

Edsall, J.T. (1953)

in 'The Proteins' (Neurath, H. and Bailey, K. eds) 1B, Chapter 7,

Academic, New York

Edwardes, D. (1892)

Quart. J. Math. 26, 70

Einstein, A. (1905)

Ann. Physik 17, 549

Einstein, A. (1906)

Ann. Physik 34, 591

Einstein, A. (1911)

Ann Physik 34, 591

Emes, C.H. (1977)

Ph. D. thesis, University of Leicester

Emes, C.H. and Rowe, A.J. (1978a)

Biochim. Biophys. Acta 537, 110

Emes, C.H. and Rowe, A.J. (1978b)

Biochim. Biophys. Acta 537, 125

Farrant, J.L. (1954)

Biochim. Biophys. Acta 13, 569

Feldman, R.J. (1976)

'Atlas of Macromolecular Structure on Microfiche', Traco Jitco Int.,

Rockville, Md. USA

Gans, R. (1928)

Ann. Physik 86, 628

Garcia Bernal, J.M. and Garcia de la Torre, J. (1980)

Biopolymers 19, 628

Garcia de la Torre, J. and Bloomfield, V.A. (1977a)

Biopolymers 16, 1747

Garcia de la Torre, J. and Bloomfield, V.A. (1977b)

Biopolymers 16, 1765

Garcia de la Torre, J. and Bloomfield, V.A. (1977c)

Biopolymers 16, 1779

Garcia de la Torre, J. and Bloomfield, V.A. (1978)

Biopolymers 17, 1605

Gardner, D.G., Gardner, J.C., Laush, G. and Meinke, W.W. (1959)

J. Chem. Phys. 31, 978

Giesekus, H. (1962)

Rheol. Acta 2, 50

Gill, P.E. and Murray, W. (1976)

Nat. Phys. Lab. report NAC 72

Gold, O. (1937)

Ph. D. thesis, University of Vienna

Goodwin, J.W. (1975)

Colloid Science 2 (Chemical Society), 246

Guoy, L.G. (1910)

J. Phys. Chem. 9, 457

Hall, C.E. and Slayter, H.S. (1959)

J. Biophys. Cytol. 5, 11

Harding, S.E. (1980a)

Biochem. J. 189 (in press)

Harding, S.E. (1980b)

mss. submitted to J. Phys. Chem.

Harrison, P.M. (1959)

J. Mol. Biol. 1, 69

Herzog, R.O., Illig, R. and Kudar, H. (1934)

Z. Phys. Chem. A167, 329

Holtzer, A. and Lowey, S. (1956)

J. Am. Chem. Soc. 78, 5954

Jablonski, A. (1961)

Naturforsch 169, 1

Jeffrey, G.B. (1922)

Proc. Roy. Soc. (London) A102, 476

Johnson, P. and Mihalyi, E. (1965)

Biochim. Biophys. Acta 102, 476

Jost, J.W. and O'Konski, C.T. (1978)

in 'Molecular Electro Optics' (O'Konski, C.T. ed.) Volume 2, 529

Kartha, G., Bello, J. and Harker, D. (1967)
Nature 213, 862

Kendrew, J.C., Bodo, G., Dintzis, H.M., Parrish, R.G., Wycoff, H.
and Phillips, D.C. (1958)
Nature 181, 665

Kim, S.H. (1974)
in 'Biochemistry' (Stryer, L.) 653, Freeman, San Francisco

Kirkwood, J.G. (1967)
'Macromolecules' (Aueur, P.L. ed.), Gordon and Breach

Koenig, S.H. (1975)
Biopolymers 14, 2421

Kratky, O., Leopold, H. and Stabinger, H. (1969)
Z. Angew. Phys. 27, 273

Kratky, O., Leopold, H. and Stabinger, H. (1969)
in 'Methods in Enzymology' (Hirs, C.H.W. and Timasheff, S.N. eds.),
27, 98, Academic, London

Krause, S. and O'Konski, C.T. (1959)
J. Am. Chem. Soc. 81, 5082

Kuff, E.J. and Dalton, A.L. (1957)
J. Ultrastructure Res. 1, 62

Kuhn, W. and Kuhn, H. (1945)

Helvetica Chimica Acta 38, 97

Kynch, G.J. (1956)

Proc. Roy. Soc. (London) A237, 90

Labaw, L.W. and Wycoff, R.W.G. (1957)

Biochim. Biophys. Acta 25, 263

Lauffer, M.A. (1942)

Chem. Rev. 31, 561

Laurent, T.C. and Killander, J. (1964)

J. Chromatog. 14, 317

Lipscomb, W.N. (1971)

Proc. Robert A. Welch Found. Conf. Chem. Res. 15, 134

Lloyd, P.H. (1974)

'Optical Methods in Ultracentrifugation, Electrophoresis and Diffusion',

Clarendon Press, Oxford

Lucas, C.W. and Terrill, C.W. (1970)

Collected Algorithms from CACM, No. 404

Manley, R. and Mason, S. G. (1954)

Canad. J. Chem. 32, 763

Martin, R.B. (1964)

'Introduction to Biophysical Chemistry' Chap. 11, McGraw—Hill, New York

McCammon, J.A., Deutch, J.M. and Bloomfield, V.A. (1975)

Biopolymers 14, 2479

Mehl, J.W., Oncley, J.L. and Simha, R. (1940)

Science 92, 132

Mendelson, R. and Hartt, J. (1980)

EMBO Workshop on Muscle Contraction, Alpbach Conf. Austria

Mihalyi, E. and Godfrey, J. (1963)

Biochim. Biophys. Acta 67, 90

Memming, R. (1961)

Z. Physik. Chem. (Frankfurt) 28, 169

Mooney, M. (1951)

J. Coll. Sci. 6, 162

Mooney, M. (1957)

J. Coll. Sci. 12, 575

Munro, I., Pecht, I. and Stryer, L. (1979)

Proc. Nat. Acad. Sci. (USA) 76, 56

Nichol, L.W., Jeffrey, P.D., Turner, D.R. and Winzor, D.J. (1977)

J. Phys. Chem. 81, 776

Nisihara, T. and Doty, P. (1958)

Proc. Nat. Acad. Sci. (USA) 44, 411

Oberbeck, A. (1876)

J. reine. angew. Math. 81, 62

O'Connor, D.V., Ware, W.R. and Andre, J.C. (1979)

J. Phys. Chem. 83, 1333

Offer, G., Moos, C. and Starr, R. (1973)

J. Mol. Biol. 74, 653

O'Hara and Smith (1968)

Comp. Journal 11, 213

O'Konski, C.T. and Haltner, A.J. (1956)

J. Am. Chem. Soc. 78, 3604

Oliver, J. (1972)

Comp. Journal 15, 141

Oncley, J.L. (1940)

J. Phys. Chem. 44, 1103

Oncley, J.L. (1941)

Ann. New York Acad. Sci. 41, 121

Paradine, C.G. and Rivett, B.H.P. (1960)

'Statistical Methods for Technologists', English Universities Press,

London

Pearce, T.C., Rowe, A.J. and Turnock, G. (1975)

J. Mol. Biol. 97, 193

Perrin, F. (1934)

J. Phys. Radium 5, 497

Perrin, F. (1936)

J. Phys. Radium 7, 1

Perutz, M.F., Rossmann, M.G., Cullis, A.F., Muirhead, H., Will, G. and

North, A.C.T. (1960)

Nature 185, 416

Powell, D.R. and MacDonald, J.R. (1972)

Comp. Journal 15, 148

Pytkowickz, R.M. and O'Konski, C.T. (1959)

J. Am. Chem. Soc. 81, 5082

Rallison, J.M. (1978)

J. Fluid Mech. 84, 237

Riddiford, C.L. and Jennings, B.R. (1967)

Biopolymers 5, 757

Ridgeway, D. (1966)

J. Am. Chem. Soc. 88, 1104

Ridgeway, D. (1968)

J. Am. Chem. Soc. 90, 18

Rowe, A.J. (1977)

Biopolymers 16, 2595

Rowe, A.J. (1978)

Techniques in Protein and Enzyme Biochem. B105a, 1

Saito, N. (1951)

J. Phys. Soc. (Japan) 6, 297

Scheraga, H.A. (1955)

J. Chem. Phys. 23, 1526

Scheraga, H.A. (1961)

'Protein Structure', Academic, New York

Scheraga, H.A. and Mandelkern, L. (1953)

J. Am. Chem. Soc. 79, 179

Simha, R. (1940)

J. Phys. Chem. 44, 25

Simha, R. (1952)

J. Appl. Phys. 23, 1020

Shaw, D.J. (1970)

'Introduction to Colloid and Surface Chemistry' (2nd edn.), Butterworths

Small, E.W. and Isenberg, I. (1977)

Biopolymers 16, 1907

Sorenson, N.A. (1930)

CR Lab. Carlsberg 18, No. 5

Squire, P.G. (1970)

Biochim. Biophys. Acta 221, 425

Squire, P.G. (1978)

in 'Molecular Electro Optics' (O'Konski, C.T. ed.) Volume 2, 565

Squire, P.G., Moser, L. and O'Konski, C.T. (1968)

Biochemistry 7, 4261

Stacey, K.A. (1956)

'Light Scattering in Physical Chemistry', Butterworths, London

Stokes, Sir G. (1851)

Trans. Cambridge Phil. Soc. 9, 8

Stokes, Sir G. (1880)

'Mathematical and Physical Papers', Cambridge University Press

Svedberg, T. and Pedersen, K.O. (1940)

'The Ultracentrifuge', Oxford University Press

Tanford, C. (1955)

J. Phys. Chem. 59, 798

Tanford, C. (1961)

'Physical Chemistry of Macromolecules', Wiley, New York

Theorell, H. (1934)

Biochem. Z. 268, 46

Vand, V. (1948)

J. Phys. Coll. Chem. 52, 277

Van de Hulst, H.C. (1957)

'Light Scattering by Small Particles', Wiley, New York

Van Holde, K.E. (1971)

'Physical Biochemistry', Prentice Hall, New Jersey

Wahl, P. (1966)

Compt. Rend. Acad. Sci. (Paris) 263D 1525

Wales, M. and Van Holde, K.E. (1954)

J. Polymer Sci. 14, 81

Wilde, D.J. (1964)

'Optimum Seeking Methods', Prentice Hall, New Jersey

Williams, R.C., Ham, W.T. and Wright, A.K. (1976)

Anal. Biochem. 73, 52

Wilson, R.W. and Bloomfield, V.A. (1979a)

Biopolymers 18, 1205

Wilson, R.W. and Bloomfield, V.A. (1979b)

Biopolymers 18, 1543

Yang, J.T. (1961)

Adv. Protein Chem. 16, 323

Zimm, B.H. (1948)

J. Chem. Phys. 16, 1093

Zimm, B.H. (1956)

J. Chem. Phys. 24, 269